KALMAN FILTERING TECHNIQUES APPLIED TO THE DYNAMIC SHIP POSITIONING PROBLEM

by

ADNAN A G AL-TAKIE

A thesis, submitted to the Council for National Academic Awards in partial fulfilment of the requirements for the degree of Doctor of Philosophy

The research was conducted at Sheffield City Polytechnic in collaboration with GEC Electrical Projects Ltd, Rugby

October 1982

TO MY FAMILY

KALMAN FILTERING TECHNIQUES APPLIED TO THE DYNAMIC SHIP POSITIONING PROBLEM

A A G Al-Takie

Abstract

The dynamic ship positioning problem using Kalman filtering techniques is considered. The main components of the system are discussed. The ship dynamics, based on a linearised model, are represented by state equations. These equations involve low and high frequency subsystems. A simplified design procedure for the implementation of a Kalman filter is described based on the linearised equations of motion. The Kalman filter involves a model of the system and is therefore particularly appropriate for separating the low and high frequency motions of the vessel. The filtering problem is one of estimating the low-frequency motions of the vessel so that control can be applied. An optimal feedback control system simulation based on optimal stochastic control theory is used. The optimal control performance criterion weighting matrices Q, R were pre-selected and the optimal feedback gain matrix was computed. This control scheme involves the low-frequency part of the ship model. The Kalman filter has been simulated on a digital computer for different modelled operating conditions. The computer simulation results showing the behaviour and responses of the Kalman filter applied to the dynamic ship positioning problem were investigated. The system dynamics vary as the weather conditions vary and can be classified from a calm sea condition (Beaufort number 5) to the worst condition (Beaufort number 9). Different tests involving systems modelling and filter mismatching have been carried out. Another field in which the robustness of a Kalman filter has been assessed involved a test in which the system observation noise covariance was increased keeping the filter with the usual noise information. Saving in both computation and computer storage requirement were achieved using a form of semi-constant filter gain and reduced-order Kalman filter respectively.

System non-linearities have been considered and a non-linear control algorithm was proposed and implemented using an extended Kalman filter. These non-linearities involve the thruster dynamics and the associated low-frequency part of the system model.

All data that have been used within this work for system implementation were obtained from two different models ("Wimpey Sealab" and "Star Hercules" vessels). Our system has been employed by GEC Electrical Projects Limited, Rugby, for a new vessel ("Star Hercules") and this has been commissioned and is currently operating successfully off Brazil.

CONTRIBUTION AND PUBLICATIONS

Summary of Contributions

1. Complete implementation of Kalman estimator together with optimal feedback control for "Wimpey Sealab" vessel.
2. In depth investigations into the non-linearities of main parts of the dynamic ship positioning systems.
3. Complete development of dynamic positioning control based on Kalman filtering and optimal feedback control for "Star Hercules" vessel.

Publications

1. AL-TAKIE, A A: "Development of a dynamic ship positioning simulation", Research Report EEE/28/1979, Sheffield City Polytechnic.
2. AL-TAKIE, A A: "Documentation report on the selection of the optimal control performance criterion", Research Report, January 1980, Sheffield City Polytechnic
3. AL-TAKIE, A A: "Kalman filtering techniques applied to the dynamic positioning problem", Research Report EEE/53/May 1980, Sheffield City Polytechnic
4. AL-TAKIE, A A and GRIMBLE, M J: "Optimal control of non-linear stochastic systems with application to dynamic ship positioning", International Conference on Systems Engineering, September 14-16, 1982, Coventry (Lanchester)Polytechnic, UK.
5. GRIMBLE, M J and AL-TAKIE, A A: "Optimal control of non-linear stochastic systems", Research Report EEE/60/September 1980, Sheffield City Polytechnic.

ACKNOWLEDGEMENTS

I would like to express my gratitude and sincere thanks to my supervisor, Professor M J Grimble, for his guidance, valuable advice and encouragement all through the period of this research work.

The work described in this thesis was partially financed by the British Science and Engineering Research Council for which the author is most grateful.

The work has been carried out in close liaison with GEC Electrical Projects, Rugby and I would particularly like to thank Mr D Wise for his valuable technical advice.

Thanks due to Mr D Abraham, Head of Department of Electrical and Electronic Engineering, Sheffield City Polytechnic and to virtually every member of his staff who have offered their help and suggestions with respect to difficulties.

My thankfulness is also extended to Dr R J Patton of the Department of Electrical Engineering, York University, for his help and advice on the software developments.

Finally, I would like to thank Mrs Lesley Walker for her meticulous care in typing this thesis.

TABLE OF CONTENTS

C H A P T E R (1)

CHAPTER 1

GENERAL ASPECTS OF THE DYNAMIC POSITIONING PROBLEM

1.1 General Introduction

Since the end of World War II, it has been increasingly realised that the seabed and rock beneath are rich in mineral resources which should be exploited. The best known example is the offshore oil reserves. Initially, exploitation was limited to shallow water close to the shore but it has moved progressively into deeper water and less hospitable locations. Early exploration for oil production was carried out from fixed platforms. Inspection and maintenance work on fixed structures involve extensive use of diving services and lifting facilities. From these has arisen the need for the floating vessel with the necessary technique to keep it stationary with respect to some reference point. Recently many floating drilling rigs and drill ships have been introduced and many of these are working in the North Sea. In addition to drilling, offshore operations involve:

(i) coring

(ii) surveying

(iii) cable laying

(iv) dredging

(v) diving

(vi) fire fighting

The most significant limitation of using the conventional floating vessel is the difficulty of anchoring in deep water. To overcome these limitations, the concept of a dynamic positioning technique was introduced. Dynamic ship positioning is defined as the technique for maintaining the position of a vessel stationary over a specific preselected

point on the seabed without the use of anchoring systems. The second definition of dynamic positioning is that the vessel may be moving at controlled speed, which can be extended to include the tracking problem.

The process of automatically controlling a ship or floating platform position and heading [13] [19] over a preselected area is concerned with providing the necessary thrust in appropriate quantity and direction to match the mean loads imposed on the vessel by environment and other forces. This will involve using:

(i) a combination of thruster mechanism and propulsion

(ii) position and heading measuring devices

(iii) wind speed sensor

(iv) control computer

The design of an automatic position and heading control system for a vessel depends on the required criteria, which must be satisfied by the vessel and its control system (or computer control system) to perform its mission, on the environmental conditions in the area where the vessel will operate and on the expected behaviours of the vessel for changing weather.

The control system is part of a closed loop system, schematically shown in Figure 1.1. The main components are:

(i) measurement subsystem, including all devices for generating the information to be processed by the computer,

(ii) the filter to attenuate the unwanted signals and to generate the required estimates for state feedback control,

(iii) the controller, of which the output is sent to the propulsors (main propellers and other thrusters),

(iv) thrust generating system to drive the vessel to the required

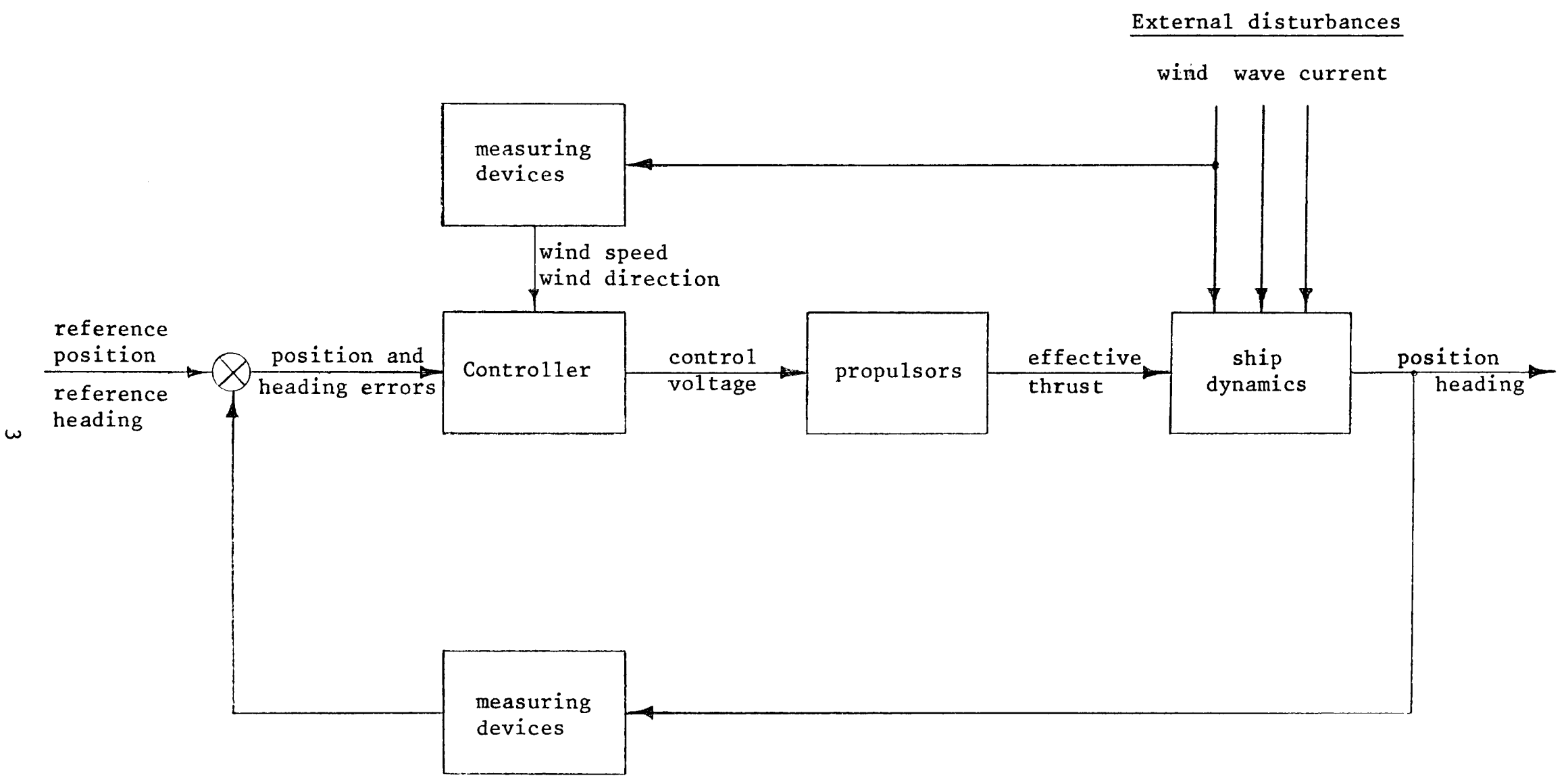

Figure (1.1): Dynamic ship positioning control systems

position.

This control scheme should be capable of:

(i) controlling the propulsors for maintaining a reference position and heading under specified weather conditions (with the ability to react to changing weather conditions), with a maximum allowable radial position error of 3 per cent of the water depth,

(ii) avoiding high-frequency fluctuations in the thrust demand (filtering problem) since this may cause unnecessary wear of the propulsors and waste of energy,

(iii) controlling the propulsors for changing the position or heading of the ship in case a new reference position or heading is selected.

Dynamic positioning systems with on-line computer control involve one of the following [30]:

(i) Simplex computer control, where longer term or more accurate position keeping is necessary, such as for support purposes. This fully automatic control system is an economic scheme and it normally comprises:

(a) one computer complete with monitoring unit and peripherals controllers

(b) one operator console, with full set-up, control and display

(c) one position measurement system

(d) set of environmental and attitude sensors

(ii) Duplex computer control, which is usually used for oil exploration drilling vessels, which is required to remain on station for long periods of time. A Full automatic duplex dynamic positioning system comprises of:

(a) two computers complete with monitoring units and peripheral controllers

(b) one operator console, with full set-up, control and display,

(c) two position measurement systems,

(d) two sets of environmental and attitude sensors.

The design of a vessel's dynamic positioning system involves a compromise between the two conflicting requirements of accuracy of position holding and the need to suppress the thrusters response to part of the wave motions. These external forces are assumed to consist of low-frequency and high-frequency forces. The thrusters response to the first order high-frequency wave motions is oscillatory in nature, and involves an extra power demand and wear and tear of the thrust-producing mechanisms, without any gains in counteracting vessel motion due to the above waves and forces.

The accuracy of the dynamic positioning system will depend to a certain extent on the philosophy of the wave filter selection method and the corresponding controller design procedure. Thus, the amount of the thrusters oscillations will depend on the wave filter attenuation and the controller bandwidth. Filtering for the dynamic positioning problem can be defined as the process of operating upon the corrupted information (the noisy measured system output) to attempt to construct a signal which can be used for control purposes [18], [22]. The control systems for the first dynamically positioned vessels [31], [30] included Notch filters and PID controllers. Using such a scheme, the position measurement signal can be filtered out to obtain a comparatively good estimate of the low-frequency part of the vessel motions, and hence, control can be applied [23]. An introduction to Notch filter networks is given in Section 1.2

Using the above conventional Notch filter scheme with PID control can cause some difficulties since a compromise should be made between improved filtering and good control system performance. Such difficulties led to the use of the alternative Kalman filtering technique together with modern stochastic optimal control theory. The Kalman-Bucy filter [58], [60], [47], [46] has assumed a role of ever increasing importance over recent years in the field of filtering and estimation of processes, and its applications in dynamic systems. Theoretically, the Kalman filter gives the unbiased, minimum variance estimation of the state vectors of a linear or linearised dynamic system when output measurements are provided which represent a linear function of the system states with some additive white noise. In practice, optimum performance will be very hard to realise since the information required to construct the Kalman filter is only approximately known. Hence, to get the best filtering and estimation, the Kalman filter has to be provided with as much information as possible concerning the noise statistics and system dynamics.

In dynamic vessel positioning the low-frequency part of the system states are required to be estimated by the Kalman filter so that control can be applied. Kalman filter dynamics, based on the separation theorem [21], [54] will involve a model of the actual low and high frequency part of the system dynamics (Figure 1.2), and hence, the estimated high-frequency state vectors can be ignored, while the estimated low-frequency states can be fed back to be used within the control loop. An introduction into the use of the Kalman-Bucy filtering scheme and its applications to the dynamic positioning problem for this study will be given in Section 1.3.

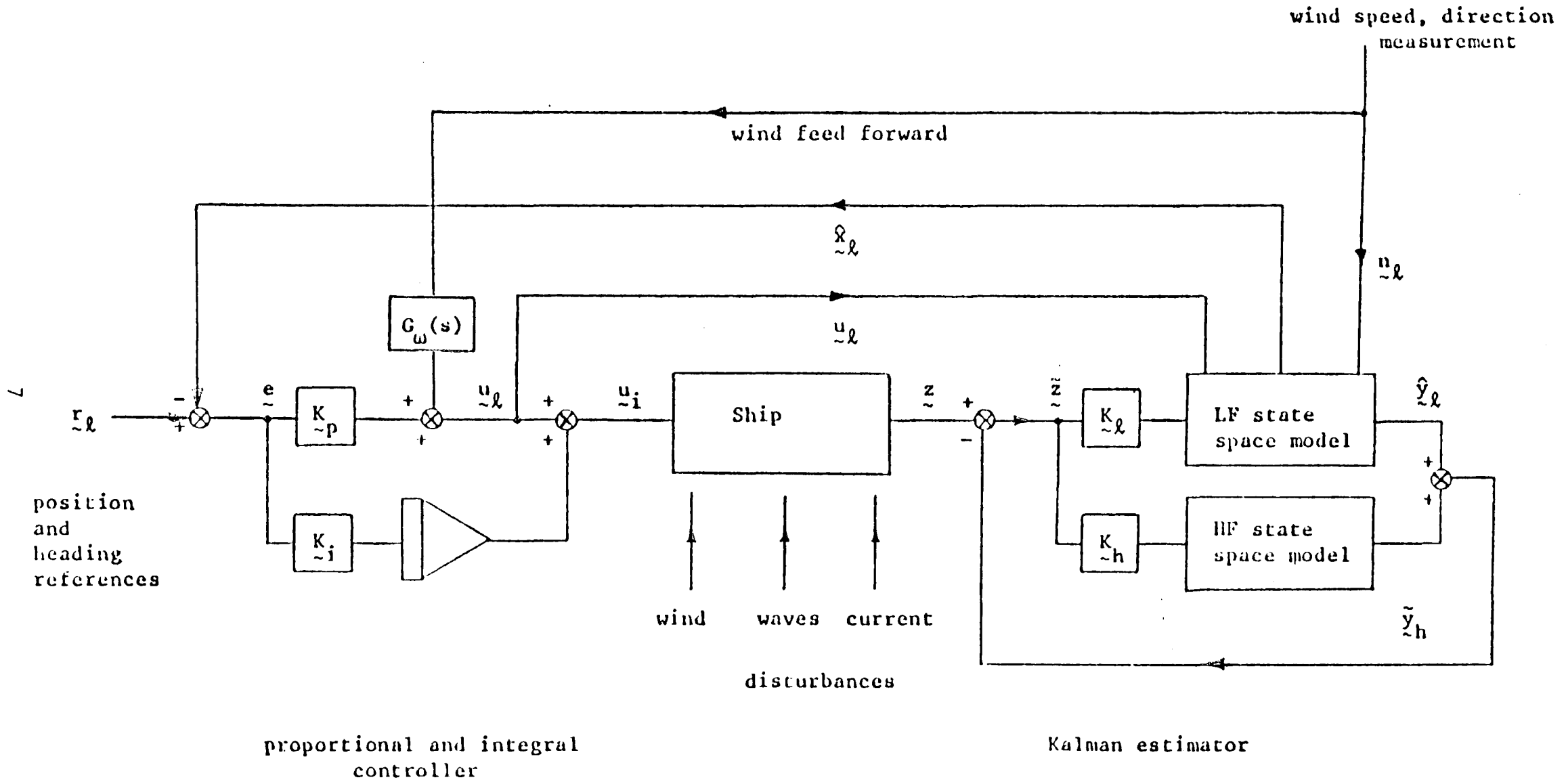

Figure (1.2): Dynamic Positioning Control System and Estimator

1.2 Notch, PID Filtering and Control

Notch filters [99], [103] have been developed and used in dynamic ship positioning for some years with relatively good results. If the control system were purely analogue, this filter would obviously be preferred. With digital processors available, other filter structures might yield additional advantages. A Kalman filter with such properties [45], [12] will be introduced in the next section. A Notch filter is often used in dynamic positioning problems to attenuate the high-frequency wave motion signals from the position measurement system. The Notch filter must be capable of providing a constant attenuation ratio either for a fixed sea wave resonant frequency or for a range of resonant frequencies. A typical range of Notch frequencies [51] would be 0.06 Hz to 0.12 Hz corresponding to Beaufort scale number 9 down to 5 (Appendix 2). To provide a wide band-stop characteristic it is necessary to use a cascaded system of Notch filters with each section tuned to a particular resonant frequency [20], [13]. In this application three such cascaded sections are normally used. The Notch filter transfer function can be defined [103] by:

$$H(s) = \frac{s^2 + \frac{bd}{\sqrt{1 - 2d^2}}\, s + \omega^2}{s^2 + \frac{b}{\sqrt{1 - 2d^2}}\, s + \omega^2} \qquad \ldots\ldots\ldots\ldots \quad (1.1)$$

where:

ω Notch centre frequency (rad/sec)

b the 3 dB bandwidth of the Notch (rad/sec)

d the attenuation ratio at the Notch centre frequency

The above parameters ω, b and d can be used to describe the Notch network. For a three cascaded section of this network the above transfer function H(s) can be written as [82]:

$$H(s) = \prod_{i=1}^{i=n} G_i(s) \qquad \ldots\ldots\ldots\ldots \quad (1.2)$$

where: n = 3 (for three cascaded sections), and:

$$G_i(s) = \frac{s^2 + \frac{b_i d_i}{\sqrt{1 - 2d_i^2}}\, s + \omega_i^2}{s^2 + \frac{b_i}{\sqrt{1 - 2d_i^2}}\, s + \omega_i^2} \qquad \ldots\ldots\ldots (1.3)$$

where:

ω_i the ith section centre frequency

b_i the ith section 3 dB bandwidth

d_i the ith section attenuation ratio

1.3 Alternative Kalman Filtering and Stochastic Optimal Control Solution

Considerable research has been devoted during the last twenty years to various problems in the estimation of the states of linear dynamic systems using system measurements corrupted by Markov noise. The Kalman-Bucy filtering technique for such applications has been thoroughly examined in the literature. The optimal, continuous time filtering problem for the case of linear system dynamics, additive measurements and Gaussian white disturbance measurement noise was first solved by Kalman (1960) [58] and Kalman and Bucy (1961) [60]. Specifically they considered the problem of finding the unbiased, minimal variance state estimate $\underline{\hat{x}}(t)$ of the system state $\underline{x}(t)$ in the presence of stochastic input disturbances and output measurement additive noise.

The problem of state estimation of noisy systems using Kalman filtering scheme requires a knowledge of the system structure and its parameters [9]. If the system is linear or linearised and its different parameters are known, the solution is a straightforward application of Kalman algorithms for filtering and estimation and is given by Kalman and Bucy (1961). In actual industrial applications, some of the plant

parameters may be unknown and hence it is necessary to estimate them together with the system states simultaneously. This parameter estimation problem requires the extension of the Kalman filtering scheme to include the system non-linearity. This will involve the implementation of the extended Kalman filter. This form of non-linear filter problem can be dealt with by constructing an additional linear dynamic model corresponding to the unknown parameters. The parameter equations are added to the system model equations and the combined states and parameter variables of this augmented model are to be estimated. Feedback control can be applied using the low-frequency part of the state estimates only (Figure 1.3). All the necessary information concerning the process and observation noise as well as system inputs have to be fed into the proposed filter dynamics for good estimation and filtering accuracy. The non-linear filtering problem for systems with random inputs is of great importance in control processes, especially in industrial situations. The Kalman filter has been proved to be efficient and reliable for many industrial applications.

The Kalman filtering scheme and its application to the dynamic positioning problem has been proposed by the Norwegians (Balchen et al, 1976 [11],[12]). Balchen's design involves a more complicated and computationally inefficient form of filter in which some of the high-frequency parameters were estimated. An alternative solution to the linear and non-linear Kalman filtering problems with their applications to the dynamic ship positioning problem was proposed and used by Grimble [51],[49]. The use of the proposed alternative solution of Kalman filtering combined with the optimal control theory to the dynamic positioning problem was part of a Case research study supported by GEC Electrical Projects Limited, Rugby

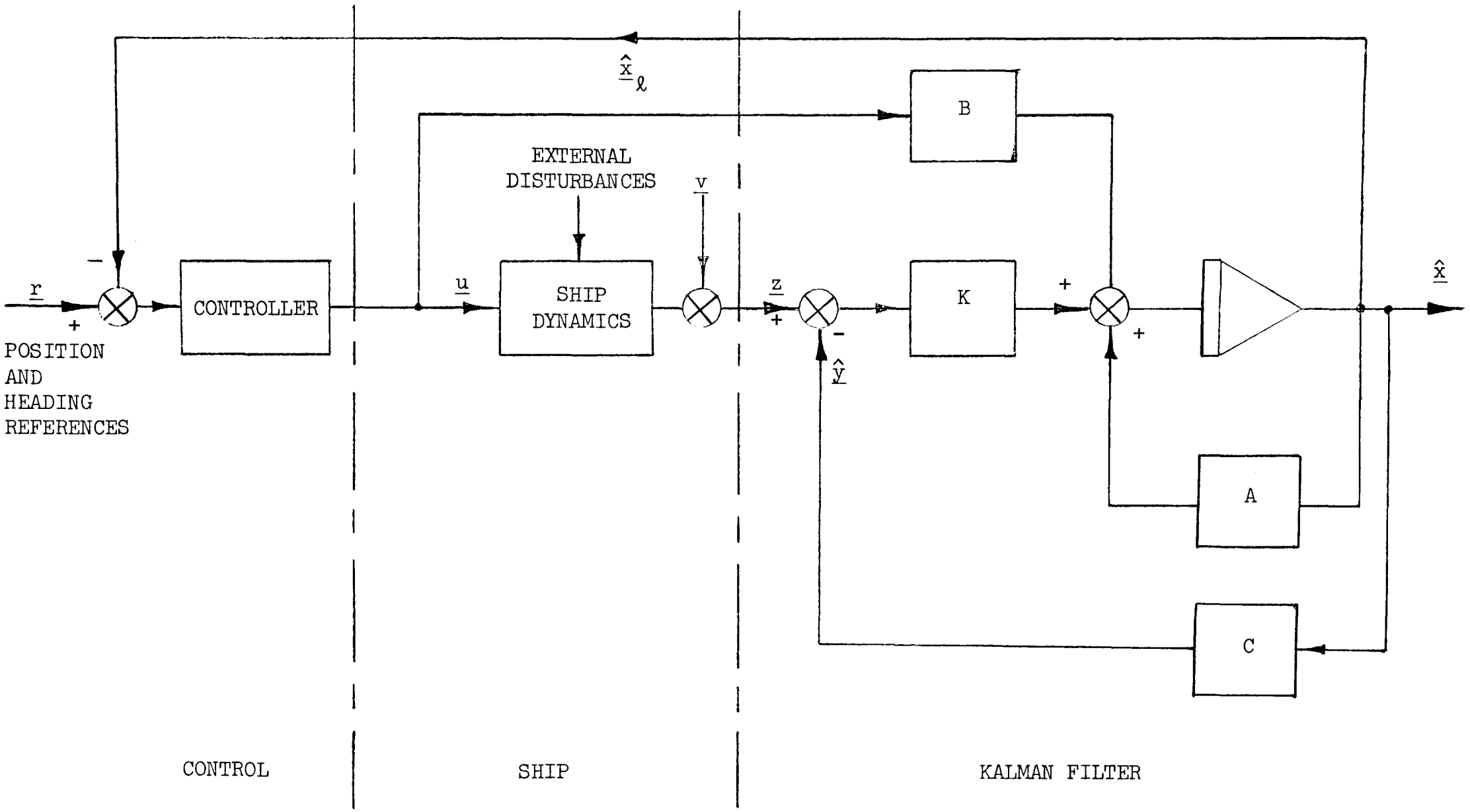

Figure (1.3): Kalman Estimator for the Dynamic Positioning Control

and carried out by a team of researchers. This work on dynamic positioning using Kalman filtering was an extension of in depth study of general filtering and control problems by Grimble [35], [33], [36]. The simulations were involved in some high-frequency parameter estimations to estimate some of the unknown parameters within the high-frequency dynamics using an extended Kalman filter [49], [52]. These estimated parameters are to affect the high-frequency block of the system dynamics structure which varies in accordance with the weather and sea conditions (Beaufort 9 for the worst sea condition down to Beaufort 5 for calm sea).

The team research provided a basic design for the dynamic ship positioning problem using Kalman filtering techniques based on data available from the "Wimpey Sealab" vessel. The author produced a complete design for the implementation of Kalman filtering and optimal stochastic control with its applications to the dynamic positioning problem based on data from the new "Star Hercules" vessel. This vessel has already been commissioned by GEC Electrical Projects Limited, Rugby. The author has also contributed to an original idea in which a special form of extended Kalman filter has been used employing the optimal control loop within the low-frequency part of the vessel dynamics. This form of non-linear control caters for the non-linearities within the low-frequency dynamics and deals specifically in detail with the non-linearity of the thruster devices which form part of the low-frequency dynamic structure (Chapter 7).

1.4 Thesis Layout

In the previous sections of Chapter 1, the overall dynamic vessel positioning problem has been introduced and its usefulness for exploitation processes and other industrial applications were outlined. An introduction for the use of Notch or Kalman filtering techniques within the dynamic positioning control loop were finally drawn in Sections 1.2 and 1.3 respectively.

Chapter 2 contains a brief description of the main basic parts of the dynamic positioning systems. This will include the overall system structure, the systems for measuring the position of the vessel, the thrust producing devices (for both "Wimpey Sealab" and "Star Hercules" vessels) and finally, the general statistics of both the process and observation noise.

Chapter 3 includes the basic linearised mathematical equations representing both the low and high frequency motions of the vessel. These differential equations have been formulated on the basis of data obtained from a set of "tank-tunnel-tests" and carried out by GEC Electrical Projects Limited, Rugby. These data were provided for both "Wimpey Sealab" and "Star Hercules" vessels. Finally, system matrices were summarised for control and system simulations.

In Chapter 4, Grimble's approach for the selection of the Q and R control weighting matrices has been implemented and used within the problem of the dynamic ship positioning. A form of the separation theorem has been used and the matrix Riccati equation was solved to calculate the optimal feedback gain matrix. Finally, the low-frequency dynamics for both "Wimpey Sealab" and "Star Hercules" vessels were simulated for the selection of the optimal Q and R matrices, and hence

the selection of the optimal gain matrix for future design (Chapters 5, 6).

Chapter 5 contains the main design results for a complete implementation and installation of the dynamic positioning system on both "Wimpey Sealab" and "Star Hercules" vessels using linear Kalman filtering and stochastic optimal control techniques. This chapter has been extended to include tests and investigations into the reliability and robustness of the Kalman filter algorithm and its application to the dynamic ship positioning problem.

In Chapter 6 the reliability and goodness of the Kalman filter and its application to the dynamic ship positioning are to be investigated and several tests to be carried out to examine the scheme robustness.

Chapter 7 deals mainly with the case of non-linear filtering and control. Non-linearities in both the high-frequency and low-frequency dynamics of the system were studied and an extended Kalman filter has been used.

Finally, in Chapter 8, all the design procedures and results were concluded, together with some future work recommendations.

C H A P T E R (2)

CHAPTER 2

MAIN PARTS OF THE DYNAMIC SHIP POSITIONING SYSTEMS

2.1 Introduction

The design of on-line computer control of a vessel position and heading under dynamic positioning control depends on certain criteria. These must be satisfied by the vessel and its control system in order to perform its mission (drilling, diving, fire fighting, etc), in the environmental conditions in the area where the vessel will operate and on the expected behaviour of the vessel under these environmental conditions. In dynamic positioning only the vessel motion in the horizontal plane (surge, sway and yaw) are controlled, where the ship will be regarded as a rigid body. The vessel motions induced by the waves are oscillatory motions with frequencies equal to the wave frequencies. At the same time the vessel drift from its original position is due to forces induced by the wind and the current. The vessel motion is assumed to consist of a low-frequency component and a high-frequency component. To keep the vessel motions, induced by the external forces, within the required allowable limits, the vessel is fitted with a set of thrusters (Section 2.2). Considering the requirements and environmental conditions, it may be stated that the control system should be designed to accept the relatively high-frequency motions without any counter-act measures, while the low-frequency motions should be reduced and controlled on the basis of the required accuracy for the different applications within the dynamic positioning technique (Table No 2.1).

As it has been defined,dynamic positioning is the technique for

DUTY	ENVIRONMENTAL CONDITION			ACCURACY
	Wind (knots)	Waves (metres)	Current (knots)	
Drilling	25	3.9	3	3% Water depth
Diving Support	30	4.5	1	± 3 m, Heading ± 2^{o}
Equipment Transfer	20	2.0	1	Heading ± 1^{o}, Excursion 1.5 m maximum
Fire Fighting	Weather up to severe gale or storm conditions			± 15 metres

Table (2.1): The required position accuracy

maintaining the position of a vessel above a reference point on the seabed without the use of anchors. This is to be achieved by employing a set of active thrusters controlled by a computer. The error within the position can be monitored using different kinds of measurement techniques. These measurements could be corrupted by noise. The main components in the dynamic positioning systems are the thrusters, the measurement systems, filter and the computer control (Figures 2.1, 2.2). System input signals from wind sensor, gyro compass and position measurements are fed into the control system and its associated computer to produce a command signal to the thrusters for appropriate action. This computer control system should be capable of:

(i) controlling the propulsors for maintaining a reference position and heading under specified adverse weather conditions, with a maximum allowable radial position error of 3 per cent of water depth or 7 metres (whichever is the smaller in case of drilling), or controlling the propulsors to maintain the vessel at a constant speed,

(ii) avoiding high-frequency fluctuations in the thrust demand since this may cause unnecessary wear of the propulsors and power consumption,

(iii) controlling the propulsors for changing the position or heading of the ship in case a new reference position or heading is selected.

In this chapter the thrusters, the measurement systems and the associated noise will be considered in detail, while the control system and the related filtering are due to be considered later.

2.2 Thruster Devices

2.2.1 Introduction

The dynamic ship positioning system has been defined as the process of automatically controlling a ship, or floating platform position and heading above a pre-selected fixed position on the seabed by using a

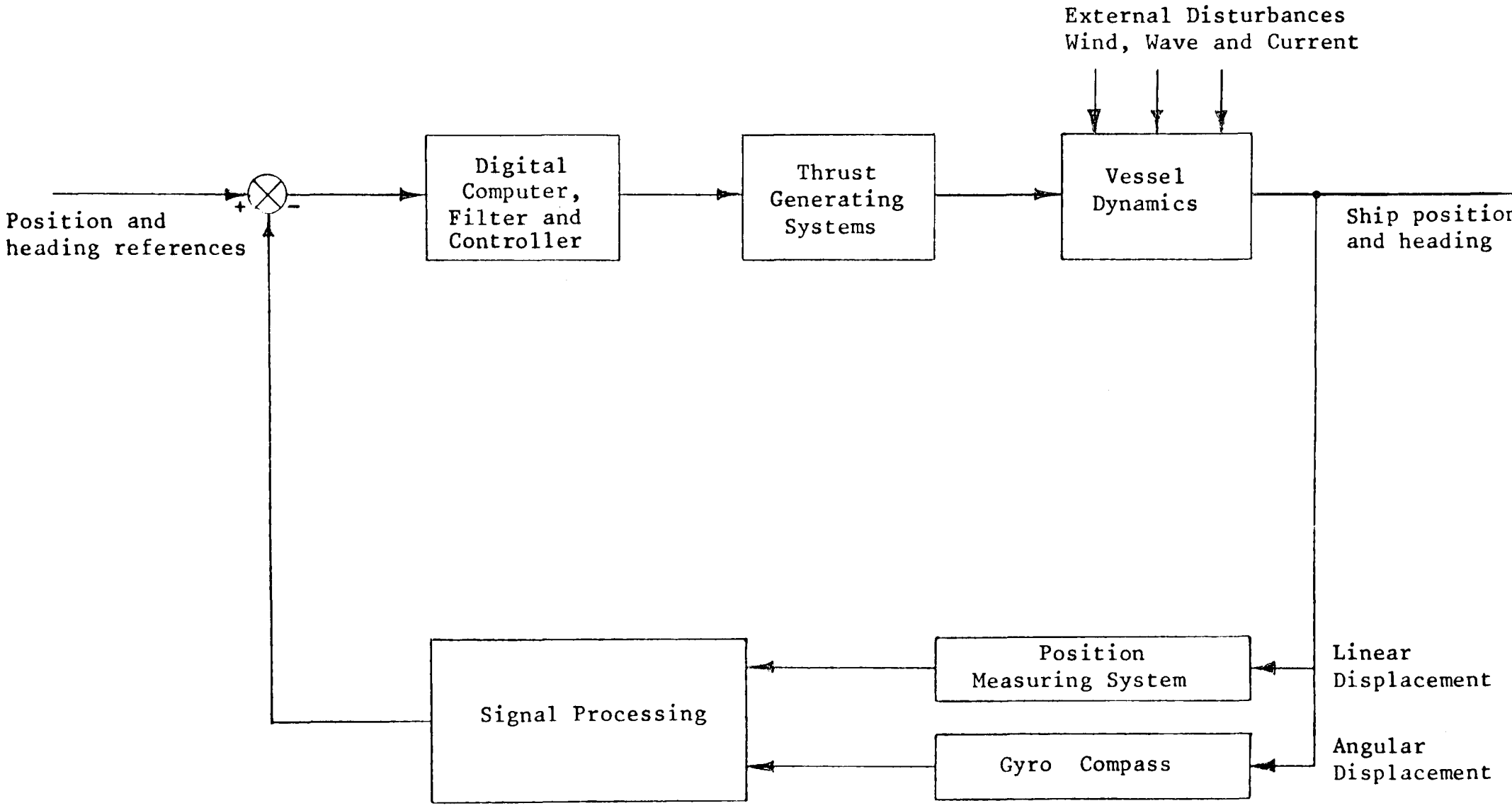

Figure (2.1): Layout of the main part for dynamic positioning systems

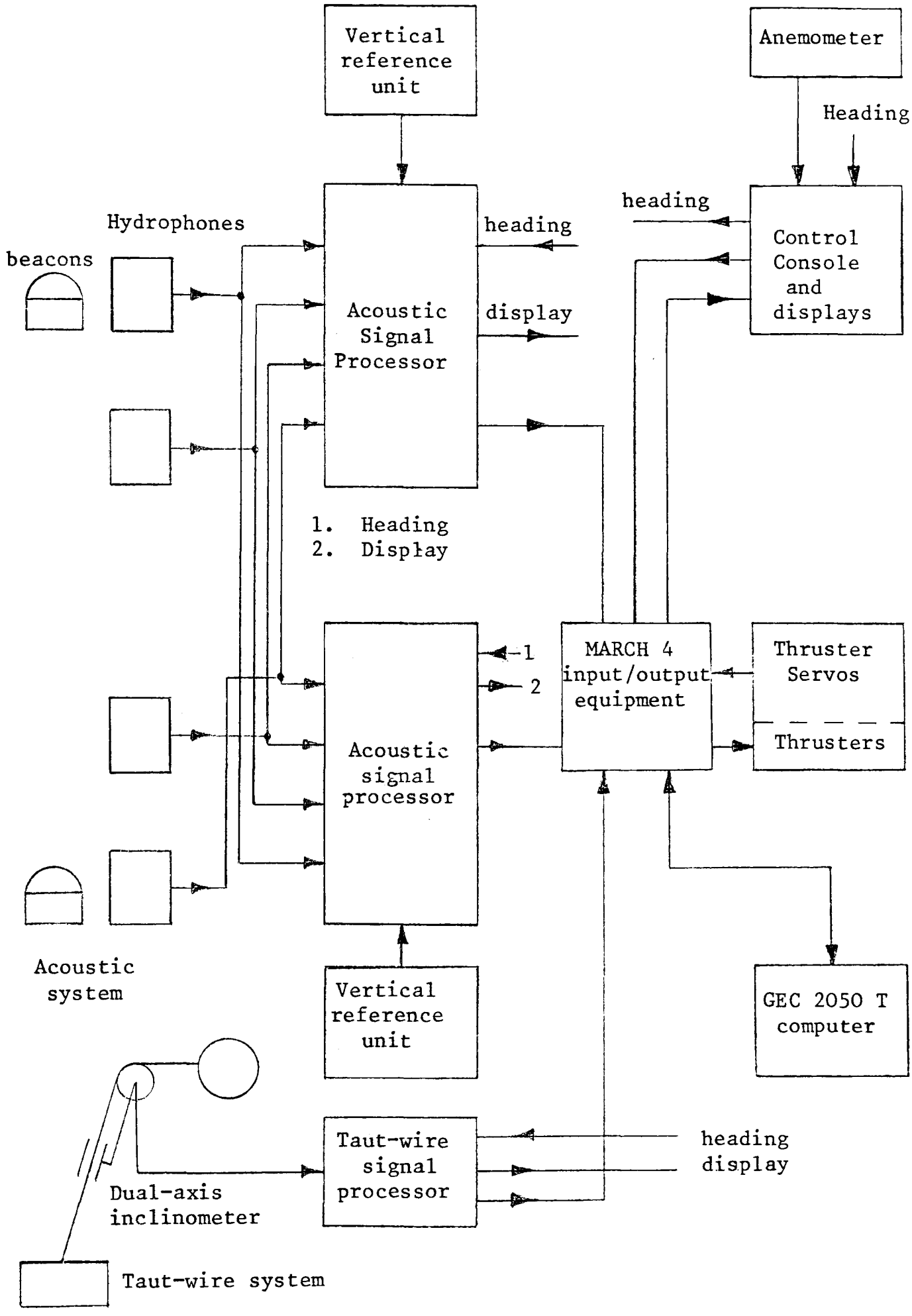

Figure (2.2): Schematic Diagram of the Dynamic Positioning System supplied for Wimpey Sealab

set of thrust-producing devices. In a dynamically positioned system the forces required to overcome the effects of wind, waves and currents are provided by propellers, and the vessel pre-selected position can be maintained by the use of a combination of thrusters and the main propulsion unit. Numerous types of thrusters are used for the dynamic ship positioning problem including plain propellers, ducted propellers and cycloidal propellers [73], (Figure 2.3). When thrusters or propellers are operated on a dynamic positioning vessel, the force and moment produced on the hull are not only due to the thrust devices since interactions arise due to pressure changes on the hull, and these should be taken into consideration in some cases.

The principal types of thrust-producing units are:

(i) screw propellers or thrusters,

(ii) cycloidal propellers (Voith Schneider units),

(iii) pump type thrusters,

(iv) transverse tunnel thrusters, and

(v) steerable thrusters.

Figure (2.3) shows the most common configuration being used. The thrusters have both dead zone and saturation characteristics (the dead zone for "Wimpey Sealab" is approximately 1-2% of the rated value of the thrusters [49]). The size of thrusters required is determined by the largest magnitude of the steady drift forces and moments. To avoid the unnecessary wear and tear on the thrusters the control system should not attempt to compensate for the high cyclic vessel motions.

2.2.2 Thrusters used on "Wimpey Sealab" vessel

George Wimpey and Company Limited have been involved in offshore drilling for many years. The dynamic positioning system, Figure 2.2, has been developed and included in the "Wimpey Sealab" vessel in

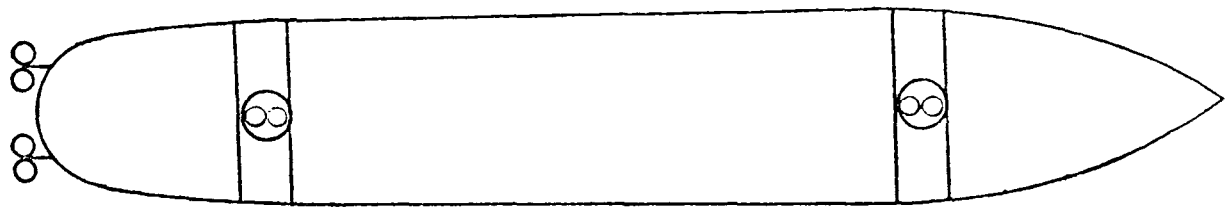

(a) Fixed Transverse Tunnel Thrusters
and Main Propellers

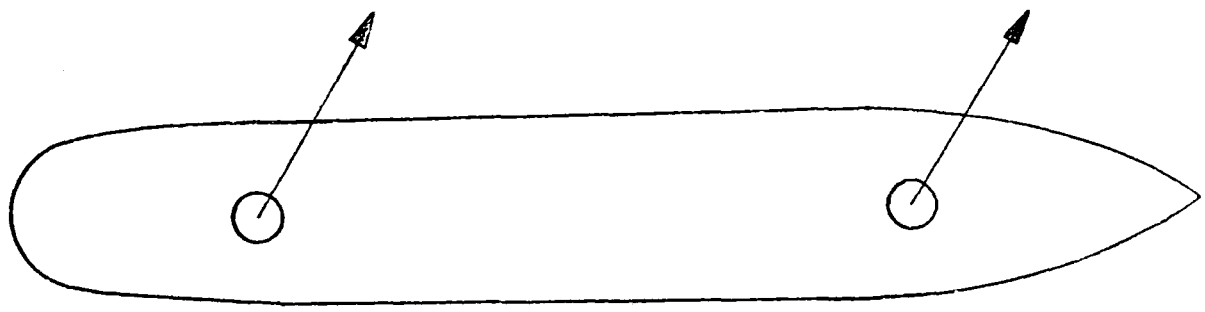

(b) Cycloidal Propellers

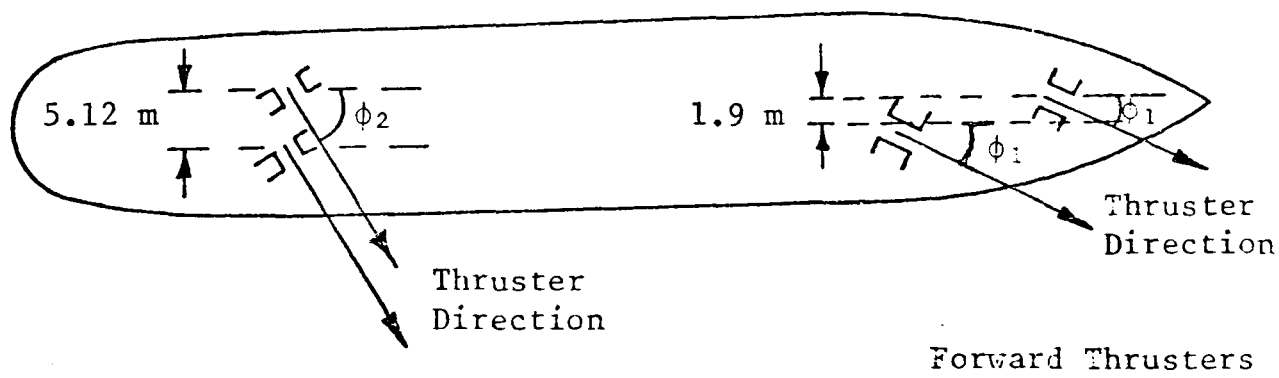

(c) Stearable Thruster

Figure (2.3): Possible Bow and Stern Thruster Configuration

November 1972. The vessel (Figure 2.4) was the first British owned dynamically positioned drillship, and it has been used for site investigation in addition to the drilling activities. "Wimpey Sealab" employs retractable a.c. motor driven thrusters with variable pitch propellers (Figure 2.5). The vessel has two rotatable bow and two rotatable stern thrusters (capable of 360^{o} rotation and each rated at 12.5 tonnes). The basic configurations of the thrusters are fully rotatable outboard propellers. Data from "Wimpey Sealab" were used as the basic information for the implementation of the dynamic positioning technique throughout this work (Chapter 3).

2.2.3 Thrusters used on "Star Hercules" vessel

"Star Hercules" vessel (Figure 2.6) is the other vessel to be considered in this work. Data from the "Star Hercules" have been obtained and used for design and simulation implementations.

The control thrust for the "Star Hercules" is provided by the main engine and by two forward and one aft tunnel thrusters. Thruster locations used on "Star Hercules" are shown in Figure 2.7 and have the following specifications:

The thrust producing device	Maximum thrust (tonne force)	Thruster lever arms relative to centre of gravity
Main Engine	28 (FWD) 19 (REV)	- -
FWD.FWD Thrusters	5.1	31.03 metres
AFT.FWD Thrusters	9.1	28.62 metres
AFT. Thrusters	5.1	28.62 metres

Figure (2.4) :Wimpey Sealab Vessel

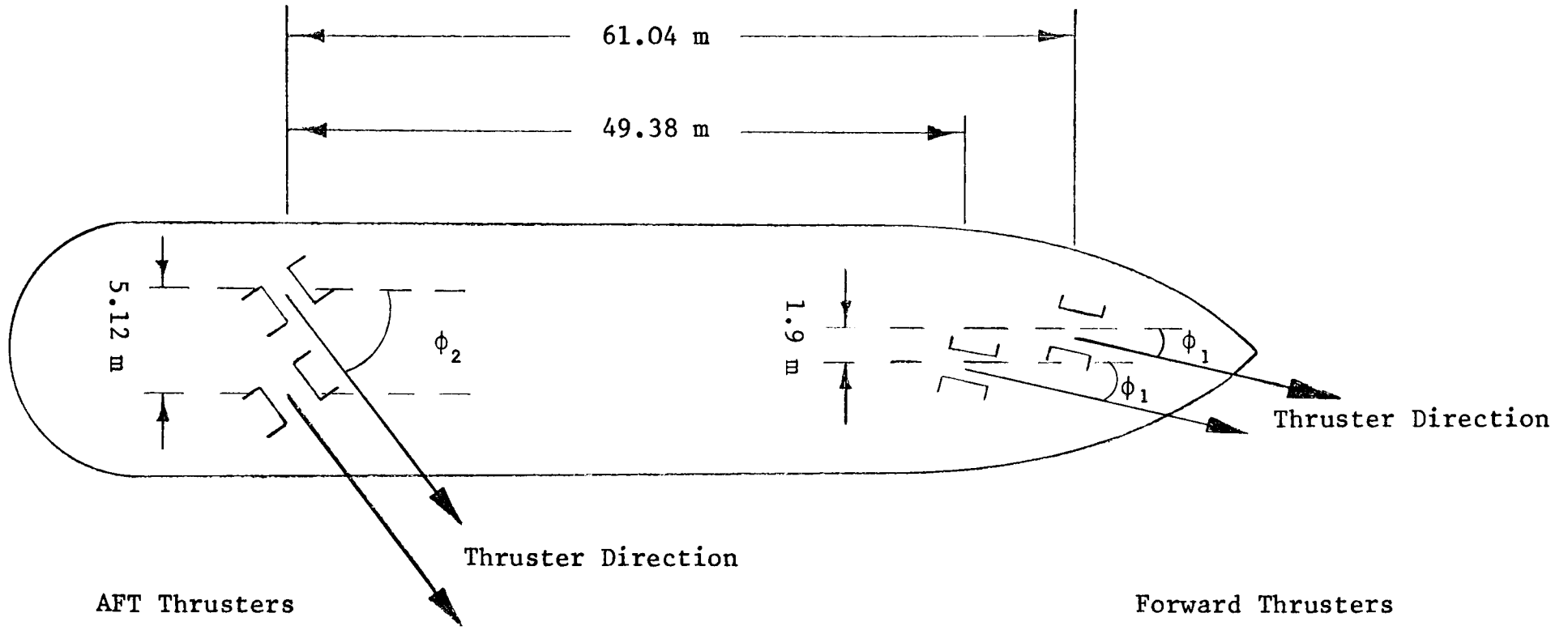

Figure (2.5): Steerable Thruster Configuration for Wimpey Sealab

Figure (2.6) :Star Hercules Vessel.

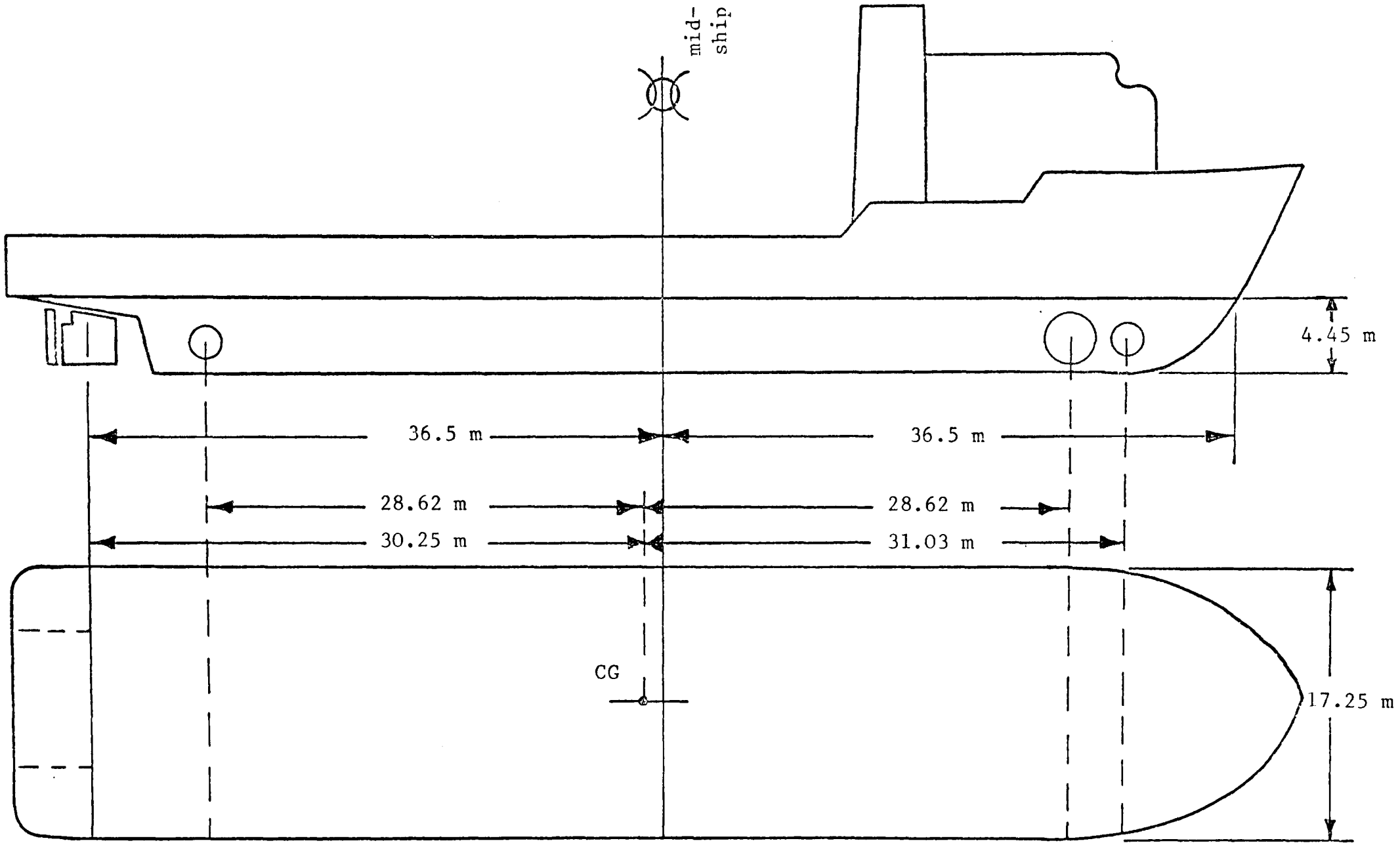

Figure (2.7): Outline Sketch of Star Hercules and its thrusters

2.2.4 Thrusters applied forces

The fore and aft thrusters on "Wimpey Sealab" act at angles ϕ_1 and ϕ_2 relative to the vessels coordinates respectively (Figure 2.5). Let the thrusters forces be f_1 and f_2 respectively for the fore and aft thrusters. Then the thrusters force in the surge direction is:

$$f_1 \cos \phi_1 + f_2 \cos \phi_2 \quad \ldots\ldots\ldots\ldots\ldots (2.1)$$

the total force in the sway direction is:

$$f_1 \sin \phi_1 + f_2 \sin \phi_2 \quad \ldots\ldots\ldots\ldots\ldots (2.2)$$

and the total force in the yaw direction is:

$$f_1 \ell_1 \sin \phi_1 - f_2 \ell_2 \sin \phi_2 \quad \ldots\ldots\ldots\ldots\ldots (2.3)$$

where $\ell_1 = \ell_2 = 10$ metres ("Wimpey Sealab"). Hence, the per-unit equations in a matrix form (Appendix 1) will be:

$$\begin{bmatrix} \text{surge force} \\ \text{sway force} \\ \text{yaw force} \end{bmatrix} = \begin{bmatrix} \cos \phi_1 & \cos \phi_2 \\ \sin \phi_1 & \sin \phi_2 \\ \frac{\ell_1}{\ell_b} \sin \phi_1 & -\frac{\ell_2}{\ell_b} \sin \phi_2 \end{bmatrix} \begin{bmatrix} \hat{f_1} \\ \hat{f_2} \end{bmatrix} \quad \ldots\ldots\ldots (2.4)$$

where:

$\hat{f_1}$, $\hat{f_2}$ are the per-unit values of f_1, f_2 respectively.

ℓ_b is the per-unit base length = 30 metres

$0 < \frac{\ell_1}{\ell_b} < 1$, $0 < \frac{\ell_2}{\ell_b} < 1$ and $\frac{\ell_1}{\ell_b} = \frac{\ell_2}{\ell_b} = \frac{1}{3}$

The matrix in equation (2.4) can be written in appropriate notation as:

$$\gamma = \begin{bmatrix} \gamma_{11} & \gamma_{12} \\ \gamma_{21} & \gamma_{22} \\ \gamma_{31} & \gamma_{32} \end{bmatrix} = \begin{bmatrix} \cos \phi_1 & \cos \phi_2 \\ \sin \phi_1 & \sin \phi_2 \\ \frac{\ell_1}{\ell_b} \sin \phi_1 & -\frac{\ell_2}{\ell_b} \sin \phi_2 \end{bmatrix} \quad \ldots\ldots\ldots\ldots (2.5)$$

2.3 Position and Heading Measurement Systems

Dynamic positioning system is basically the technique in which control signals can be applied to propellers and thrusters for specific action based on information concerning position and heading deviations from the pre-determined limits. In recent years the need for dynamic positioning has been increased by the problems associated with oil exploration and production. With these applications, accuracy will be one of the main requirements. Accuracy within dynamic positioning systems depends to some extent upon the reliability and availability of the information regarding position, heading and different wind and environmental forces as measured and fed into the system.

System inputs (Figure 2.2) could come from:

(i) wind sensor, measuring the wind speed and direction,

(ii) gyro compass, for heading measurements,

(iii) position measurements, which could be provided by one or more of the following techniques:

(a) hydroacoustic systems (with 122-305 m ideal depth of operation)

(b) radionavigation systems, and

(c) taut wire systems.

Due to the demand for accuracy within the dynamic positioning systems, the most commonly used technique for measuring the position (Figure 2.8) is based on an acoustic system where a beacon is deployed on the seabed and designed to transmit signals at a frequency around 20 KHz [15] at specific time intervals. The pulses transmitted by the beacon are received at an array of hydrophones fitted at the hull underneath the vessel, and the position of the vessel relative to the beacon is computed from the time differences in receiving the signal. These

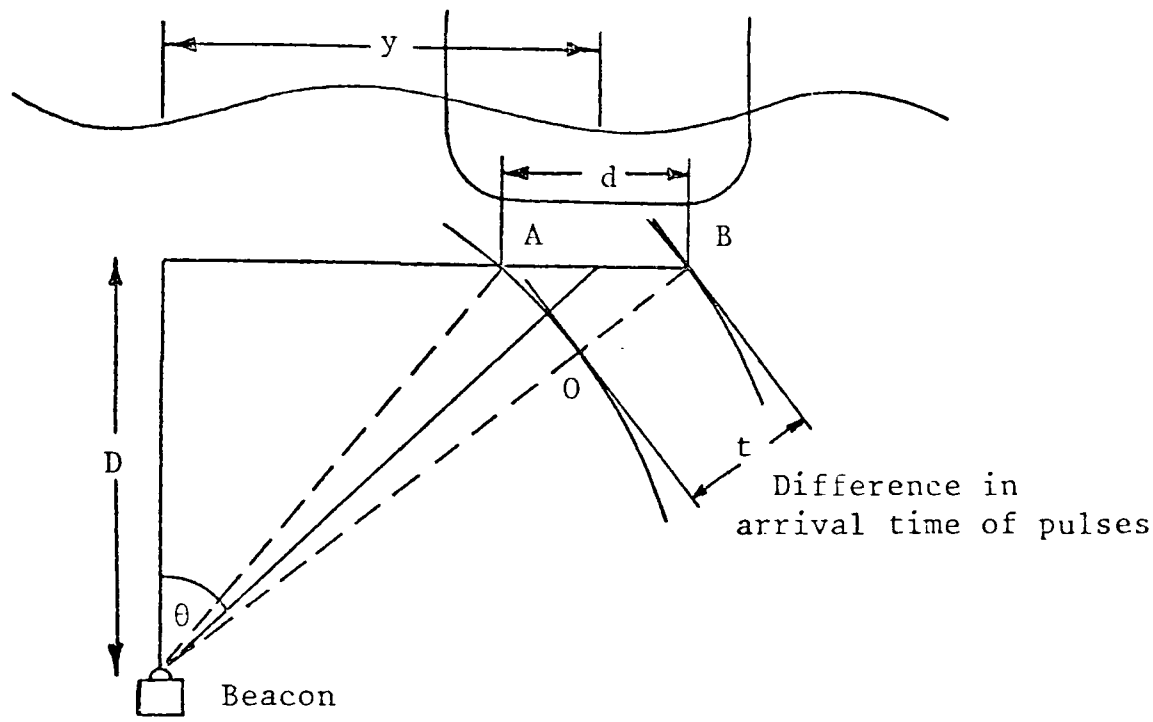

Figure (2.8): Simplified Two Dimensional Representation of the Acoustic System

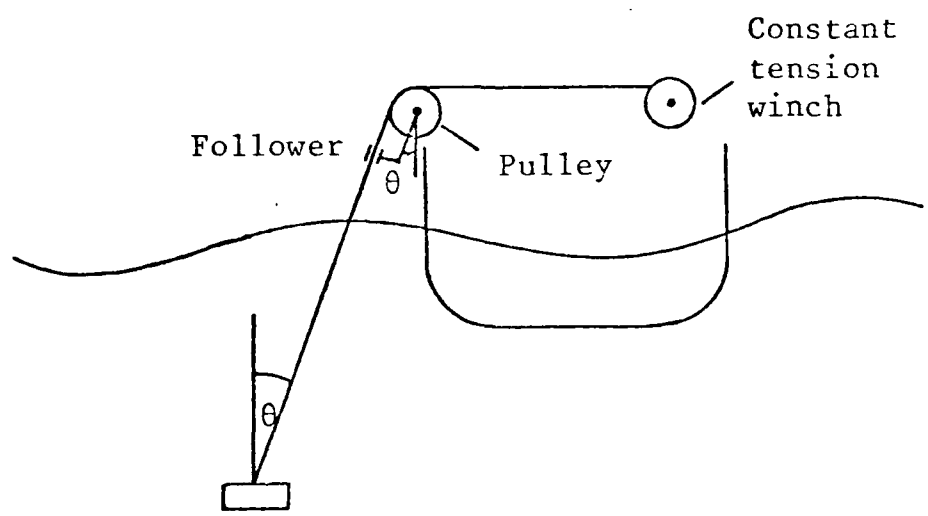

Figure (2.9): Simplified Diagram of the Taut-Wire System

position calculations are carried out by the on-board computer on the basis of the following formula:

$$y = D \tan (\sin^{-1} \frac{v\delta t}{d}) \simeq \frac{Dv\delta t}{d} \qquad \ldots\ldots\ldots\ldots (2.6)$$

where:

y	the displacement of the vessel
δt	the difference in the time of arrival of the pulses at two of the hydrophones set
v	the velocity of sound in water
D	the water depth
d	the separation between the two hydrophones

The great disadvantage with this technique in providing position reference deviations are the sensitivity to acoustic noise and air bubbles in the signal transmission line [16]. In addition to the accuracy requirement of the measurements, reliability and repeatability are also required. With the hydroacoustic system in operation alone, blocking of measurements in 20-40 per cent of the operation time may occur. To avoid the loss of the measurement signal, and to improve the reliability of the measurement systems, various back up systems can be used. The most commonly used system is the taut wire system shown in Figure 2.9, which consists of a sinker weight, wire, tensioning winch and inclinometer. The wire is maintained in tension by means of the constant-tension winch, which is also used to raise and lower the sinker weight when required. The measurement inaccuracy within the taut wire system may arise from the effect of the sea currents and the catenary effect on the wire due to its weight. Measurement systems developed by GEC and installed on "Wimpey Sealab" are to consist of one beacon and two sets of hydrophones using the computer to calculate the vessel position. These acoustic position measurement systems are backed by the

taut wire measuring system shown in Figure 2.10. The vessel heading measurements are obtained by the ship gyro compass.

As to the applications of dynamic ship positioning, considered in this work, the vessel position accuracy is about ±3 per cent of the water depth of 200 metres and ±2 per cent in 500 metres of water depth. The vessel positional accuracy can be defined by the following expression:

$$\text{Radial Error} = e_1.d + W/2 + e_2 \qquad \ldots\ldots\ldots (2.7)$$

where:

e_1 is the per unit error of the position measurement system

d is the water depth

W is the peak to peak wave motion

e_2 is the accuracy of the control loop

2.4 Process and Measurement Noise Analysis

The vessel motions under dynamic positioning control are assumed to consist of low and high frequency components. Our main concern in this section is the low-frequency part of the motions, which are assumed to be due to the current, wind and the second order wave forces (Section 3.2). The mean wind forcing level and the sea current speed and direction are all normally assumed constant over a period of time and up to several hours [74]. Like all environmental phenomena, wind has a stochastic nature which greatly depends on time and location. To compensate for such uncertain forces, the low-frequency part of the system dynamic is excited by random variables. These random variables are modelled as stationary zero mean and Gaussian white noise sequences. Stationarity of these sequences [87] can be pictured as the absence of any drift in the ensemble of realisations as time proceeds.

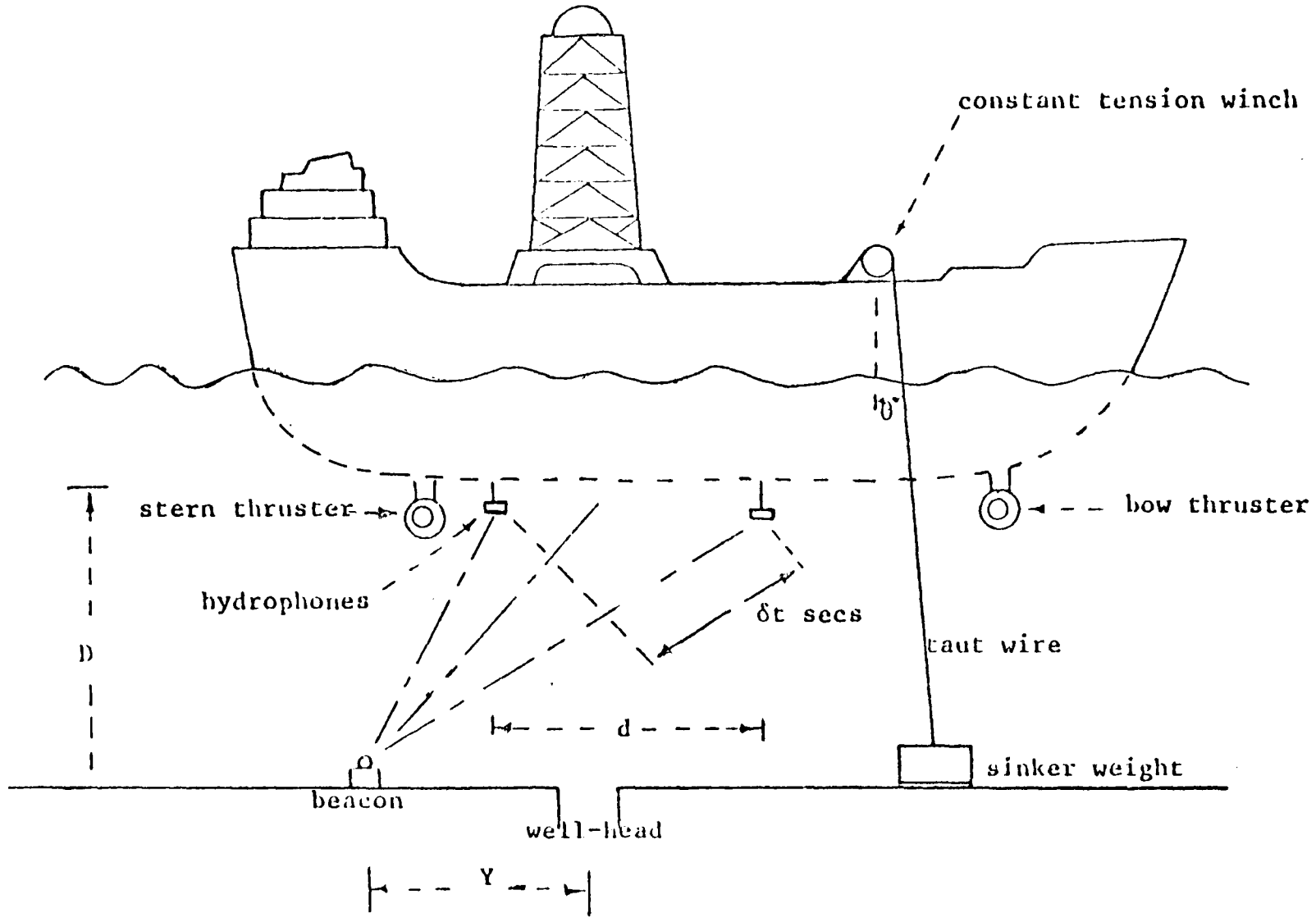

Figure (2.10) : Taut wire and Acoustic Position Measuring Systems used in Wimpey Sealab

Mathematically, this means that the probability distribution and density functions are unchanged over some specific period of time.

The wind forces are often the most important disturbance acting on the vessel. Wind feedforward control is often used to counteract the effect of steady wind (Figure 1.1) and hence, it will be assumed that the vessel positioning will be affected by a white component of wind only. The noise analysis can be extended to include the study of both process and observation noise, which in turn affect the system estimation for them causing the plant uncertainties.

2.4.1 The Process Noise

The process noise will be considered here in terms of their covariance matrices. The continuous or discrete time noise covariance matrices are related by the step length of the system simulations time interval (Δt), and hence the discrete process covariance matrix will be:

$$Q_D = \frac{Q}{\Delta t} \qquad \ldots\ldots\ldots\ldots\ldots (2.8)$$

where Δt is the step length time interval = 0.1 and Q_D is the discrete form of Q. The process covariance matrix (Q) is assumed to consist of a Q_ℓ submatrix corresponding to the low-frequency part of the system dynamics, and a Q_h submatrix corresponding to the high-frequency part of the dynamics.

The high-frequency submatrix in Q is determined by the least squares fitting procedure [34] and assumed to be unity (i.e. $Q_h = I$).

The low-frequency part of the system dynamics has a Q_ℓ matrix determined by the mean wind forcing level (in per-unit, see Appendix 1).

Hence, per-unit sway force = 126.8/55620 = 0.00228, and per-unit yaw torque = 1636/(55620 x 94.5) = 0.00031. Thus, for two degrees of freedom in sway and yaw, the low-frequency part of Q-matrix will be:

$$Q_{\ell} = \begin{bmatrix} (0.00228)^2 & 0.0 \\ 0.0 & (0.00031)^2 \end{bmatrix}$$

2.4.2 The Observation Noise

The observation or measurement noise and their related covariances will be examined here. The position measuring systems are always contaminated by superimposed noise and assumed to have a standard deviation $\sigma = 1/3$ metre. The per-unit position measurement noise covariance (Appendix 1) therefore will become:

$$\hat{\sigma} \text{ (sway)} = 0.0033 \text{ and } (\hat{\sigma})^2 = 0.1 \times 10^{-4}$$

The yaw angle standard deviation is assumed to be one degree, and hence

$$\hat{\sigma} \text{ (yaw)} = 0.02 \text{ radians in per-unit and } (\hat{\sigma})^2 = 4 \times 10^{-4}.$$

C H A P T E R (3)

CHAPTER 3

THE SHIP MOTION

3.1 Introduction

The motion of a ship induced by the waves is an oscillatory motion with frequencies equal to the wave frequencies [18]. At the same time the ship drifts off from its original position in the wave direction. Drift of the ship is also induced by the external environmental forces of wind and current. The current speed and direction may be constant over some period of time. Current speed and direction changes could occur but these changes are slow compared with fluctuations of wind speed and direction. The wind may be treated as a random Gaussian process (white Gaussian noise throughout the modelling and simulation). The ship motion is also induced by the wave forces which consist of a small drift second-order component and a very large first-order oscillatory component.

Depending on the type of the external acting forces the ship motion [3] is assumed to consist of a low-frequency component and a high-frequency component. The combined motion of the vessel due to both low and high frequency components [12] is indicated in Figure 3.1. The low-frequency motion in the range of 0.0 - 0.04 Hz (which is 0.0 - 0.251 rad/sec) is assumed to be induced by:

(i) forces generated by the thrusters and propellers,

(ii) hydrodynamic and interaction forces due to the ship motion relative to the water [25],

(iii) wind forces,

(iv) induced second-order wave forces.

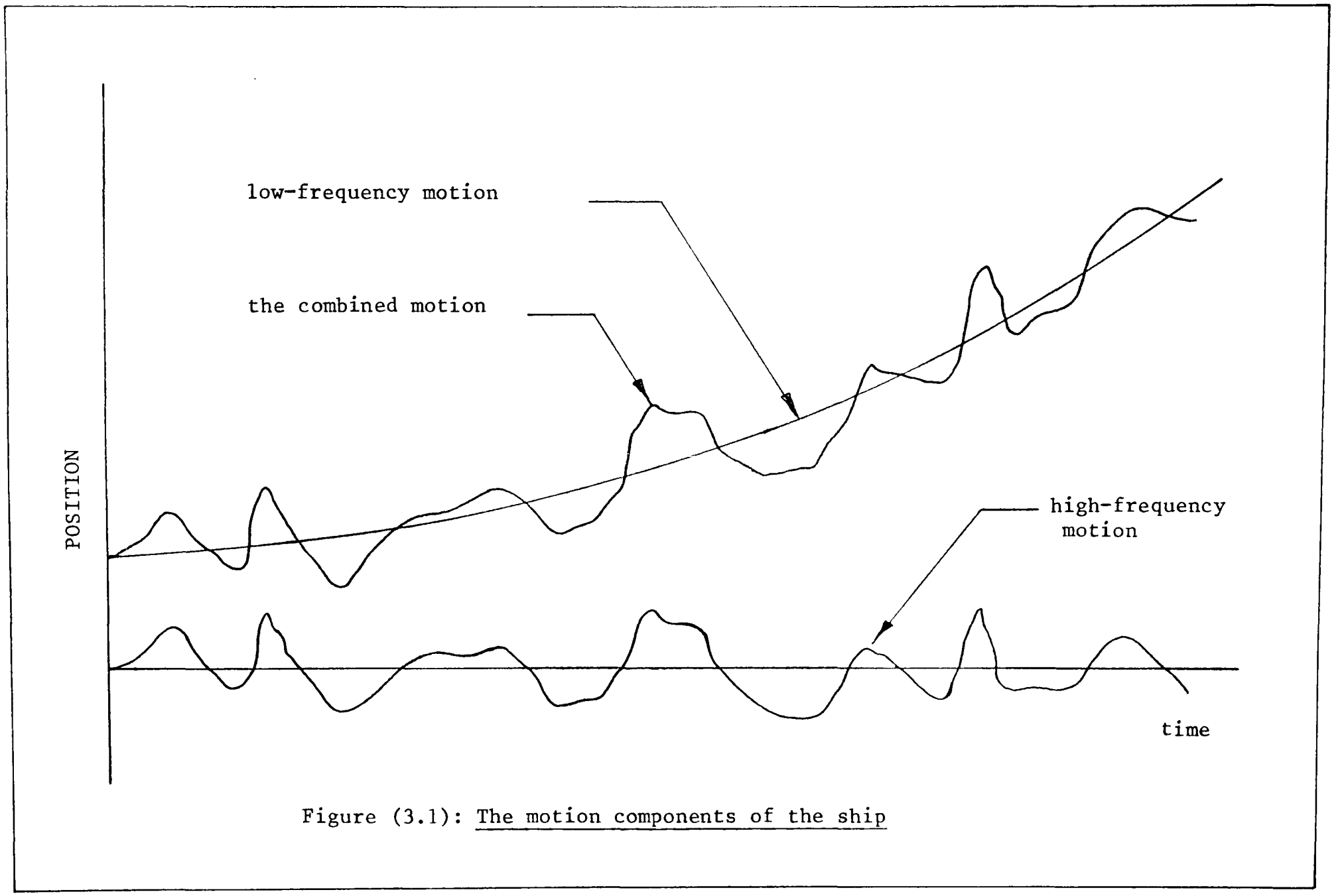

Figure (3.1): The motion components of the ship

The low-frequency motion will be the combination of the applied forces due to the thrust devices and due to the wind and waves. So that for one degree of freedom:

$$\text{Total force} = f_a + f_b \qquad \ldots\ldots\ldots\ldots\ldots (3.1)$$

where:

f_a represents the applied forces due to (i), (iii) and (iv) above.

f_b represents the hydrodynamic forces in (ii) above.

The high-frequency motions in the range 0.05 - 0.25 Hz (equivalent to 0.314 - 1.57 rad/sec depending on the actual sea spectrum) are assumed to be due to the first-order wave motions. These motions are of a very large level and cause the oscillatory motions of the vessel. These motions cannot be effectively counteracted because of the limited thrust of the propulsors. The basic assumption for the development of models of the vessel to correspond to the high-frequency motion is that the sea state is known and can be described by a spectral density function. The high-frequency wave motions are normally modelled using the Pierson-Moskowitz sea spectrum [51].

In the worst case the vessel motions are simply the Pierson-Moskowitz excitation since the vessel dynamics filter the sea wave spectrum.

In dynamic positioning, only the vessel motions in the horizontal plane (surge, sway and yaw) are controlled. Heave, roll and pitch motions (Figure 3.2a) are neglected. All motions will be referred to the body axes of the vessel (Figure 3.2b).

Surge motion has only a minor effect upon the directional stability of the ship. Sway motion mainly occurs due to the imbalance of wind and tidal forces acting upon the vessel. Yawing is induced by orbital

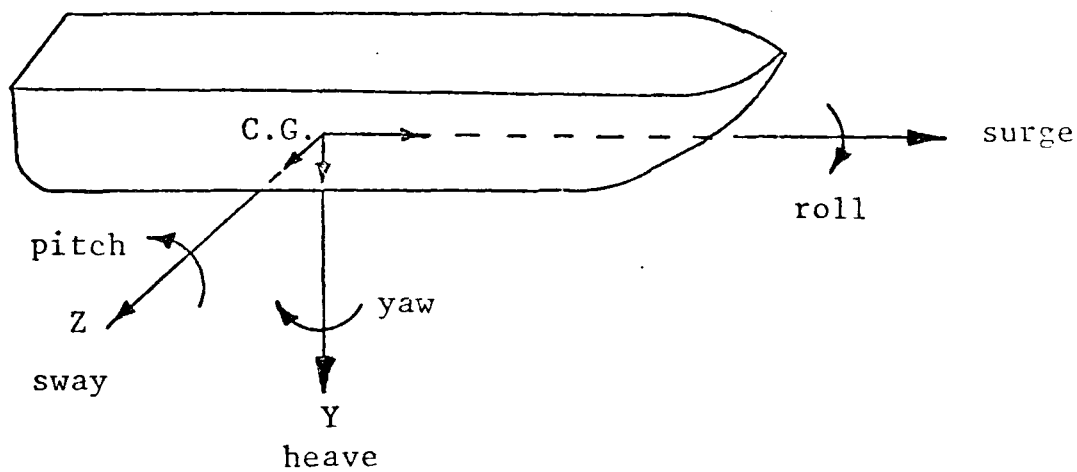

Figure (3.2) (a): Cartesian Coordinate System

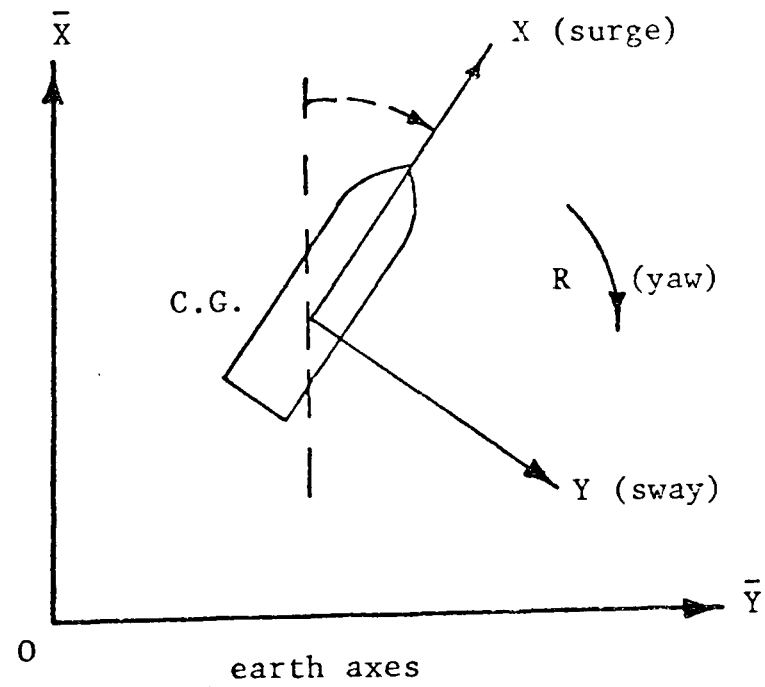

Figure (3.2) (b): Earth and Body Axes Coordinate System

motions of the water in the wave [73]. There is differential static pressure on the hull because of the shape and the gyroscopic couple due to the imposition of rolling motion on the pitching ship. Sway and yaw motions are normally associated with each other. To simplify the situation, the equations of motion of the vessel in sway and yaw only will be considered. This is possible because the linearised equations of motion indicate that surge motion can be assumed decoupled from the sway and yaw motions, and hence it can be considered and controlled separately.

3.2 Low-Frequency Dynamics

3.2.1 Introduction

A study of the dynamic positioning control of a vessel at sea requires the formulation of a set of equations which describe its dynamic behaviour under the forces imposed on it by the environment of wind, waves and current flow as well as by its own thrust producing devices [104][7]. These equations of motion which represent the vessel dynamics are assumed to involve a complex multiplicity of coefficients for reasonable accuracy and good modelling to be achieved. Such equations will be regarded as the basis of the whole modelling and simulation involving the position control scheme of the vessel. However, the need is apparent for a simplification of the set of equations which give a more realistic feel of the vessel dynamics.

For an efficient control scheme using Kalman filtering, a good mathematical model of the vessel dynamic is required. The reason for this is that the Kalman filter uses the model dynamics, together with some knowledge of the noise statistics, to generate the unbiased estimates of the system states. This assumption will introduce the need for some reasonable means of linearisation based on common practice,

and at the same time provide reasonable representation, good accuracy and simplicity.

The low-frequency part of the vessel dynamics should describe:

(i) the wind and wave forces,

(ii) the part of the vessel dynamic to be controlled,

(iii) the thruster dynamics, and

(iv) the interaction between the thrusters devices and the vessel dynamics.

The dynamic ship positioning system controls the low-frequency part of the ship motion in surge, sway and yaw. Treating the ship as a rigid body [104] having freedom of movement in surge, sway and yaw, but restricted in heave, pitch and roll. These movements are taken with respect to the body axes (Figure 3.2b). The vessel dynamics are represented by a set of non-linear differential equations, then linearisation procedure has to be applied to these equations for control purpose. The linearised form of the ship equations have the following differential state equation form:

$$\dot{\underline{x}}_\ell = A_\ell \underline{x}_\ell + B_\ell \underline{u}_\ell + D_\ell \underline{\omega}_\ell + E_\ell \underline{n}_\ell \qquad \ldots\ldots\ldots (3.2)$$

where:

$x_\ell(t) \in R^9$ are the system state vectors

$u_\ell(t) \in R^3$ are the control inputs to the thrusters

$\omega_\ell(t) \in R^3$ are white noise signals representing the random forces applied to the vessel

$n_\ell(t) \in R^3$ are the wind disturbance forces

A_ℓ is the system matrix

B_ℓ is the input matrix

D_ℓ and E_ℓ are the noise matrices.

Different parameters and coefficients of equation (3.2) above have been obtained from a set of tank and wind tunnel tests, carried out by the National Physical Laboratory on two different models, namely "Wimpey Sealab" and "Star Hercules". The obtained non-linear set of equations have to be linearised, time-scaled and converted into per-unit form, before it can be used in the control loop. Originally, these dynamic equations were provided by GEC Electrical Projects Limited, Rugby, and derived from first principles of Newton's laws of motion.

3.2.2 Derivation of the Low-Frequency Dynamics

The body axes are chosen to be the principle axes of the vessel for the derivation of the dynamic equations with its origin located at the centre of gravity (Figure 3.2b). For the position control of a vessel, interest is directly concerned with the motions in the horizontal plane of surge, sway and yaw (Figure 3.2a).

Regarding the vessel as a rigid body having freedom in surge, sway and yaw, but restricted in heave, roll and pitch, the equations of motion can simply be represented by [104] :

$$X = m(\dot{u} - rv) \qquad \ldots\ldots\ldots (3.3)$$

$$Y = m(\dot{v} + ru) \qquad \ldots\ldots\ldots (3.4)$$

$$N = I_{zz}\dot{r} \qquad \ldots\ldots\ldots (3.5)$$

The forces and moment acting on the vessel in equations (3.3) to (3.5), X, Y and N respectively can be considered as a sum of two components as shown in the following equations:

$$X_A + X_H = m(\dot{u} - rv) \qquad \ldots\ldots\ldots (3.6)$$

$$Y_A + Y_H = m(\dot{v} + ru) \qquad \ldots\ldots\ldots (3.7)$$

$$N_A + N_H = I_{zz}\dot{r} \qquad \ldots\ldots\ldots (3.8)$$

where X_A, Y_A and N_A represent the applied forces and moment due to the thrust-producing devices, and to the environment of wind and second-order wave drifts.

X_H, Y_H and N_H represent the hydrodynamic forces and moment due to relative motion between the vessel and the water. To determine the equations of motion, expressions for X_H, Y_H and N_H are required, appropriate to a vessel making small movements about a fixed reference position.

X_H, Y_H and N_H are assumed to be a function of the velocities and accelerations (u, v, r, $\dot{u}$, $\dot{v}$ and $\dot{r}$). It is assumed that the velocity and acceleration dependent forces can be separated. Acceleration dependent forces, referred to as added masses and added inertia are $X_{\dot{u}}$, $Y_{\dot{v}}$ and $N_{\dot{r}}$, which depend on the nature of the body motion and flow pattern.

m : mass of the vessel.

I_{zz} : radius of gyration.

The above equations in (3.6) to (3.8) can now be written as:

$$X_A + X_{\dot{u}}\dot{u} - Y_{\dot{v}}rv + X_H(u,v,r) = m(\dot{u} - rv) \quad \ldots\ldots\ldots (3.9)$$

$$Y_A + Y_{\dot{v}}\dot{v} + X_{\dot{u}}ru + Y_H(u,v,r) = m(\dot{v} + ru) \quad \ldots\ldots\ldots (3.10)$$

$$N_A + N_{\dot{r}}\dot{r} + N_H(u,v,r) = I_{zz}\dot{r} \quad \ldots\ldots\ldots (3.11)$$

Equations (3.9) to (3.11) can be rearranged into the following form:

$$(m - X_{\dot{u}})\dot{u} - (m - Y_{\dot{v}})rv = X_A + X_H(u,v,r) \quad \ldots\ldots\ldots (3.12)$$

$$(m - Y_{\dot{v}})\dot{v} + (m - X_{\dot{u}})ru = Y_A + Y_H(u,v,r) \quad \ldots\ldots\ldots (3.13)$$

$$(I_{zz} - N_{\dot{r}})\dot{r} = N_A + N_H(u,v,r) \quad \ldots\ldots\ldots (3.14)$$

These non-linear equations can be dimensioned using the appropriate base units, based on the specifications and dimension of the vessel under

consideration. The per-unit variables are shown by using a primed symbol, and are obtained using the following base units:

$$u' = \frac{u}{\sqrt{L_{pp}g}} \quad , \quad v' = \frac{v}{\sqrt{L_{pp}g}} \quad , \quad r' = \frac{r}{\sqrt{g/L_{pp}}}$$

$$\dot{u}' = \frac{\dot{u}}{g} \quad , \quad \dot{v}' = \frac{\dot{v}}{g} \quad , \quad \dot{r}' = \frac{\dot{r}}{g/L_{pp}}$$

$$X' = \frac{X}{mg} \quad , \quad Y' = \frac{Y}{mg} \quad , \quad N' = \frac{N}{mgL_{pp}}$$

$$t' = \frac{t}{\sqrt{L_{pp}/g}} \quad , \quad K'_{zz} = \frac{K_{zz}}{L_{pp}}$$

$$I_{zz} = m'(K'_{zz})^2 = (K'_{zz})^2$$

where:

L_{pp} is the length between the perpendiculars

g is the gravitational acceleration (= 9.81 m/sec^2)

K_{zz} is the radius of gyration in yaw (= 0.243)

The above per-unit system formulas are valid for a vessel with small fixed displacement, which is the case of the dynamic positioning problem.

3.2.3 Low-Frequency Equations for "Wimpey Sealab" Vessel

There are a variety of methods by which an estimation of the different coefficients in equations (3.12) to (3.14) can be achieved. These methods are mainly based on experimental results on a model of the vessel in tank tests, or on a theoretical basis using previous experimental evidence. An estimation of the coefficients for the drill ship "Wimpey Sealab" is obtained by a combination of results from tank tests and theory, performed at the National Physical Laboratory [104]. After reference to the base unit details of "Wimpey Sealab" in Appendix 1, the set of non-linear equations (3.12) to (3.14) can be expressed as:

$$(1 + 0.044)\dot{u}` - (1 + 0.84)r`v` = X_A` + 0.092(v`)^2 - 0.138u`U` \quad \ldots\ldots\ldots\ldots (3.15)$$

$$(1 + 0.84)\dot{v}` + (1 + 0.044)r`u` = Y_A` - 2.58v`U` - 1.84(v`)^3/U` + 0.068r`|r`| \quad \ldots\ldots\ldots\ldots (3.16)$$

$$((K_{zz}`)^2 + 0.0431)\dot{r}` = N_A` - 0.764u`v` + 0.258v`U` - 0.162r`|r`| \quad \ldots\ldots\ldots\ldots (3.17)$$

where:

$U` \equiv$ modulus of the vessel velocity (surge and sway) $= \sqrt{(u`)^2 + (v`)^2}$. The prime is used to denote the per-unit variable. Equations (3.15) to (3.17) above represent the vessel motions in surge, sway and yaw with respect to the vessel axes.

For the dynamic ship positioning system, the vessel deviations from its reference position are assumed relatively small, and hence a reasonable linearisation process can be applied to get a form of linear state equations for simulation and control. Previous experience with Notch filter designs [51],[99] suggests that a linear low-frequency model can be good enough for the design and control of the dynamic ship positioning system using a Kalman filtering scheme. The linear state equations can be obtained using Taylor expansions [65] and some useful approximation to the non-linear dynamics [104]. However, a number of linearised models could be obtained for different sea current and state of environment. The following linearised dynamics have been used which correspond to a Beaufort number 8 sea state with a mean wind velocity of 19 m/sec:

$$1.044\dot{u}` = X_A` - 0.01593u` \quad \ldots\ldots\ldots\ldots (3.18)$$

$$1.84\dot{v}` = Y_A` - 0.1004v` + 0.002981r` \quad \ldots\ldots\ldots\ldots (3.19)$$

$$0.1022\dot{r}` = N_A` - 0.007101r` + 0.005859v` \quad \ldots\ldots\ldots\ldots (3.20)$$

As a result of the little interaction between the surge and the sway and yaw motions within the above equations, simulation and control will be applied initially using the sway and yaw motions only and described by equations (3.19) and (3.20). Surge motion then can be simulated separately.

The low-frequency model for sway and yaw motions is to include the velocity, position and heading of the sway and yaw, as well as to represent the thruster dynamics. The thrusters have been modelled by simple first order lag terms with two seconds time constant real time. Referring to Section 2.2, Section 2.4 and Figure 3.3, the overall low-frequency dynamics for "Wimpey Sealab" can be represented by the following state space equation and its related details:

$$\dot{\underline{x}}_\ell = A_\ell \underline{x}_\ell + B_\ell \underline{u}_\ell + D_\ell \underline{\omega}_\ell + E_\ell n_\ell \qquad \ldots\ldots\ldots (3.21)$$

where:

$\underline{x}_\ell(t) \in R^6$ is the system state vectors in which,

$x_1(t) \equiv$ sway velocity

$x_2(t) \equiv$ sway position

$x_3(t) \equiv$ angular velocity

$x_4(t) \equiv$ yaw heading

$x_5(t)$, $x_6(t) \equiv$ thruster outputs

$\underline{u}_\ell(t) \in R^2$ are the control inputs

$\underline{\omega}_\ell(t) \in R^2$ and $\underline{n}_\ell(t) \in R^2$ are process and disturbance noise.

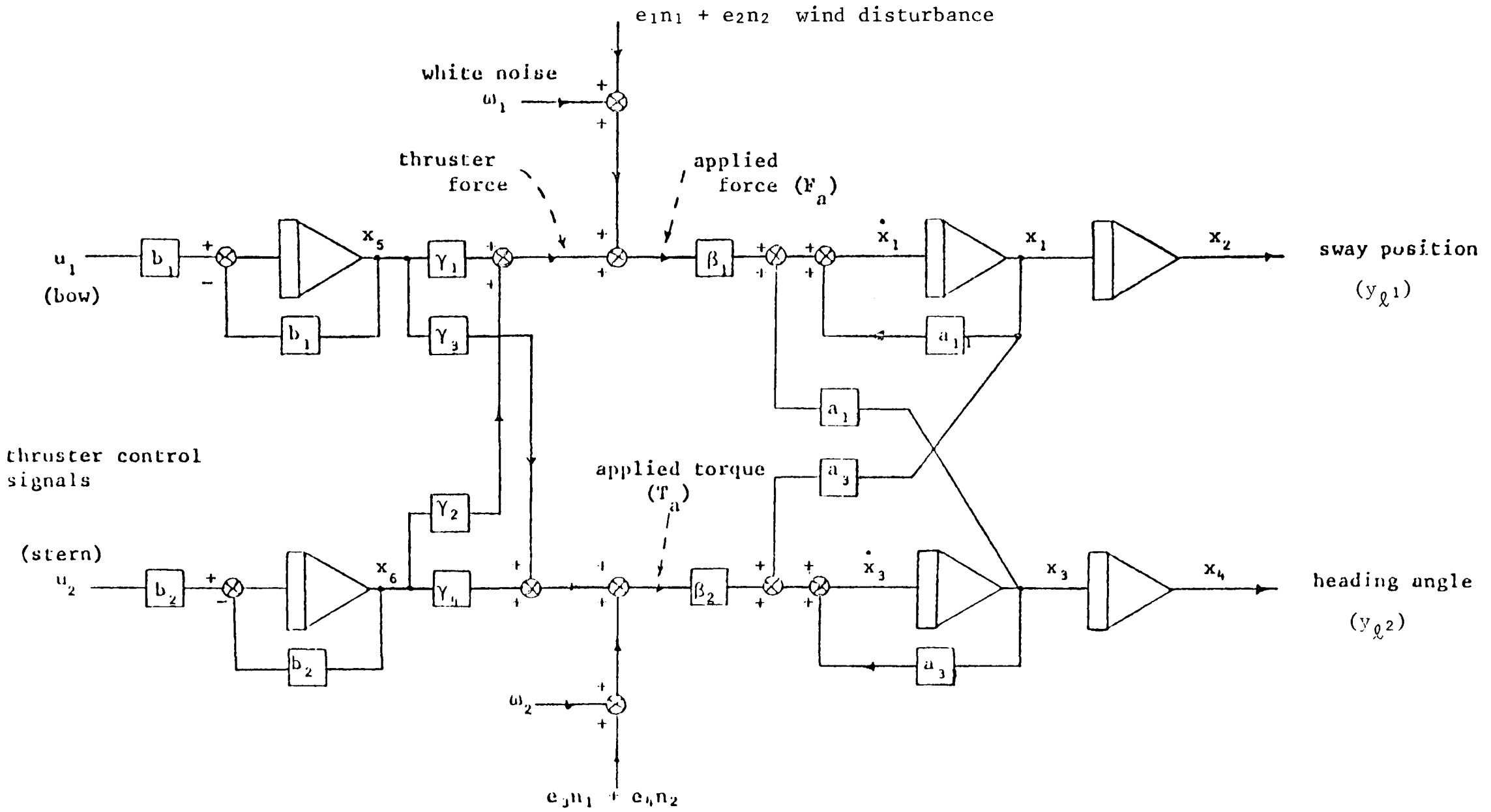

Figure 3.3: Low Frequency Model of a Vessel

With:

$$A_\ell = \begin{bmatrix} a_{11} & 0.0 & a_{13} & 0.0 & \gamma_1\beta_1 & \gamma_2\beta_1 \\ 1.0 & 0.0 & 0.0 & 0.0 & 0.0 & 0.0 \\ a_{31} & 0.0 & a_{33} & 0.0 & \gamma_3\beta_2 & \gamma_4\beta_2 \\ 0.0 & 0.0 & 1.0 & 0.0 & 0.0 & 0.0 \\ 0.0 & 0.0 & 0.0 & 0.0 & -b_1 & 0.0 \\ 0.0 & 0.0 & 0.0 & 0.0 & 0.0 & -b_2 \end{bmatrix}, \quad B_\ell = \begin{bmatrix} 0.0 & 0.0 \\ 0.0 & 0.0 \\ 0.0 & 0.0 \\ 0.0 & 0.0 \\ b_1 & 0.0 \\ 0.0 & b_2 \end{bmatrix}$$

$$D_\ell^T = \begin{bmatrix} \beta_1 & 0.0 & 0.0 & 0.0 & 0.0 & 0.0 \\ 0.0 & 0.0 & \beta_2 & 0.0 & 0.0 & 0.0 \end{bmatrix}$$

$$E_\ell^T = \begin{bmatrix} e_1\beta_1 & 0.0 & e_3\beta_2 & 0.0 & 0.0 & 0.0 \\ e_2\beta_1 & 0.0 & e_4\beta_2 & 0.0 & 0.0 & 0.0 \end{bmatrix}$$

The low-frequency components of the position and heading is given by:

$$\underline{y}_\ell = \begin{bmatrix} \underline{y}_{\ell 1} \\ \underline{y}_{\ell_2} \end{bmatrix} = C_\ell \underline{x}_\ell \qquad \ldots\ldots\ldots\ldots (3.22)$$

where:

$$C_\ell = \begin{bmatrix} 0.0 & 1.0 & 0.0 & 0.0 & 0.0 & 0.0 \\ 0.0 & 0.0 & 0.0 & 1.0 & 0.0 & 0.0 \end{bmatrix}$$

Substituting for the above different variables in terms of the respective approximated and calculated values, the following system matrices can be obtained:

$$A_\ell = \begin{bmatrix} -0.0546 & 0.0 & 0.0016 & 0.0 & 0.5435 & 0.272 \\ 1.0 & 0.0 & 0.0 & 0.0 & 0.0 & 0.0 \\ 0.0573 & 0.0 & -0.0695 & 0.0 & 3.268 & -1.634 \\ 0.0 & 0.0 & 1.0 & 0.0 & 0.0 & 0.0 \\ 0.0 & 0.0 & 0.0 & 0.0 & -1.55 & 0.0 \\ 0.0 & 0.0 & 0.0 & 0.0 & 0.0 & -1.55 \end{bmatrix} \qquad \ldots (3.23)$$

$$B_{\ell} = \begin{bmatrix} 0.0 & 0.0 & 0.0 & 0.0 & 1.55 & 0.0 \\ 0.0 & 0.0 & 0.0 & 0.0 & 0.0 & 1.55 \end{bmatrix} \quad \ldots\ldots (3.24)$$

$$D_{\ell} = \begin{bmatrix} 0.5435 & 0.0 & 0.0 & 0.0 & 0.0 & 0.0 \\ 0.0 & 0.0 & 9.785 & 0.0 & 0.0 & 0.0 \end{bmatrix} \quad \ldots\ldots (3.25)$$

$$E_{\ell} = \begin{bmatrix} 0.384 & 0.0 & 0.0 & 0.0 & 0.0 & 0.0 \\ 0.0 & 0.0 & 6.92 & 0.0 & 0.0 & 0.0 \end{bmatrix} \quad \ldots\ldots (3.26)$$

The above linearised equations have been time-scaled with 3.104 as the time normalisation factor for "Wimpey Sealab" vessel (Appendix 1).

3.2.4 Low-Frequency Dynamics of "Star Hercules" Vessel

Using the step by step procedures outlined in Section 3.2.3 above, the linearised equations of motion for the three degrees of freedom, (surge, sway and yaw), based on per-unit data from the "Star Hercules" (Appendix 1) are:

$$1.033\dot{u}` = X_A` - 0.01088u` \quad \ldots\ldots (3.27)$$

$$1.709\dot{v}` = Y_A` - 0.03307v` + 0.00221r` \quad \ldots\ldots (3.28)$$

$$0.1042\dot{r}` = N_A` - 0.003272r` + 0.004344v` \quad \ldots\ldots (3.29)$$

Taking a time normalisation factor of 2.728 and considering sway and yaw motions for simulation and control, different elements of the system matrix will be:

a_{11} = -0.03307/1.709 = -0.01935 per-unit

a_{13} = 0.002210/1.709 = 0.00129

a_{15} = 1.0/1.709 = 0.585

a_{31} = 0.004344/0.1042 = 0.04168

a_{33} = -0.003272/0.1042 = -0.0314

a_{36} = 1.0/0.1042 = 9.596

$$a_{55} = a_{66} = -1.364$$

Therefore the A-B-C matrices building up the low-frequency dynamics for "Star Hercules" will be:

$$A_\ell = \begin{bmatrix} -0.01935 & 0.0 & 0.00129 & 0.0 & 0.585 & 0.0 \\ 1.0 & 0.0 & 0.0 & 0.0 & 0.0 & 0.0 \\ 0.04168 & 0.0 & -0.0314 & 0.0 & 0.0 & 9.596 \\ 0.0 & 0.0 & 1.0 & 0.0 & 0.0 & 0.0 \\ 0.0 & 0.0 & 0.0 & 0.0 & -1.364 & 0.0 \\ 0.0 & 0.0 & 0.0 & 0.0 & 0.0 & -1.364 \end{bmatrix} \quad \ldots (3.30)$$

$$B_\ell^T = \begin{bmatrix} 0.0 & 0.0 & 0.0 & 0.0 & 1.364 & 0.0 \\ 0.0 & 0.0 & 0.0 & 0.0 & 0.0 & 1.364 \end{bmatrix} \quad \ldots (3.31)$$

$$C_\ell = \begin{bmatrix} 0.0 & 1.0 & 0.0 & 0.0 & 0.0 & 0.0 \\ 0.0 & 0.0 & 0.0 & 1.0 & 0.0 & 0.0 \end{bmatrix} \quad \ldots (3.32)$$

3.3 High-Frequency Dynamics

3.3.1 Introduction

Section 3.1 outlined a brief introduction to the high-frequency motion of the vessel. The high-frequency motions are the linear wave induced ship motions, which take place at the wave frequency. A mathematical model of the vessel for automatic control system implementation can only be made if the characteristics of all its components are known. Therefore, the high-frequency motions of the vessel have to be determined and fed into the system together with the low-frequency part of the vessel dynamics.

The automatic control system must be capable of avoiding high-frequency fluctuations since this may cause unnecessary wear of the thruster devices. Balchen, J G [12],[11] modelled the high-frequency part of the

ship dynamics using separate harmonic oscillators in each degree of freedom (surge, sway and yaw).

Since the frequency of the wave motion is time-variant and unknown, the dominant oscillator frequency must be estimated as a parameter in the state space equations [49]. For simplicity, all oscillators are assumed to be running with the same frequency and that will reduce the cost of simulation. The oscillator frequency can be estimated individually using an extended Kalman filter.

As an alternative to the above approach by Balchen, Grimble adopted a fundamental assumption for the development of models for the high-frequency motion of a vessel, in which the sea state is regarded as known and can be described by a spectral density function. An internationally accepted sea spectrum is similar to the Pierson-Moskowitz sea spectrum. The vessel dynamics act as a filter on the sea spectrum for different Beaufort sea states [17]. The worst case high-frequency motion of the vessel is determined by the Pierson-Moskowitz spectrum alone. Grimble's approach for estimating the unknown parameters within the high-frequency dynamics using extended Kalman filters will be considered in Chapter 7.

3.3.2 Development of the High-Frequency Model

The internationally accepted sea wave spectrum, which is similar to the Pierson-Moskowitz spectrum for a stationary wave system can be defined by the following sea spectrum:

$$S(\omega) = \frac{a}{\omega} e^{-b/\omega^4} \quad m^2 sec \qquad \ldots\ldots\ldots (3.33)$$

where

ω is the frequency in rad/sec

$$a = 4.894$$

$$b = 3.109\ (h_{1/3})^2$$

$h_{1/3}$ is the significant wave height in metres, which is defined by taking 99 waves, choosing the 33 largest waves and then calculating the mean of one third of the peak to peak magnitude of these waves.

The above sea spectrum can be obtained by passing a white noise source into a rational transfer function [49]. Therefore, to fit the sea spectrum $S(\omega)$ above, consider:

$$S_o(\omega) = (|G(j\omega)|)^2 . A_o \qquad \ldots\ldots\ldots\ldots\ldots\ldots (3.34)$$

in which A_o is the white noise amplitude.
For a unit magnitude white noise,

$$S_o(\omega) = (|G(j\omega)|)^2 . 1 \qquad \ldots\ldots\ldots\ldots\ldots\ldots (3.35)$$

where:

$$G(s) = \frac{Ks^2}{(s^2 + \sigma_1 s + \omega_1^2)(s^2 + \sigma_2 s + \omega_2^2)} \qquad \ldots\ldots\ldots\ldots\ldots\ldots (3.36)$$

in which σ_1, σ_2, ω_1, ω_2 and K are constants for a given sea spectrum, and given in Appendix 2. These constants can be determined by minimising the integral of the squared error criterion:

$$J = \int_o^{\omega m} (S(\omega) - S_o(\omega))^2\ d\omega \qquad \ldots\ldots\ldots\ldots\ldots\ldots (3.37)$$

over a range of frequency from zero to ωm. The worst case high-frequency dynamic of a vessel can be represented by a white noise source input to the above transfer function G(s) in each degree of freedom. The state space representation of the high-frequency dynamic of the vessel in sway and yaw motions can be expressed in a companion form as:

$$\dot{\underline{x}}_h = A_h \underline{x}_h + D_h \underline{\omega}_h \qquad \ldots\ldots\ldots\ldots (3.38)$$

where:

$\underline{x}_h(t) \in R^4$ for each degree of freedom,

$$A_h = \begin{bmatrix} A_h^{s\omega} & 0.0 \\ 0.0 & A_h^{ya} \end{bmatrix}$$

$$D_h = \begin{bmatrix} D_h^{s\omega} & 0.0 \\ 0.0 & D_h^{ya} \end{bmatrix} \qquad \ldots\ldots\ldots\ldots (3.39)$$

The above sub-matrices $A_h^{s\omega}$ and A_h^{ya} in sway and yaw directions have the same structure of:

$$A_h^{s\omega} = A_h^{ya} = \begin{bmatrix} 0.0 & T_b & 0.0 & 0.0 \\ 0.0 & 0.0 & T_b & 0.0 \\ 0.0 & 0.0 & 0.0 & T_b \\ -\alpha_4 & -\alpha_3 & -\alpha_2 & -\alpha_1 \end{bmatrix}$$

and

$$D_h^{s\omega} = D_h^{ya} = \begin{bmatrix} 0.0 \\ 0.0 \\ 0.0 \\ k \end{bmatrix} \qquad \ldots\ldots\ldots\ldots (3.40)$$

where T_b = 3.104 sec for the "Wimpey Sealab" and = 2.728 for the "Star Hercules". The parameters α_1, α_2, α_3 and α_4 are constant for a given weather condition and a specific vessel as indicated in Appendix 2 for both the "Wimpey Sealab" and the "Star Hercules" vessels. The values displayed in both tables are to correspond to Beaufort number 5 (calm sea) to Beaufort number 9 (the worst weather condition) for the "Wimpey Sealab" and the corresponding Beaufort number 5 and number

8 for the "Star Hercules" vessel.

The high-frequency component of the position of the vessel is given by the following output equation:

$$\underline{y}_h = \begin{bmatrix} \underline{y}_{h1} \\ \underline{y}_{h2} \end{bmatrix} = C_h \underline{x}_h \qquad \text{..... (3.41)}$$

where:

$$C_h = \begin{bmatrix} 0.0 & 0.0 & 1.0 & 0.0 & 0.0 & 0.0 & 0.0 & 0.0 \\ 0.0 & 0.0 & 0.0 & 0.0 & 0.0 & 0.0 & 1.0 & 0.0 \end{bmatrix} \quad \text{....(3.42)}$$

C H A P T E R (4)

CHAPTER 4

THE STOCHASTIC OPTIMAL CONTROL PROBLEM

4.1 Introduction

Optimal control problem,have attracted and received a great deal of attention during recent years owing to an increasing demand for systems of high performance especially for industrial applications. A solution to the stochastic control problem [40],[42],[10],[27] is the next step in applying the optimal control theory to the multivariable industrial systems with noisy observations [43],[63],[90],[95].

The essential components of a control system are:

(i) the system dynamics of the plant to be controlled,

(ii) measurement systems, and

(iii) the controller, which is the heart of the control system, which compares the measured values to their desired values and adjusts the input variables to the plant.

There are two traditions in control, which may be classified as, classical, which is based on a transfer function representation of the system, and modern control theory which deals directly with the differential equations, representing the system dynamics and often uses optimisation theory. Throughout this work the state space differential equations procedure will be adopted to implement the controllers. One basic difficulty with these optimal controllers is that they are often impractical, if not physically impossible to implement. Typically, the feedback portion of the optimal control system is a function of all the states of the system [85]. This would be satisfactory provided that all the states were accessible [63],[8] or available for measurements. In this case

a straightforward solution to the optimal stochastic control problem using the system states for direct feedback control would be extremely difficult. However, [21],[51],[59], since the system is linear or linearised (non-linear systems control will be considered in Chapter 7), and the measurements are directly or indirectly available then a special form of the separation theorem can be used and the optimal stochastic controller calculations can be separated (Figure 4.1) into:

(i) a filter (Kalman filter in our case) to generate the conditional mean of the system states, and

(ii) a solution to the linear optimal control problem using the estimated states in (i) as true states of the system.

Hence, the separation theorem as applied to this specific problem can be defined as follows: "In linear/linearised systems with quadratic error criterion and subjected to Gaussian inputs, the optimal stochastic controller is synthesised by combining an optimal estimation (Kalman estimator) with a deterministic optimal control".

In the dynamic ship positioning problem the system is assumed to consist of a low-frequency part to be controlled and a high-frequency part to be attenuated using the filtering scheme. The dynamic positioning control systems use the state estimates corresponding to the low-frequency model in the Kalman filter for closed loop feedback control. If the filter is working efficiently the control system will only respond to the low-frequency position error signal and thus the thruster modulation will be minimised. Hence, the purpose of the on-board computer [104] is to input error signals of the ship position and operate on them to output thrust magnitude and direction commands to the thrusters, so that ship position and heading are maintained at their fixed reference values against the environmental disturbance. Thus, the

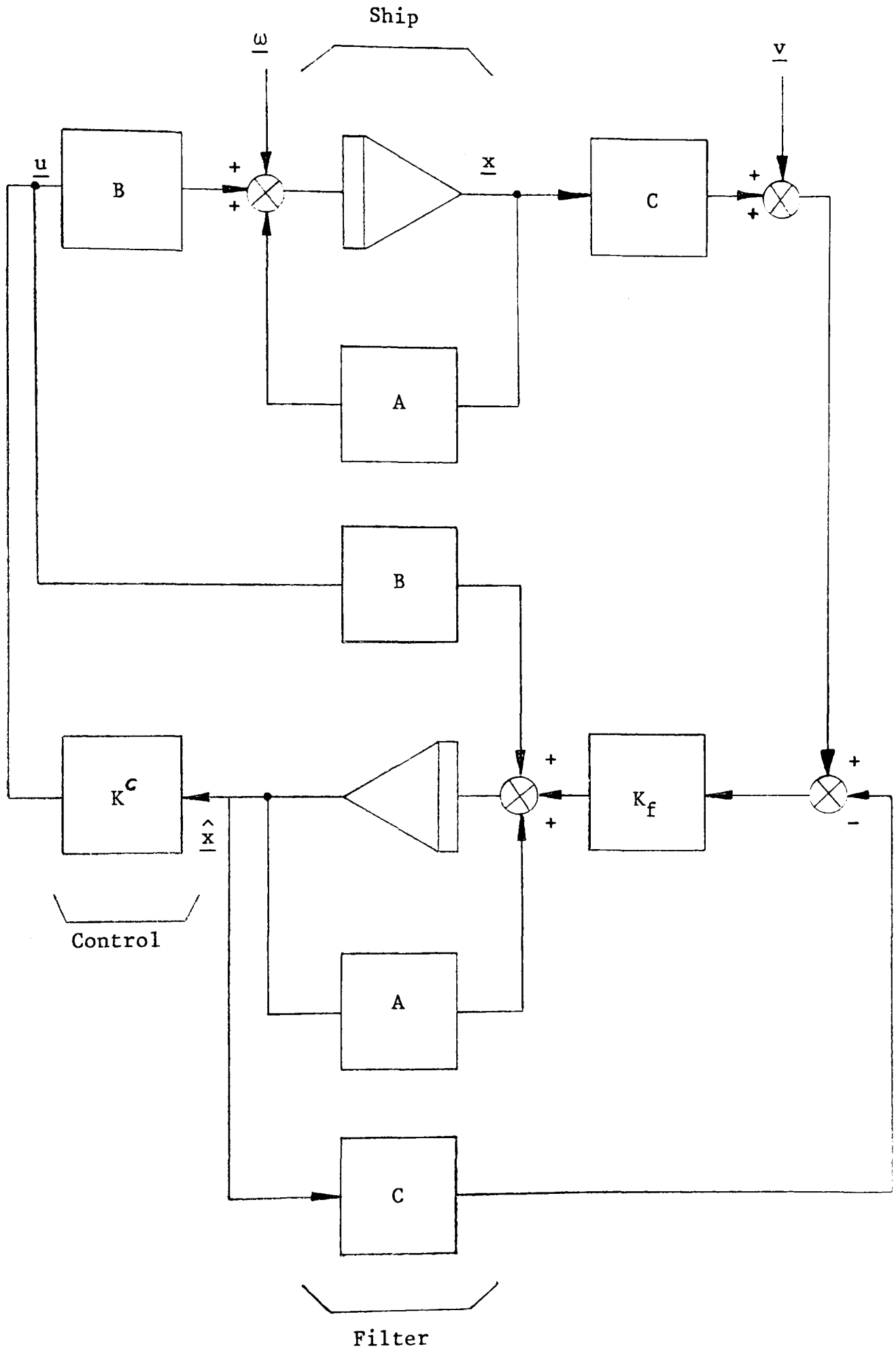

Figure (4.1): Filter and control using a form of the separation theorem

control system is mainly required to:

(i) maintain the vessel within the radial position error tolerance band (Table 2.1),

(ii) control the heading of the vessel (specially in the worst weather conditions), and

(iii) minimise thruster modulation and the consequence of energy losses.

In general, there are some difficulties in applying optimal control to multivariable industrial systems. Two problems are of relative importance to this work and were investigated in some detail. The first is concerned with the implementation of the optimal control algorithms (Section 4.2) and the second arises in the selection of the performance criterion weighting matrices Q and R (Section 4.3).

4.2 Control Algorithm

An optimal control algorithm for the stochastic multivariable system of the dynamic positioning problem is summarised in this section. The plant linearised state equations may be derived as:

$$\dot{\underline{x}}(t) = A\underline{x}(t) + B\underline{u}(t) + D\underline{\omega}(t) \quad \ldots\ldots\ldots (4.1)$$

$$\underline{z}(t) = C\underline{x}(t) + \underline{v}(t) \quad \ldots\ldots\ldots (4.2)$$

where:

$\underline{x}(t) \in R^n$ ($n = 6$ as system low-frequency states in sway and yaw)

$\underline{u}(t) \in R^m$ ($m = 2$)

$\underline{z}(t) \in R^r$ ($r = 2$) is the observations

$\underline{v}(t)$, $\underline{\omega}(t)$ are the uncorrelated additive measurement and process noise respectively.

The stochastic control strategy employing Kalman estimator can be assumed to include two procedures:

(i) Obtain the conditional mean estimate of the low-frequency part of the dynamics to be controlled, using a Kalman filter, and assume the estimates as truely representative of the system states for the state feedback loop.

(ii) Calculate the feedback control gain matrix by solving the deterministic control law [14],[28],[32],[41],[66].

The above assumptions in (i) and (ii) are often referred to as the separation theorem [21], which involves two separate problems of estimation and control (Figure 4.2) to solve the optimal stochastic control (Section 4.1).

In solving the above optimal control problem, some rules or measures need to be specified subject to certain constraints in order to minimise the deviations of the system behaviour from the ideal pre-selected ones. Such measures are usually provided by the optimisation of the performance criterion (index). The performance criterion is important because, to a large degree it determines the nature of the resulting optimal control through its cost weighting matrices Q, R. Details of the selection procedure of both Q and R are considered in Section (4.3).

The steady state performance criterion to be minimised may be defined as:

$$J(\underline{u}) = \lim_{T\to\infty} \frac{1}{2T} E \{ \int_{-T}^{T} \underline{x}^T(t).Q.\underline{x}(t) + \underline{u}^T(t).R.\underline{u}(t)dt \} \quad .... (4.3)$$

where $Q \geq 0$ and $R > 0$ are the positive semi-definite and positive definite weighting matrices respectively, while $\underline{x}^T(t)$ is the transpose of $\underline{x}(t)$. From the above separation principle, the optimal control signal can be found as:

$$\underline{u}^c(t) = -K^c\hat{\underline{x}}(t) \quad ..... (4.4)$$

where $\hat{\underline{x}}(t)$ are the best current conditional mean estimates of the system

SOLUTION OF STATE MEASURABLE PROBLEM GAIN MATRIX K^c:

SOLUTION OF KALMAN FILTERING PROBLEM GAIN MATRIX K_f:

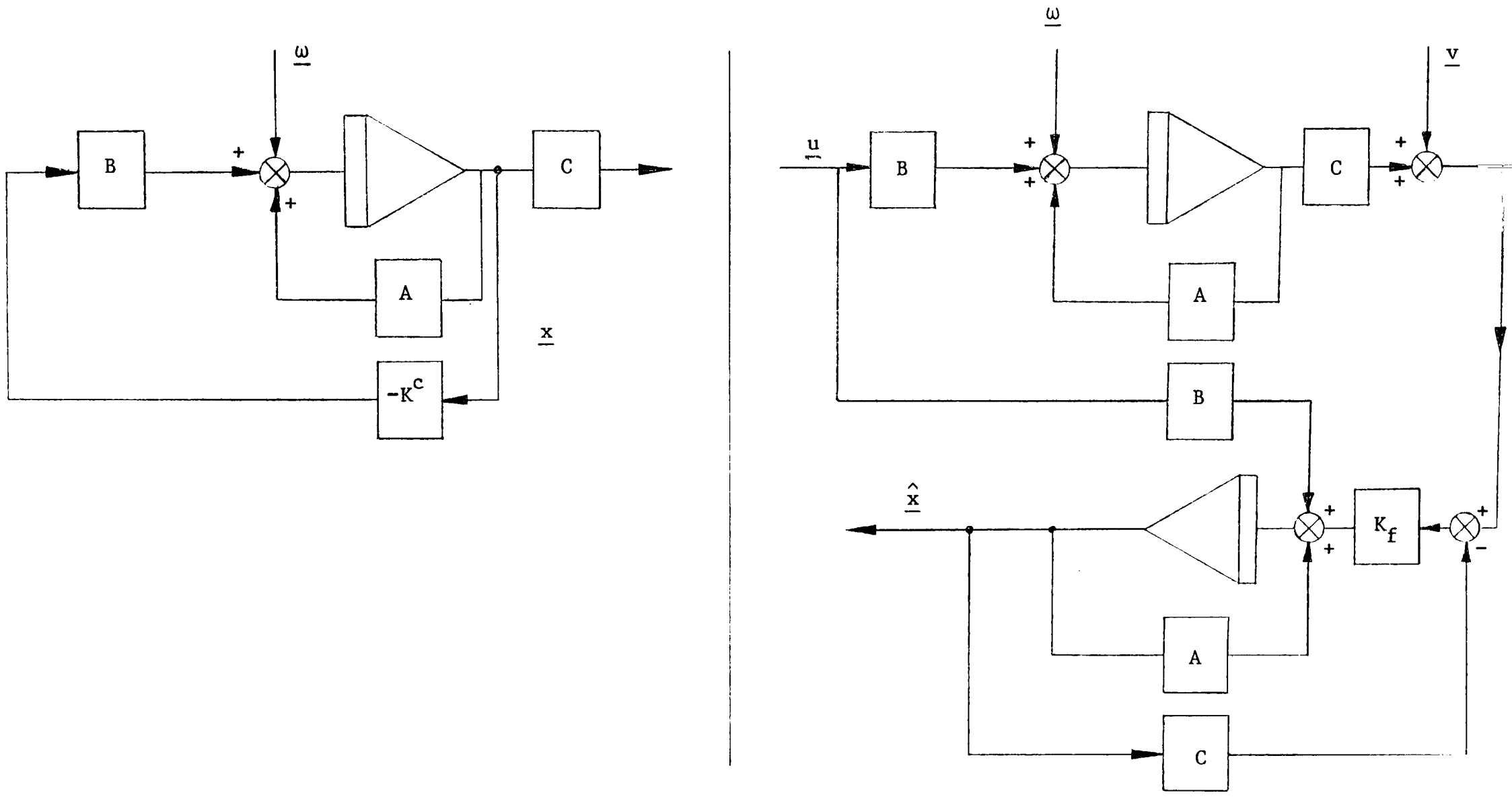

Figure (4.2): Combining the two problems of estimation and control

states $\underline{x}(t)$, and K^c is the optimal feedback gain matrix.

In dynamic ship positioning,control is not needed for the high-frequency subsystem, and hence the overall gain matrix of the feedback control loop will have the following form:

$$K^c = [\, K^{c\ell} \quad 0 \,] \qquad \ldots\ldots\ldots\ldots\ldots (4.5)$$

and the corresponding control signal will be:

$$\underline{u}^c(t) = [\, K^c \qquad 0 \,] \begin{bmatrix} \hat{\underline{x}}_\ell(t) \\ \hat{\underline{x}}_h(t) \end{bmatrix} \qquad \ldots\ldots\ldots\ldots\ldots (4.6)$$

where $\hat{\underline{x}}_h(t)$ are the high-frequency system state estimates. The gain matrix $K^{c\ell}$ may now be calculated by solving the steady state Riccati equation [70]:

$$0 = A_\ell^T P_{\ell\infty} + P_{\ell\infty} A_\ell - P_{\ell\infty} B_\ell R^{-1} B_\ell^T P_{\ell\infty} + Q \qquad \ldots\ldots\ldots\ldots\ldots (4.7)$$

and

$$K^{c\ell} = R^{-1} B_\ell^T P_{\ell\infty} \qquad \ldots\ldots\ldots\ldots\ldots (4.8)$$

Subscript (ℓ) is used to refer to the low-frequency subsystem, while subscript (∞) denotes the steady state solution of the matrix Riccati equation. A_ℓ and B_ℓ of equation (4.7) are the low-frequency plant system and input matrices respectively. $P_{\ell\infty}$ is the steady state solution of the matrix Riccati equation corresponding to the low-frequency part of the system dynamics to be controlled.

The solution of the above Riccati equation can be obtained by a number of methods [14],[62],[77],[81]. The solution to the steady state or algebraic matrix Riccati equation used throughout this work is an extension to the work done by Grimble and Patton [49] and it has been using the eigenvector method of MacFarlane (1963) [70]. The method used is to

form the 2n x 2n matrix of:

$$W = \begin{bmatrix} A_\ell & B_\ell R^{-1} B_\ell^T \\ Q & -A_\ell^T \end{bmatrix} \qquad \ldots\ldots\ldots\ldots (4.9)$$

where n = 6 (the system dimension of the low-frequency part of the ship dynamics for sway and yaw motions). Now, compute eigenvalues and eigenvectors of the above matrix (W). The eigenvalues of this matrix are symmetrically disposed in the complex plane, and if the eigenvectors corresponding to the most stable eigenvalues with negative real parts are found, then the following (2n x n) eigenvectors matrix can be written as:

$$U = \begin{bmatrix} U1 \\ U2 \end{bmatrix} \qquad \ldots\ldots\ldots\ldots (4.10)$$

then the $P_{\ell\infty}$ - matrix can be found as:

$$P_{\ell\infty} = -U2.U1^{-1} \qquad \ldots\ldots\ldots\ldots (4.11)$$

where $P_{\ell\infty}$ is the solution of the steady state matrix Riccati equation. The feedback gain matrix ($K^{c\ell}$) can now be computed using equation (4.8).

4.3 Selection of the Performance Criterion Weighting Matrices

One of the main criticisms in dealing with the design of optimal controllers for industrial applications is concerned with the selection of the performance criterion weighting matrices Q and R. For some time there has been no neat method of selecting a suitable value for the Q and R weighting matrices and thus the designer must resort to trial and error procedures to achieve reasonable values of Q, R for improved performance of the system responses. An investigation and simulation work have been carried out [2] to help with the selection of the

weighting matrices Q, R for the control loop as applied to the dynamic ship positioning problem. These investigations were based on recent techniques developed by Grimble [39],[38] on the design of an optimal controller using multivariable root loci. The author contributed to the computer implementation of the technique and the applications of the technique to the dynamic ship positioning problem. Expressions are obtained below from which the performance criterion weighting matrices Q and R may be calculated.

Consider the optimal output regulating problem [39],[72] as applied to the following linear multivariable system:

$$\dot{\underline{x}}(t) = A\underline{x}(t) + B\underline{u}(t) \qquad \ldots\ldots\ldots\ldots\ldots (4.12)$$

$$\underline{y}(t) = C\underline{x}(t) \qquad \ldots\ldots\ldots\ldots\ldots (4.13)$$

with

$$\underline{x}(t) \in R^n$$

$$\underline{u}(t) \in R^m$$

$$\underline{y}(t) \in R^m$$

and the system (A,B,C) is assumed to be square, since additional plant outputs may be defined in (4.13) to square up the system. This action only affects the following performance criterion:

$$J(0,\infty) = \int_0^\infty \underline{y}^T(t) Qy\, \underline{y}(t) + \underline{u}^T(t)\, Ry\, \underline{u}(t)\, dt \qquad \ldots\ldots\ldots\ldots (4.14)$$

for zero cross-products matrix (i.e. no interaction between the input and the output of the system). Qy and Ry are the weighting matrices for the output regulator control loop [68]. Now a straightforward conversion can be performed on equation (4.14) to obtain the energy weighting Q, R for the state (estimated state) feedback control as applied to our dynamic positioning problem (R values will be as those of Ry).

$$\underline{y}(t) = C\underline{x}(t) \qquad \ldots\ldots\ldots\ldots\ldots\ldots \quad (4.15)$$

Substitute (4.15) in (4.14) with $\underline{y}^T(t) = C^T\underline{x}^T(t)$ and derive the weighting Q-matrix for the state feedback control case as:

$$Q = C^T Q_y C \qquad \ldots\ldots\ldots\ldots\ldots\ldots \quad (4.16)$$

Hence the values of Q and R matrices can be selected on the same principle as in Grimble [39], with the necessary above conversion for the state feedback loop.

$$Q = ((CBN)^T)^{-1}(CBN)^{-1} \qquad \ldots\ldots\ldots\ldots\ldots\ldots \quad (4.17)$$

$$R = (N^T)^{-1}\Lambda^{\infty} N^{-1} \qquad \ldots\ldots\ldots\ldots\ldots\ldots \quad (4.18)$$

where:

$$N = \left[\underline{v}_1^{\infty} , \underline{v}_2^{\infty} , \ldots\ldots \underline{v}_m^{\infty} \right]$$

and $\underline{v}_1^{\infty}$, $\underline{v}_2^{\infty}$, ... are the set of the system eigenvectors.

$$\Lambda^{\infty} \triangleq \text{diag}\{ \left(\frac{1}{\lambda_1^{\infty}}\right)^2 , \left(\frac{1}{\lambda_2^{\infty}}\right)^2 , \ldots, \left(\frac{1}{\lambda_m^{\infty}}\right)^2 \}$$

and λ_i (i = 1, 2,..., m) are the system eigenvalues.

The above expressions of equations (4.17) and (4.18) were derived for the case when CB is full rank, i.e.,

$$\text{rank } (CB) = m \quad \text{or} \quad |CB| \neq 0 \qquad \ldots\ldots\ldots\ldots\ldots\ldots \quad (4.19)$$

The case when CB is not full rank will be considered now as applied to the example of the dynamic positioning problem using the dynamics of the "Wimpey Sealab" vessel [3], [2]. In applying the above technique to this example (Section 3.2.3), the following have to be noted. The first Markov parameter ($C_\ell B_\ell$) is not full rank, the second Markov parameter ($C_\ell A_\ell B_\ell$) is not full rank either, but the third Markov parameter ($C_\ell A_\ell^2 B_\ell$) is full

rank, and thence

$$C_\ell A_\ell^2 B_\ell = \begin{bmatrix} 0.84243 & 0.4216 \\ 5.0654 & -2.5327 \end{bmatrix}$$

$\det.(C_\ell A_\ell^2 B_\ell) = -4.2692.$

where A_ℓ, B_ℓ, C_ℓ are the low-frequency part of the ship system, input and output matrices based on data from the "Wimpey Sealab" vessel (Section 3.2.3).

Expressions for Q and R from equations (4.17) and (4.18) can be repeated to obtain:

$$Q = ((C_\ell A_\ell^2 B_\ell N)^T)^{-1}(C_\ell A_\ell^2 B_\ell N)^{-1} \quad \ldots\ldots\ldots\ldots (4.20)$$

$$R = \rho\left[(N^T)^{-1}.\Lambda_3^\infty.N^{-1}\right] \quad \ldots\ldots\ldots\ldots (4.21)$$

where ρ is a positive real scalar which affects the values of the control energy R-weighting matrix to shape the system responses.

$$\Lambda_3^\infty \equiv \text{diag}\{\frac{1}{(\lambda_1^\infty)^6}, \frac{1}{(\lambda_2^\infty)^6}, \ldots, \frac{1}{(\lambda_m^\infty)^6}\}$$

In a more general case where the first (k) Markov parameters are zero ($|CB| = 0, |CAB| = 0, \ldots, |CA^{k-1}B| = 0$), and (CA^kB) is full rank, the expressions of equations (4.20) and (4.21) become:

$$Q = ((CA^kBN)^T)^{-1}(CA^kBN)^{-1} \quad \ldots\ldots\ldots\ldots (4.22)$$

$$R = \rho\left[(N^T)^{-1}.\Lambda_{k+1}^\infty.N^{-1}\right] \quad \ldots\ldots\ldots\ldots (4.23)$$

where

$$\Lambda_{k+1}^\infty \equiv (-1)^k \text{diag}\{(\frac{1}{\lambda_1^\infty})^{2(k+1)}, \ldots, (\frac{1}{\lambda_m^\infty})^{2(k+1)}\}$$

Using equations (4.20) and (4.21) above for Q and R, different

combinations of Q and R values have been selected and system simulations for different cases were investigated based on data from the "Wimpey Sealab". These cases were summarised in the next section in which full simulation of the low-frequency part of the ship and calculation of the optimal feedback gain matrix were considered.

4.4 Simulations and Results

4.4.1 Case (a)

In this test, the control signal for the first input (sway motion) is 1.5 times faster than that of the second input (yaw motion), i.e.,

$\lambda_1^\infty = 1.5 \quad \lambda_2^\infty$, assume unity eigenvectors ($N = I_2$), and

$\lambda_2^\infty = 1$, then, $\lambda_1^\infty = 1.5$

$$\Lambda_3^\infty = \text{diag}\{(\frac{1}{\lambda_1^\infty})^6, (\frac{1}{\lambda_2^\infty})^6\}$$

$$= \text{diag}\{0.08799, 1.0\}$$

$$R = \rho\Lambda_3^\infty = \rho \begin{bmatrix} 0.08779 & 0.0 \\ 0.0 & 1.0 \end{bmatrix}$$

$$Q = \begin{bmatrix} 0.0 & 0.0 & 0.0 & 0.0 & 0.0 & 0.0 \\ 0.0 & 1.7597 & 0.0 & -0.17555 & 0.0 & 0.0 \\ 0.0 & 0.0 & 0.0 & 0.0 & 0.0 & 0.0 \\ 0.0 & -0.17555 & 0.0 & 0.0487 & 0.0 & 0.0 \\ 0.0 & 0.0 & 0.0 & 0.0 & 0.0 & 0.0 \\ 0.0 & 0.0 & 0.0 & 0.0 & 0.0 & 0.0 \end{bmatrix}$$

R- matrix for system simulations varies as ρ takes the following values for best response to be chosen.

$$\rho = \{10^{-4}, 10^{-3}, 1, 10, 10^3, 10^6\}$$

System responses of the low-frequency dynamics of the "Wimpey Sealab"

are shown in Figures 4.3a - d for $\rho = 10^{-3}$ and in Figure 4.4a - d for $\rho = 1.0$. Both system responses were presented here as the best responses of case (a) for a step input of 0.02 p.u. into sway. The optimal feedback gain matrices for both systems have been calculated, for $\rho = 10^{-3}$, as:

$$K^{c\ell} = \begin{bmatrix} -26.87 & -63.67 & -4.39 & -10.48 & -5.18 & -0.024 \\ -23.81 & -37.46 & -3.95 & 6.24 & -0.002 & -3.22 \end{bmatrix}$$

and for $\rho = 1.0$,

$$K^{c\ell} = \begin{bmatrix} -2.87 & -2.05 & -0.44 & -0.32 & -1.20 & -0.024 \\ -2.54 & -1.17 & 0.41 & 0.19 & -0.002 & -0.66 \end{bmatrix}$$

4.4.2 Case (b)

Throughout this test, the two inputs are non-interactive and required to be at the same speed. Hence choose $\lambda_1^\infty = \lambda_2^\infty = 1.0$. Let $N = I_2$ and the Q-matrix remains unchanged as from case (a).

$$R_1 = \text{diag}\{1.0 , 1.0\}$$

$$R_1 = \begin{bmatrix} 1.0 & 0.0 \\ 0.0 & 1.0 \end{bmatrix}$$

$$R = \rho R_1$$

The systems of the "Wimpey Sealab" have been simulated for different values of ρ,

$$\rho = \{10^{-6}, 10^{-5}, 10^{-4}, 10^{-3}, 1.0, 10\}$$

and the responses for a step input of 0.02 p.u. into sway are presented here in Figures 4.5a - d for the case when $\rho = 1.0$. The optimal feedback gain matrix $K^{c\ell}$ for this case is:

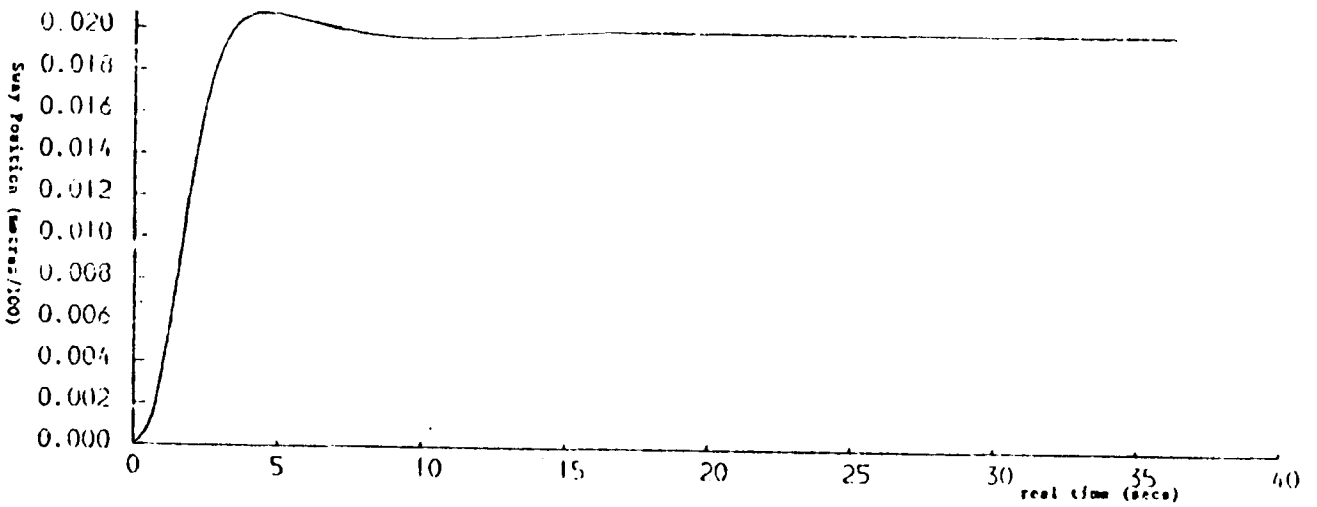

a- Sway Output Signal for case (a), $\rho = 10^{-1}$

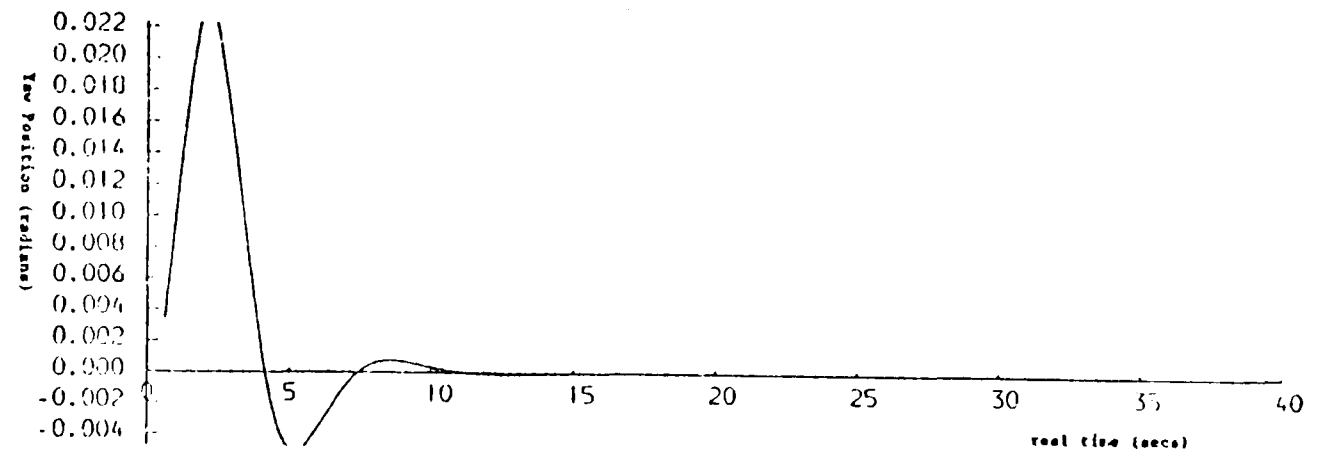

b- Yaw Output Signal for case (a), $\rho = 10^{-1}$

Figures(4.3-a,b) :Output signals for step into sway (Wimpey Sealab)

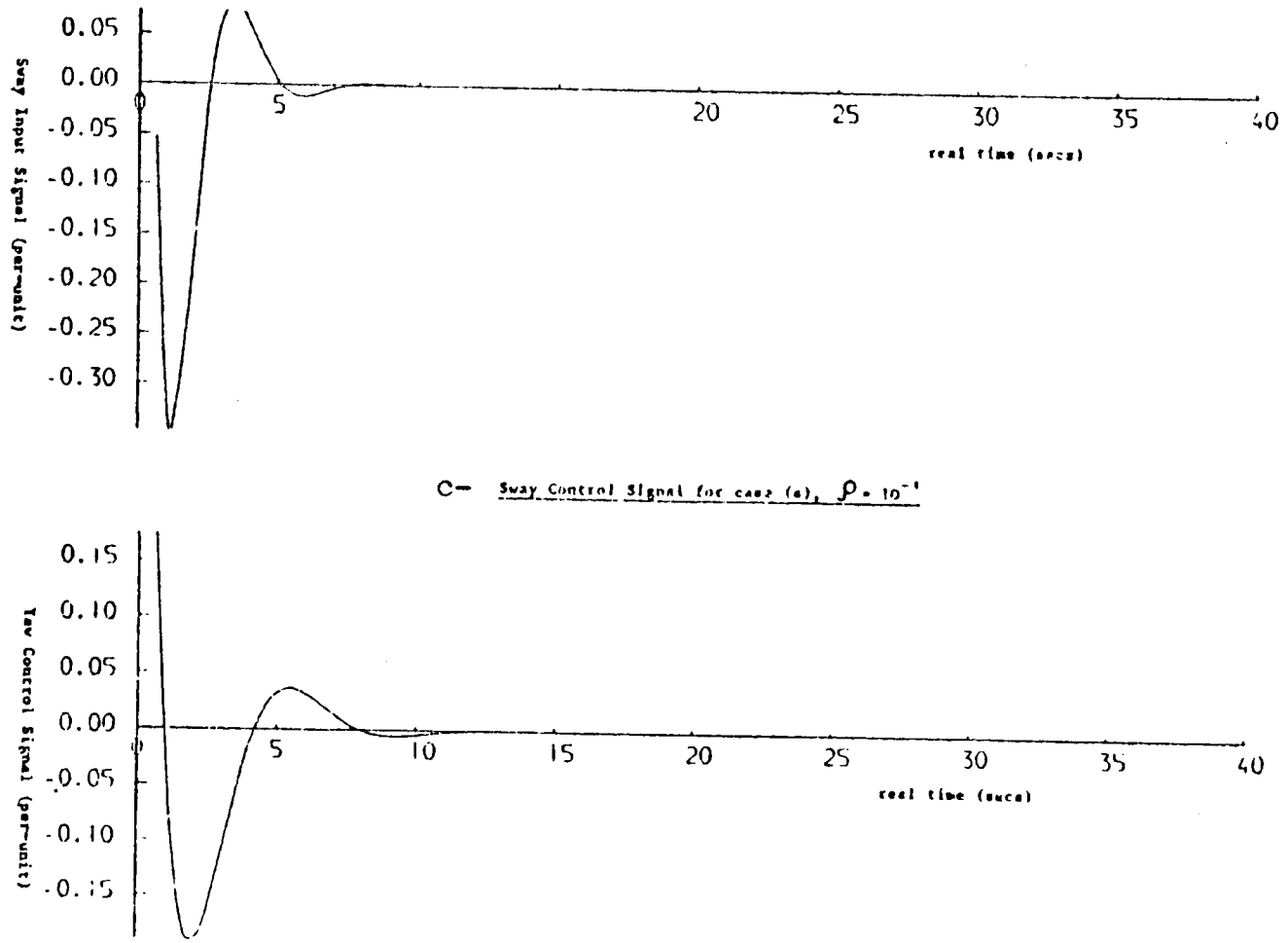

c- Sway Control Signal for case (a), $\rho = 10^{-1}$

d- Yaw Control Signal for case (a), $\rho = 10^{-1}$

Figures(4.3-c,d) :Control signals for step into sway (Wimpey Sealab)

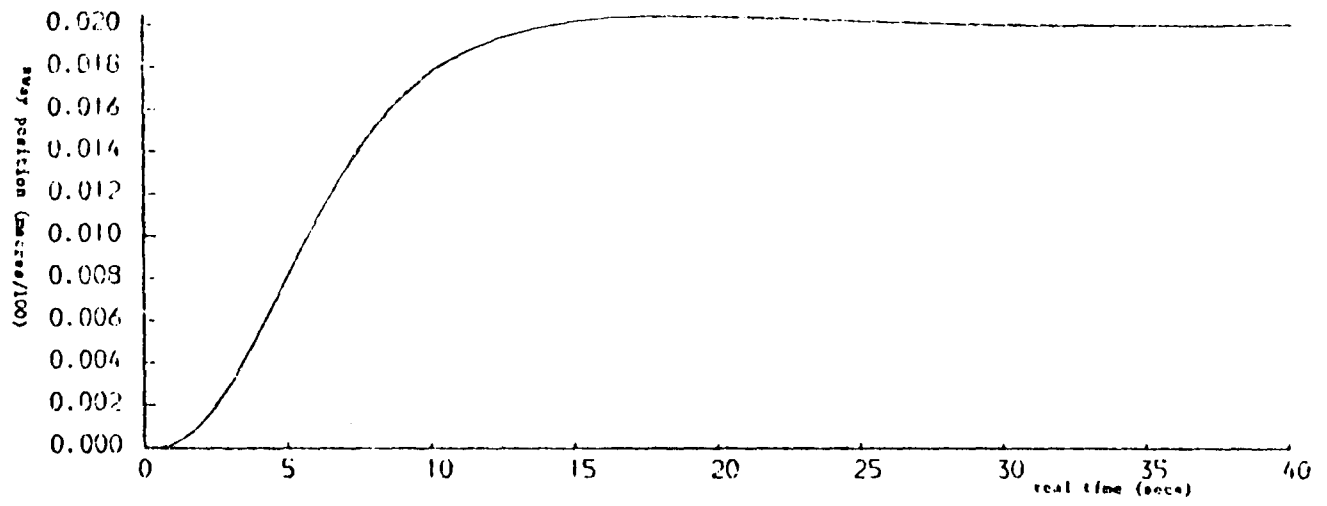

a- Sway Output Signal for case (a), ρ = 1

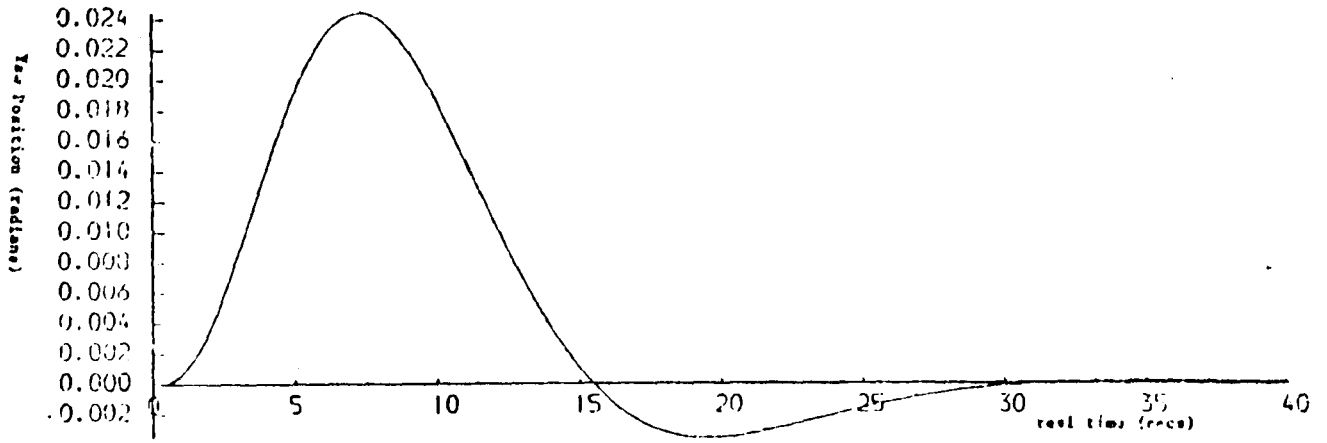

b- Yaw Output Signal for case (a), ρ = 1

Figures(4.4-a,b) :Output signals for step into sway (Wimpey Sealab)

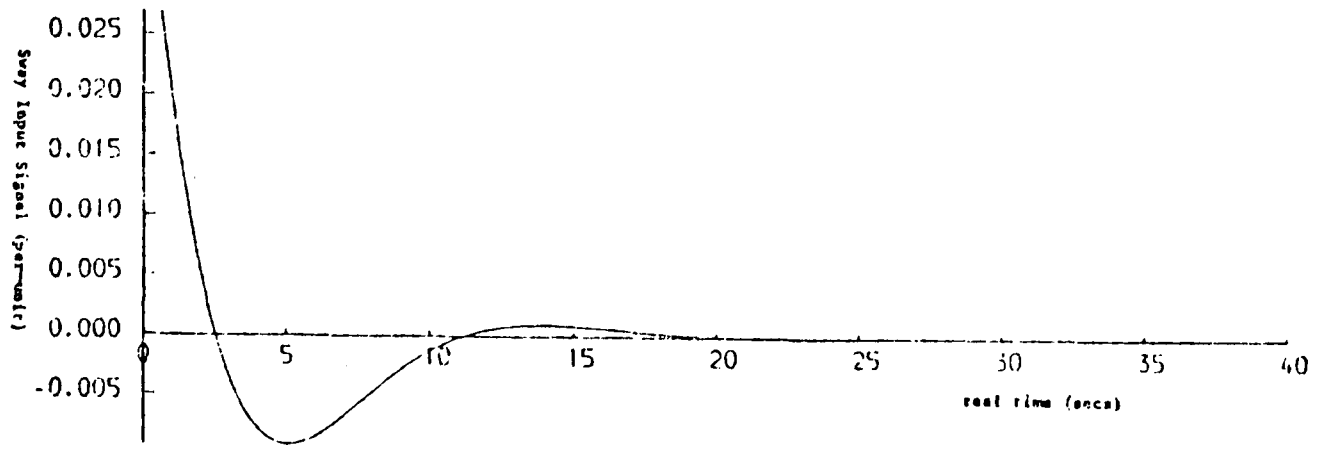

C— Sway Control Signal for case (a), ρ = 1

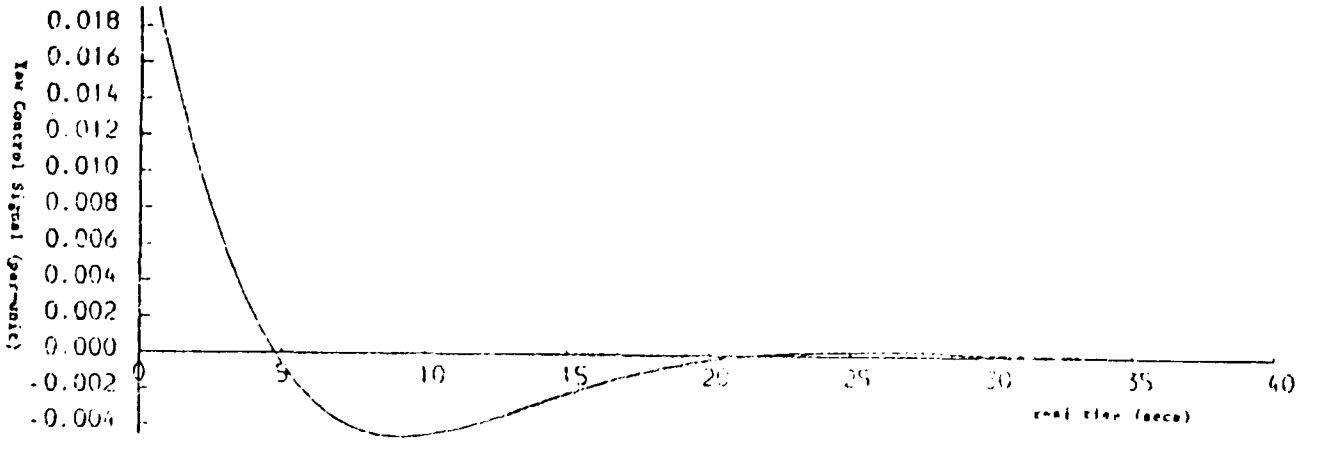

d— Yaw Control Signal for case (a), ρ = 1

Figures(4.4-c,d) :Control signals for step into sway (Wimpey Sealab)

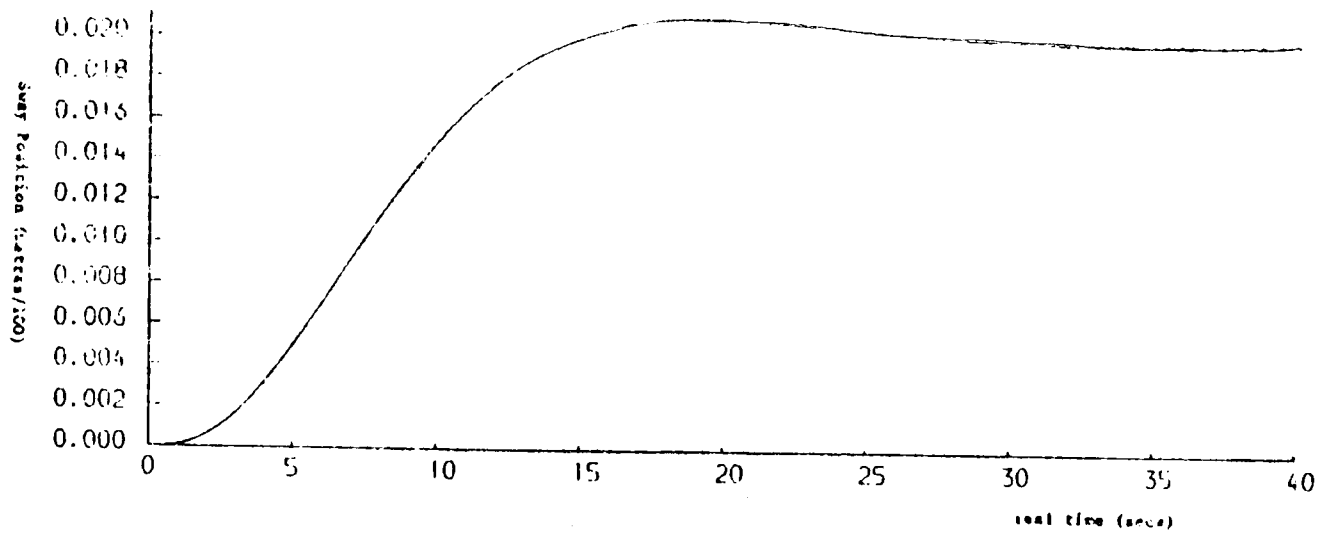

a- Sway Output Signal for case (b), ρ = 1

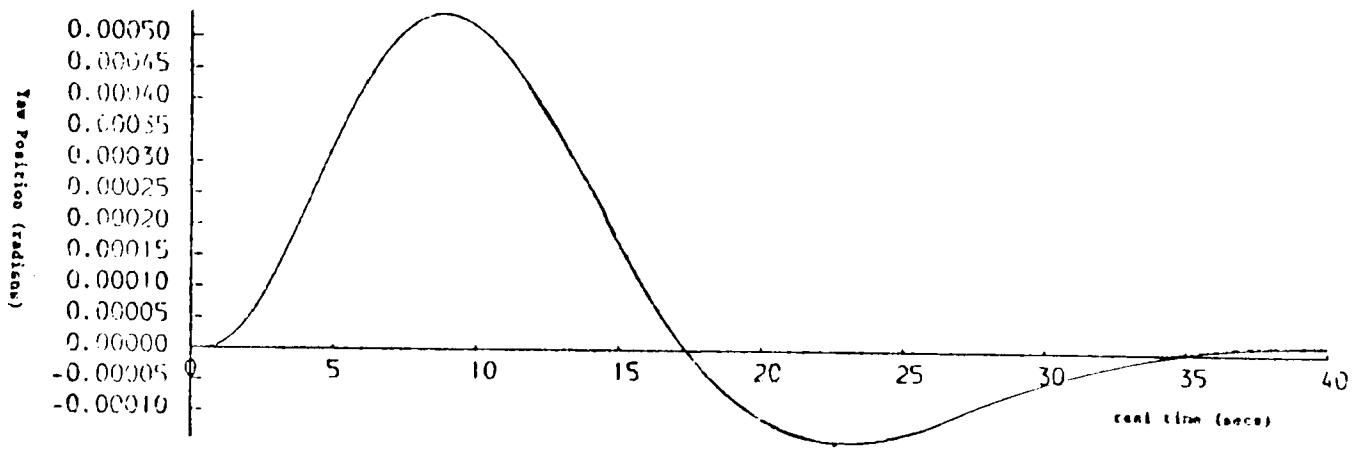

b- Yaw Output Signal for case (b), ρ = 1

Figures(4.5-a,b) :Output signals for step into sway (Wimpey Sealab)

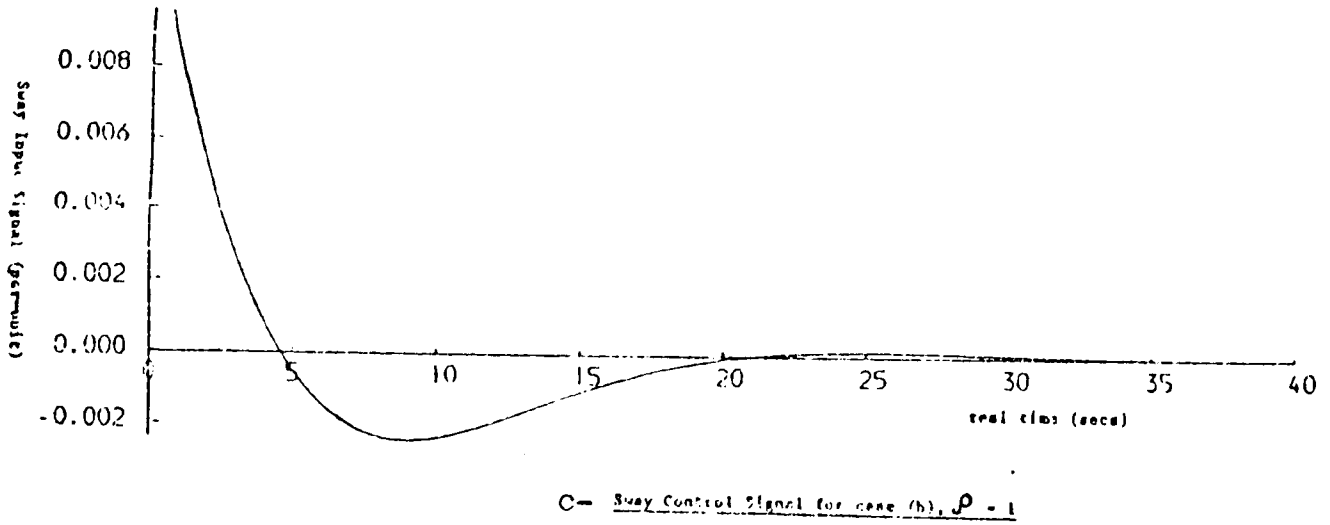

C- Sway Control Signal for case (b), $\rho = 1$

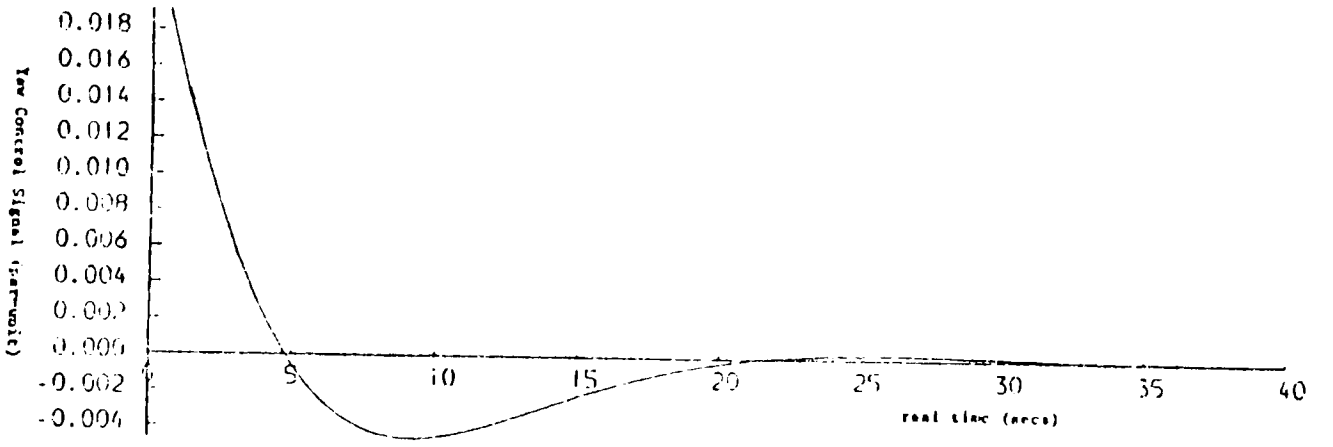

d- Yaw Control Signal for case (b), $\rho = 1$

Figures(4.5-c,d) :Control signals for step into sway (Wimpey Sealab)

$$K^{c\ell} = \begin{bmatrix} -1.30 & -0.59 & -0.21 & -0.097 & -0.67 & -0.005 \\ -2.54 & -1.18 & 0.41 & 0.19 & -0.005 & -0.67 \end{bmatrix}$$

4.4.3 Case (c)

In this case (see Grimble [39]),

$$R_1 = \begin{bmatrix} 26.36797 & -12.47397 \\ -42.47397 & 6.59232 \end{bmatrix}$$

$$R = \rho R_1$$

while:

$$Q = C^T \cdot C$$

$$Q = \begin{bmatrix} 0.0 & & & & & \\ & 1.0 & & 0.0 & & \\ & & 0.0 & & & \\ & & & 1.0 & & \\ & 0.0 & & 0.0 & & \\ & & & & & 0.0 \end{bmatrix}$$

and ρ takes values of the following range:

$$\rho = \{10^{-3},\ 1.0,\ 10.0\}$$

Based on the above selected values of Q and R, system responses of the "Wimpey Sealab" for 0.02 p.u. step input into sway are presented in Figures 4.6a-d for the selected case when ρ = 1.0 with the following feedback gain matrix:

$$K^{c\ell} = \begin{bmatrix} -1.28 & -0.58 & -0.26 & -0.13 & -0.74 & 0.038 \\ -2.57 & -1.19 & 0.30 & 0.13 & -0.17 & -0.59 \end{bmatrix}$$

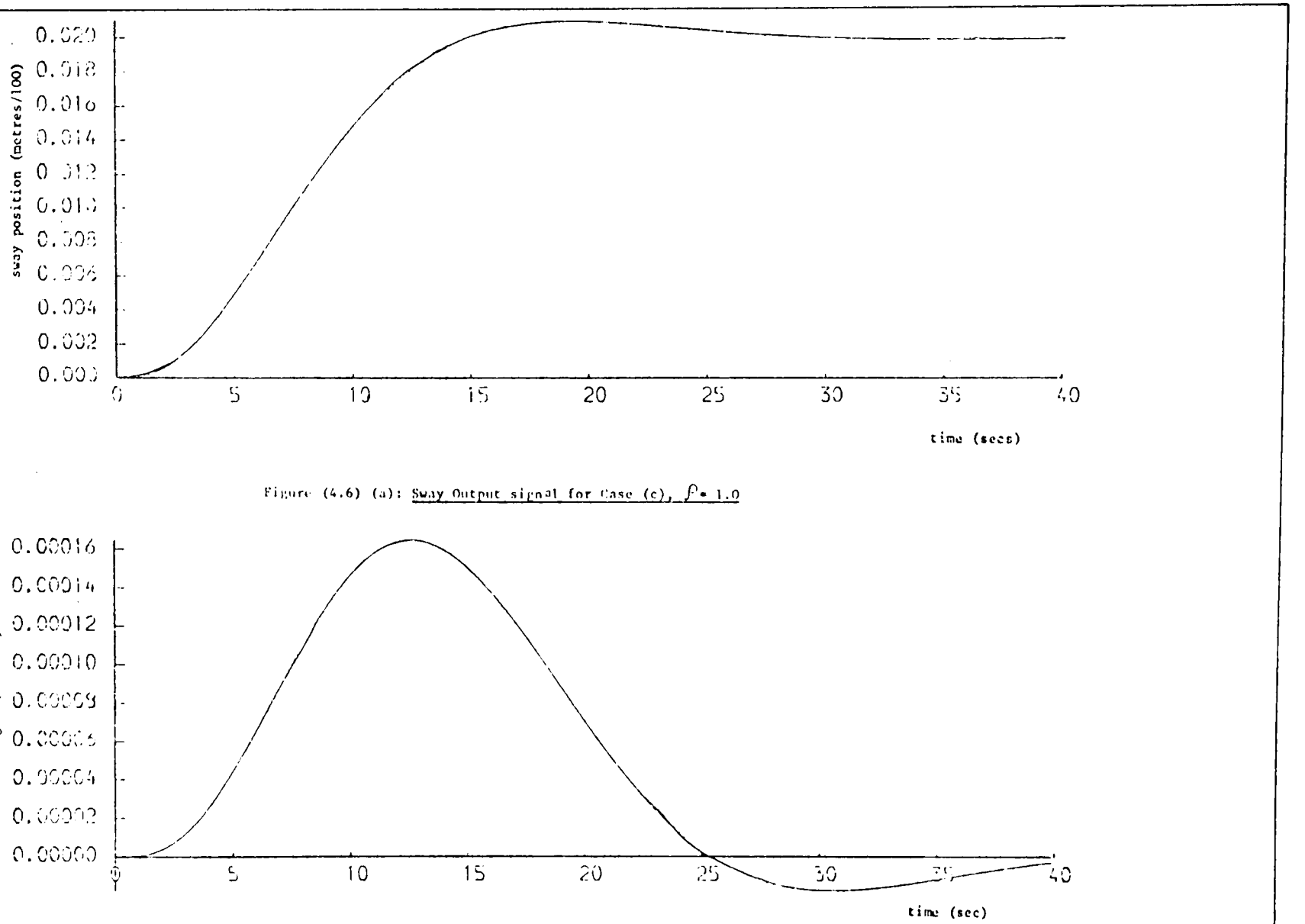

Figure (4.6) (a): Sway Output signal for Case (c), $\rho = 1.0$

Figure (4.6) (b): Yaw Output Signal for Case (c), $\rho = 1.0$

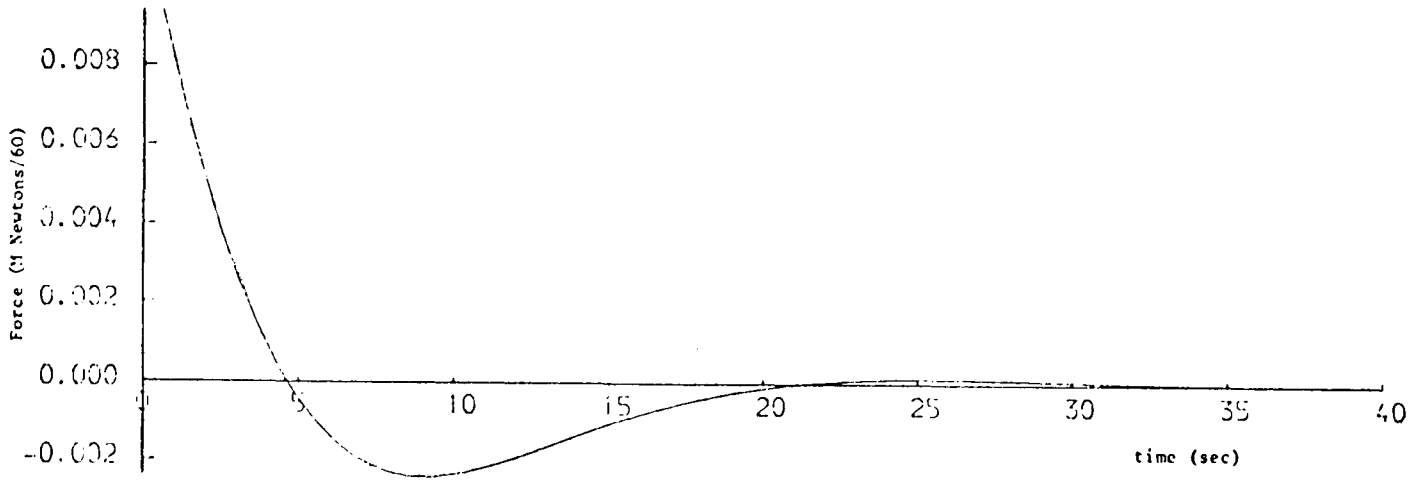

Figure (4.6) (c): Sway control signal for case (c), $\rho = 1.0$

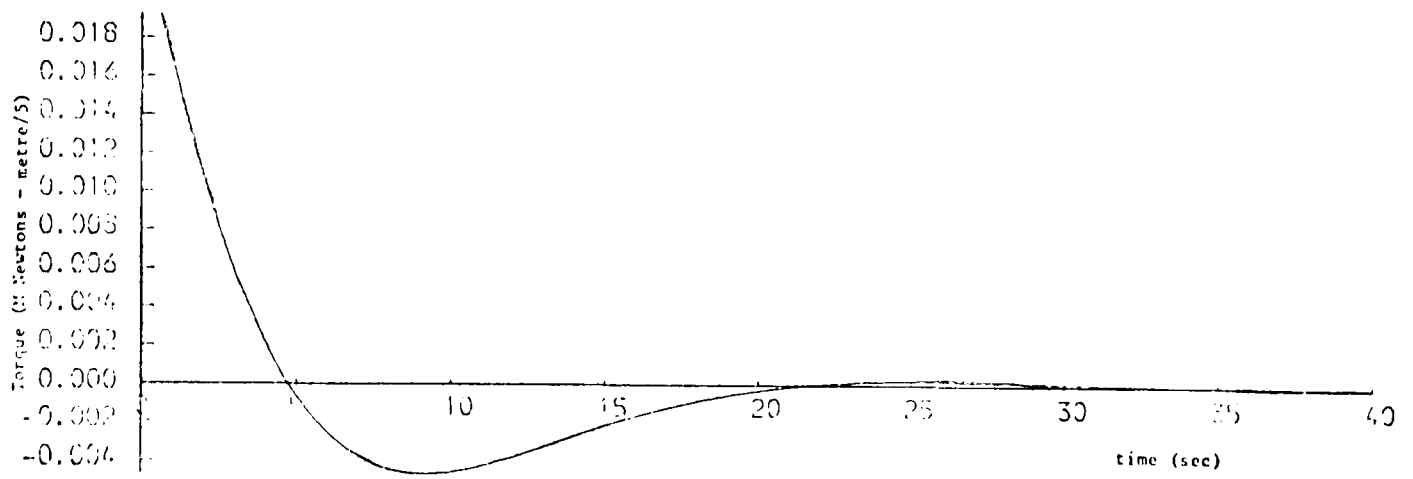

Figure (4.6) (d): Yaw control signal for case (c), $\rho = 1.0$

4.5 Concluding Remarks

Values of the weighting matrices Q and R were selected using the new technique by Grimble [39] which showed that these weightings depend on the choice of the eigenvalues (λ_i^∞) and the eigenvectors (v_i^∞). The chosen values of Q, R have been used in solving the matrix Riccati equation to obtain the optimal feedback gain and hence to simulate the system. The dynamics of the "Wimpey Sealab" have been simulated over a range of Q and R values (cases (a) to (e)), in which R-matrix took multiple values for a range of ρ values. Some selected tests were presented and the system responses for sway and yaw input-output vectors were considered. The rest of the simulation, including case (d) and case (e) was documented in a separate report by the author [2]. Among the presented responses, case (b) with ρ = 1.0 has been selected for the control loop and its application to the dynamic ship positioning problem. It has been selected, since it has given a good system response and since it represents a test for a non-interactive, same speed input, which is the case of the dynamic positioning problem. After Q and R are specified there remain the procedures of solving the Riccati equation and calculating the feedback gain matrix thereafter, and for any specified system. Solution of the Riccati equation is the process of obtaining the steady state P-matrix. For systems based on data from the "Wimpey Sealab" vessel (Section 3.2.3), the P-matrix was found to be:

$$P_\infty = \begin{bmatrix} 8.40 & 4.61 & -0.82 & -0.46 & 0.84 & 1.67 \\ 4.61 & 4.07 & -0.45 & -0.40 & 0.38 & 0.77 \\ -0.82 & -0.45 & 0.22 & 0.12 & 0.13 & -0.27 \\ -0.46 & -0.40 & 0.12 & 0.11 & 0.063 & -0.12 \\ 0.84 & 0.38 & 0.13 & 0.063 & 0.43 & 0.003 \\ 1.67 & 0.77 & -0.27 & -0.12 & 0.003 & 0.43 \end{bmatrix}$$

and hence the corresponding optimal gain matrix is:

$$\begin{bmatrix} -1.30 & -0.59 & -0.21 & -0.097 & -0.67 & -0.005 \\ -2.54 & -1.18 & 0.41 & 0.19 & -0.005 & -0.67 \end{bmatrix}$$

The calculation of the optimal feedback control using the above selected values of Q and R for a system based on data from the "Star Hercules" vessel of Section 3.2.4 was performed, and the optimal feedback gain matrix found as:

$$\begin{vmatrix} -1.40 & -0.44 & 0.0 & 0.0 & -0.51 & 0.0 \\ 0.0 & 0.0 & -0.09 & -0.03 & 0.0 & -0.53 \end{vmatrix}$$

The above calculated feedback gain matrices for both the "Wimpey Sealab" and the "Star Hercules" will be used for closed loop control for different applications of the dynamic positioning problem considered throughout this work. At this stage, the low-frequency part of the "Wimpey Sealab" and the "Star Hercules" have been simulated using their corresponding values of the feedback gain and for a step input of 0.02 p.u. into yaw rather than sway. These responses are shown in Figures 4.7a - d for the "Wimpey Sealab" and in Figures 4.8a - d for the "Star Hercules" dynamics.

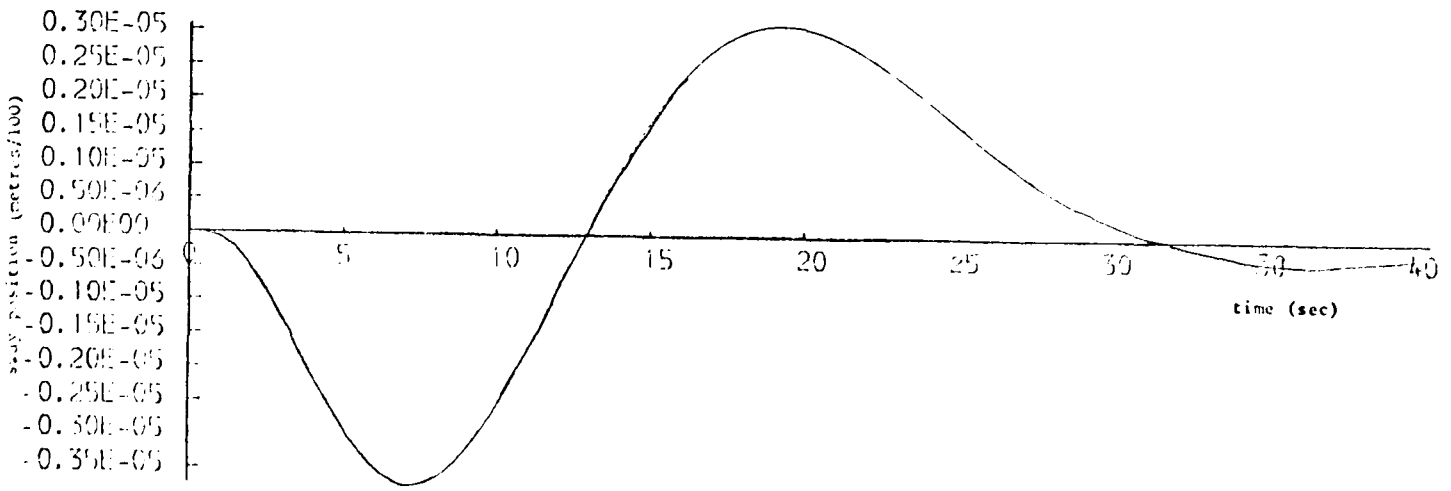

Figure (4.7) (a): Output (1) for step into yaw (Wimpey SeaLab)

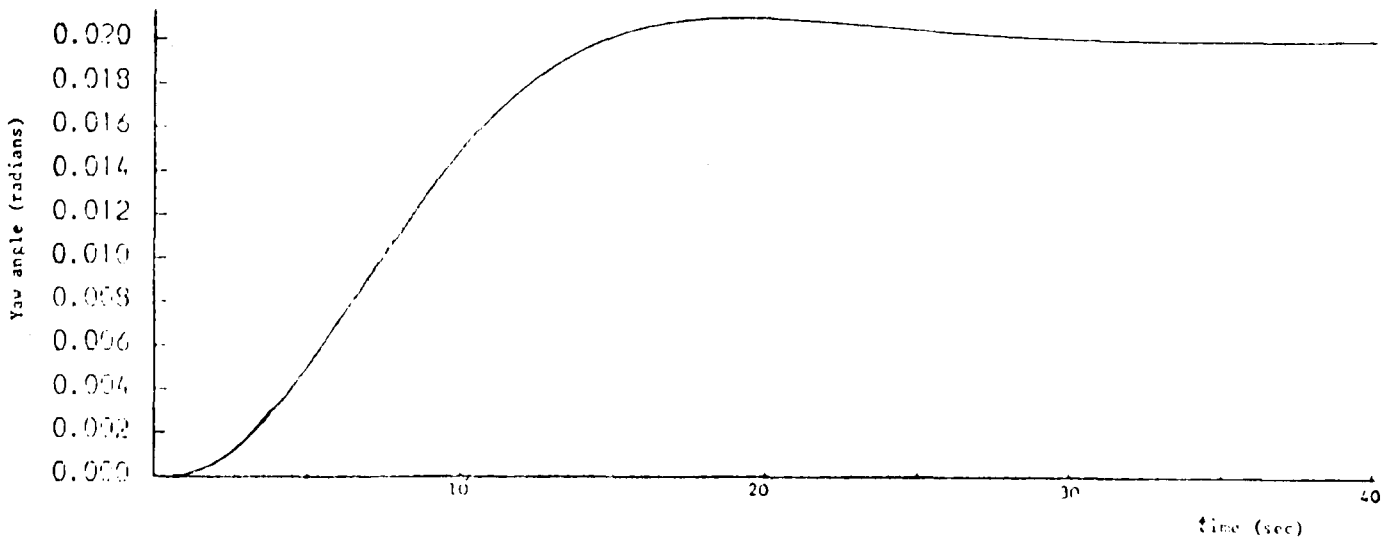

Figure (4.7) (b): Output (2) for step into yaw (Wimpey Sealab)

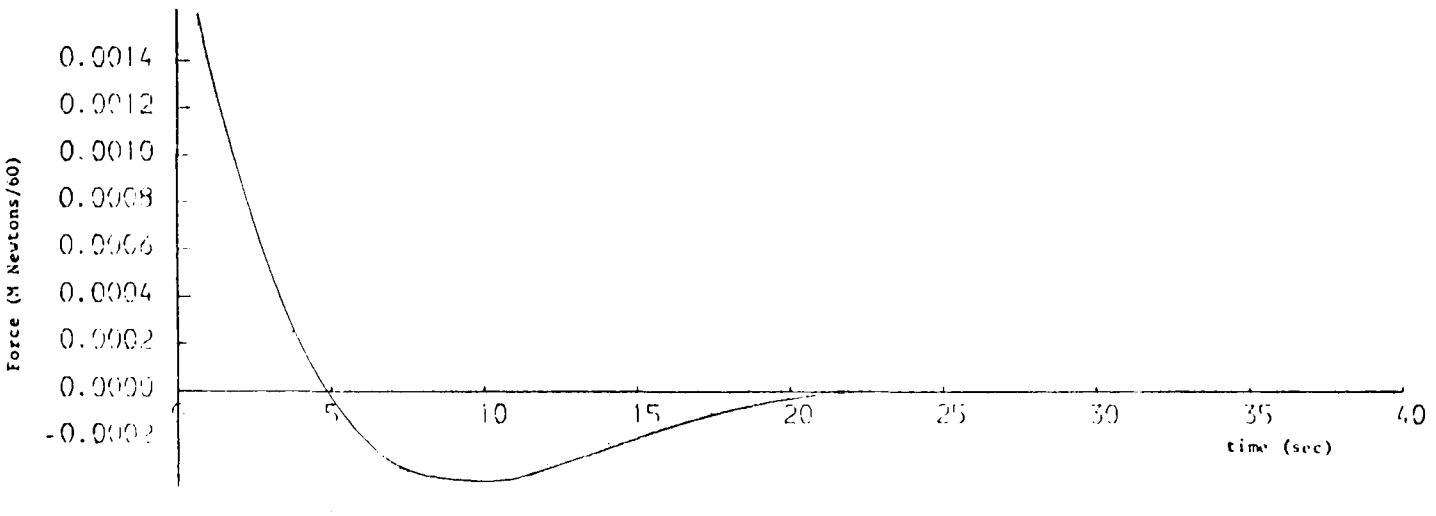

Figure (4.7) (c): Sway control signal (Wimpey Sealab)

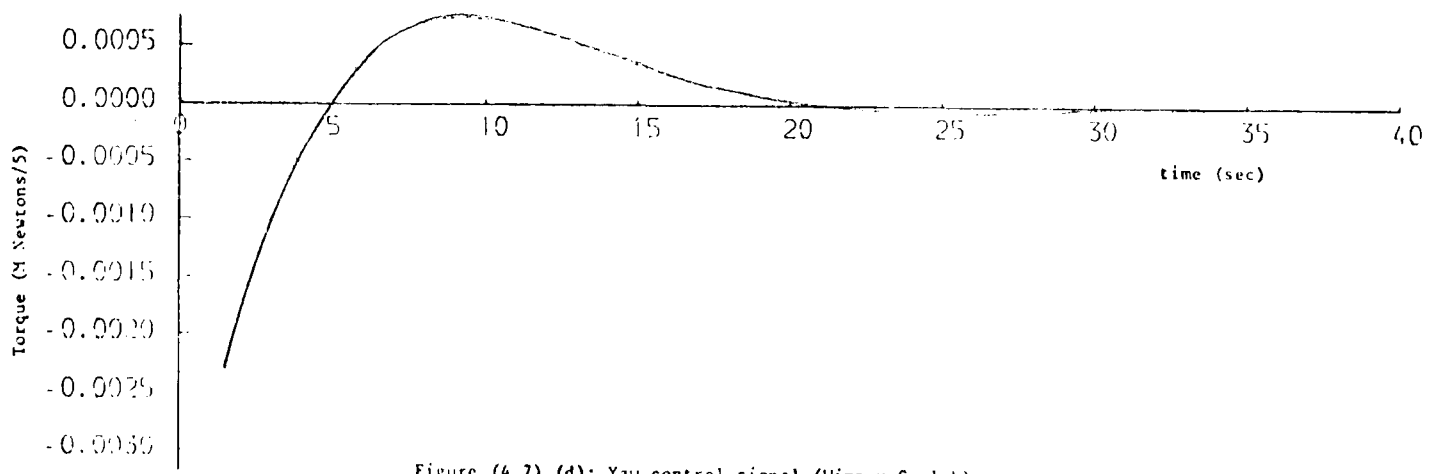

Figure (4.7) (d): Yaw control signal (Wimpey Sealab)

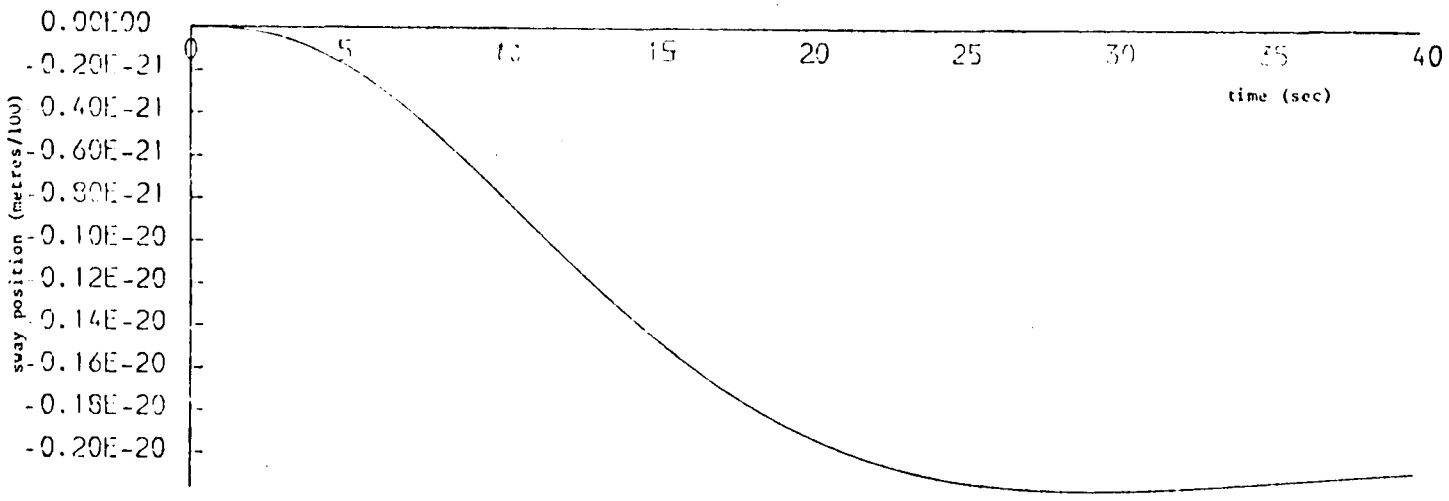

Figure (4.8) (a): Output (1) for step into yaw (Star Hercules)

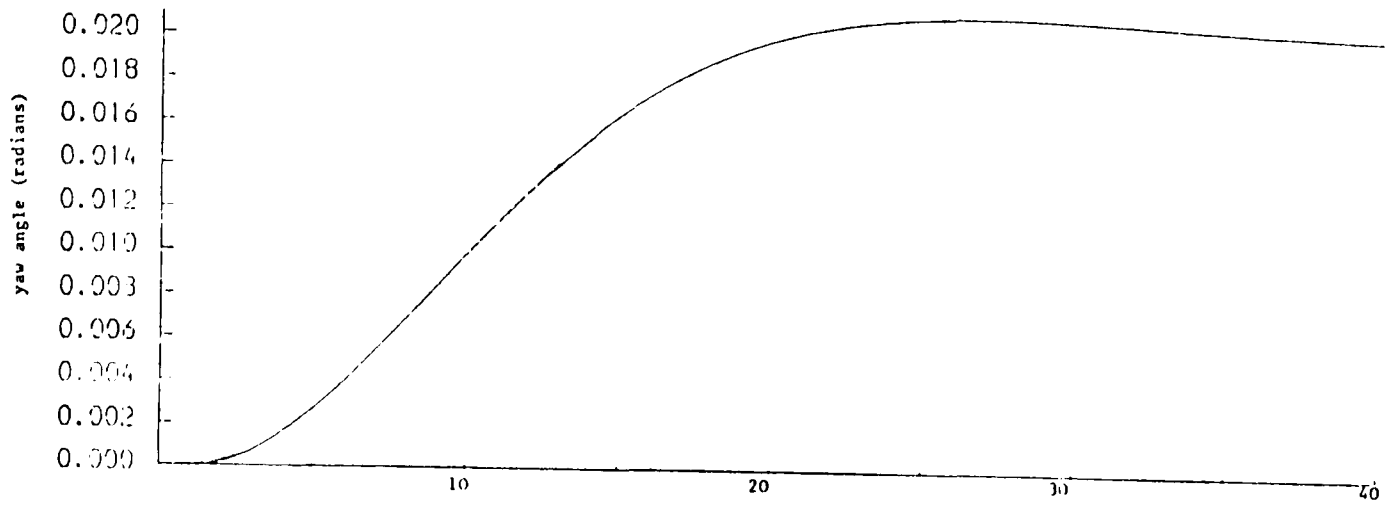

Figure (4.8) (b): Output (2) for step into yaw (Star Hercules)

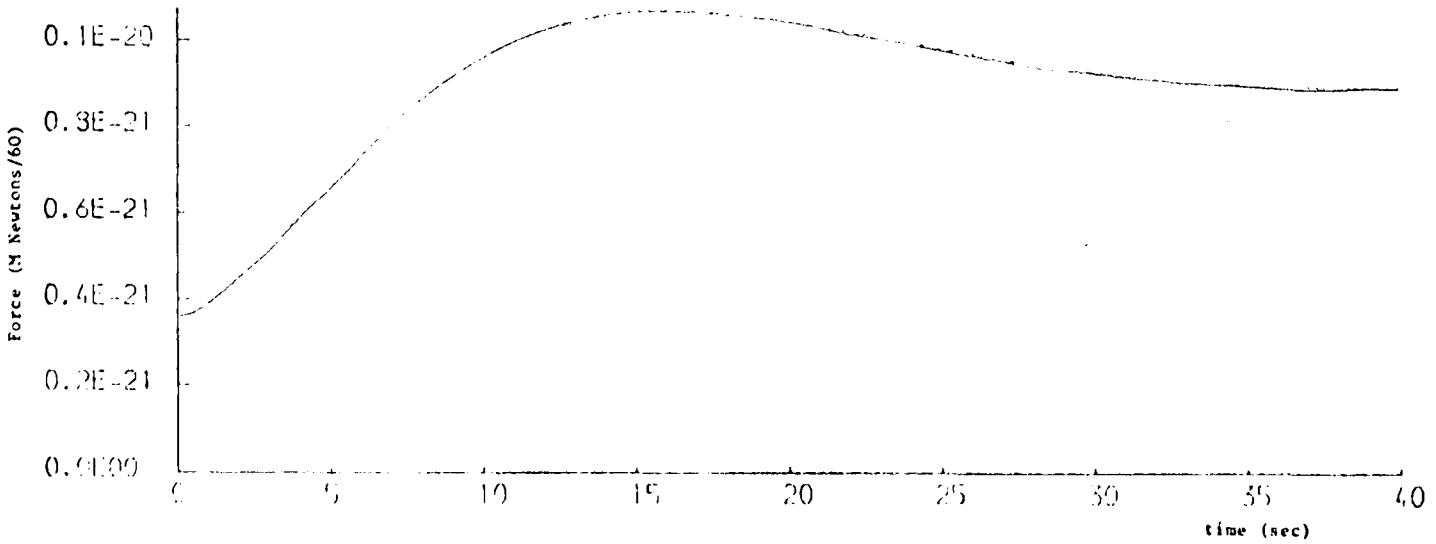

Figure (4.8) (c): Sway control signal (Star Hercules)

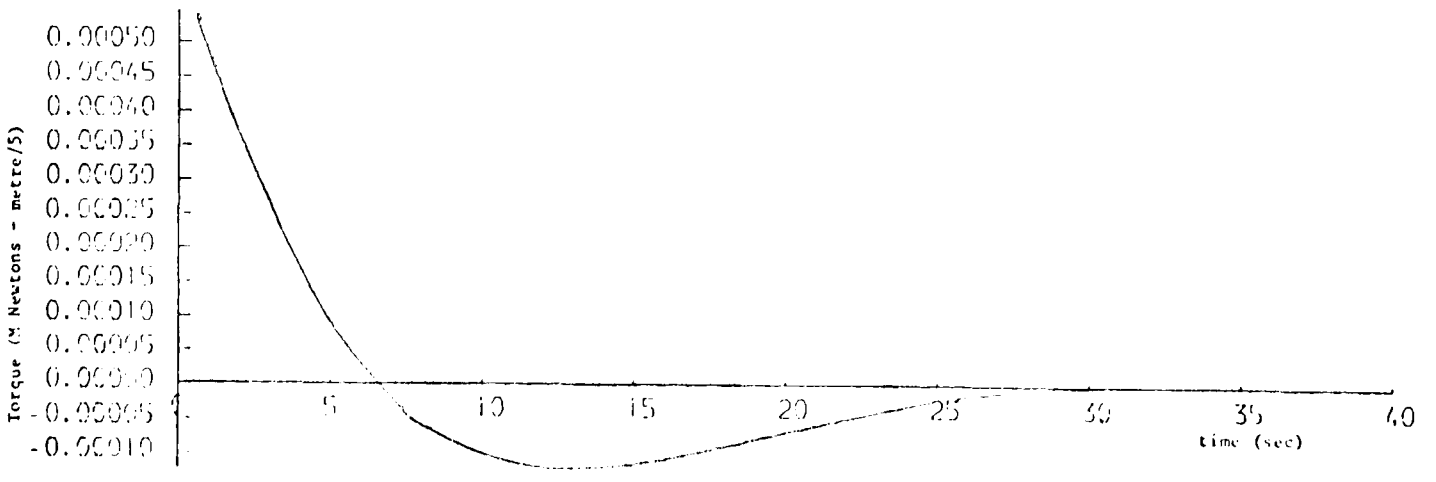

Figure (4.8) (d): Yaw control signal (Star Hercules)

C H A P T E R (5)

CHAPTER 5

LINEAR FILTERING/KALMAN FILTERING PROBLEM

5.1 Introduction

Dynamic ship positioning control systems require filters to remove the large high-frequency wave motion signals [99]. This ensures that the thrusters do not respond to the high-frequency wave motion and, consequently, reduces energy loss and wear on the thrusters. Some dynamic positioning systems employ Notch filters [13],[57]. However, Kalman filtering techniques have been used throughout this work.

Kalman filtering is a technique which produces an optimum estimate of the state of a system, from a succession of measurements. A knowledge of the dynamic behaviour and error characteristics of the system is an essential pre-requisite. The Kalman filter includes a model of the system dynamics and can therefore provide separate low and high frequency state estimates. The Kalman estimator is shown in Figure 5.1 and is defined by the following state and output equations:

$$\dot{\hat{\underline{x}}} = A\hat{\underline{x}} + K(\underline{z} - \hat{\underline{y}}) + B\underline{u} \qquad \ldots\ldots\ldots\ldots\ldots (5.1)$$

$$\hat{\underline{y}} = C\hat{\underline{x}} \qquad \ldots\ldots\ldots\ldots\ldots (5.2)$$

where

$A \equiv$ filter system matrix

$K \equiv$ filter gain matrix

$\underline{z} \equiv$ observations

$\hat{\underline{y}} \equiv$ filter output

$\hat{\underline{x}} \equiv$ state estimates

$B, C \equiv$ filter input and output matrices

The Kalman gain matrix K(t) of equation (5.1) above can be partitioned

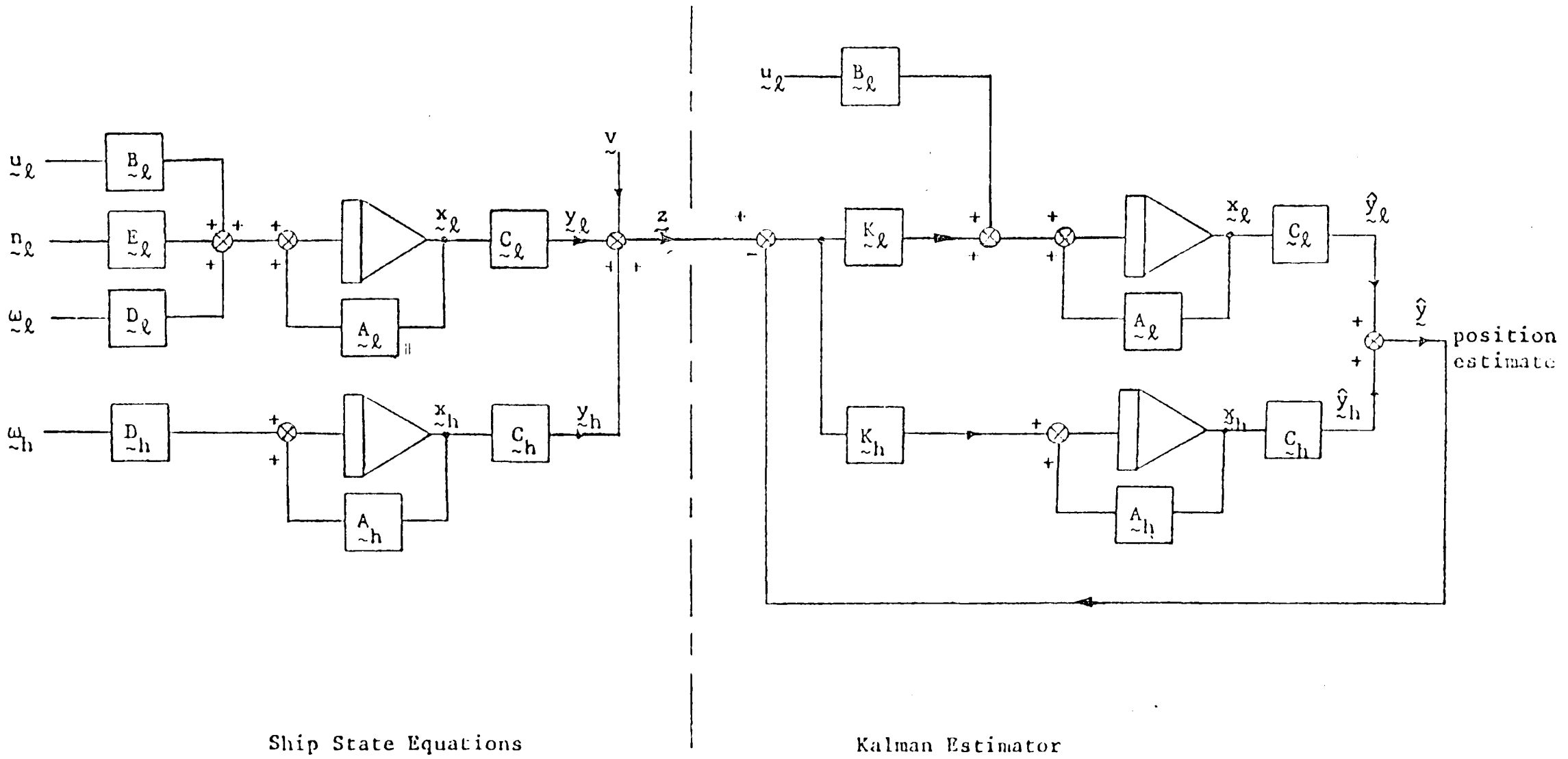

Figure (5.1): The Ship Represented by State Equations and the Kalman Estimator

into low and high frequency gain matrices as:

$$K(t) = \begin{bmatrix} K_{\ell}(t) \\ \hline K_{h}(t) \end{bmatrix} \qquad \ldots\ldots\ldots\ldots \quad (5.3)$$

This matrix can be evaluated for a given noise information (Appendix 3- Kalman algorithm). The process noise covariance matrix related to ran-dom forces, is defined on the basis of common practice, while the measurement noise covariance matrix can be defined with acceptable accuracy from a knowledge of the measuring system. The evaluated time-varying Kalman gain matrix elements settle to a constant value after approximately 20 seconds (Section 5.3), and thus these gains can be pre-computed off-line in some cases and stored (Section 6.3). By using a constant or semi-constant gain Kalman filter, the overall cost of the control system can be reduced by saving some computing time.

5.2 Kalman Algorithm

Kalman filter theory is well known [58], [60], [98]. A step by step application to the dynamic ship positioning systems can be summarised as follows:

(i) Develop a system model in order to formulate a state vector ($\underline{x}$) which describes the system at any given time.

(ii) Determine the state of the input ($\underline{u}$) and the dynamic relationship between ($\underline{u}$) and ($\underline{x}$).

(iii) Assess the likely process noise ($\underline{\omega}$) and its covariance matrix (Q).

(iv) Determine the measurements to be made ($\underline{y}$), and the associated output matrix (C) relating the vector ($\underline{y}$) to the state vector ($\underline{x}$).

(v) Assess the likely error or noise in the measurements ($\underline{v}$) and its covariance matrix (R).

(vi) Finally determine the initial state estimate and its error covariance matrix (P).

The Kalman filter can be implemented using the continuous-time differential equations of the system represented in state-space form, but the simulations using digital computer have been performed in discrete-time form. In actual practice, a Kalman filtering scheme involves digital computations on an on-line process control by computer, and hence the discrete-time form of the system description is more appropriate for implementation and can be written as:

$$\underline{x}(k+1) = \Phi\underline{x}(k) + \Delta\underline{u}(k) + \Gamma\underline{\omega}(k) \quad \ldots\ldots\ldots\ldots (5.4)$$

$$\underline{z}(k) = H\underline{x}(k) + \underline{v}(k) \quad \ldots\ldots\ldots\ldots (5.5)$$

where:

$\Phi \equiv$ state transition matrix

$\Delta \equiv$ input driving matrix

$\Gamma \equiv$ noise driving matrix

$H \equiv$ output matrix

Having fed the filter with the necessary information, the next operational stages will be as follows:

(i) Store the previous best estimate (the initial values at the start) of the state ($\hat{\underline{x}}$) and its covariance matrix (P) at time instant (t).

(ii) The system represented by the usual differential equation and in the discrete form (Figure 5.2a) will be:

$$\underline{x}(k+1) = \Phi\underline{x}(k) + \Delta\underline{u}(k) + \Gamma\underline{\omega}(k) \quad \ldots\ldots\ldots\ldots (5.6)$$

$$\underline{z}(k) = H\underline{x}(k) + \underline{v}(k) \quad \ldots\ldots\ldots\ldots (5.7)$$

(iii) The prediction (Figure 5.2b). The problem is to obtain $\underline{x}(k+1|k)$, i.e. to estimate the value of ($\underline{x}$) at (k + 1) instant, given

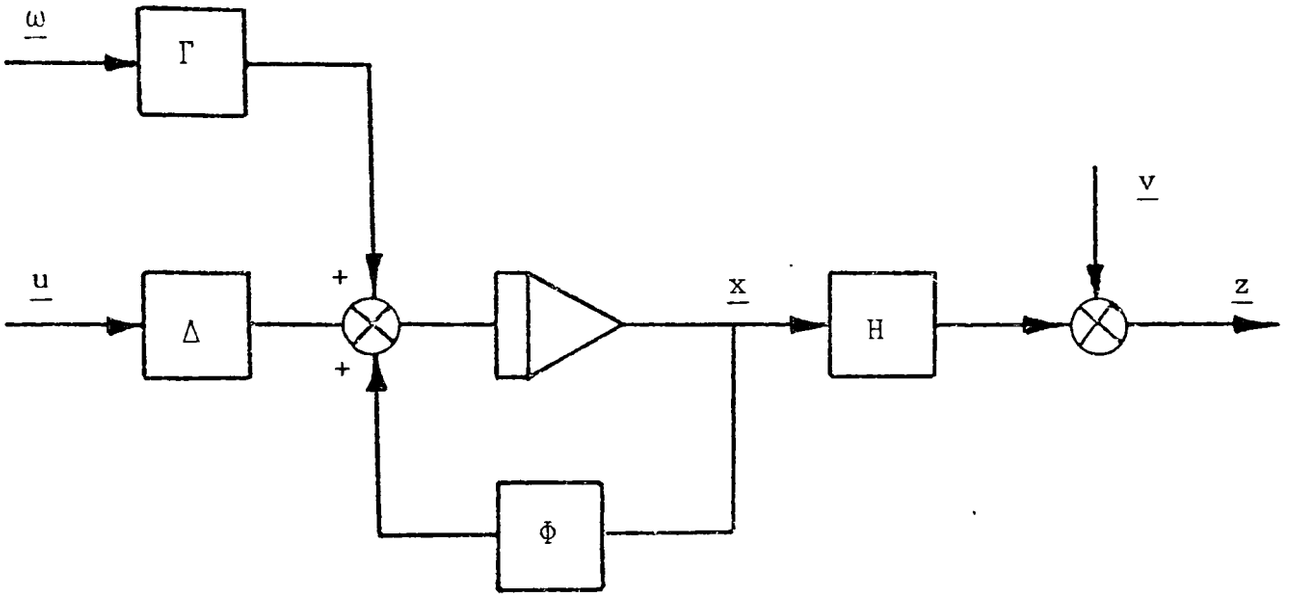

Figure (5.2) (a): The System in Discrete Form Representation

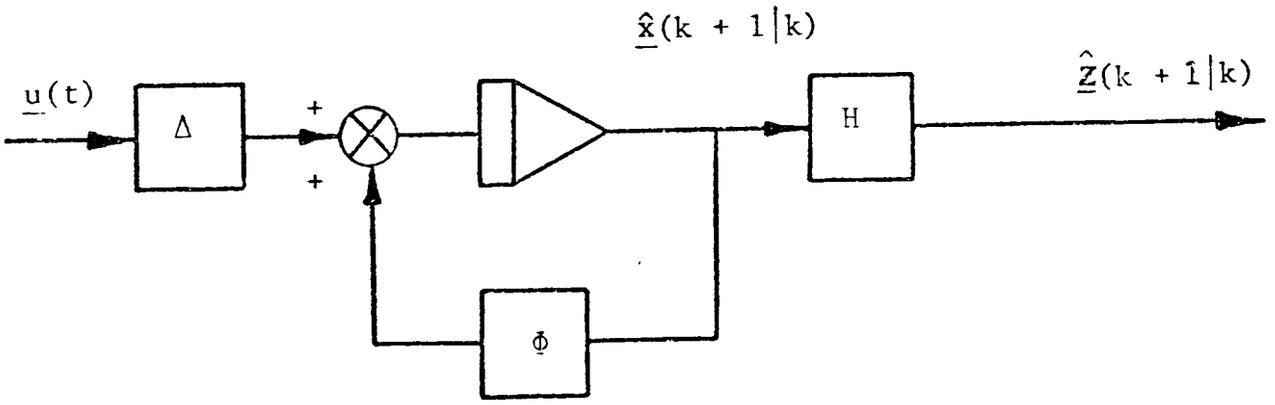

Figure (5.2) (b): Open Loop Prediction (the filter)

all the measurements up to instant (k). The previous estimate $\hat{\underline{x}}(k|k)$ is known:

$$\hat{\underline{x}}(k+1|k) = \Phi\hat{\underline{x}}(k|k) + \Delta\underline{u}(k) \quad \ldots\ldots\ldots\ldots (5.8)$$

$$\hat{\underline{z}}(k+1|k) = H\hat{\underline{x}}(k+1|k) \quad \ldots\ldots\ldots\ldots (5.9)$$

(iv) The correction. There will be an error between the measured and the predicted output:

$$\tilde{\underline{z}}(k+1|k) = \underline{z}(k+1) - \hat{\underline{z}}(k+1|k) \quad \ldots\ldots\ldots\ldots (5.10)$$

To compensate for such differences:

$$\hat{\underline{x}}(k+1|k+1) = \hat{\underline{x}}(k+1|k) + K\tilde{\underline{z}}(k+1|k) \quad \ldots\ldots\ldots\ldots (5.11)$$

which defines the Kalman filter, where:

$$K(k) = \begin{bmatrix} K_{\ell}(k) \\ \hline K_{h}(k) \end{bmatrix}$$

is the Kalman gain matrix, with $K_{\ell}(k)$ and $K_{h}(k)$ as the low and high frequency parts of the gain matrix respectively.

(v) The estimation. For a given instant (k + 1),

$$\hat{\underline{x}}(k+1|k+1) = (I - KH)(\Phi\hat{\underline{x}}(k|k) + \Delta\underline{u}(k)) + K\underline{z}(k+1) \quad \ldots\ldots (5.12)$$

where $\hat{\underline{x}}(k|k)$ is the previous estimate, and $\underline{z}(k+1)$ is the current measurement.

As mentioned above, Kalman filter basically involves a model of the system and is therefore particularly appropriate for separating the low and high frequency motions of the vessel. The filtering problem is thus one of estimating the low-frequency motion of the vessel so that control can be applied. The Kalman filter will be shown to be suitable

for obtaining the estimates of the low-frequency states. The Kalman algorithm is illustrated in Appendix 3, while the schematic diagram of the Kalman filter applied to the dynamic ship positioning problem is shown in Figure 5.3.

5.3 Implementations and Simulation Results

5.3.1 Software Descriptions

The application of Kalman filtering technique to the dynamic positioning problem is a complicated process of estimation and control, and hence, the availability of a high-speed, digital computer is the prime contributing factor to the success of such applications.

The full Kalman filter together with ship dynamics and the related control were simulated on an ICL 1906S digital computer using the FORTRAN4 computer language and GEORGE4 operating system. The computer program has been written in a form suitable for making changes for different practical investigations of using the reduced-order Kalman filter, semi-constant gain filter, etc. Calculations of the optimal feedback control matrix have been performed and fed into the main data block. Subroutines for generating the uncorrelated measurement and process noise signals have been written by Patton [51] and used here [75]. Two different subroutines were used for simulating the filter and the ship and basically called FILTER and DYN. The initial part of the program sets up the ship and filter parameters. Subroutine PHIDELTA is used to compute the state transition matrix Φ_k and the driving matrix Δ_k for the simulations. Subroutine DYN is used to advance the state variables of the ship model by one step interval using the transition equation. The control input signals are also calculated in this subroutine. The Kalman filter gain, state estimates

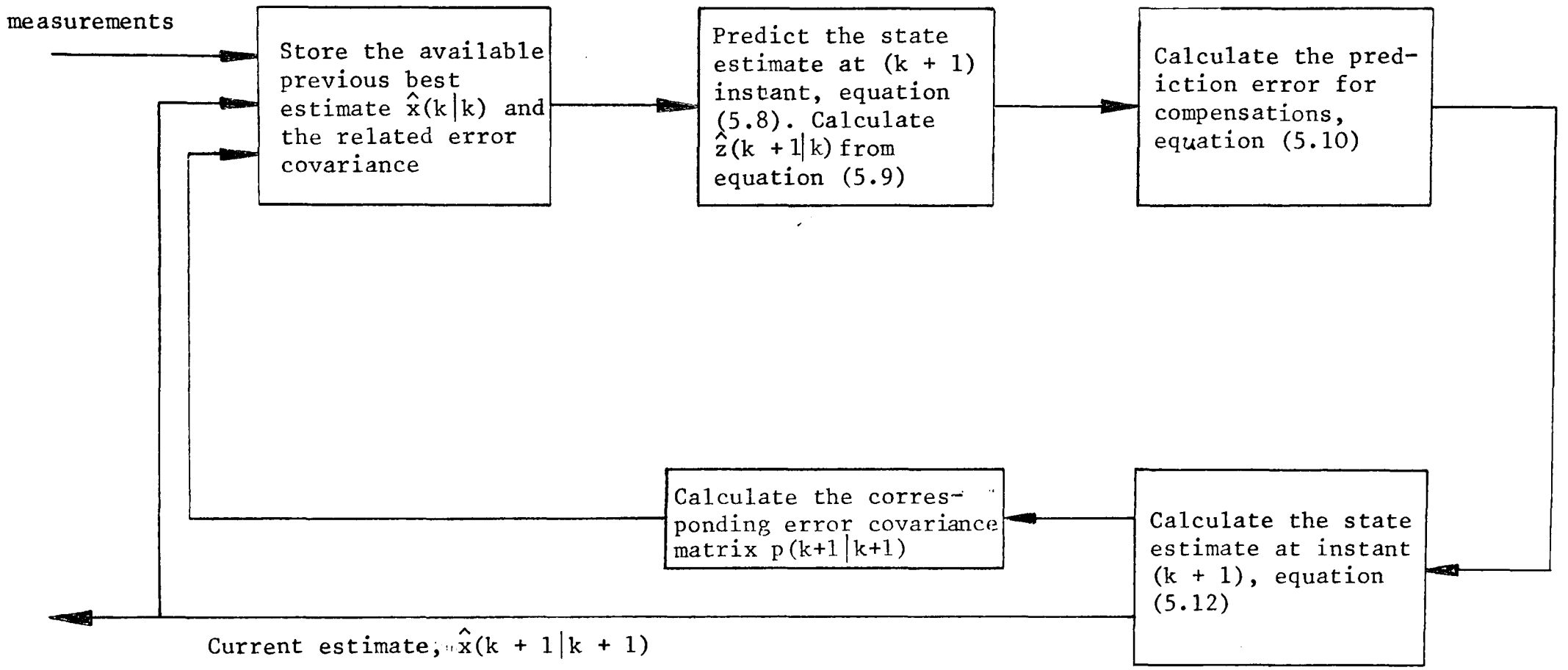

Figure (5.3): Schematic diagram of the process of the implementations of Kalman filter estimates

and the associated error covariance matrix are calculated by a successive call to subroutine FILTER using the filter algorithm given in Section 5.2. The basic computer flow chart for the whole system simulations using the full Kalman filter algorithm is shown in Figure 5.4, [1].

5.3.2 Filter and Control Implementations for "Wimpey Sealab" Vessel

Dynamic positioning control for "Wimpey Sealab" ship has been performed using the linear Kalman filter and the stochastic optimal state estimate feedback control. The Kalman filter is time-varying although the filter gain matrix becomes constant after about twenty seconds. Full Kalman filter algorithms for this application have been implemented using results from Section 5.2. The low-frequency part of the ship and filter dynamics are independent of the weather conditions variations and have been assumed linear for closed loop feedback control. Hence, the optimal control gain matrix assumed constant which were calculated off-line and stored.

As the weather conditions vary, different parameters of the sea-wave simulator change (Appendix 2). Different tests were performed, and results for Beaufort number 8 conditions will be presented here. The ship is assumed to be subjected to disturbance forces of 4×10^{-6} per-unit force for sway and 9×10^{-8} per-unit turning moment for yaw. Computer plots shown in Figures 5.5 to 5.15 inclusive illustrate the system behaviour together with the filter estimates (shown by a dotted curve) for a step input of 0.02 per-unit into sway motions. These responses represent full low and high frequency parts of the ship dynamics using Kalman estimator with the following definitions:

State (1): low-frequency sway velocity

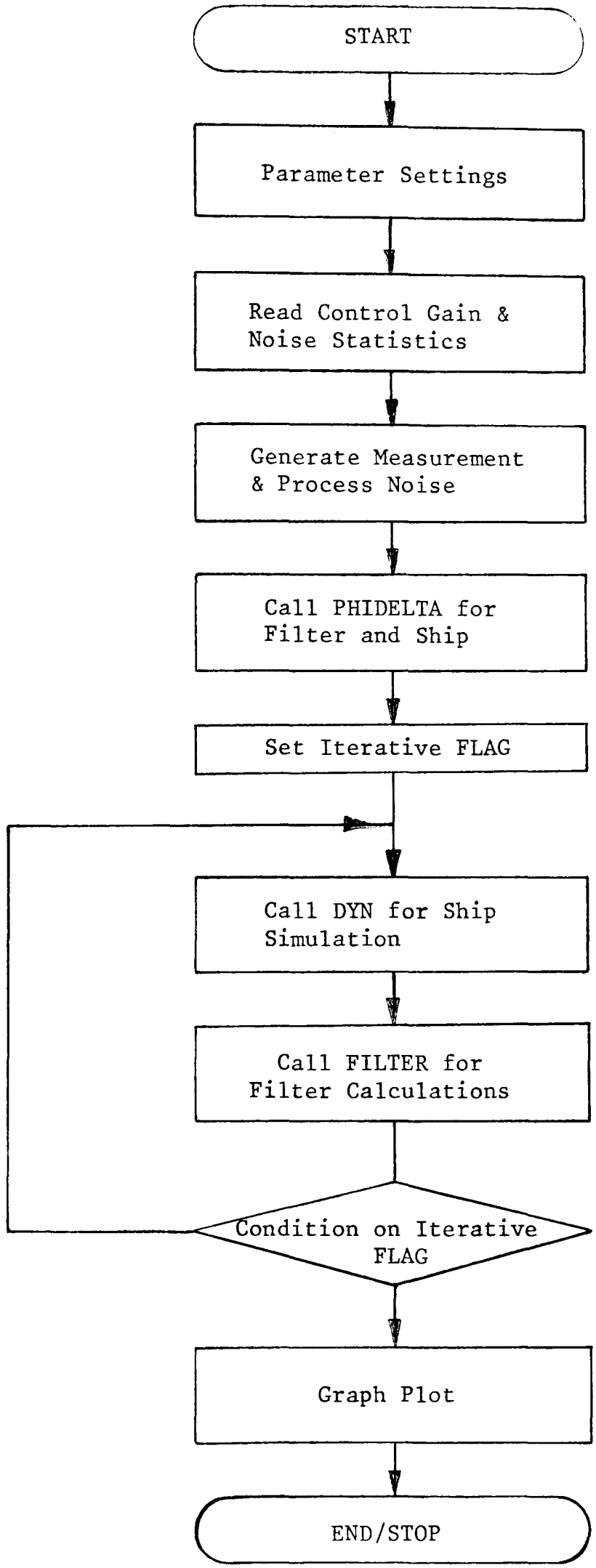

Figure (5.4) : Computer Flow Chart of Kalman Filtering and Control

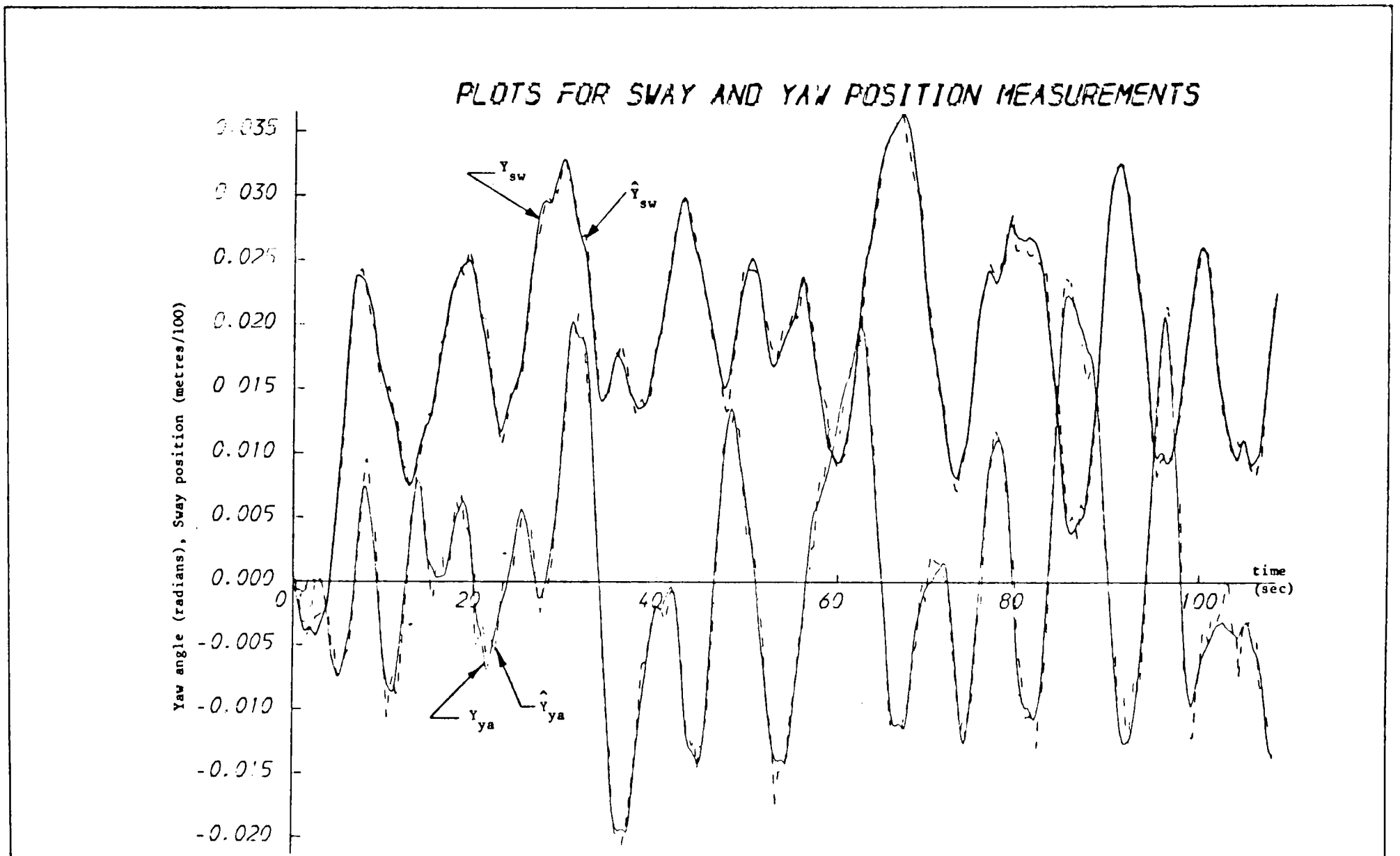

Figure (5.5): Optimal stochastic control with linear Kalman filter

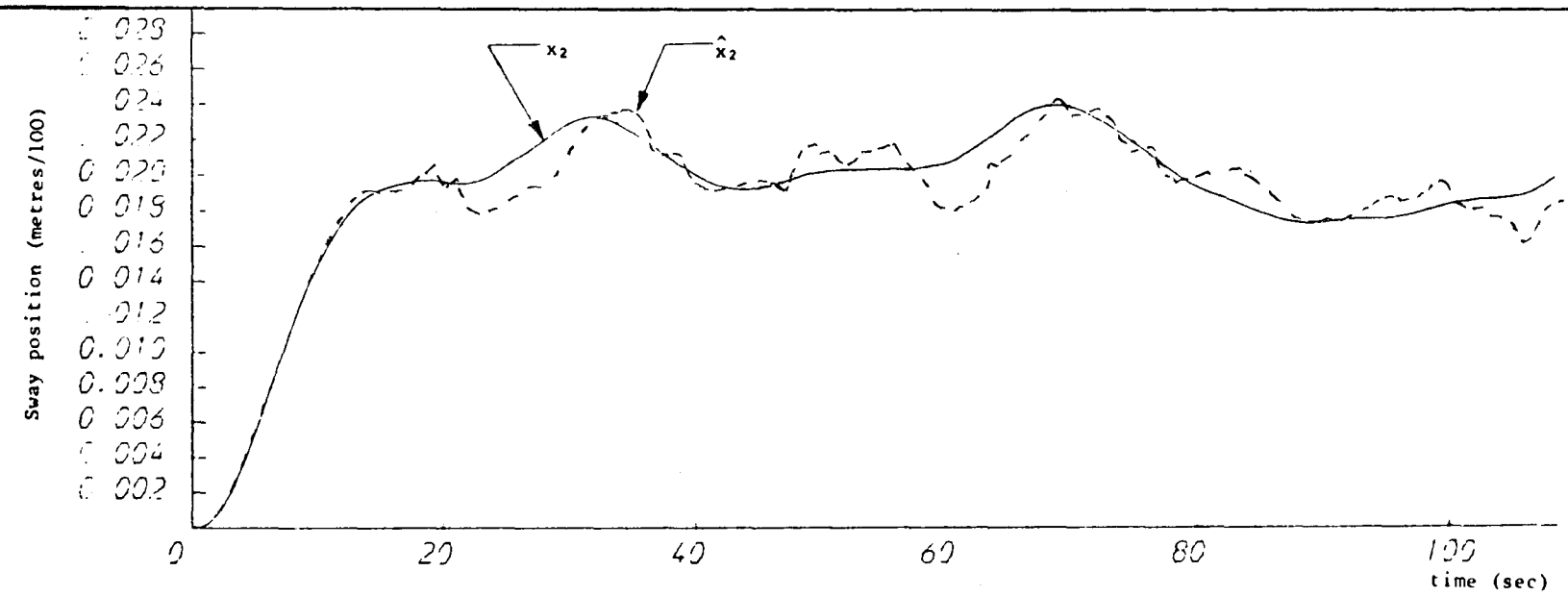

Figure (5.6): Sway low-frequency true and estimated position - state 2

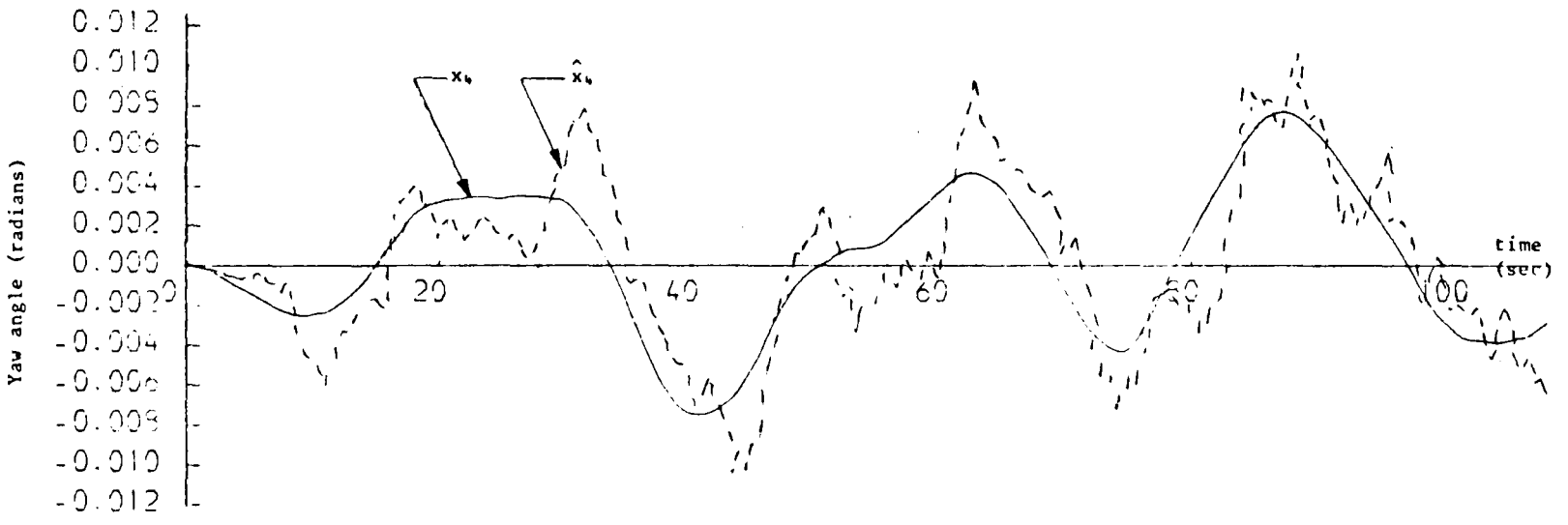

Figure (5.7): Yaw low-frequency true and estimated position - state 4

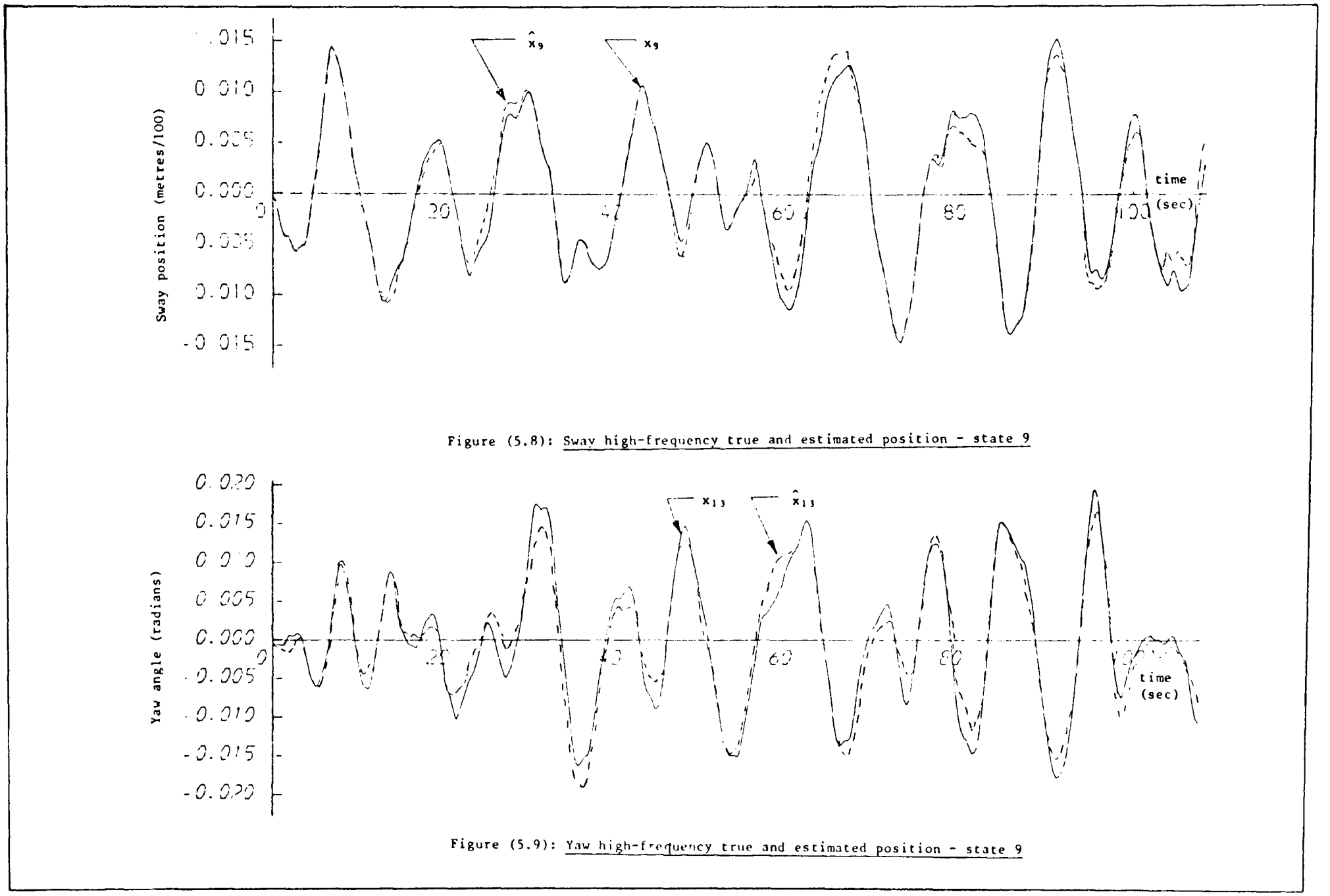

Figure (5.8): Sway high-frequency true and estimated position - state 9

Figure (5.9): Yaw high-frequency true and estimated position - state 9

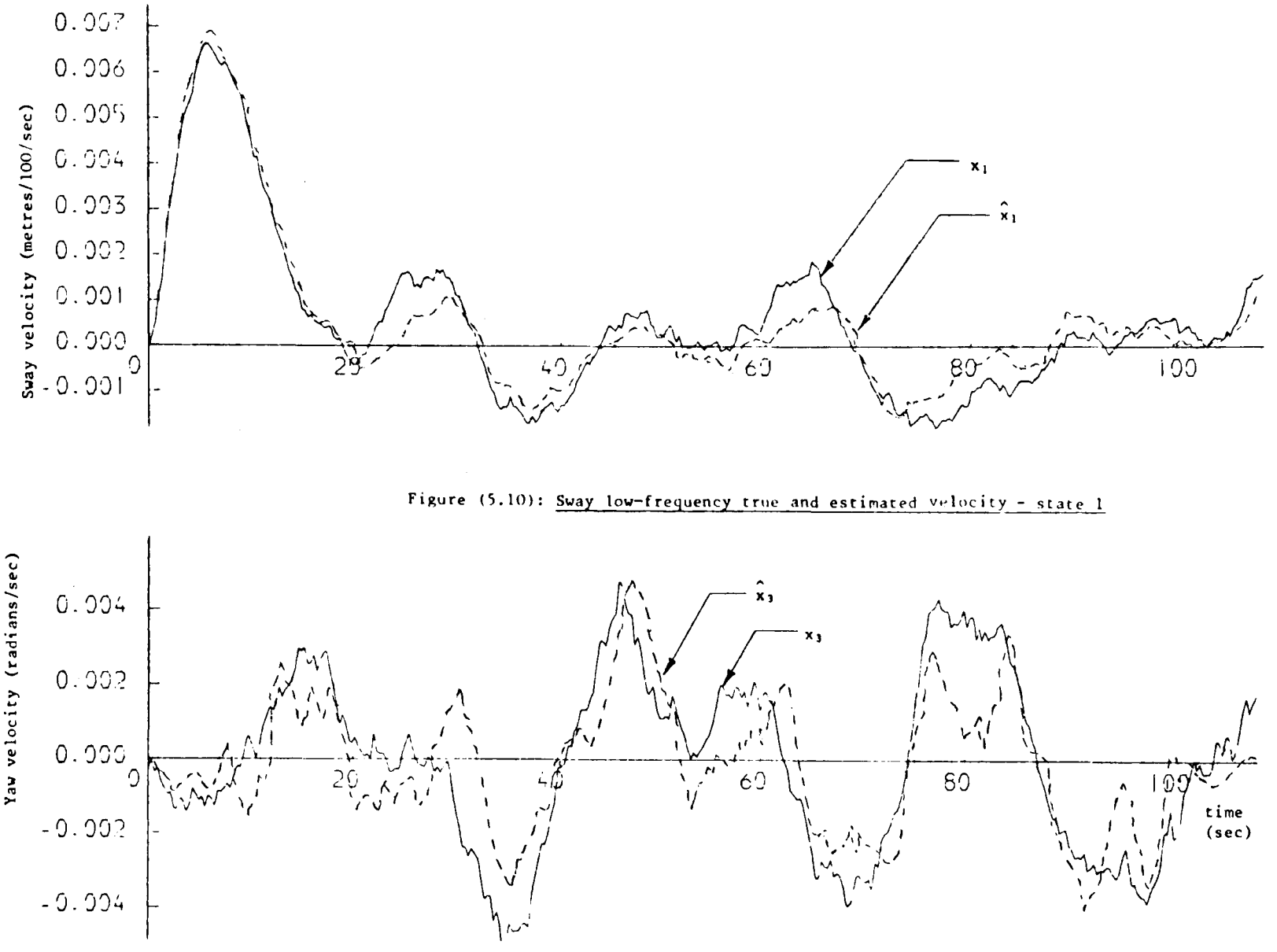

Figure (5.10): Sway low-frequency true and estimated velocity - state 1

Figure (5.11): Yaw low-frequency true and estimated velocity - state 3

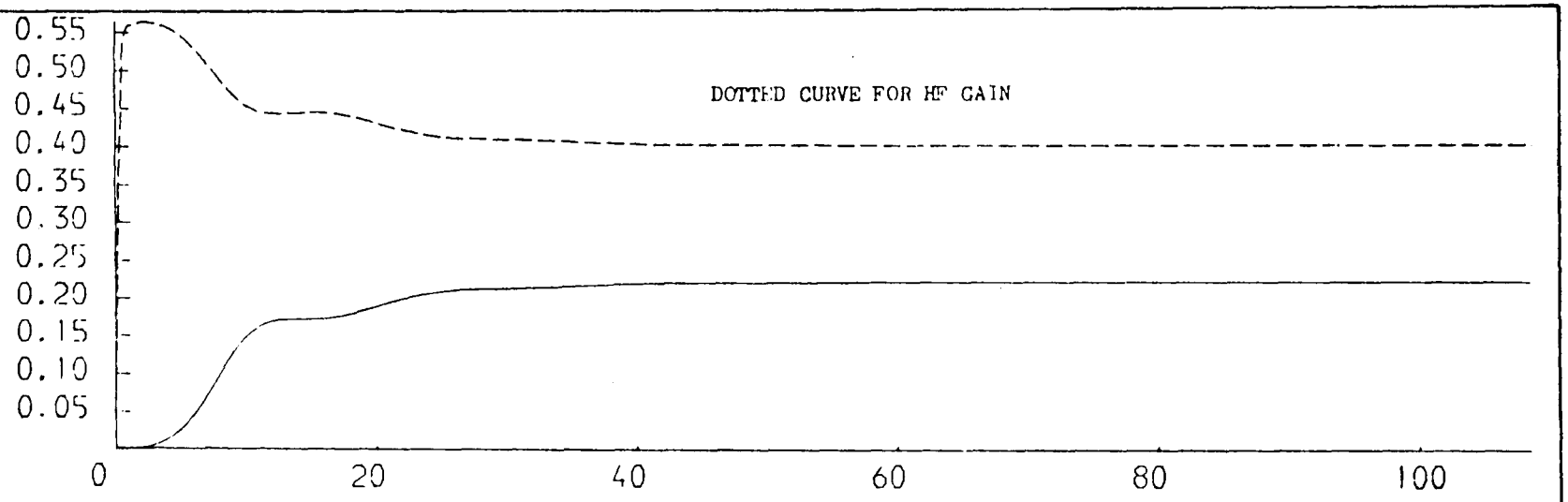

Figure (5.12) :Low and high frequency Kalman gains for sway position

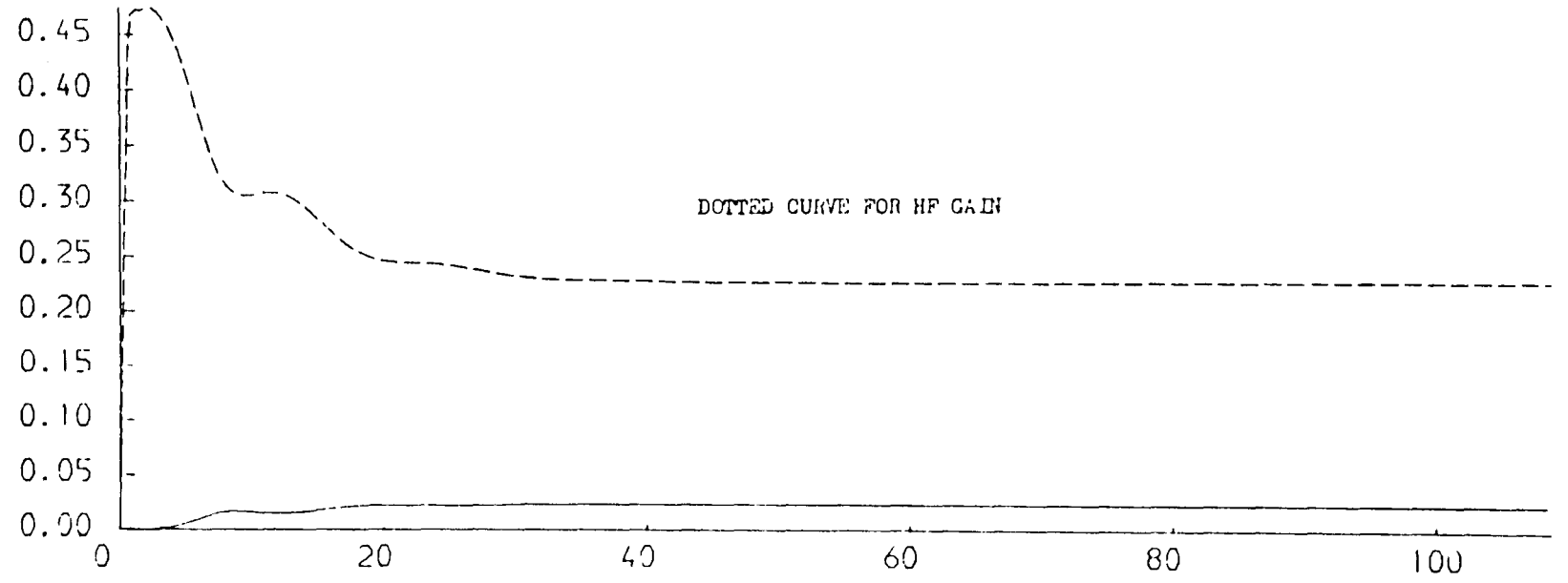

Figure (5.13): Low and high frequency Kalman gains for yaw position

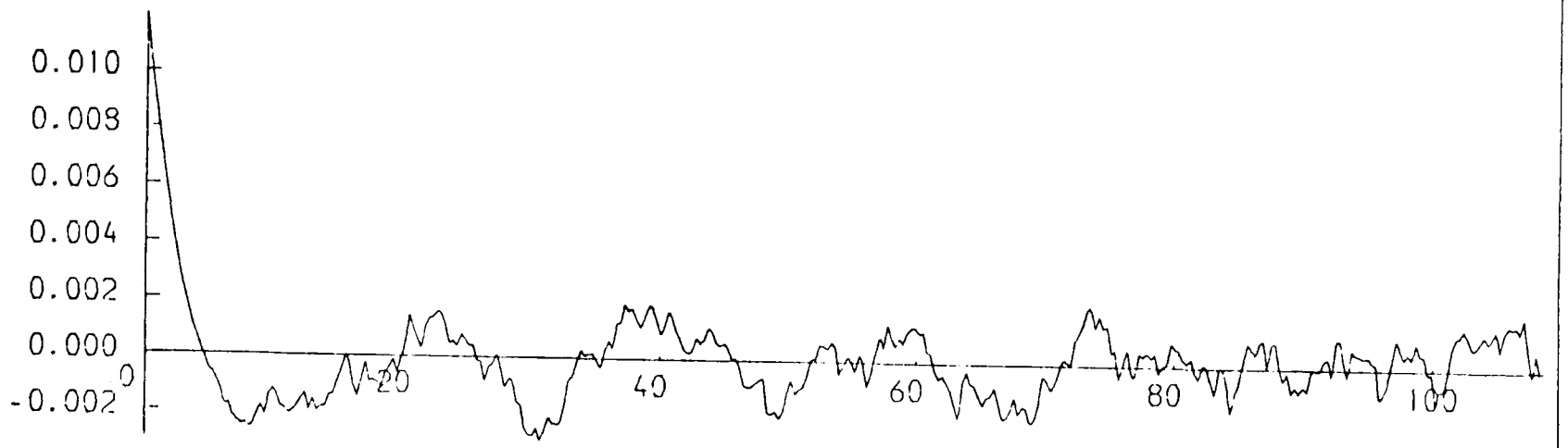

Figure (5.14) :Optimal control signal 1.

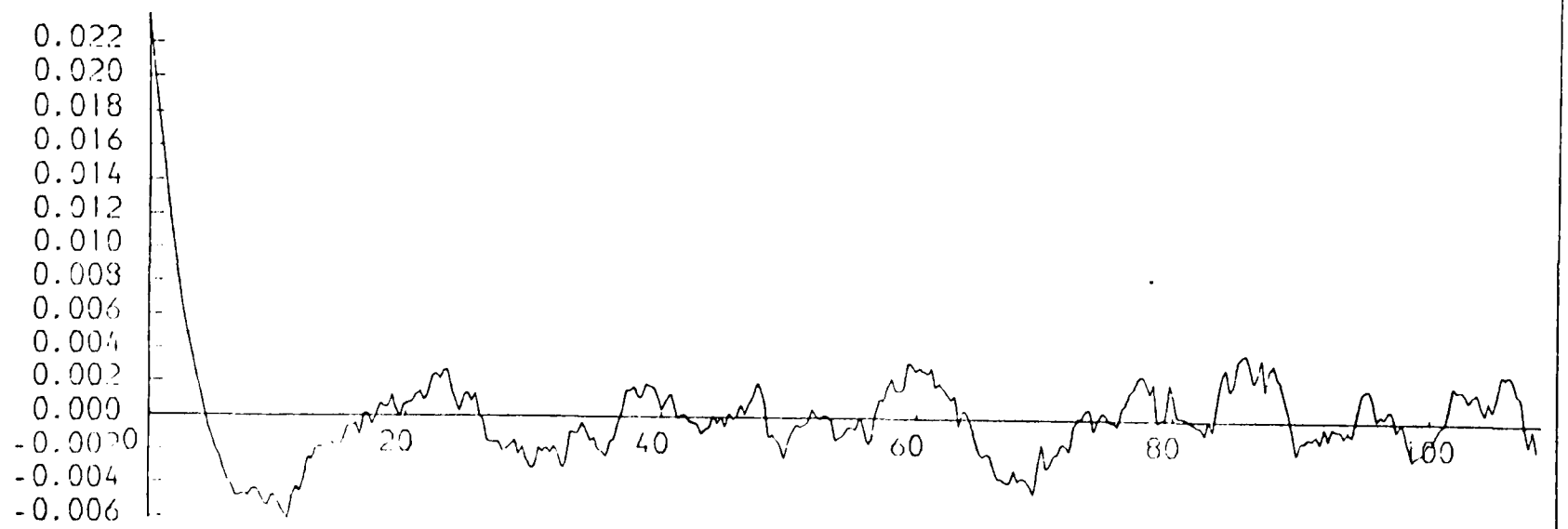

Figure (5.15) :Optimal control signal 2.

State (2): low-frequency sway position

State (3): low-frequency yaw angular velocity

State (4): low-frequency yaw angle

State (9): high-frequency sway position

State (13): high-frequency yaw angle

Figures 5.16 and 5.17 display the control signals into sway and yaw motions respectively for the system simulations with some saturation on the thrusters (such saturations and other non-linearities within the thruster devices will be considered in detail in Chapter 7). Figure 5.18 illustrates the effect of the control signal saturation on the speed of the system responses in sway motion.

5.3.3 Filter and Control Implementations for "Star Hercules" Vessel

The same software structure was used here for the implementation of Kalman filter algorithms and dynamic positioning control for the vessel "Star Hercules" as that of Section 5.3.2 of the vessel "Wimpey Sealab".

Computer plots of Figures 5.19 to 5.29 demonstrate the system responses with the corresponding filter estimates (shown by a dotted curve) of "Star Hercules" motions under dynamic positioning control and for a step input of 0.02 per-unit into sway motion. These responses show the system behaviour when the ship is subjected to a disturbance force of 4×10^{-6} per-unit force for sway and 9×10^{-8} per-unit turning moment for yaw.

Results displayed in this section were based on the "Star Hercules" dynamics of Section 3.2.4 and the corresponding optimal control obtained from Section 4.5.

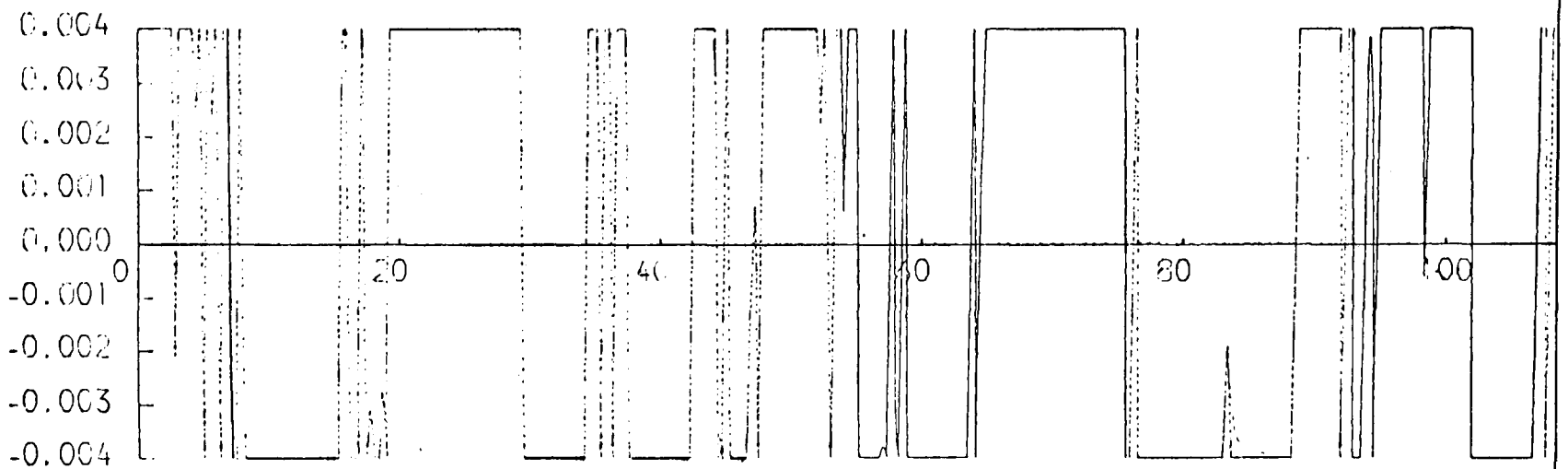

Figure (5.16) :Optimal control signal 1.

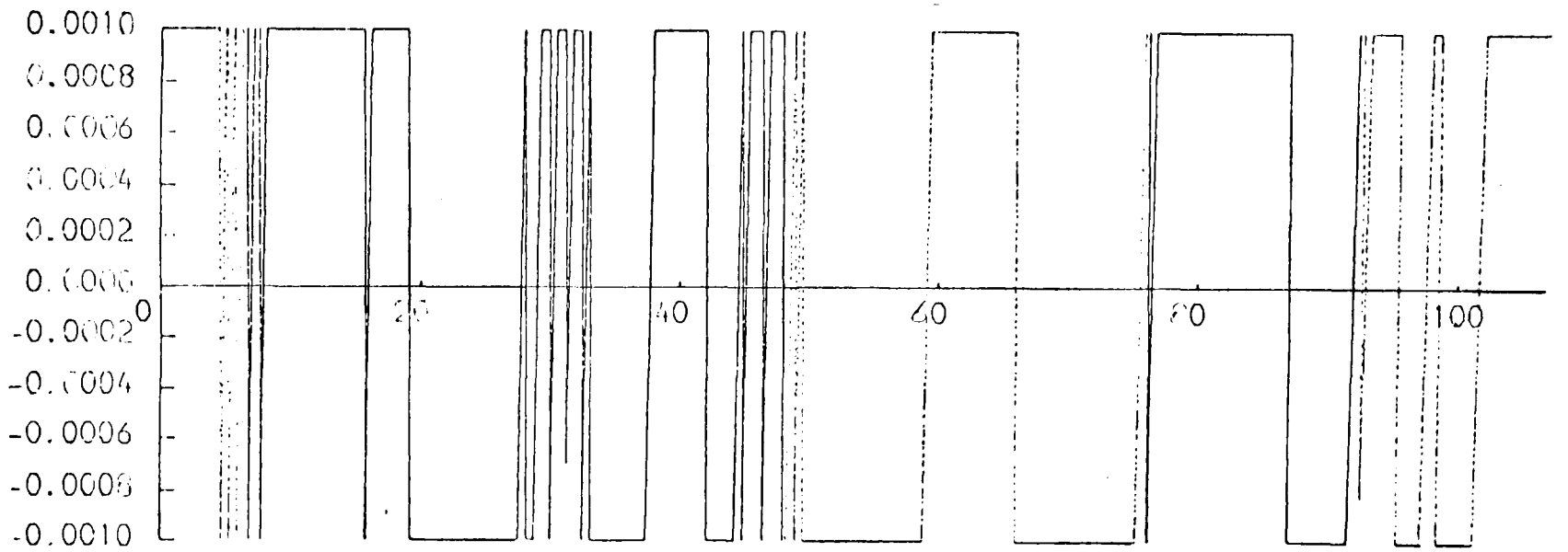

Figure (5.17) :Optimal control signal 2.

PLOTS OF TRUE AND ESTIMATED TRAJECTORIES FOR SWAY POSITION

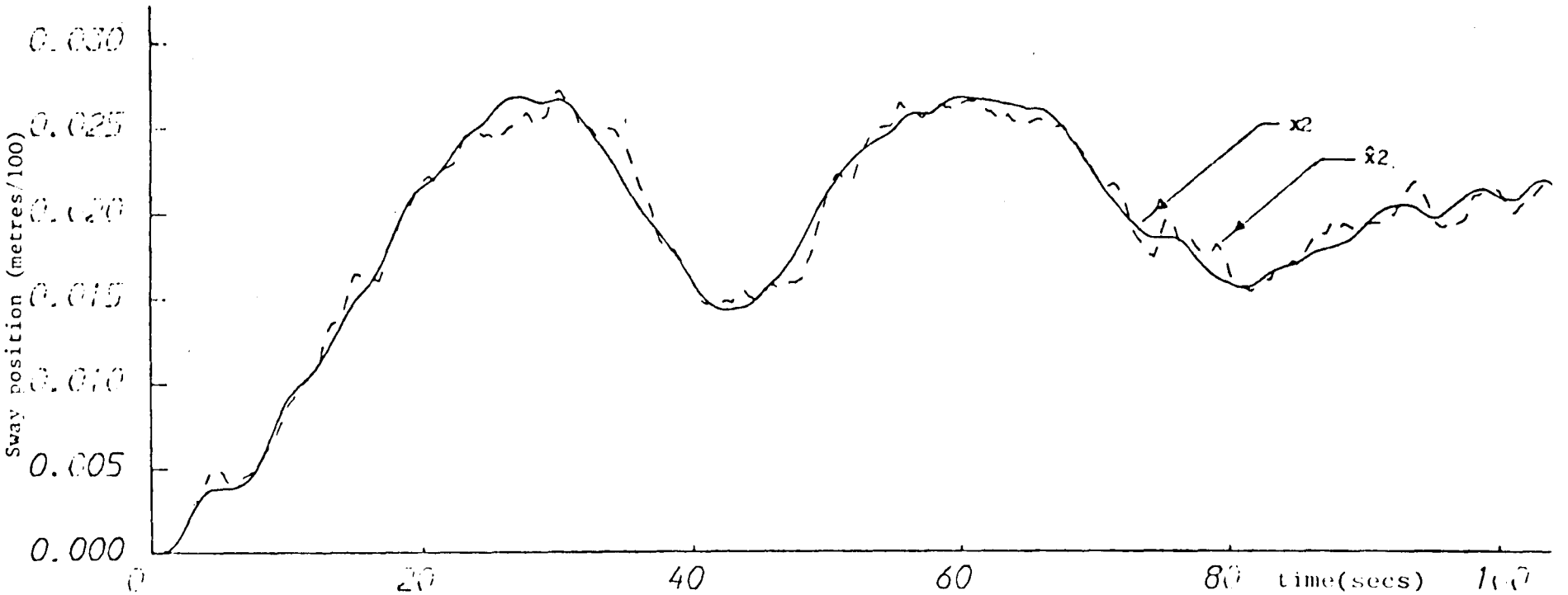

Figure (5.18)

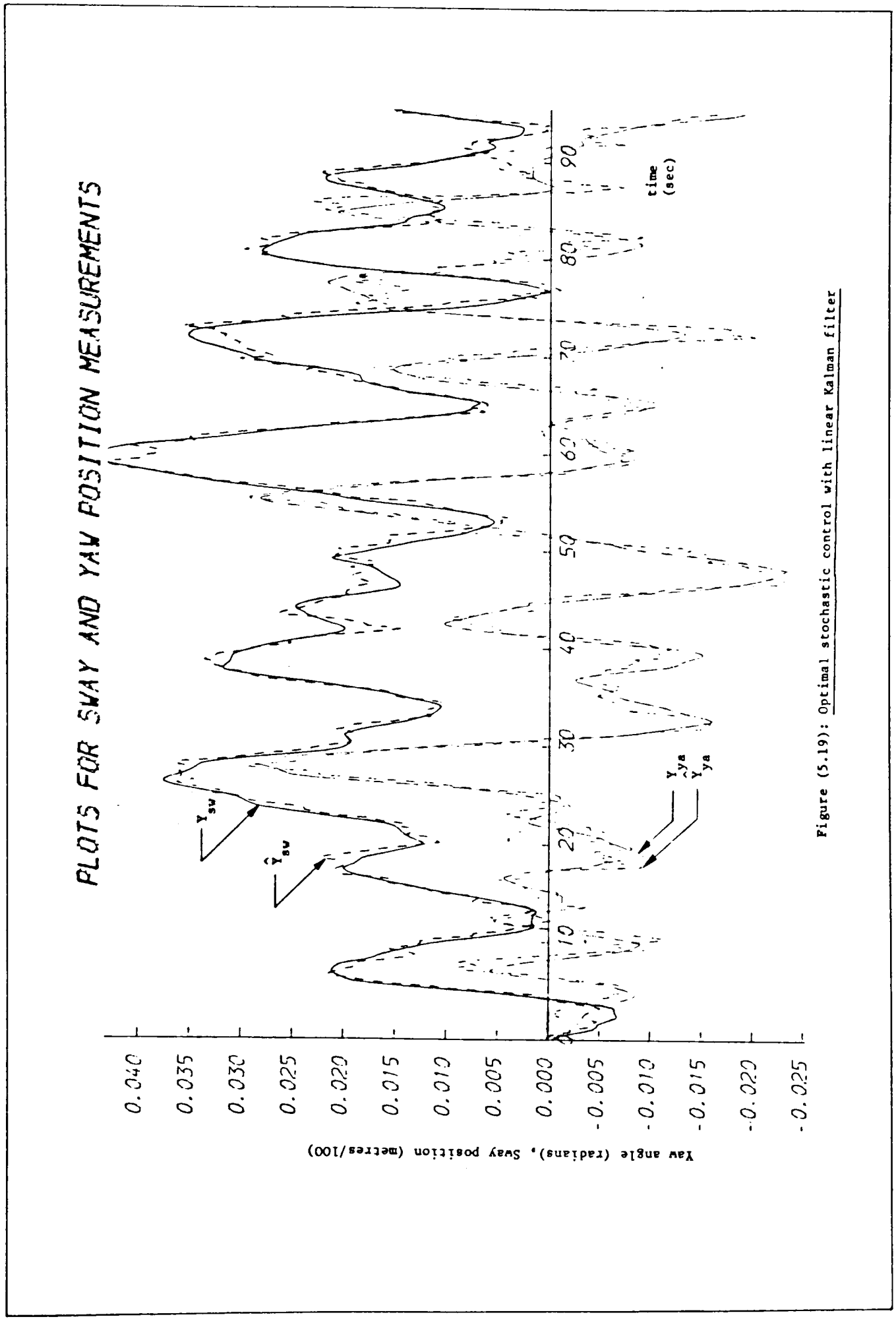

Figure (5.19): Optimal stochastic control with linear Kalman filter

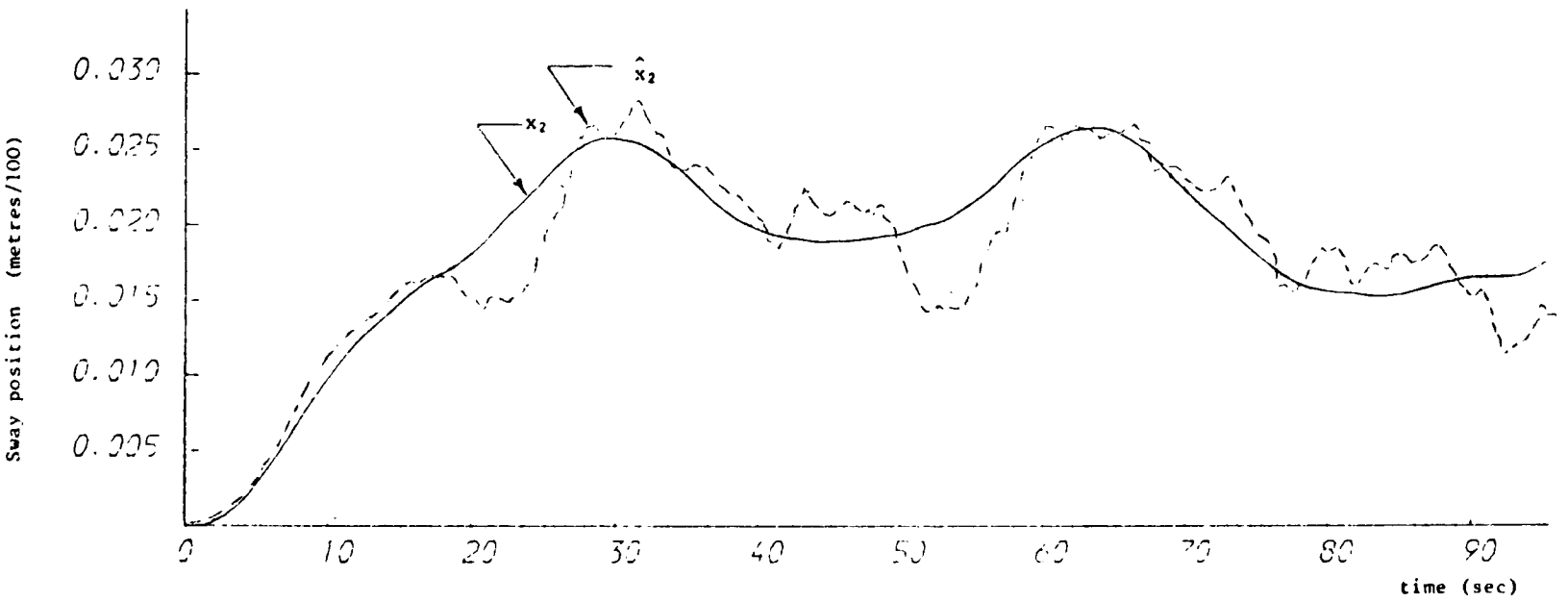

Figure (5.20): Sway low-frequency true and estimated position - state 2

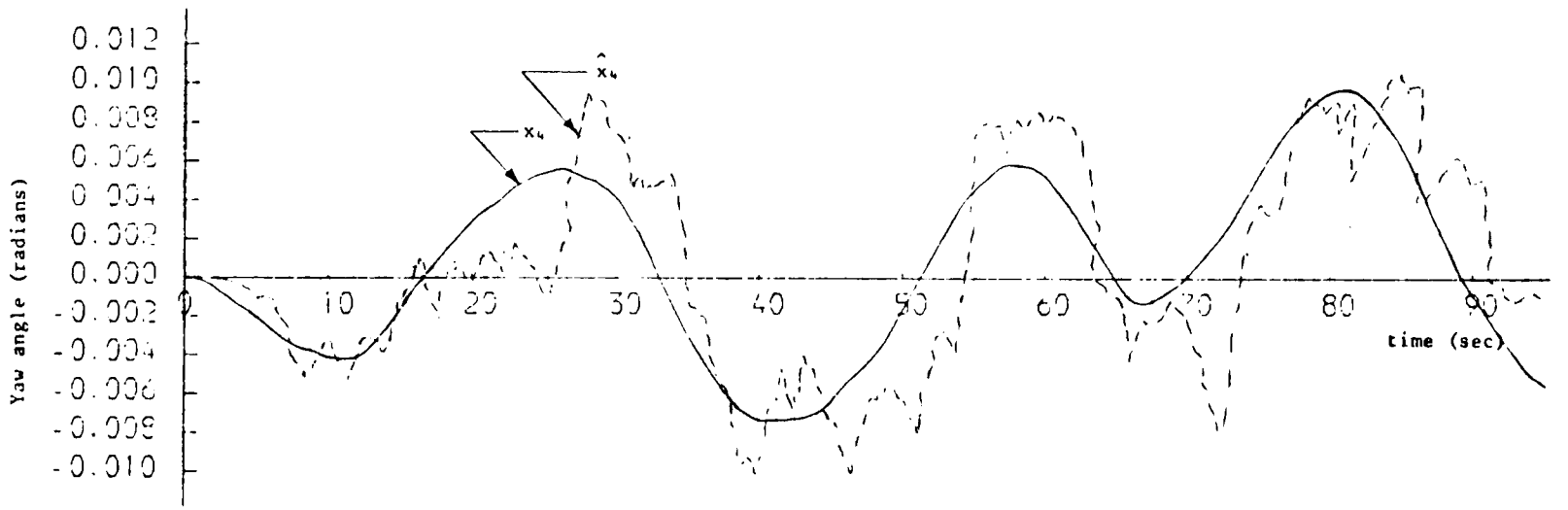

Figure (5.21): Yaw low-frequency true and estimated position - state 4

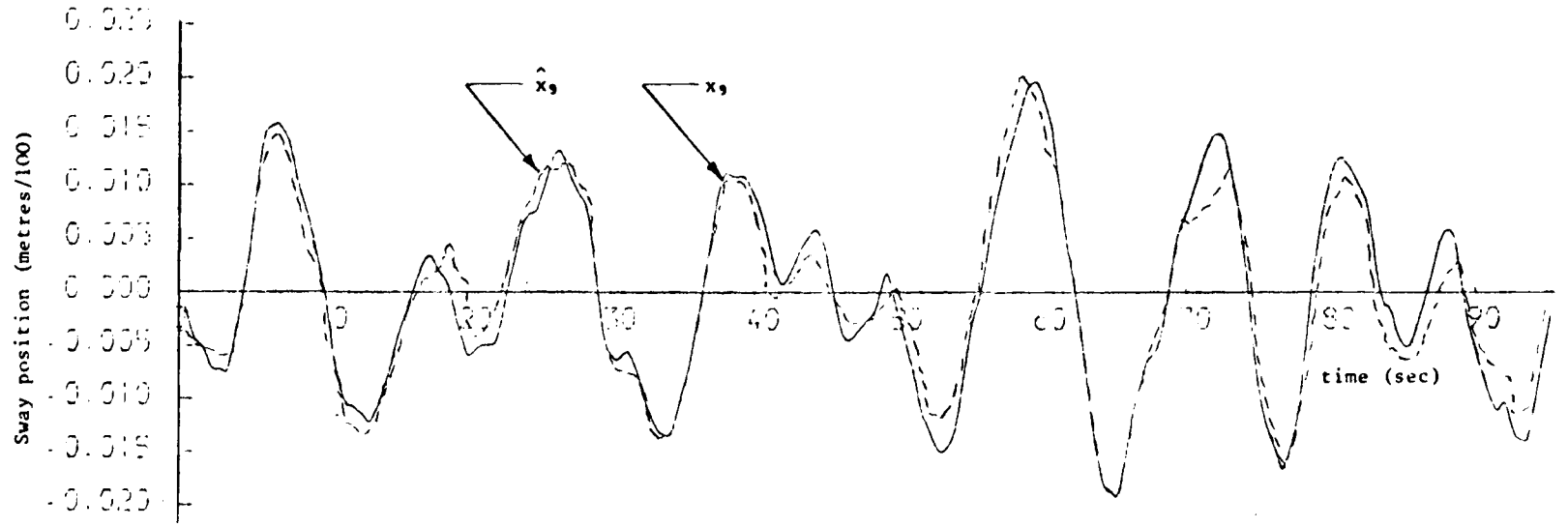

Figure (5.22): Sway high-frequency true and estimated position - state 9

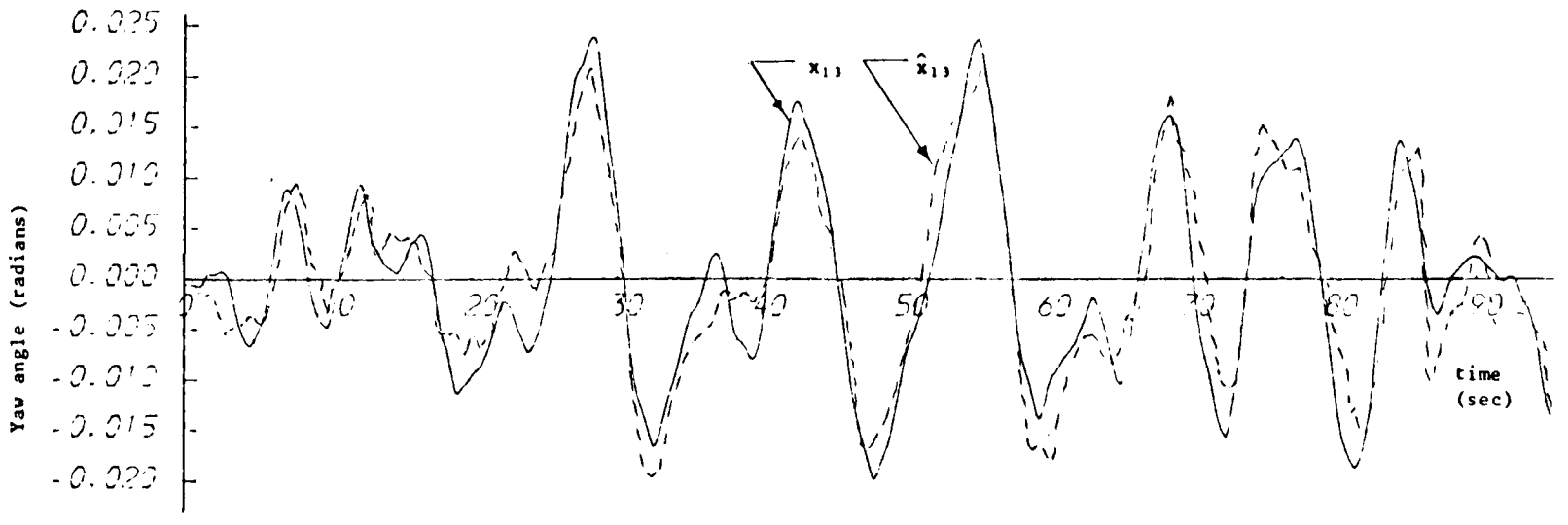

Figure (5.23): Yaw high-frequency true and estimated position - state 13

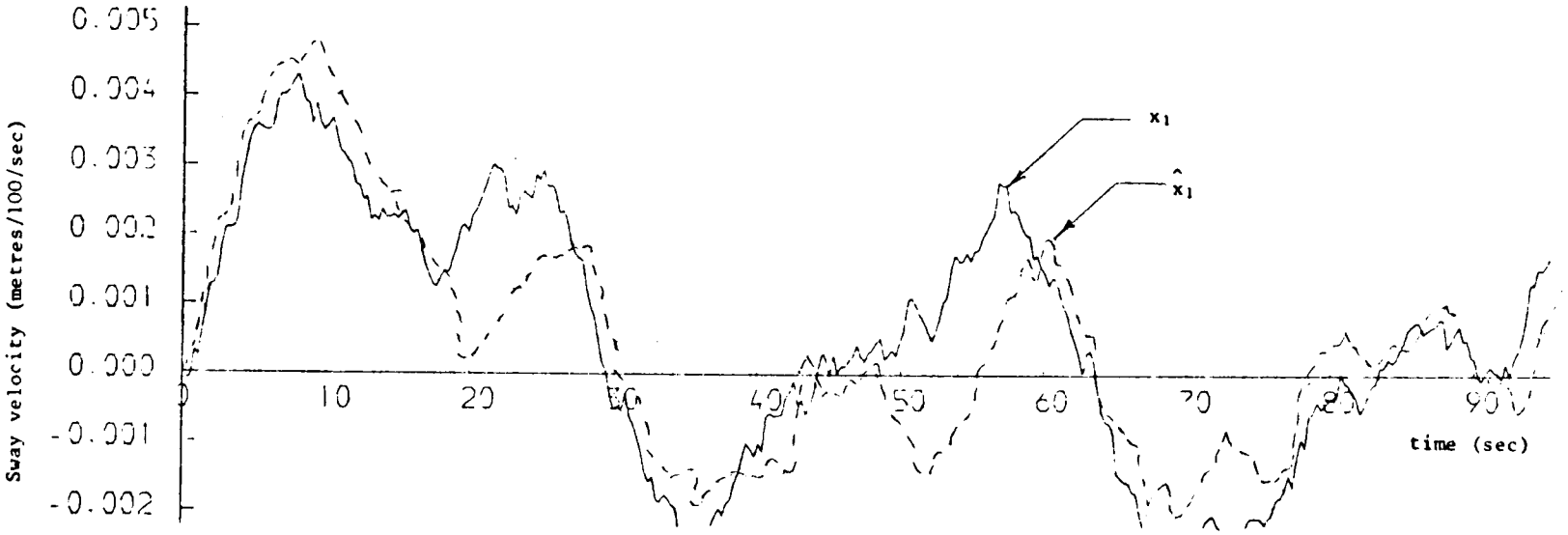

Figure (5.24): Sway low-frequency true and estimated velocity - state 1

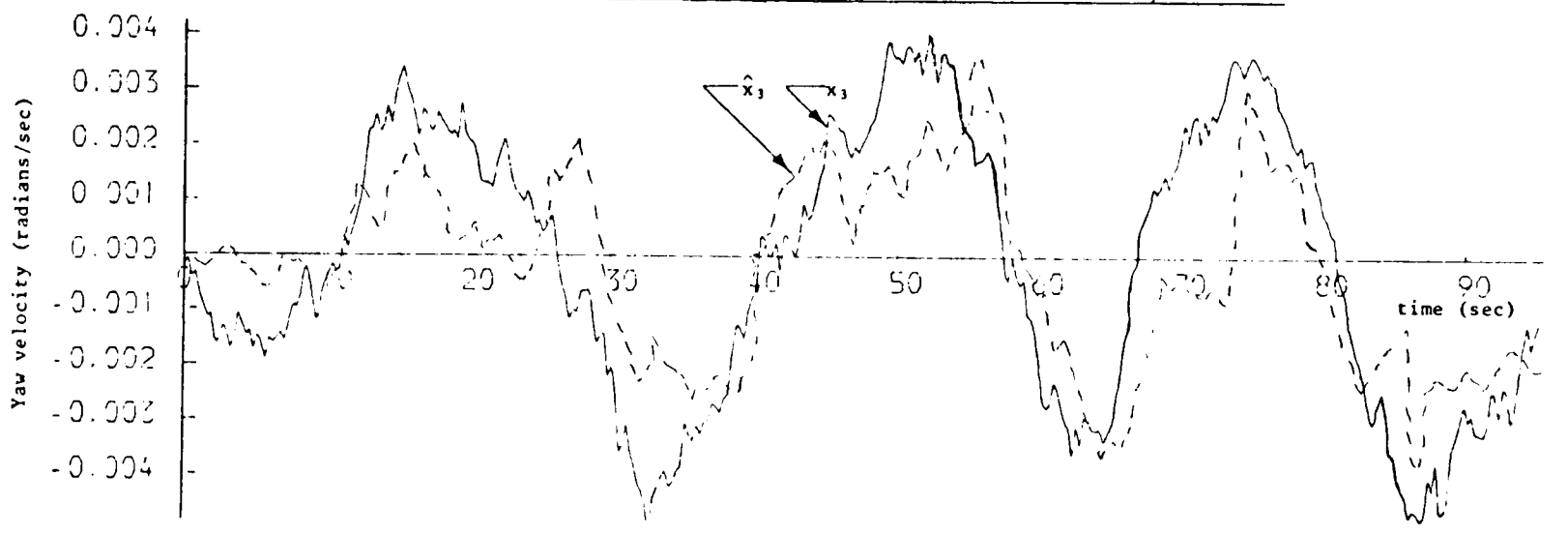

Figure (5.25): Yaw low-frequency true and estimated velocity - state 3

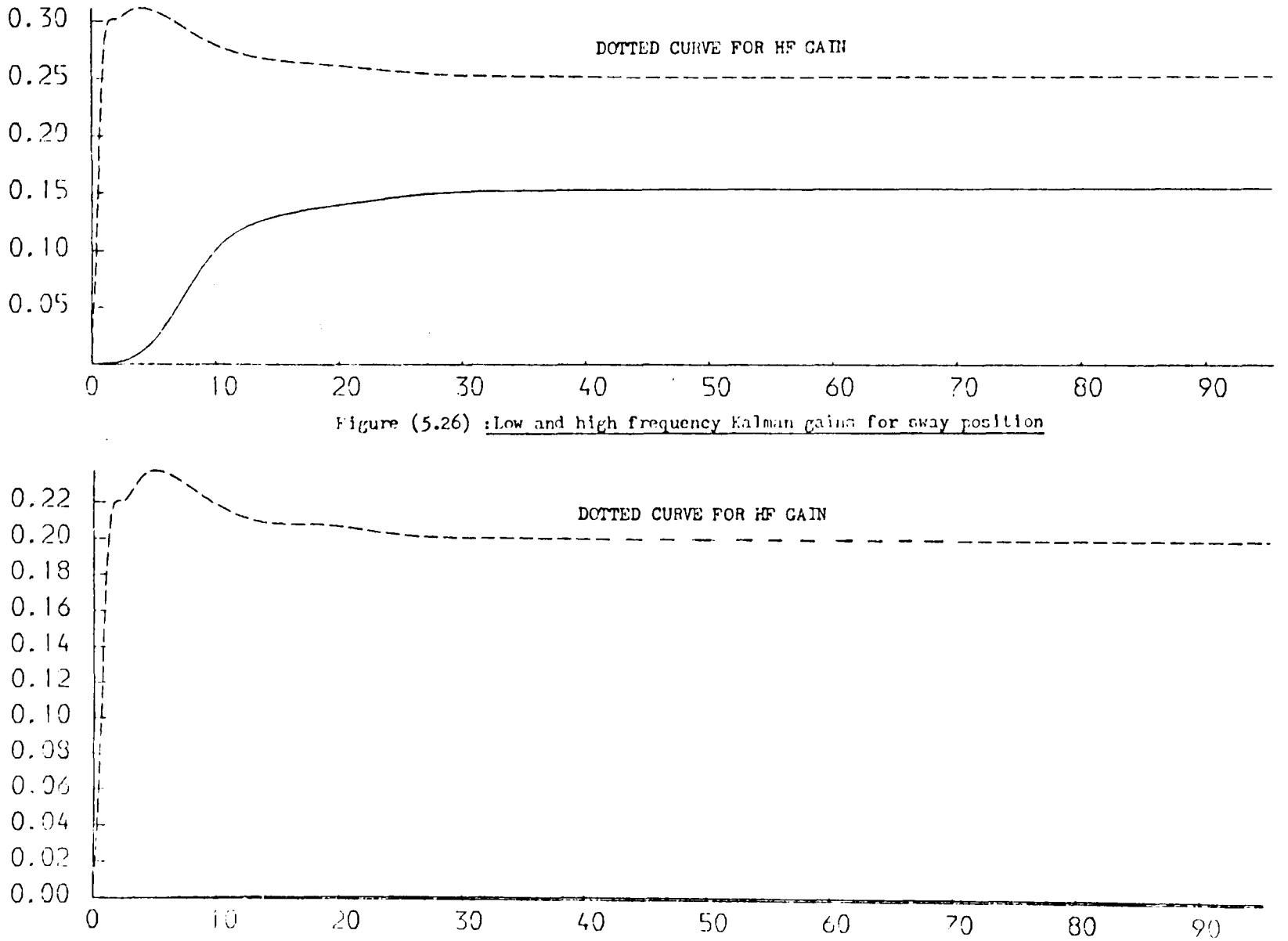

Figure (5.26) :Low and high frequency Kalman gains for sway position

Figure (5.27) :Low and high frequency Kalman gains for yaw position

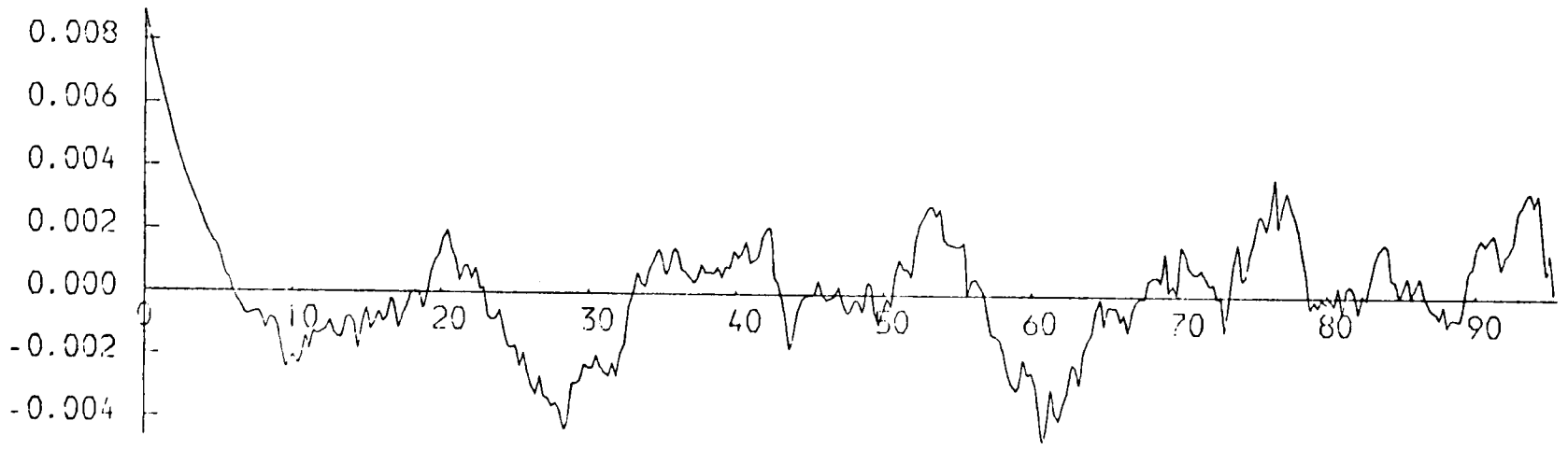

Figure (5.28) :Optimal control signal 1.

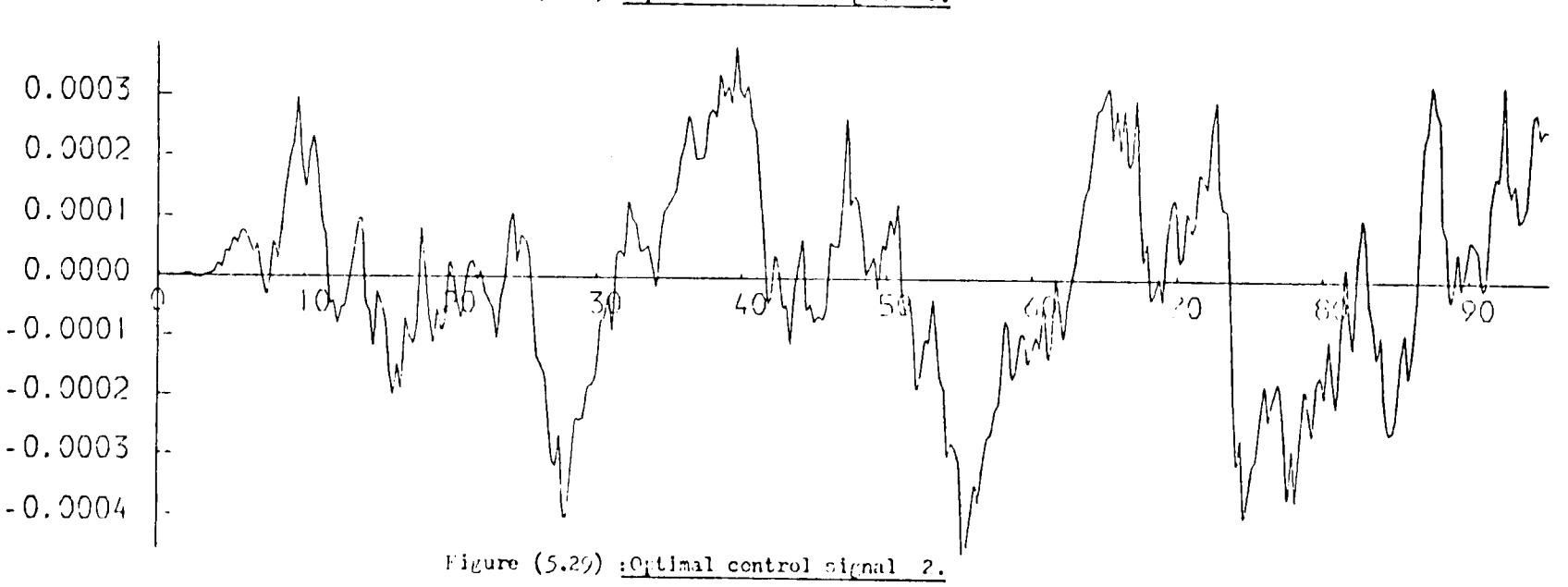

Figure (5.29) :Optimal control signal 2.

5.4 Concluding Remarks

In this chapter, dynamic ship positioning control has been implemented successfully using Kalman filtering techniques and optimal stochastic control. This scheme has been implemented based on models of the vessels "Wimpey Sealab" and "Star Hercules". System responses show good estimation and control. The saturation on the thrusters, illustrated by Figures 5.16 and 5.17, has a damping effect demonstrated by the slow sway position response of Figure 5.18. Saturation in the thrusters is an inherent feature of the actual system implementation. The Kalman filter is a time-varying filter, and hence the filter gain matrix has been computed at each sampling instant. Typical values of the filter gain for both "Wimpey Sealab" and "Star Hercules" will be listed below, corresponding to the constant filter gain region:

(i) Filter gain (Wimpey Sealab) =

$$\begin{bmatrix} 0.0618 & 0.0125 \\ 0.2235 & 0.0234 \\ 0.0383 & 0.1390 \\ 0.0658 & 0.3460 \\ 0.0013 & 0.0026 \\ 0.0000 & 0.0000 \\ -3.0208 & 0.0837 \\ -1.0127 & -0.0465 \\ 0.4034 & -0.0216 \\ 0.9550 & 0.0035 \\ 0.2312 & -1.8244 \\ -0.1203 & -1.0832 \\ -0.0584 & 0.2267 \\ 0.0118 & 0.7270 \end{bmatrix}$$

(ii) Filter gain (Star Hercules) =

$$\begin{bmatrix} 0.0443 & 0.0005 \\ 0.1544 & 0.0014 \\ 0.0047 & 0.0440 \\ 0.0062 & 0.1418 \\ 0.0012 & 0.0000 \\ 0.0000 & 0.0000 \\ -1.3888 & 0.0019 \\ -0.5104 & -0.0038 \\ 0.2515 & -0.0010 \\ 0.3689 & 0.0006 \\ 0.0193 & -0.9929 \\ -0.0071 & -0.3887 \\ -0.0046 & 0.2006 \\ 0.0011 & 0.2459 \end{bmatrix}$$

These filter gains represent a sample from the constant region of the gain matrix shown in Figures 5.12, 13, 26 and 27. The system responses are acceptable from the practical point of view; however, the response speed can be varied by tuning the controller and its related weightings (Chapter 4).

C H A P T E R (6)

CHAPTER 6

PRACTICAL INVESTIGATION INTO THE USE OF KALMAN FILTERING FOR DYNAMIC POSITIONING

6.1 Introduction

Kalman filtering techniques have been found suitable for many industrial applications in recent years. They have been implemented successfully for a nuclear reactor control problem,for a marine navigation system [53] and in the metal industry [44]. The filtering scheme has shown to be very reliable and practical in its applications to the dynamic ship positioning problem. However, inaccuracies in the system model and incorrect filter dynamics representation, especially with the required approximations and necessary linearisations could frequently cause a loss of system reliability. Theoretically, the Kalman filter is a statistical technique which produces the optimum estimates of the state vectors of the linear/linearised dynamic system from a succession of noisy measurements. A knowledge of the dynamical behaviour and error characteristics of the system is an essential pre-requisite. In practice, the necessary information required to construct the Kalman filter is only approximately known. Hence, one of the objectives of this chapter is to investigate the quality of the system representation in the filter structure.

The Kalman filter scheme has been widely used to solve the linear/non-linear estimation problem because of its practicability and robustness. However, this solution adds some complexity and also the large number of dimensions in the augmented state is a severe computational disadvantage for large multivariable systems [76]. Contribution will be made here to reducing such filtering and control computational

cost by two different ways as applied to our specific ship positioning scheme [93],[97]:

(i) Semi-constant gain Kalman filter (Section 6.3).

(ii) Reduced-order Kalman filter (Section 6.2)

Dynamic ship positioning using the Kalman filtering techniques gives a system performance substantially better than can be obtained by systems employing conventional filtering networks [91]. In previous chapters, a fundamental implementation of the Kalman filter and optimal stochastic control were established and applied to the two vessels under consideration (Chapter 3). However, to evaluate the goodness of any scheme, the following steps should be noticed and investigated:

(i) Cost.

(ii) Reliability and robustness.

(iii) Accuracy.

Hence, the above factors will be considered and investigated in this chapter since adequate filter models, enough initial condition information and realistic noise statistics can be difficult to achieve in practice.

6.2 Reduced-Order Kalman Filter

It is normally assumed that none of the states may be measured directly and in this case, the Kalman filter has the same dimension as that of the plant. In dynamic positioning problems, Kalman filter estimates the low-frequency states for state feedback control [3]. Part of the low-frequency states are associated with the actuators output, which may be measured without contamination by noise [6] [37]. It follows that a reduction in the dimension of Kalman filter may be achieved, equal to the number of the measurable states [80]. In such cases, the feedback control scheme will consist of direct state-feedback combined

with state-estimate-feedback.

The use of direct state-feedback from the measurable states, and the consequent reduction in size of the filter has several indirect advantages [96]. Direct state-feedback improves the transient response of the system, since this feedback loop would otherwise contain a filter which degrades performance. The reduction in the dimension of the filter also reduces modelling errors, since only part of the plant is represented in the filter for state estimation. The actuators are non-linear elements, and hence assuming their states as measurable variables will reduce the effect of the non-linearities within the modelled plant.

In applying the above simplification to the dynamic positioning problem using Kalman filtering techniques and considered for sway and yaw motions only, two states can be measured corresponding to the states of the two sway and yaw thrusters [37]. Hence, the dimension of the Kalman filter will be reduced from 14 states down to 12 states. The reduction in size of the Kalman filter is particularly valuable in dynamic ship positioning control systems since the size of on-board computer is limited.

The following analysis will illustrate the application of the combined state and state estimate control to the dynamic ship positioning control systems [37]. The ship dynamics can be represented by the usual linear state equation as:

$$\begin{bmatrix} \dot{\underline{x}}_1 \\ \dot{\underline{x}}_2 \end{bmatrix} = \begin{bmatrix} A_{11} & A_{12} \\ 0 & A_{22} \end{bmatrix} \begin{bmatrix} \underline{x}_1 \\ \underline{x}_2 \end{bmatrix} + \begin{bmatrix} 0 \\ B_2 \end{bmatrix} u + \begin{bmatrix} \underline{\omega}_1 \\ \underline{\omega}_2 \end{bmatrix} \quad \ldots\ldots\ldots (6.1)$$

$$\underline{y} = \begin{bmatrix} C_1 & 0 \end{bmatrix} \underline{x} \quad \ldots\ldots\ldots (6.2)$$

$$\underline{z} = \begin{bmatrix} C_1 & 0 \end{bmatrix} \underline{x} + \underline{v} \quad \ldots\ldots\ldots (6.3)$$

where the system has been partitioned into a measurable part $\underline{x}_2$ which includes the thrusters, and the remaining state variables $\underline{x}_1$. $\underline{u}$ is the thrusters control signals and $\underline{y}$ is the total position of the vessel from some reference point.

$\underline{\omega}_1$, $\underline{\omega}_2$ and $\underline{v}$ are white noise signals with covariance matrices Q_1, Q_2 and R respectively. $A_{21} = 0$, since the thruster states do not depend upon the other state variables in most industrial problems. The system is illustrated in Figure 6.1.

Since some of the states are assumed to be measurable (the thruster states), the size of Kalman filter algorithm and the related filter model structure used in Chapter 5 for simulation will be reduced in proportion to those measurable states. The structure of the ship model will remain unchanged.

The system responses based on the above proposed reduced-order Kalman filter for estimation are illustrated in Figures 6.2 to 6.6. These simulations have been carried out using data from "Wimpey Sealab" vessel of Section 3.2.3. States (7) and (11) and their estimates of Figures 6.5 and 6.6 are the high-frequency sway position and yaw heading respectively which correspond to states (9) and (13) and their estimates in the full Kalman filter of Chapter 5.

6.3 Semi-Constant Gain Kalman Filter

The implementation of Kalman or extended Kalman filters for estimation and control is a straightforward process copied from the actual plant dynamics to be controlled. This nature of the filter dynamics gives it the practicability for on-line estimation. However, the computation time required to implement the filter could exceed the usual practical limit for real-time applications. This difficulty can be clearly

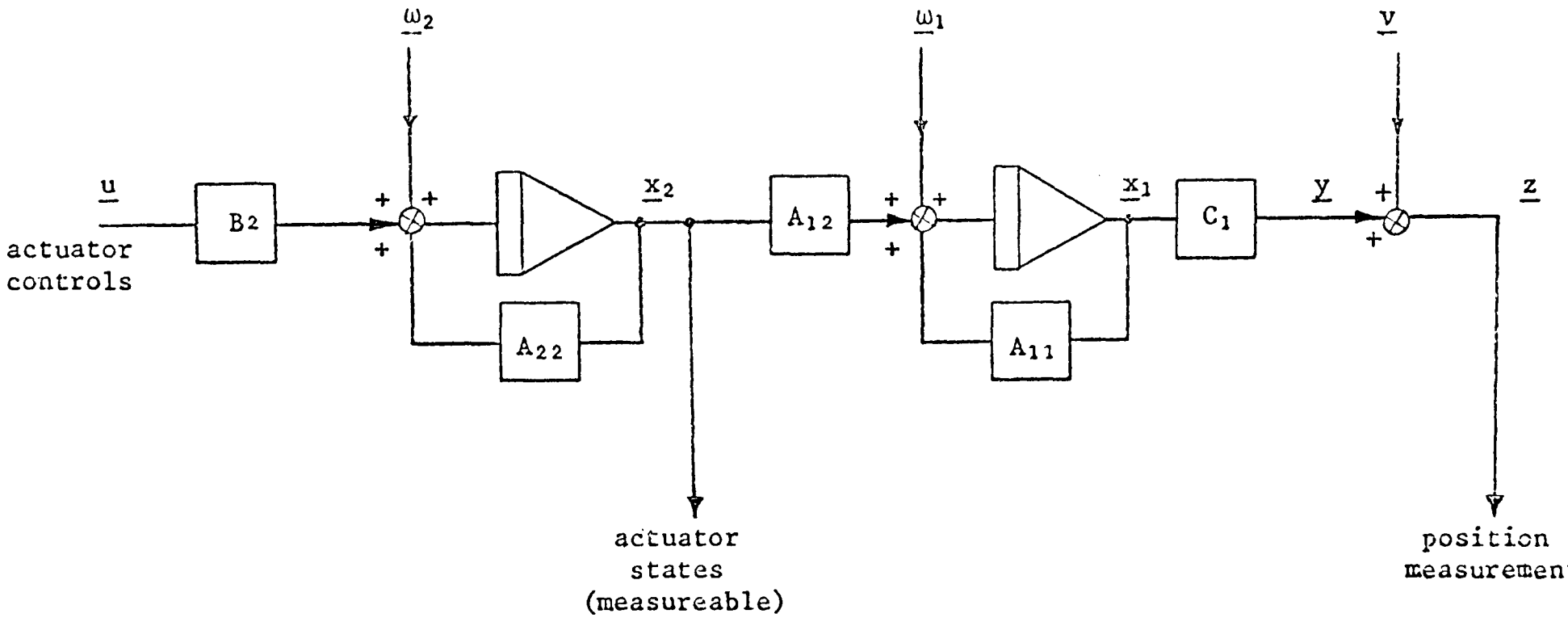

Figure (6.1): The State Description of a Dynamically Positioned Vessel

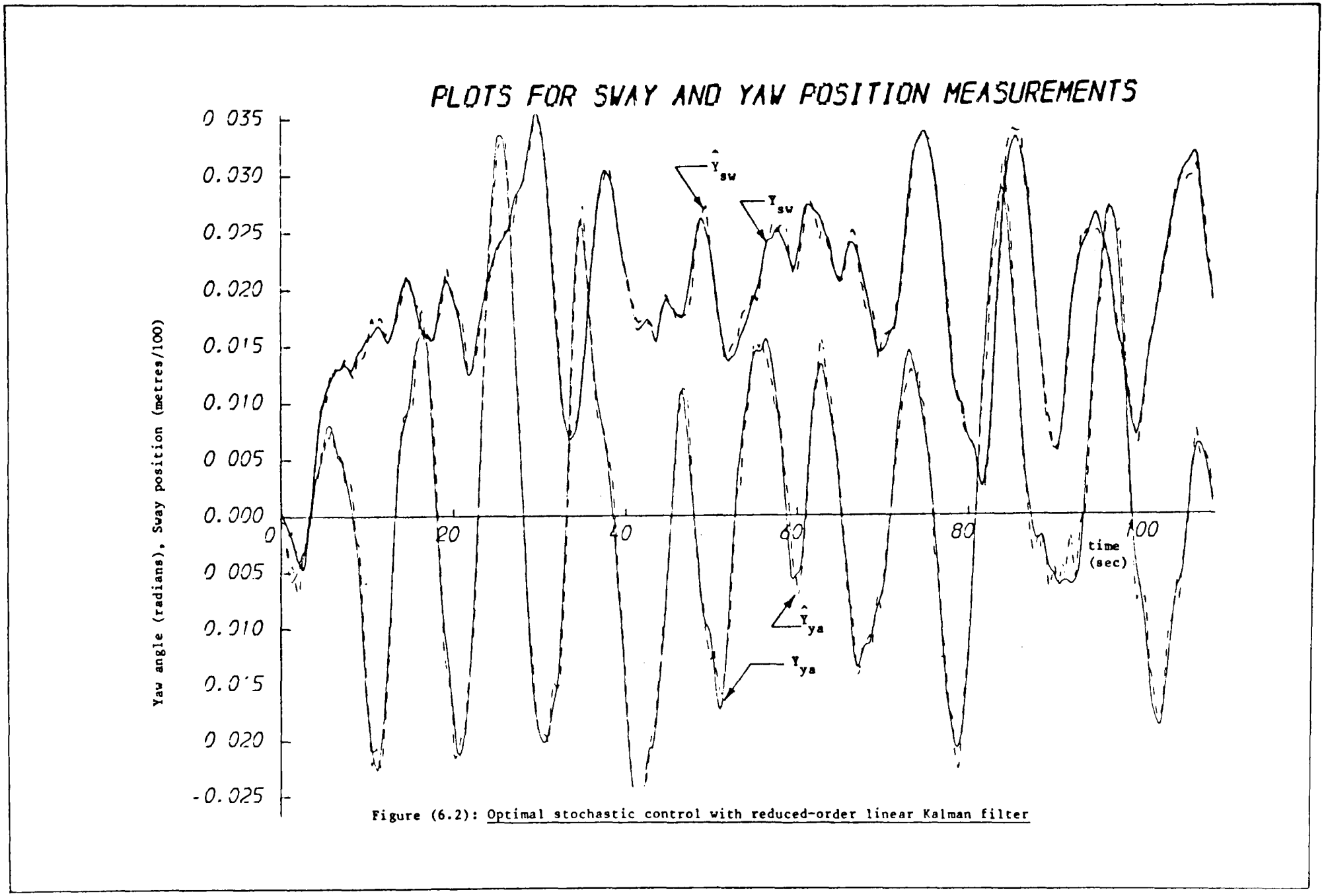

Figure (6.2): Optimal stochastic control with reduced-order linear Kalman filter

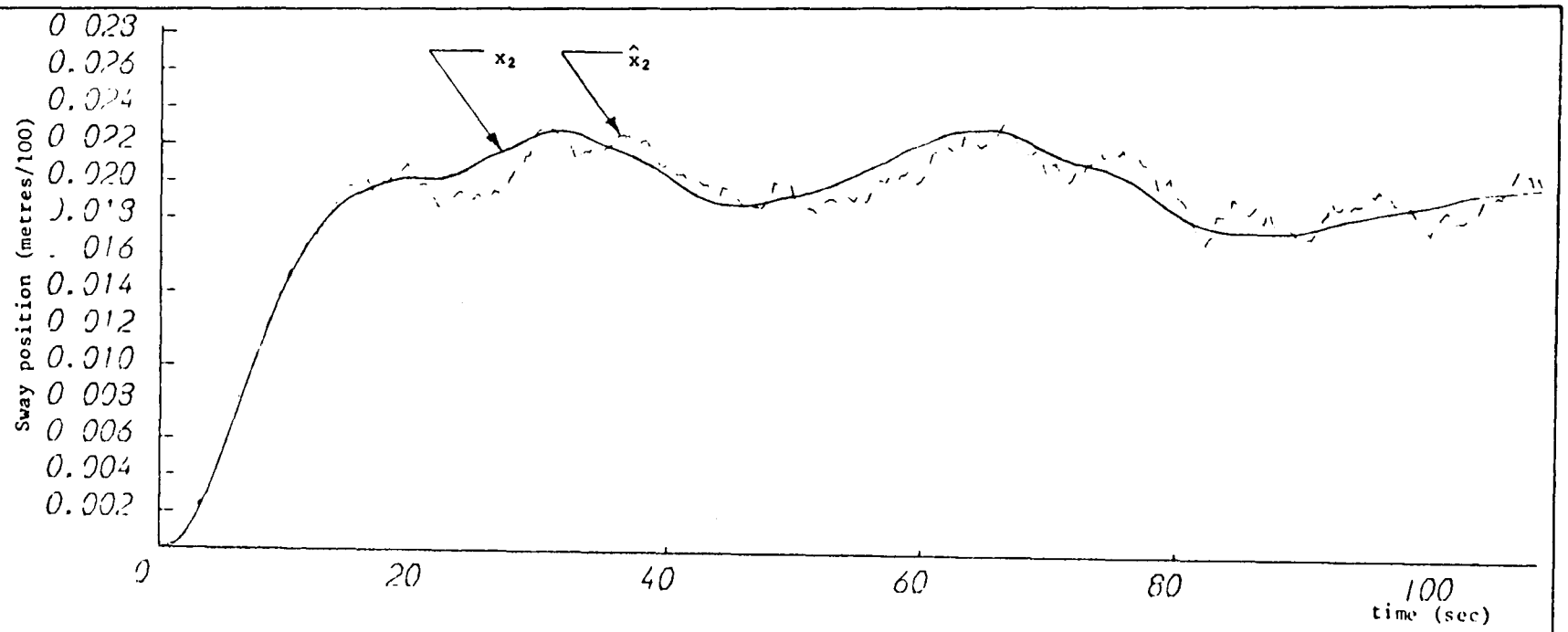

Figure (6.3): Sway low-frequency true and estimated position - state 2

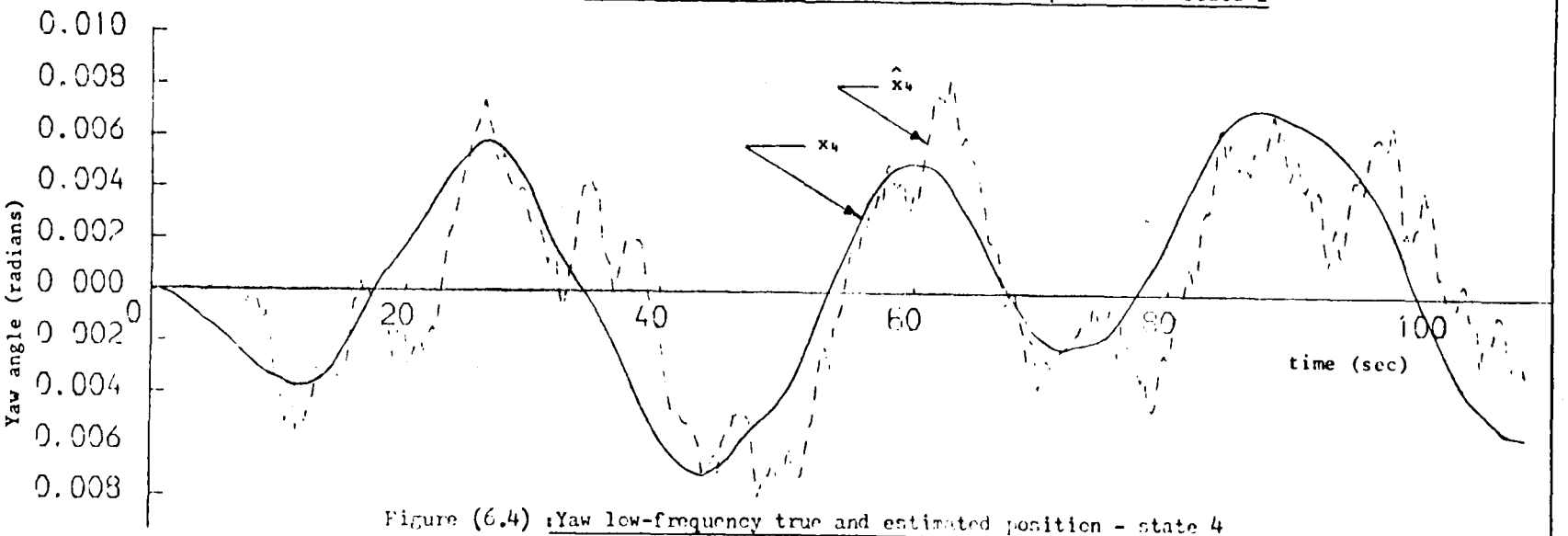

Figure (6.4) :Yaw low-frequency true and estimated position - state 4

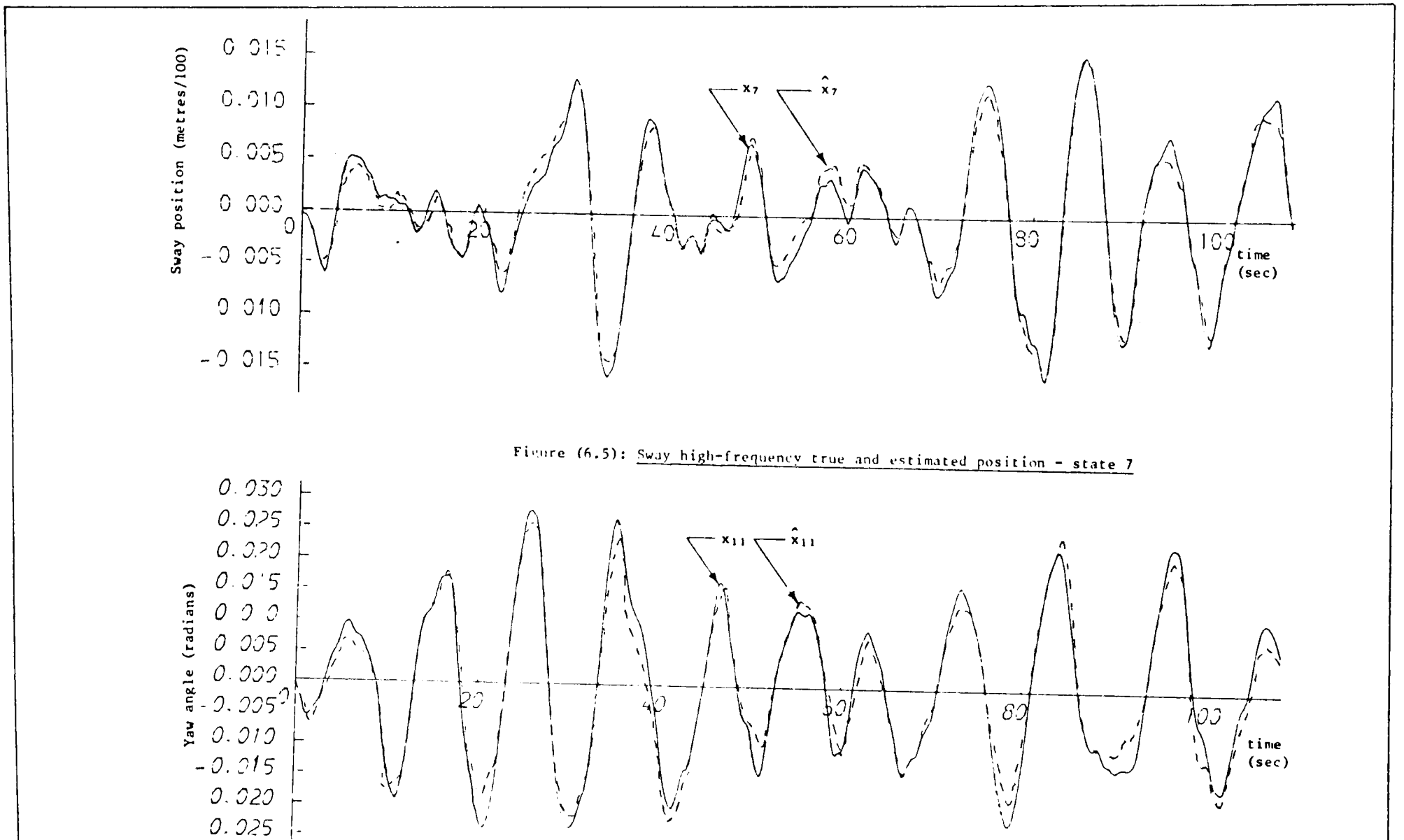

Figure (6.5): Sway high-frequency true and estimated position - state 7

Figure (6.6): Yaw high-frequency true and estimated position - state 11

realised when a limited space only is available for on-board computers and processing equipment especially for ship positioning or space applications. Basically, the high computational burden encountered by using Kalman algorithms for estimation is mainly concerned with the re-computations of the error covariance matrix by solving the Riccati equation and with the calculations of the related Kalman gain matrix, and hence a great saving in computing time can be obtained by pre-computing and storing the filter gain matrix. In the linear case, the system simulation results for both "Wimpey Sealab" and "Star Hercules" vessels of Chapter 5 have shown that elements of Kalman gain matrix settle to a constant value after approximately twenty seconds from the initial condition. This fact could give the possibility of applying a partitioning process on the gain calculations in which the gain matrix can be assumed constant and need not be computed on-line after twenty seconds. [57], [24], [56].

In this section, full simulation of the ship using Kalman filter for estimation and based on data from "Wimpey Sealab" were performed on the basis of the above partitioning procedure of the filter gain calculations. To ensure the stability of the system behaviour and to reduce the effect of using constant Kalman gain for system implementation, the filter gain has been assumed constant after 28 seconds rather than after 20 seconds. System responses for the ship low-frequency controlled position and heading together with the total low and high frequency ship trajectory are shown in Figures 6.7, 6.8 and 6.9 respectively, and are for step input of 0.02 per-unit into sway with the ship hull subjected to the same disturbance forces described in Section 5.3.2. These responses show no loss of accuracy with the advantage of reduced computing time. Selected elements of the Kalman gain matrix have also been shown in Figures 6.10 and 6.11.

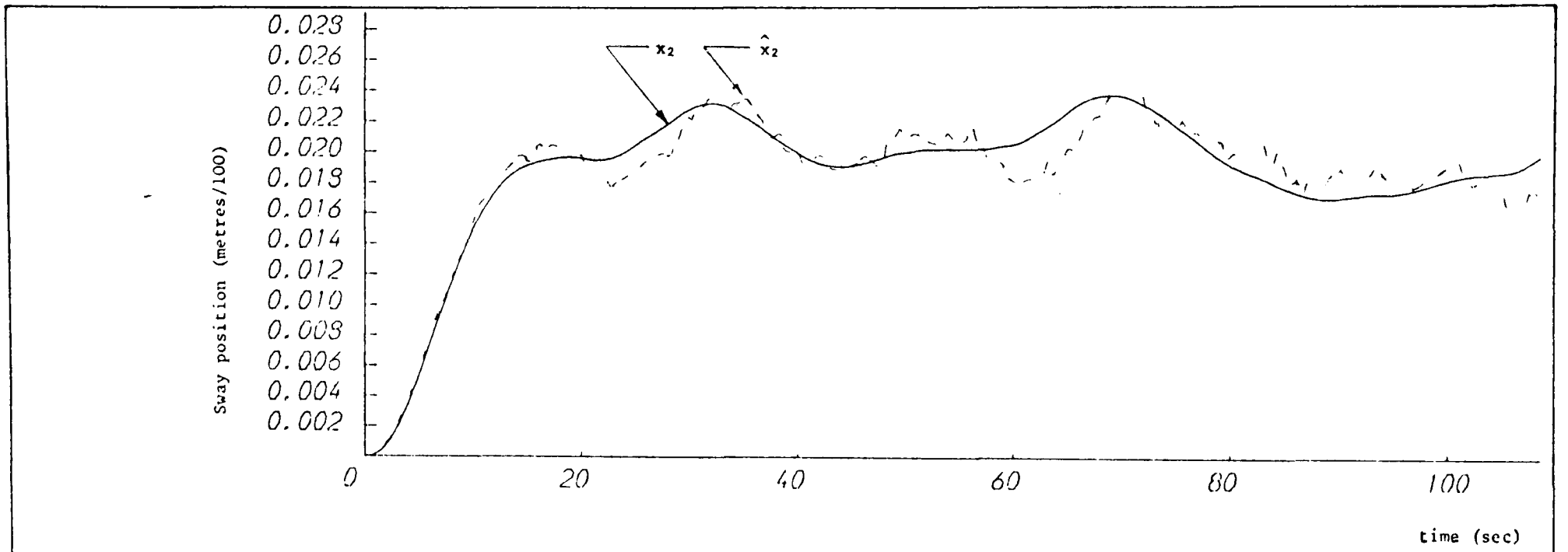

Figure (6.7): Ship low-frequency true and estimated position - state 2

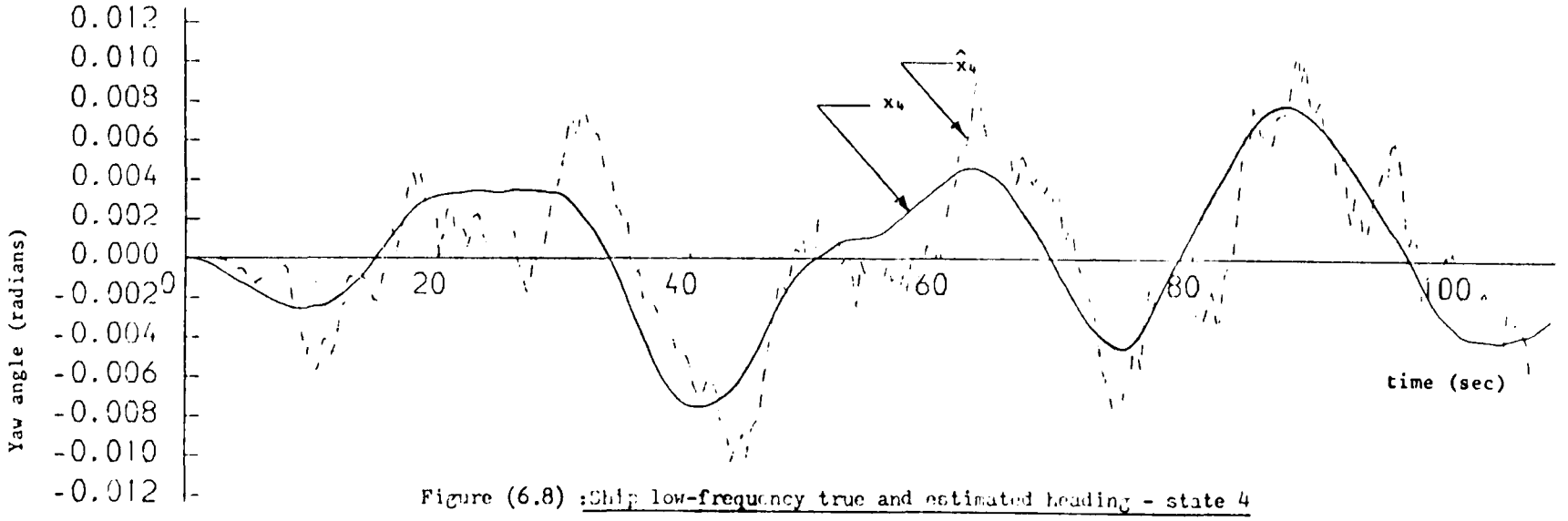

Figure (6.8) :Ship low-frequency true and estimated heading - state 4

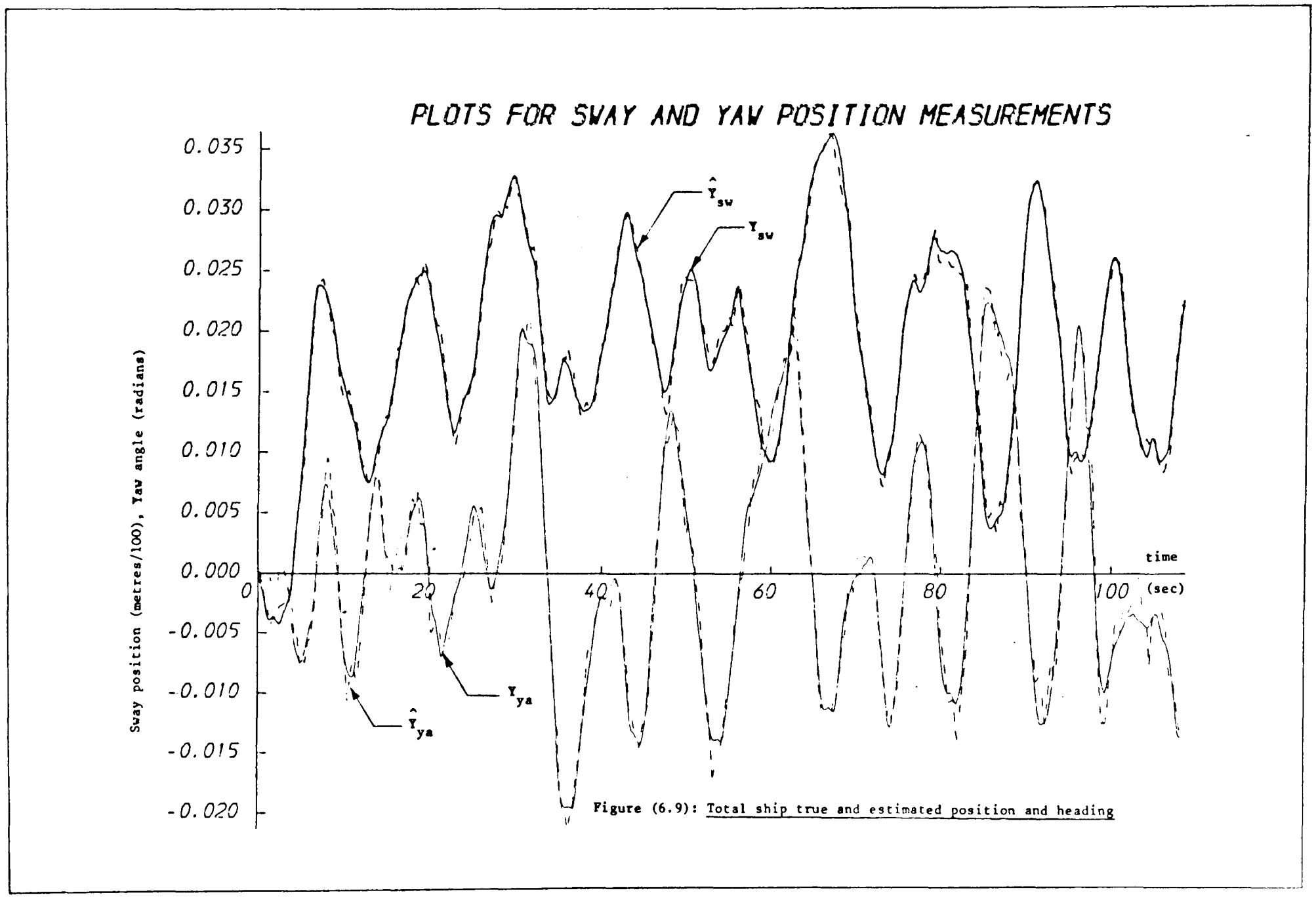

Figure (6.9): Total ship true and estimated position and heading

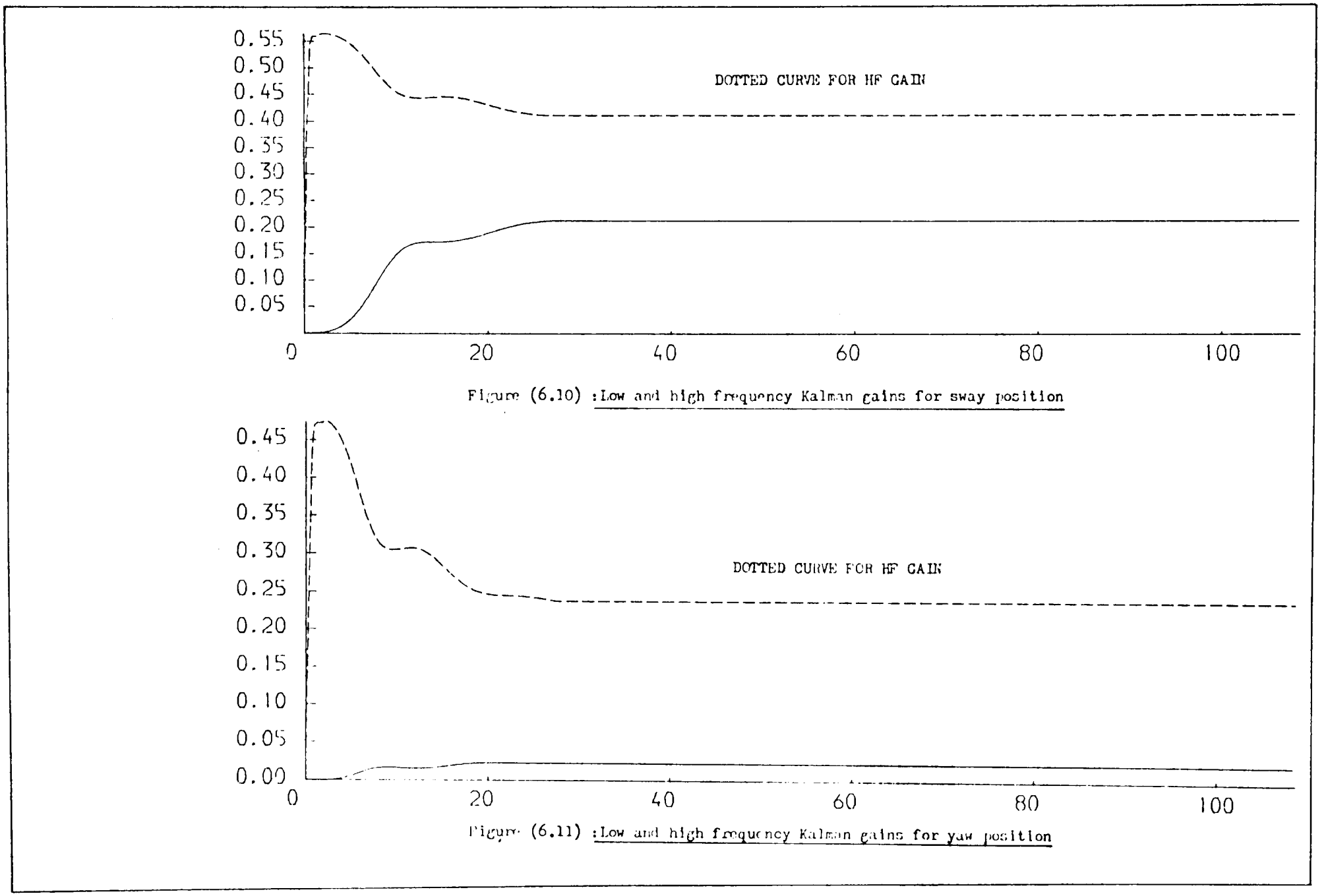

Figure (6.10) :Low and high frequency Kalman gains for sway position

Figure (6.11) :Low and high frequency Kalman gains for yaw position

6.4 Filter Mismatching

Before an effective control strategy can be implemented, there must be available an adequate model of the dynamics of the controlled plant, so that simulation settings may be chosen in more realistic fashion. The applications of Kalman filtering theory developed to date assume that system dynamics are completely known and are precisely modelled in the filter. Clearly, this will never be true in practice since for a highly complex system, there is often a lack of knowledge of part of the plant behaviour. Although the Kalman filtering scheme has proved to be practically useful in a variety of industrial applications, it has become apparent that insufficient care in constructing the filter can easily lead to entirely unacceptable system responses [29] [55] [92]. Such mismatch between the filter and the plant models can cause sensitivity problems and even divergence of a Kalman filter [26] [89] [100] [86]. Such modelling errors can arise when the nominal parameters used to construct Kalman filter are different from the parameters used to construct the actual plant. Mismodelling may arise from individual or combined effects of errors in:

(i) the actual mathematical formulation of the system dynamics,

(ii) measurement signal processing,

(iii) noise and environmental statistical considerations.

For the purpose of this study, a Kalman filter has been implemented for dynamic positioning control and constructed to consist of low and high frequency subsystems. The high-frequency dynamics are to represent the simulated sea waveform (Section 3.3). Tests were obtained for different sea conditions and vary from Beaufort number 5 for a calm sea state to the worst sea condition of Beaufort number 9. Throughout the design and

implementation of Kalman filtering for the dynamic ship positioning under consideration, the high-frequency dynamics were developed on the basis of data for Beaufort number 8 sea conditions. These system developments of the high-frequency dynamics for Beaufort number 8 sea conditions were copied into the filter, and hence, the filter structure will represent a model of the actual ship dynamics (the high-frequency part).

The purpose of this section is to investigate the mismatching effect on system behaviour by using the filter model of Beaufort number 5 data, but using information for the ship dynamics derived from Beaufort number 8 conditions. The actual changes in the system and filter dynamics can be noticed from the system and filter sub-matrices of the sway high-frequency motion.

$$\text{Ship sway high-frequency sub-matrix} = \begin{bmatrix} 0.0 & 2.728 & 0.0 & 0.0 \\ 0.0 & 0.0 & 2.728 & 0.0 \\ 0.0 & 0.0 & 0.0 & 2.728 \\ -0.22 & -0.662 & -1.572 & -2.455 \end{bmatrix}$$

$$\text{Filter sway high-frequency sub-matrix} = \begin{bmatrix} 0.0 & 2.728 & 0.0 & 0.0 \\ 0.0 & 0.0 & 2.728 & 0.0 \\ 0.0 & 0.0 & 0.0 & 2.728 \\ -1.292 & -2.626 & -3.853 & -4.037 \end{bmatrix}$$

The above data and full system simulations were based on "Star Hercules" dynamics. Selected system responses are shown in Figure 6.12 to 6.16 and titled as appropriate.

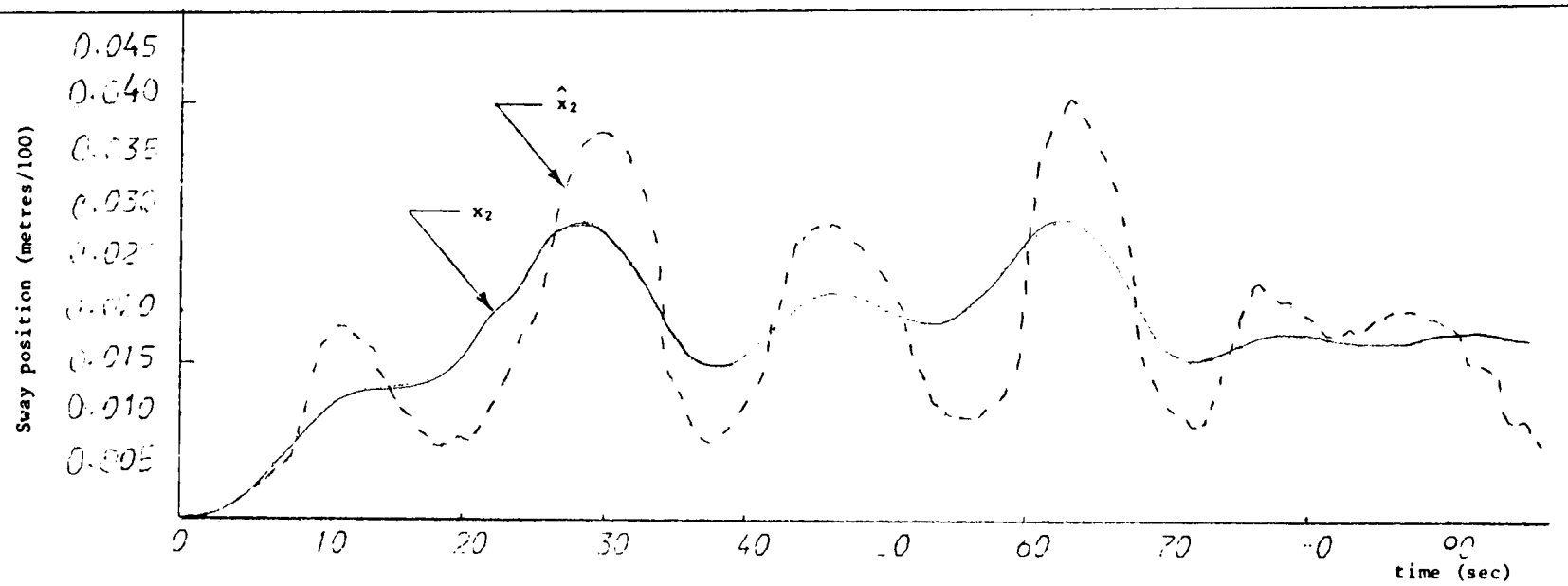

Figure (6.12): Sway low-frequency true and estimated position - state 2

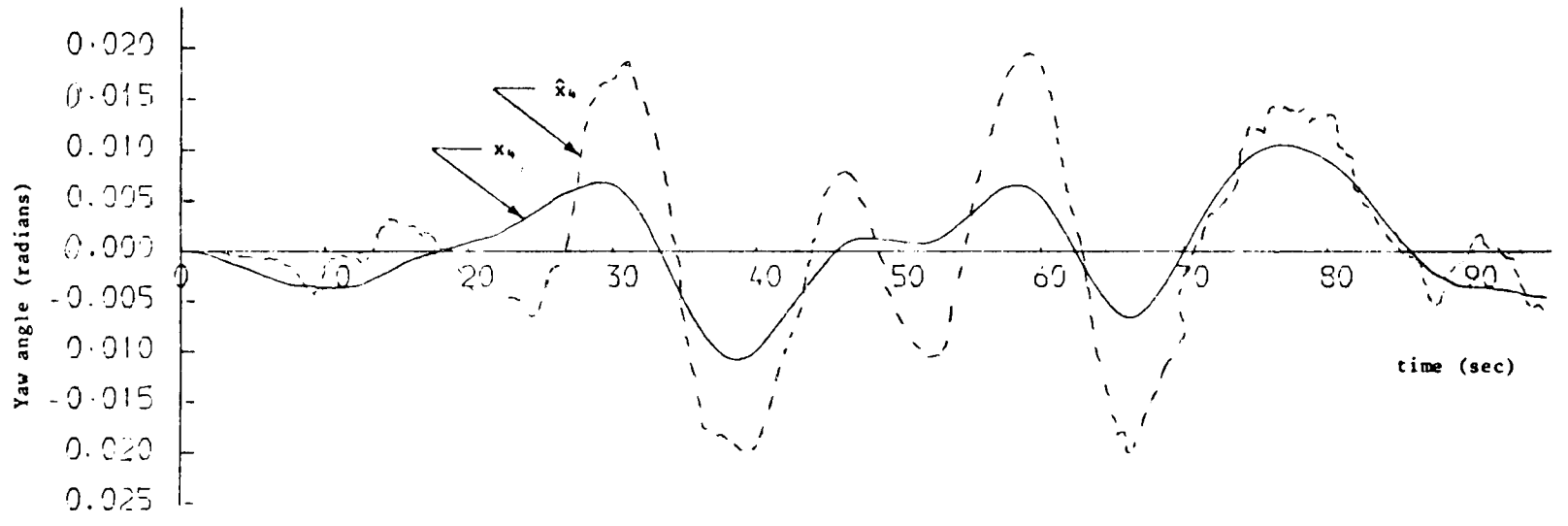

Figure (6.13): Yaw low-frequency true and estimated position - state 4

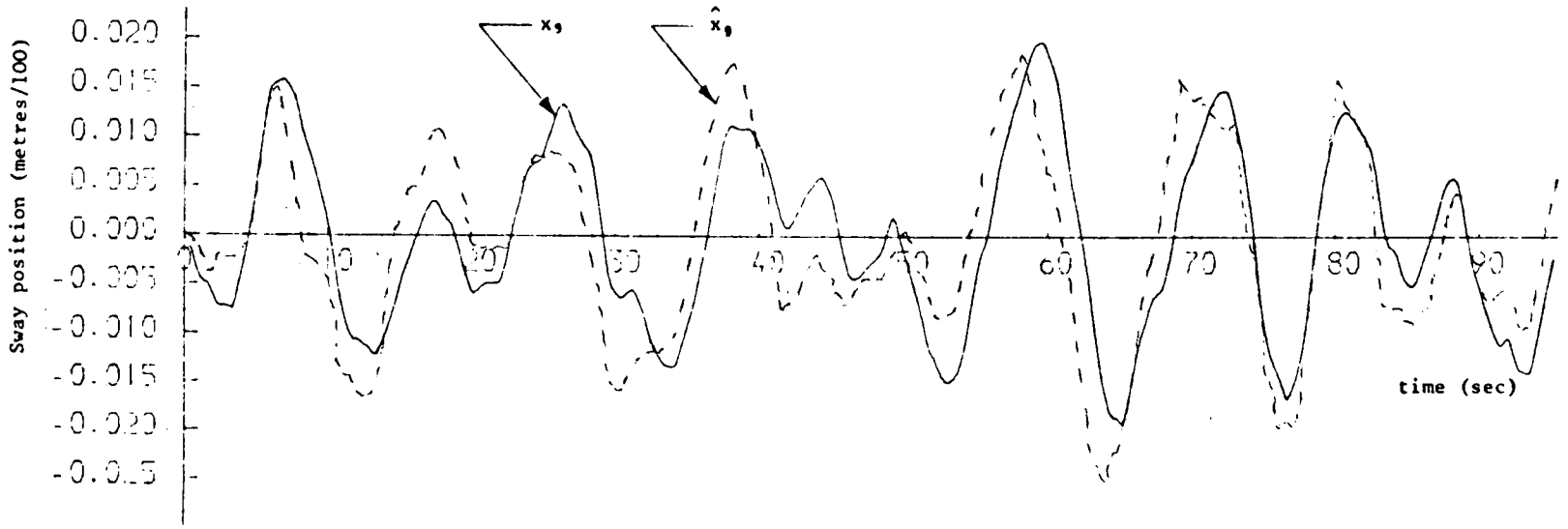

Figure (6.14): Sway high-frequency true and estimated position - state 9

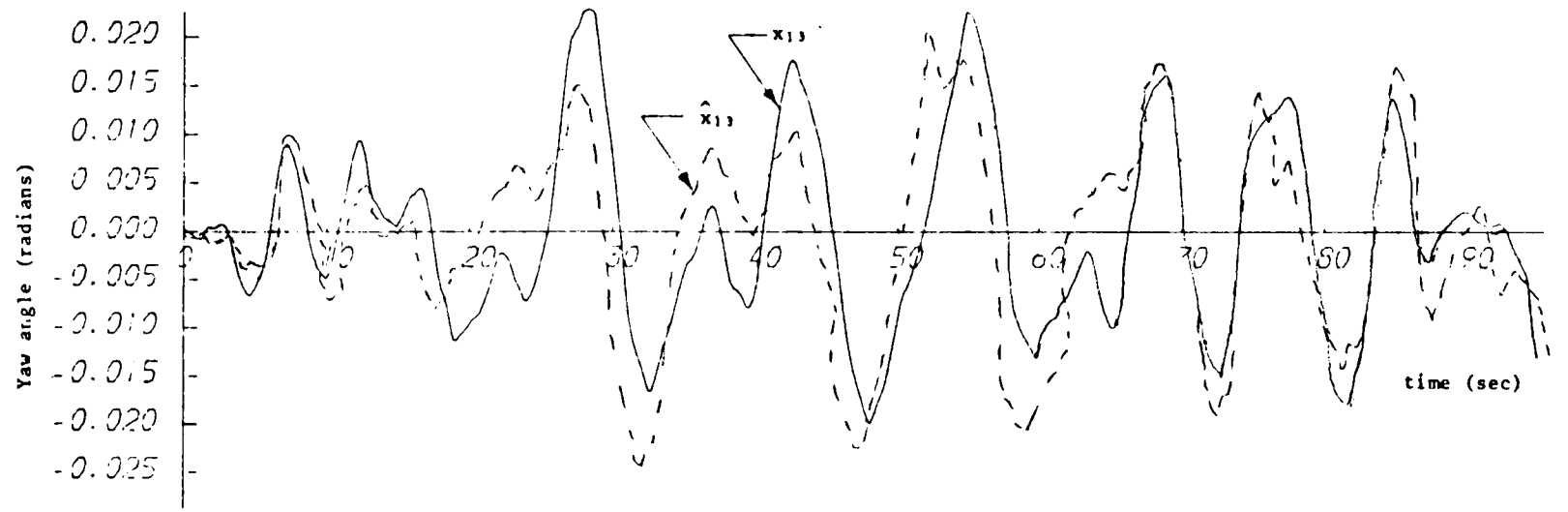

Figure (6.15): Yaw high-frequency true and estimated position - state 13

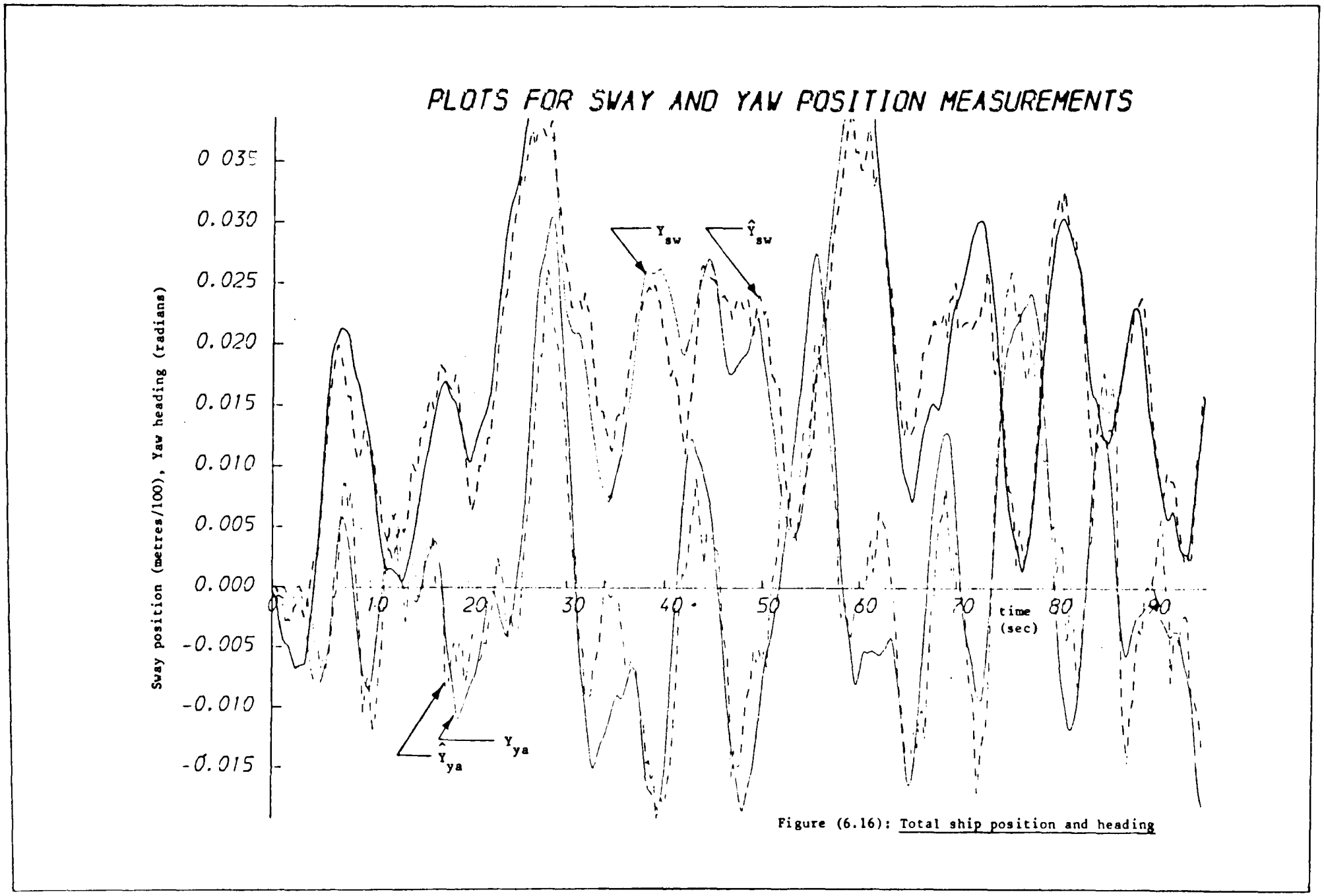

Figure (6.16): Total ship position and heading

6.5 Reliability Tests

Ship dynamics and filter structure are traditionally determined from the formulation of a set of mathematical equations representing the ship motions together with the hydrodynamic forces acting on the hull. These are usually obtained from tests on scaled models on the basis of a reasonably good knowledge of the environmental and measurement noise statistics. Estimation of the system state vectors for control from noisy observations is the prime principle of Kalman filtering operations. Kalman algorithms for dynamic positioning applications provide the conditional mean of the state estimates. This widely known algorithm assumes exact knowledge of the system dynamics, of the initial error and state statistics, and of both system and measurement noise statistics. In practice, however, the stochastic environmental forces represented by the appropriate noise streams are not necessarily constant, and their characteristics are not always certain. The purpose of this section is to investigate the effect of a misidentified noise on the system response and filter estimations. Hence, Kalman algorithm reliability and robustness can be assessed by examining its applicability when the noise factor of the dynamics information is subject to uncertainty. This is carried out by increasing the plant and measurement noise included in the simulation of the plant itself, whilst the filter algorithm operates with the old usual noise conditions.

System simulations were investigated using the full Kalman filter algorithm with the ship observation noise covariance being increased, keeping the filter with the usual noise information. Figures 6.17 to 6.20 show the low-frequency and high-frequency of the ship trajectories together with the filter estimates of these trajectories (the dotted curves) for both sway and yaw motions. These computer plots show the

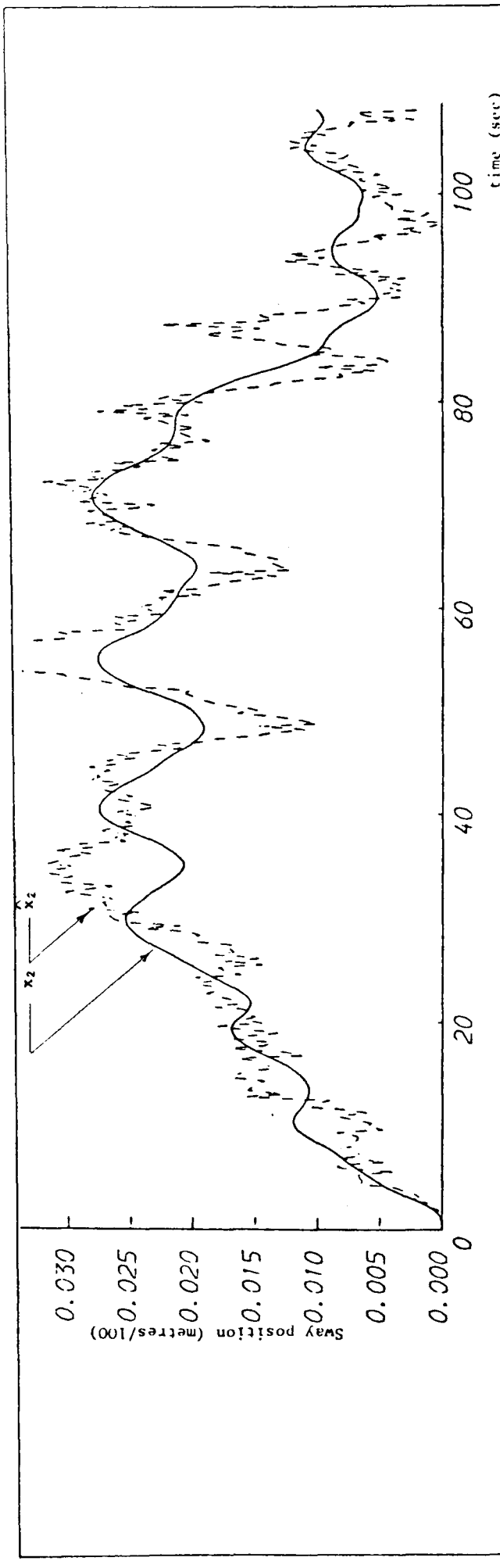

Figure (6.17): Sway low-frequency true and estimated position - state 2

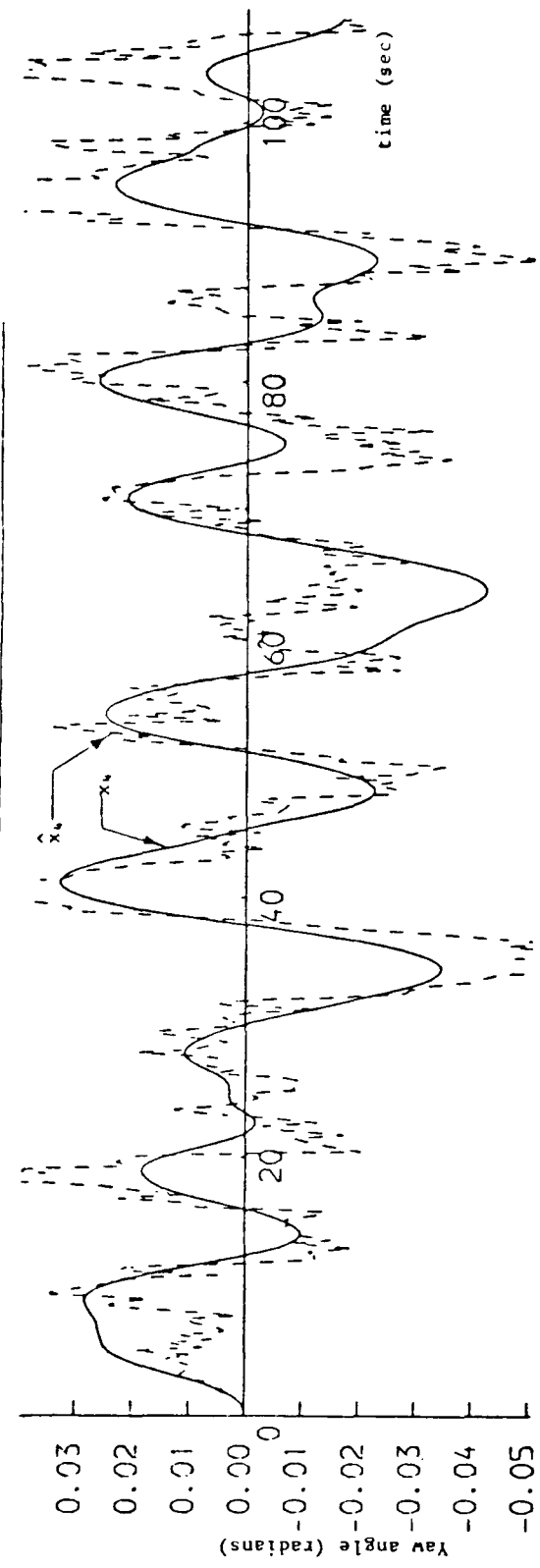

Figure (6.18): Yaw low-frequency true and estimated position - state 4

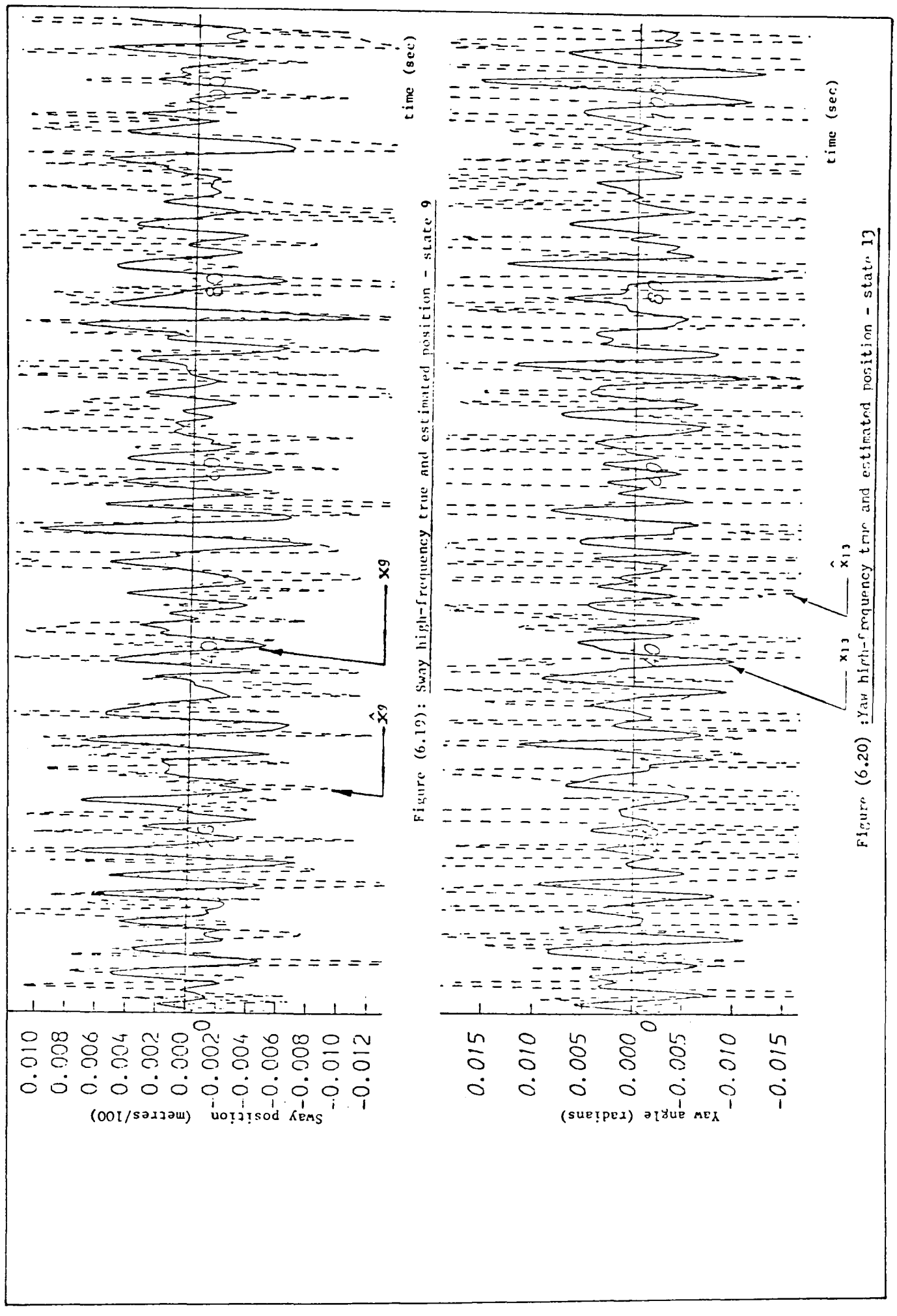

Figure (6.19): Sway high-frequency true and estimated position - state 9

Figure (6.20) :Yaw high-frequency true and estimated position - state 13

system responses under dynamic positioning control for the case when the observation noise covariance within the system has been increased 100 times. Data from "Wimpey Sealab" of Sections 3.2.3 and 3.3 were employed in here for the above simulations and used for Kalman implementations of Chapter 5.

6.6 Concluding Remarks

The main remarks which can be made here will outline the robustness and practicability of using the Kalman filtering technique for estimation within the proposed dynamic positioning control loop. Such remarks can be assessed by a straightforward examination of the system behaviour for the different tests and investigations carried out throughout this chapter. These concluding remarks can be summarised now and listed as follows:

(i) Measuring the thruster output reduces the size of the system and hence reduces the uncertainty throughout the linearisations and approximations in developing the system dynamics.

(ii) The time-varying Kalman gain matrix settles to a constant value after twenty seconds, and hence, using a constant gain matrix at this point, and for the rest of the operations will produce significant savings in computation, cost and storage.

(iii) Deviations of the filter estimations from the actual system state output is very clear when operating under dynamic positioning control with the ship model represented by Beaufort number 8 sea conditions keeping the filter model represented by Beaufort number 5 sea conditions (calm sea state).

(iv) Finally, system responses are presented for the case when system observation noise was increased by 100 times the usual noise statistics used within the filter. Many tests were carried out to show that the results represent the limit for reliable filter performance.

C H A P T E R (7)

CHAPTER 7

NON-LINEAR FILTERING/EXTENDED KALMAN FILTER

7.1 Introduction

An obvious extension of the technique of employing Kalman filtering scheme to the dynamic ship positioning (Chapter 5), is the consideration of the non-linearity of the dynamics of the system (low and high frequency parts of the ship dynamics), and hence the required filtering and control strategy. As shown in Chapter 3, the system dynamics can be represented by a set of non-linear differential equations. These equations were obtained from a set of tests carried out on a scaled model, Section 3.2. However, Chapter 3 outlined a reasonable scaling and linearisation of the non-linear dynamics, as well as an approximation to the formulation of the high-frequency part of the dynamics. Thence, a straightforward application of Kalman filtering and state estimate feedback control, Chapter 5, proved efficient and produced improved system response. In practice, the low-frequency part of the system dynamics needs to be simulated using the actual stochastic non-linear based differential euqations. Hence, an extended form of Kalman filter must be used.

The proposed extended Kalman filter can be used for both state and parameter estimation [49] [69]. Such an extended Kalman filter for the high frequency non-linear system model was first proposed by Grimble and Patton (Section 7.3) [49] based upon a linearisation of the system function of non-linearity about the most recent update of the estimate of the state vector ($\underline{\hat{x}}(t)$) at time (t). The dynamics of the filter are thus locally linear. The linearisation and discretisation process at

each step should be repeated, and the Kalman gain matrix must be re-computed.

The actual non-linear low-frequency part of the system dynamics can be represented by the following differential state equation:

$$\frac{d}{dt}\underline{x}(t) = f_{\ell}(\underline{x}_{\ell}(t), t) + D_{\ell}\underline{\omega}_{\ell}(t) + B_{\ell}\underline{u}(t) \qquad \ldots\ldots\ldots (7.1)$$

with the measurement equation:

$$\underline{z}_{\ell}(t) = H_{\ell}\underline{x}(t) + \underline{v}_{\ell}(t) \qquad \ldots\ldots\ldots (7.2)$$

where $\underline{\omega}_{\ell}(t)$ and $\underline{v}_{\ell}(t)$ are the process and measurement noise vectors respectively [101]. The above proposed scheme of extended Kalman filter for high-frequency non-linearities and parameter estimation can be applied here for the low-frequency dynamics of the system of equation (7.1). The linearisation of $f_{\ell}(\underline{x}_{\ell}(t), t)$ above and the updating of the filter dynamics will be based on the same strategy as that of the high-frequency case. In addition, the system matrix of the LF dynamics needs the same linearisations and system updating processes for control calculations (Section 7.2).

7.2 Non-Linear Filtering and Control

This section extends the discussion of optimal estimation and control for linear systems to the more general case described by the non-linear stochastic differential equation of (7.1). The non-linearities within the low-frequency dynamics will be considered here. The main part of these non-linearities is the non-linearities of the thruster devices, and hence, will be considered in detail [94]. The main goal of this section is to provide insight into the applications of non-linear estimation, hence optimal feedback control can be applied. The extended Kalman

filter system can be combined with optimal feedback control and applied to the low-frequency part of the dynamics by analogy with the separation principle [21] of linear stochastic control theory. The extended Kalman filter dynamics will be assumed locally linear about some operating point, and hence, the filter gain matrix and the estimation process would be followed as from the linear filtering rules. It is postulated that the optimal control gain matrix can be calculated using a similar philosophy to that used for calculating the filter gain matrix [48],[4] Figure 7.1.

7.2.1 System Description including Thrusters Non-Linearities

To indicate the non-linear control problem, the thruster devices (Section 2.2 and Figure 2.3) and their associated non-linearities are to be considered. The type of thrusters fitted on "Wimpey Sealab" vessel is considered in here with its related data (Figure 2.5). The thruster has both dead zone and saturation characteristics (the dead zone for "Wimpey Sealab" is approximately 1-2 per cent of the rated value of the thrust) (Figure 7.2).

The non-linear continous time low-frequency model may be represented by the following non-linear stochastic differential equation:

$$\frac{d}{dt}\underline{x}_\ell(t) = f_\ell(\underline{x}_\ell(t), t) + D_\ell\underline{\omega}_\ell(t) + B_\ell\underline{u}_\ell(t) \quad \ldots\ldots\ldots\ldots (7.3)$$

where $\underline{\omega}_\ell(t)$ is a Wiener process with incremental covariance of $\underline{Q}_\ell dt$. The state vector $\underline{x}_\ell(t)$ contains the sway and yaw velocities and positions as well as the thruster states for sway and yaw ($\underline{x}_5$ and $\underline{x}_6$ respectively). Now, consider the thruster devices non-linearities of Figure 7.2, system state space representation of the low-frequency model including the proposed non-linearities can be written as:

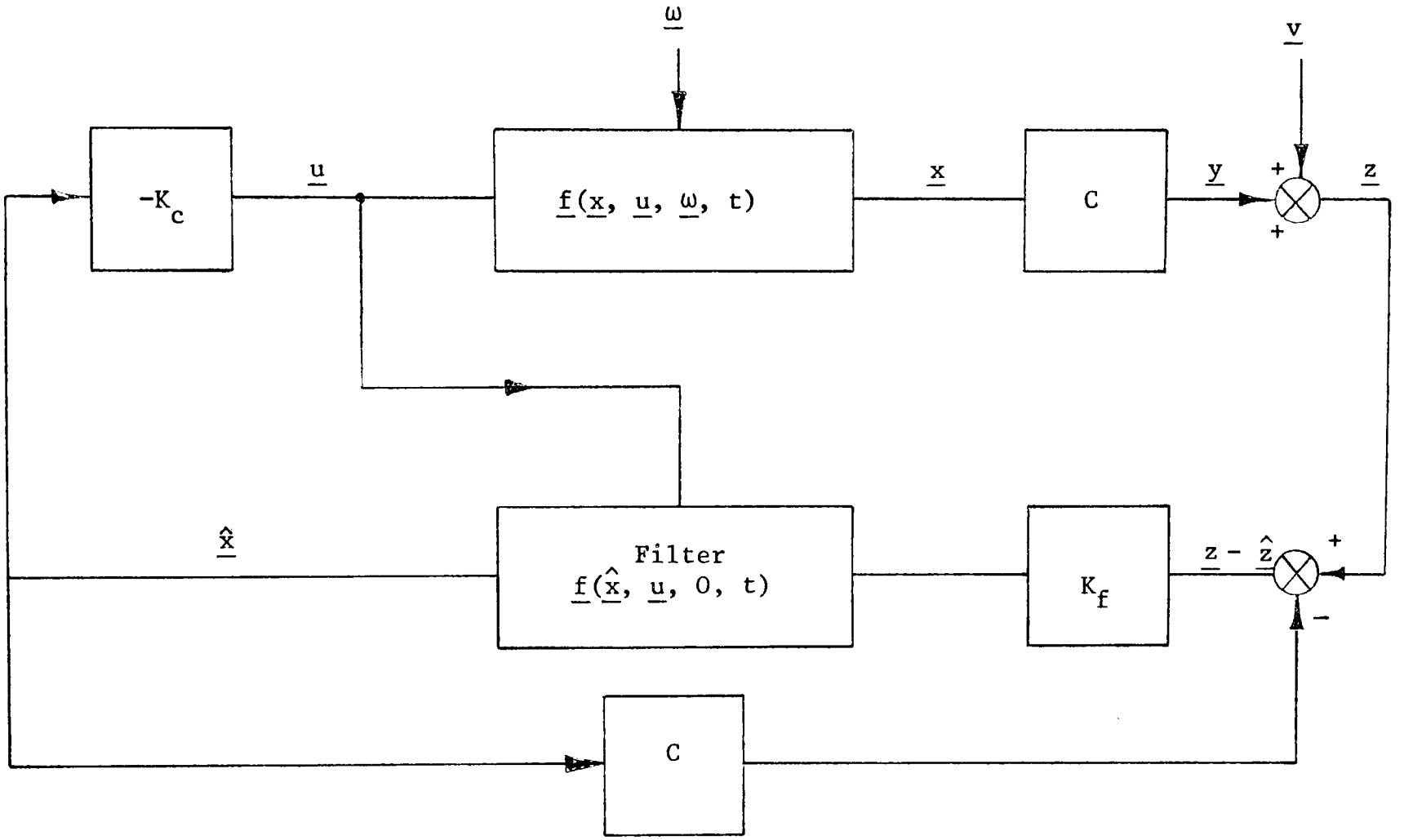

Figure (7.1): Control Strategy involving Thruster's Non-Linearity

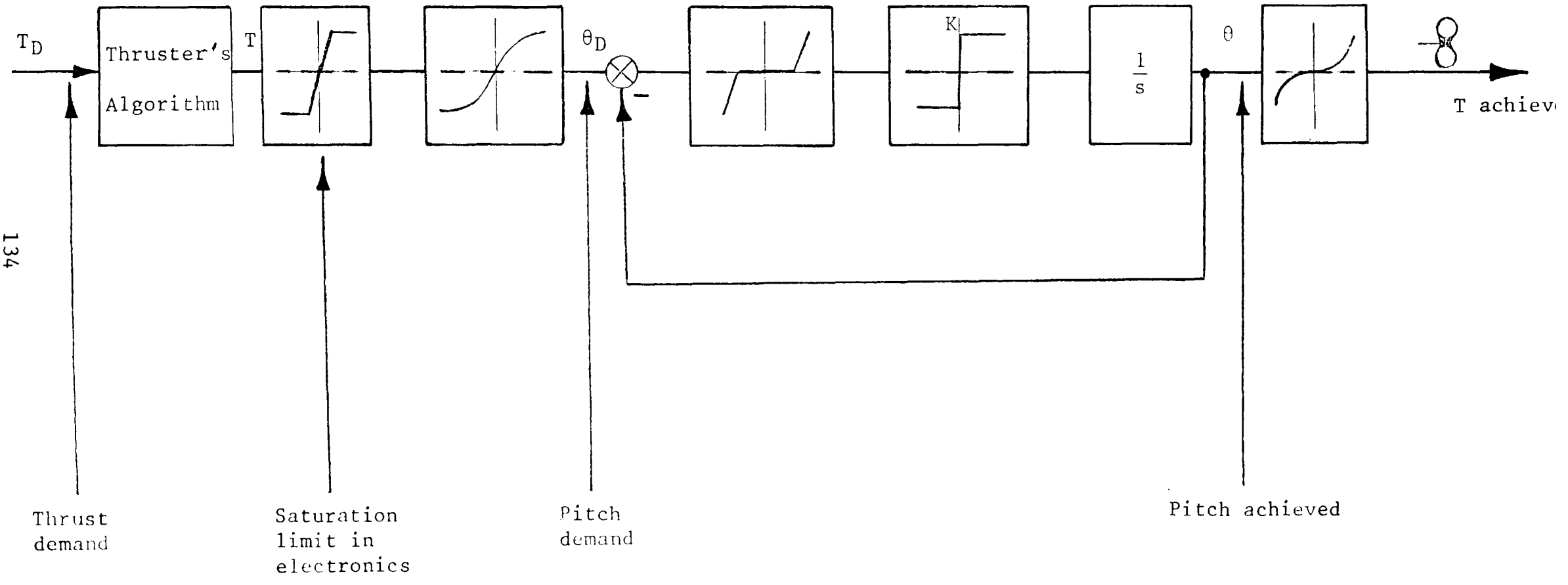

Figure (7.2): The Thruster's Algorithm and the Related Non-Linearities

$$\dot{\underline{x}}_1 = a_{11}\underline{x}_1 + a_{13}\underline{x}_3 + \beta_1\gamma_1\mathcal{N}_1(\underline{x}_5)\underline{x}_5 + \beta_1\gamma_2\mathcal{N}_2(\underline{x}_6)\underline{x}_6$$

$$\dot{\underline{x}}_2 = \underline{x}_1$$

$$\dot{\underline{x}}_3 = a_{31}\underline{x}_1 + a_{33}\underline{x}_3 + \beta_2\gamma_3\mathcal{N}_1(\underline{x}_5)\underline{x}_5 + \beta_2\gamma_4\mathcal{N}_2(\underline{x}_6)\underline{x}_6$$

$$\dot{\underline{x}}_4 = \underline{x}_3$$

$$\dot{\underline{x}}_5 = -b_1\underline{x}_5 + b_1\underline{u}_1$$

$$\dot{\underline{x}}_6 = -b_2\underline{x}_6 + b_2\underline{u}_2 \qquad \text{.....(7.4)}$$

where $\mathcal{N}_1(\underline{x}_5)$ and $\mathcal{N}_2(\underline{x}_6)$ are non-linear functions of the thruster devices in sway and yaw respectively. The thruster non-linearities have been approximated and assumed to be of the following exponential form:

$$\mathcal{N}_1(\underline{x}_5) = (\text{sign } (\underline{x}_5)).F_1.(1 - e^{-F_2\underline{x}_5}) \qquad \text{..... (7.5)}$$

$$\mathcal{N}_2(\underline{x}_6) = (\text{sign } (\underline{x}_6)).F_1.(1 - e^{-F_2\underline{x}_6}) \qquad \text{..... (7.6)}$$

where $F_1 = 0.02$ and $F_2 = \frac{1}{0.02}$. F_1 and F_2 values have been approximated to an exponential function with some saturation. This gross approximation of the low-frequency dynamics is better than the linear approximation normally employed.

Now, the next step will be considered, in which the linearisation of the system and filter matrices can proceed. To obtain these linearised matrices for filter gain and optimal feedback gain calculations, some partial differentiations must be performed (Appendix 4).

$$\frac{\partial}{\partial \underline{x}} (\mathcal{N}(\underline{x}))$$

must be defined for the following two separate regions of each state:

$$0 < \underline{x}_5 < \infty \quad \text{and} \quad -\infty < \underline{x}_5 < 0$$

$$0 < \underline{x}_6 < \infty \quad \text{and} \quad -\infty < \underline{x}_6 < 0$$

Thence, for

$$\underline{x}_5 > 0, \quad \frac{\partial}{\partial \underline{x}_5}(N_1(\underline{x}_5)) = F_1F_2e^{-F_2(|\underline{x}_5|)}$$

and

$$\underline{x}_5 < 0, \quad \frac{\partial}{\partial \underline{x}_5}(N_1(\underline{x}_5)) = F_1F_2e^{F_2(|\underline{x}_5|)} \qquad \ldots\ldots\ldots\ldots\ldots\ldots (7.7)$$

Similarly, for

$$\underline{x}_6 > 0, \quad \frac{\partial}{\partial \underline{x}_6}(N_2(\underline{x}_6)) = F_1F_2e^{-F_2(|\underline{x}_6|)}$$

and

$$\underline{x}_6 < 0, \quad \frac{\partial}{\partial \underline{x}_6}(N_2(\underline{x}_6)) = F_1F_2e^{F_2(|\underline{x}_6|)} \qquad \ldots\ldots\ldots\ldots\ldots\ldots (7.8)$$

a_{15}, a_{16}, a_{35} and a_{36} of the system matrix of equation (7.4) can be formulated in terms of the current system state estimate using the non-linear equations (7.5), (7.6) for the actual system simulations, and updated using the linearised equations (7.7) and (7.8) for filter gain and control gain calculations.

7.2.2 The Filtering Algorithm

Consider the general case of a non-linear system described by the following stochastic differential equation:

$$\dot{\underline{x}}(t) = f(\underline{x}(t), t) + B\underline{u}(t) + D\underline{\omega}(t) \qquad \ldots\ldots\ldots\ldots (7.9)$$

with the output equation:

$$\underline{y}(t) = C\underline{x}(t) \qquad \ldots\ldots\ldots\ldots (7.10)$$

and observations of:

$$\underline{z}(t) = C\underline{x}(t) + \underline{v}(t) \qquad \ldots\ldots\ldots\ldots (7.11)$$

where f is a non-linear function of the state vector, and B, D and C are the input, noise and output matrices respectively. The process noise ($\underline{\omega}$) and the measurement noise ($\underline{v}$) are both Gaussian zero mean

signals with covariances of Q_f and R_f respectively, and with the following expectations:

$$E\{\underline{\omega}(k)\} = 0$$

$$E\{\underline{v}(k)\} = 0$$

$$E\{\underline{\omega}(k)\ \underline{\omega}^T(j)\} = Q_f\delta_{kj}$$

$$E\{\underline{v}(k)\ \underline{v}^T(j)\} = R_f\delta_{kj}$$

$$E\{\underline{\omega}(k)\ \underline{v}(j)\} = 0$$

for all k and j since all the noise sequences are independent, with Kronecker delta function of:

$$\delta_{kj} = 0, \qquad \text{for all } k \neq j$$

$$\delta_{kj} = 1, \qquad \text{for all } k = j$$

System states for the purpose of this study (Chapter 3) can be expressed as:

$$x(t) = \begin{bmatrix} \underline{x}_\ell(t) \\ \hline \underline{x}_h(t) \end{bmatrix}$$

in which $\underline{x}_\ell(t)$ here will refer to the non-linear low-frequency part of the system dynamics.

The discrete-time Kalman filter scheme for the above non-linear system of equations (7.9) and (7.11) [49],[3],[48] has the problem of getting the required state estimate to be used for closed loop control.

A step-by-step implementations of the filter scheme as it has been used within the system simulations can be summarised as follows:

(i) The predicted state at (k + 1) instant is,

$$\hat{\underline{x}}(k+1|k) = f(\hat{\underline{x}}(k|k)) + \Delta_f\ \underline{u}(k) \qquad \ldots\ldots\ldots (7.12)$$

since the system input has been fed into the filter as well as into the plant (Figure 7.1).

(ii) Based on (i), the state estimates at (k + 1) can now be calculated.

$$\underline{\hat{x}}(k+1|k+1) = \underline{\hat{x}}(k+1|k) + K(k+1)\left[\underline{y}(k+1) - C\underline{\hat{x}}(k+1|k)\right] \quad \ldots\ldots (7.13)$$

where K(k + 1) is the Kalman gain matrix which has been calculated from the linearised filter dynamics.

(iii) The linearisation and updating processes of the filter system matrices(A_k) and (A_f) can now begin. The filter matrix (A_f) will be used for actual filter simulations thereafter, while the linearised (A_k) matrix will be used for Kalman gain matrix calculations:

$$A_k(\text{linearised}) = \frac{\partial}{\partial \underline{x}} A_f\ (\underline{x},\ (k+1))\Big|_{\underline{x} = \underline{\hat{x}}} \quad \ldots\ldots\ldots (7.14)$$

(iv) Now Kalman gain matrix K(k + 1) can be obtained, first by calculating the predicted error covariance matrix,

$$P(k+1|k) = \Phi_k(k+1|k)P(k|k)\Phi_k^T(k+1|k) + \Gamma_k(k+1|k)\ Q_f\Gamma_k^T(k+1|k) \quad \ldots\ldots\ldots (7.15)$$

where

$P(k|k) = \left[\ 0.0\ \right]_{14}$ is the initial error covariance matrix.

Therefore

$$K(k+1) = P(k+1|k)\ C^T\left[\ CP(k+1|k)C^T + R_f\ \right]^{-1} \quad \ldots\ldots\ldots (7.16)$$

where R_f and Q_f are the measurement and process covariance matrices respectively.

(v) Finally, the error covariance matrix is:

$$P(k+1|k+1) = (I - K(k+1)C)P(k+1|k)(I - K(k+1)C)^T + K(k+1)R_f\ K^T(k+1) \quad \ldots\ldots\ldots (7.17)$$

(vi) Given the expected values of the initial state, error covariance matrices and filter dynamics, one can use the above equation iteratively to obtain the state estimates at any future sampling instant (k + i).

7.2.3 The Control Algorithm

In the dynamic positioning problem under consideration, the control problem is one of using the filter low-frequency estimates for a closed feedback loop. These estimates will be assumed to represent the true system states for the control purpose. The next step in here is to calculate the feedback control gain matrix on the basis of optimal stochastic control theory.

In the linear stochastic optimal control problem (Chapter 4), determination of the optimal feedback control requires the solution of the matrix Riccati equation [102]. The optimal control philosophy for the non-linear stochastic system under consideration can be explained as follows:

(i) Linearise the system locally around the most recent state estimates using the extended Kalman filter philosophy.

(ii) Estimate the step ahead conditional mean of the state vector (Chapter 5).

(iii) In here, linearisation and updating of the system matrix can be carried out in analogy to the process in Section 7.2.2 (iii). The A-matrix is to include the actual non-linearities for system simulations, while the A_1-matrix is to represent the linearised structure of the system matrix for control gain calculations.

$$A_1 \text{ (linearised)} = \frac{\partial}{\partial \underline{x}} A(\underline{x}, (k+1)) \Big|_{\underline{x} = \hat{\underline{x}}} \qquad \ldots\ldots\ldots (7.18)$$

(iv) The process of calculating the control gain matrix (K_c) can now begin to control the non-linear system of equation (7.1). This process will involve the iterative solution of the following steady-state Riccati equation over the specific sampling instant [84][88]:

$$0 = A_{1\ell}^T P_c + P_c A_{1\ell} - P_c B_\ell R_c^{-1} B_\ell^T P_c + Q_c \quad \ldots\ldots\ldots (7.19)$$

and it is such that the performance criterion,

$$J = \int_o^T (\underline{x}^T(t)\ Q_c\ \underline{x}(t) + \underline{u}^T(t)\ R_c \underline{u}(t)\ dt \quad \ldots\ldots\ldots (7.20)$$

is minimised, where $A_{1\ell}$ is the locally-linearised low-frequency part of the system matrix for control calculations. B_ℓ is the low-frequency part of the input matrix. R_c and Q_c are the control weighting matrices. These matrices were chosen optimally [39], [2], (Section 4.3).

(v) Finally, once solution to the Riccati equation P_c of equation (7.19) is obtained, the control gain matrix at that specific instant can be calculated as:

$$K_c = R_c^{-1} B_\ell^T P_c \quad \ldots\ldots\ldots (7.21)$$

7.2.4 Simulation Results

Simulation results will be presented in here to illustrate the idea of non-linear control of the above section (7.2). These simulations are based on data from the vessel "Wimpey Sealab" (Chapter 3), with control weightings of Chapter 4 and filter specifications of Chapter 5. Non-linearities within the low-frequency part of the system will be considered in here with the high-frequency dynamics assumed constant and the canonical state-space form for both sway and yaw motions have been used as from Chapter 3.

Full system simulations combining both low and high frequency dynamics

using extended Kalman filter for control can now be summarised. The system responses for a step input of 0.02 per-unit into the sway direction are shown in Figures 7.3 to 7.7 inclusive, where Figures 7.3 and 7.4 show the non-linear behaviour of the low-frequency vessel position and heading respectively, while Figures 7.5 and 7.6 show the corresponding high-frequency vessel position and heading respectively. Figure 7.7 shows the combined low and high frequency trajectories. Throughout these simulations, the ship and filter matrices were updated and linearised every two intervals of the simulations. However, linearising every five intervals (Figures 7.8 to 7.10) for sway and yaw low-frequency position and heading as well as the ship total position shows no loss of accuracy and a significant saving in system simulation cost. Filter estimates are again shown by dotted curves.

7.3 Parameter Estimations

Kalman filtering for estimating the state vectors of system under dynamic positioning control has been widely applied because of the reliability of the filter performance. Such performance depends mainly on the availability of the required information to construct the Kalman filter. Most of this information is approximately known with some parameter uncertainties within the main body of the plant model. Such uncertainties could cause the requirement for non-linear estimations using the extended Kalman filter as state and parameter estimator. Hence, the problem of doing accurate estimation when some of the ship and filter models parameters are not precisely known involve parameter estimations with all the consequences of increased system dimensions and undesirable complexity in implementing the filter algorithm [64].

The problem of parameter estimation in a noisy stochastic dynamic system using extended Kalman filter for state and parameter estimation

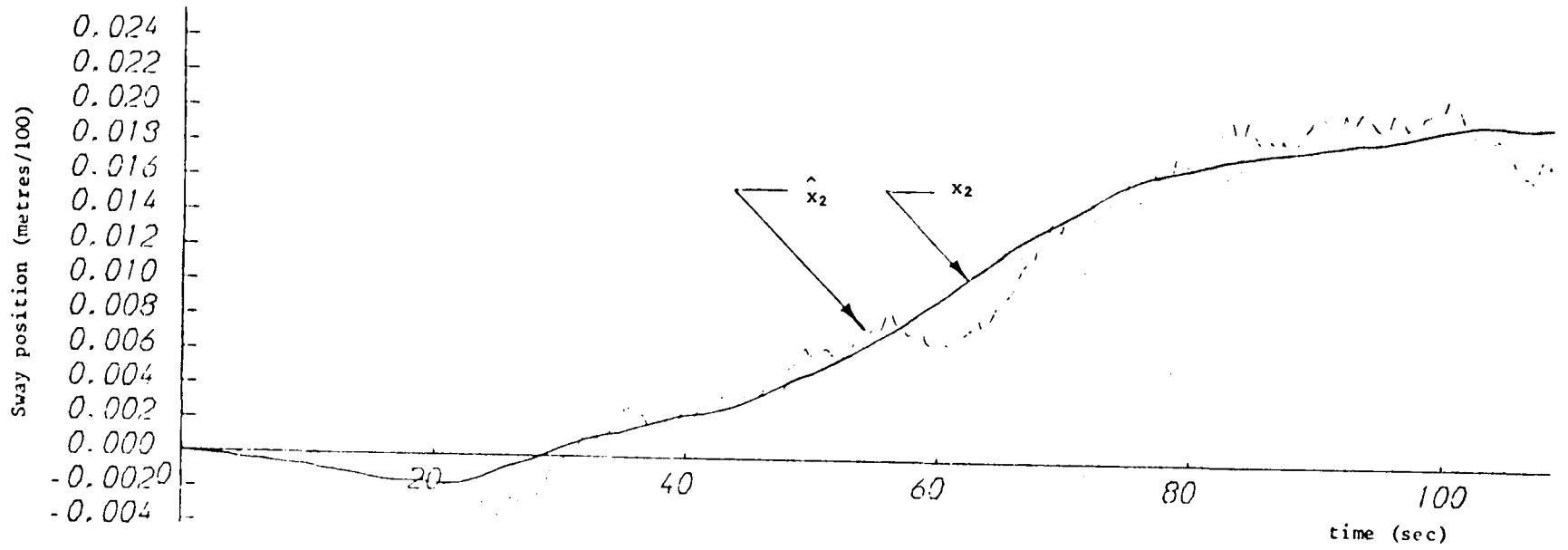

Figure (7.3) :Sway low-frequency true and estimated position (2 steps linearisation)

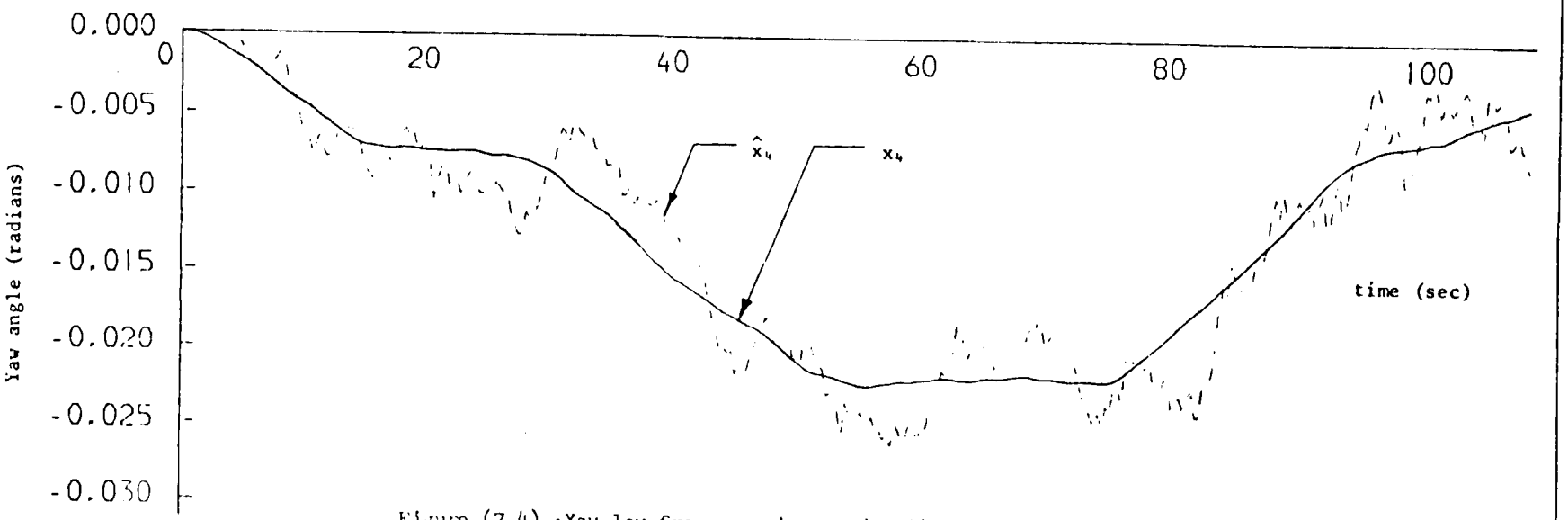

Figure (7.4) :Yaw low-frequency true and estimated position (2 steps linearisation)

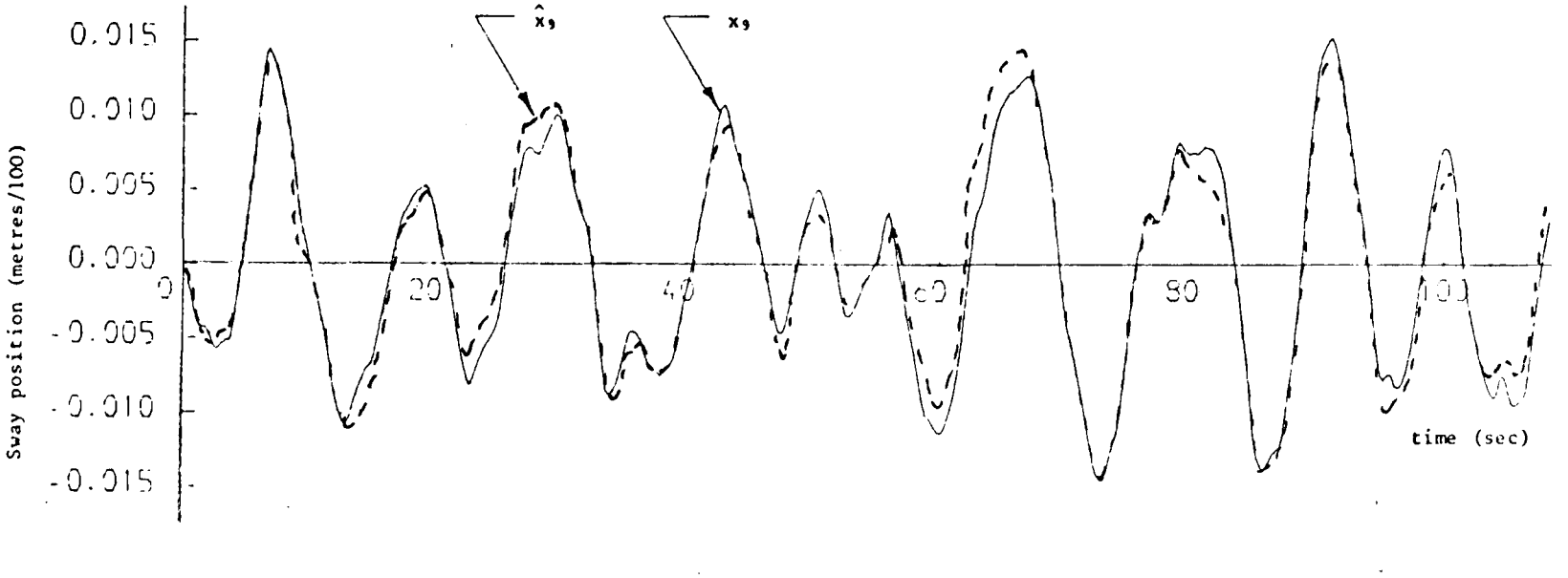

Figure (7.5): Sway high-frequency true and estimated position (2 steps linearisation)

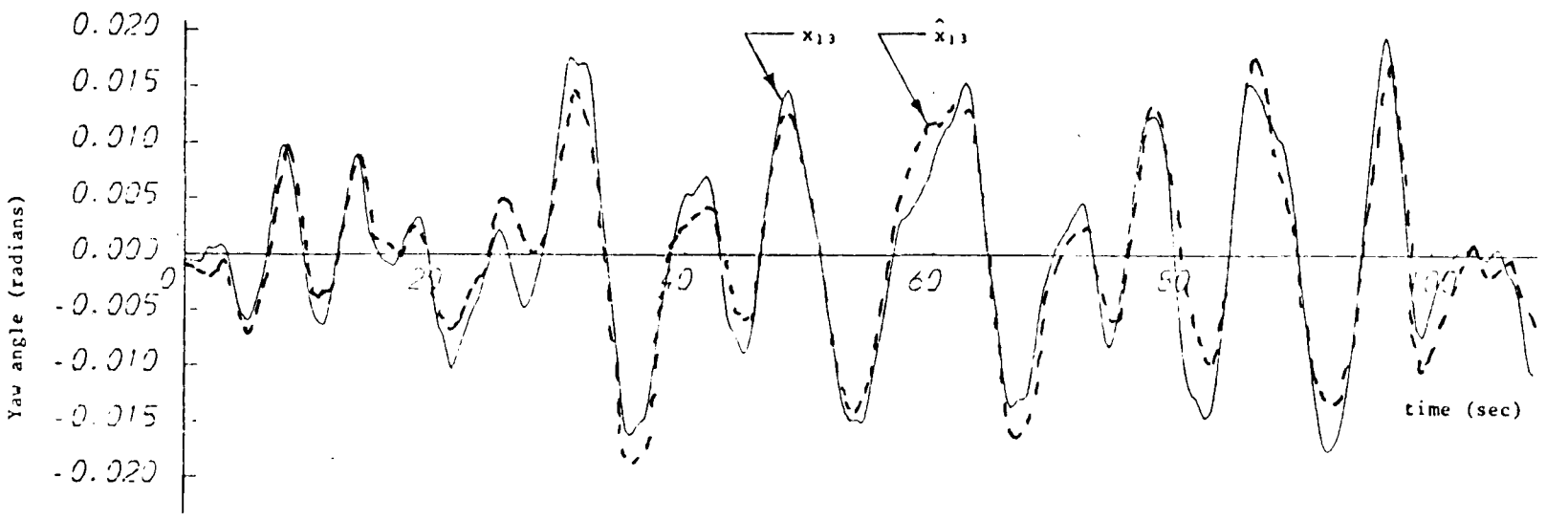

Figure (7.6): Yaw high-frequency true and estimated position (2 steps linearisation)

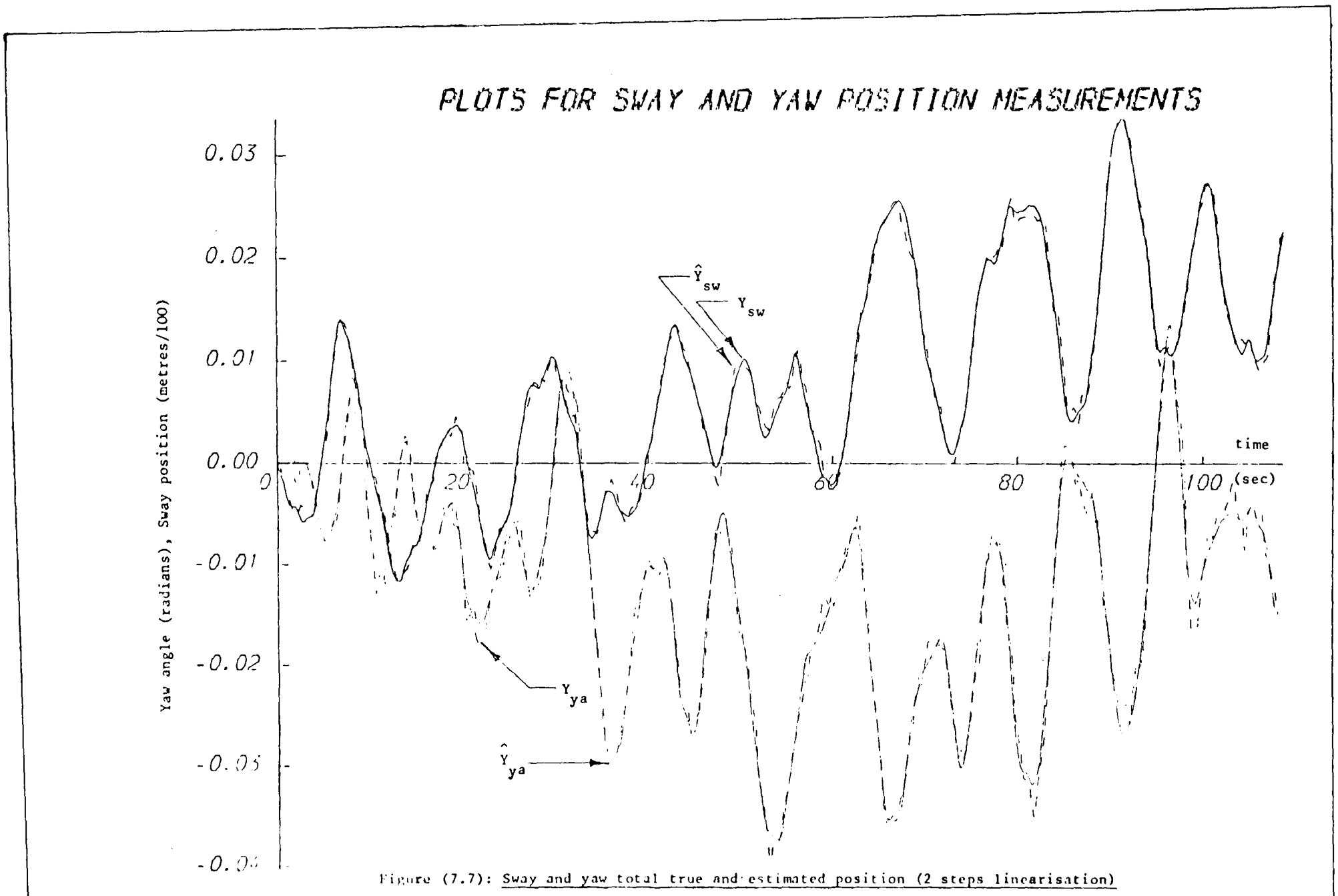

Figure (7.7): Sway and yaw total true and estimated position (2 steps linearisation)

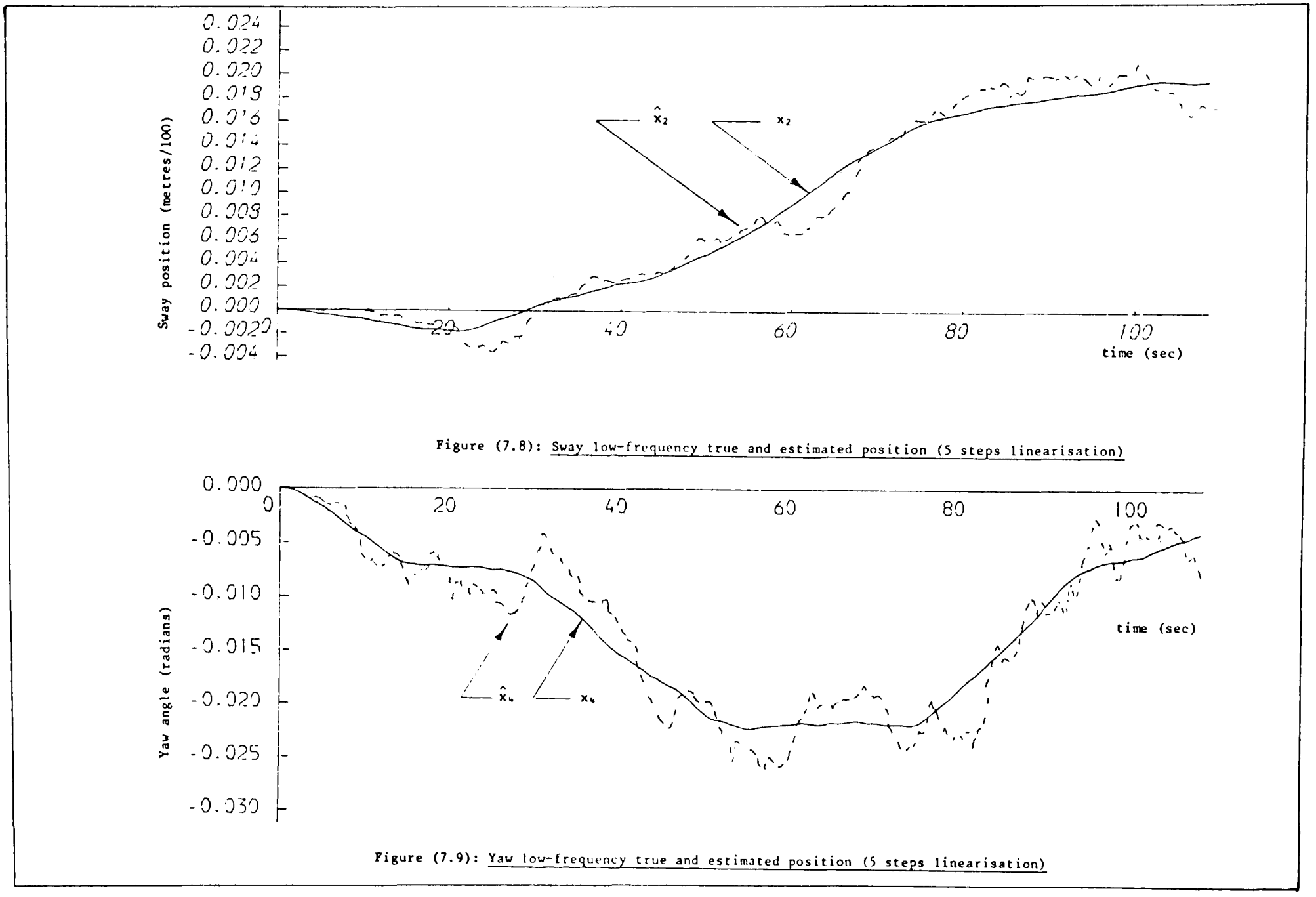

Figure (7.8): Sway low-frequency true and estimated position (5 steps linearisation)

Figure (7.9): Yaw low-frequency true and estimated position (5 steps linearisation)

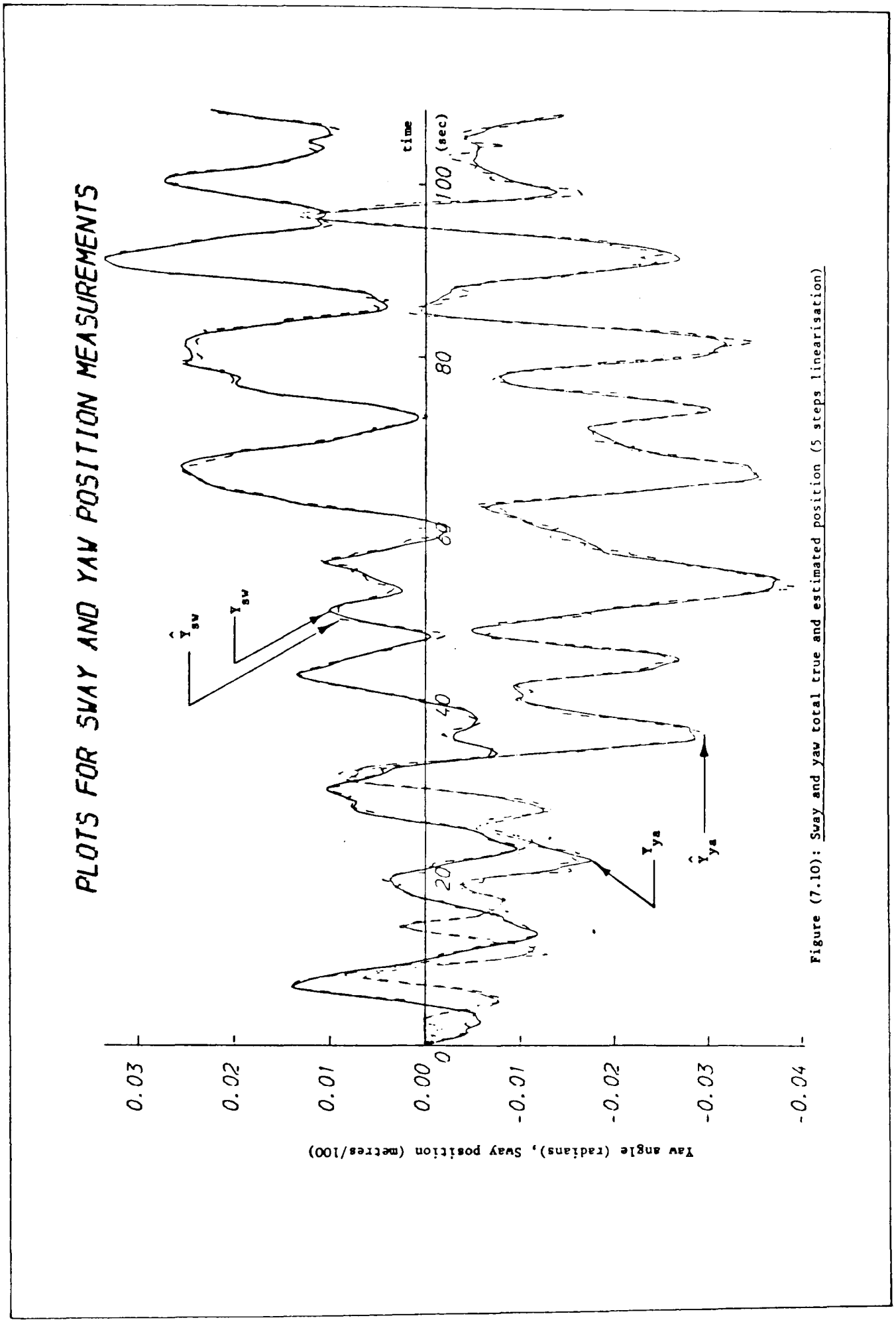

Figure (7.10): Sway and yaw total true and estimated position (5 steps linearisation)

has received considerable attention [61],[67],[79],[83] because of its importance in system model building and control. Basically, the unknown parameters to be estimated must be represented dynamically within the whole system structure and estimated in a similar way to that of the state estimation procedure. Hence, the filter dimension will be increased by the number of the unknown parameters to be estimated. Kalman theory cannot be applied in here directly and a form of extended Kalman filter is required with all the necessary applications of the linearisation and updating procedures.

Previous chapters outlined the step by step implementations of Kalman filtering techniques for dynamic positioning applications. The system was assumed to consist of low-frequency and high-frequency parts and so the filter model. Non-linearities within the low-frequency part of the system dynamics have been considered in Section 7.2 using extended Kalman filter to estimate the system states vectors for control.

In this section, work done by Balchen [12] and Grimble and Patton [49] will be summarised, which has been mainly involved with the investigation of the non-linearities within the high-frequency part of the system dynamics and the related state and parameter estimations using extended Kalman filter. J G Bålchen (1976) has proposed an extended Kalman filter for dynamic ship positioning problem in which the high-frequency subsystems have been modelled by harmonic oscillators. The frequency of the oscillators is assumed equal for both sway and yaw motions and needs to be estimated as an unknown parameter using an additional state variable. Hence, the system matrix for sway motion which is identical to the yaw motion will be:

$$A_h^{s\omega} = \begin{bmatrix} 0 & (x_3^h)^2 & 0 \\ 1 & 0 & 0 \\ 0 & 0 & 0 \end{bmatrix}$$

with system state vectors of:

$$\begin{bmatrix} x_1^h \\ x_2^h \\ x_3^h \end{bmatrix}$$

where x_1^h represents the high-frequency sway velocity, x_2^h represents the high-frequency sway position, and x_3^h represents the dominant angular wave frequency to be estimated.

Disadvantages with using Balchen's method led to the use of the alternative technique proposed by Grimble and Patton [49]. This alternative approach uses an extended Kalman filter which is based on a more accurate model of the sea wave energy spectrum (Section 3.3). An assumption for an approximate non-linear sea spectrum was made in Section 3.3 to develop and implement the high-frequency part of the system dynamics. The state space representation of the system high-frequency model were developed in companion canonical form for different Beaufort numbers and sea conditions and assumed identical for both sway and yaw. The system matrix for sway motion can be presented as:

$$A_h^{s\omega} = \begin{bmatrix} 0 & T_b & 0 & 0 \\ 0 & 0 & T_b & 0 \\ 0 & 0 & 0 & T_b \\ -\alpha_4 & -\alpha_3 & -\alpha_2 & -\alpha_1 \end{bmatrix}$$

where T_b is the per-unit system time constant, and α_1, α_2, α_3 and α_4 are constant parameters for a specific Beaufort number and vary in

proportion to the weather conditions. The main purpose of the proposed extended Kalman filter in here in addition to estimating the system state vectors is to include a subsystem for estimating the above four parameters (α_1, α_2, α_3 and α_4) for different weather conditions, together with the rest of the system states. Thence, the new filter high-frequency system matrix for both sway and yaw will have the following structure:

$$A_h = \begin{bmatrix} A_h^s & & 0 \\ & A_h^{ya} & \\ 0 & & A_h^p \end{bmatrix}$$

in which A_h^p is a (4 x 4) matrix corresponding to the unknown four parameters to be estimated. In this case, the discrete-time Kalman filter for the dynamic positioning problem may be defined as:

$$\underline{\hat{z}}(t+1) = f(\underline{\hat{z}}, \underline{u}(t)) + K(t)\left[\underline{y}(t) - C\underline{\hat{x}}(t)\right] \qquad \text{.....(7.22)}$$

where

$$\underline{\hat{z}}(t) = \begin{bmatrix} \underline{\hat{x}}(t) \\ \hline \underline{\hat{\theta}}(t) \end{bmatrix}$$

and $\underline{\hat{x}}(t)$ are the original low and high frequency system state estimates while $\underline{\hat{\theta}}(t)$ are the parameter estimates. K(t) is the Kalman gain matrix, and can be partitioned as:

$$K(t) = \begin{bmatrix} K_\ell(t) \\ \hline K_h(t) \\ \hline K_\theta(t) \end{bmatrix}$$

where $K_\ell(t)$ and $K_h(t)$ are the filter low and high frequency gain matrices respectively while $K_\theta(t)$ is the parameter estimator gain. The filter

gain matrix should be computed at each sampling instant and linearisations and system updating should be performed in a similar manner to those of Section 7.2.

7.4 Concluding Remarks

Work in this chapter has shown that the structure of the extended Kalman filtering scheme can be used for control. The use of such an approach to control system design has been shown to produce more realistic system responses. For the purpose of studying the non-linear control of the low-frequency part of the ship under dynamic positioning control, the thrust-producing devices and their related non-linearities were considered. Figure 7.8 shows the sway position for a step input of 0.02 into sway motion which indicates good estimation but with slow overall system response. Control weighting matrices were adjusted but with little improvement on the speed of the system responses. Such slowness of response is mainly caused by the non-linearities considered and the extended Kalman filter applications with all the related linearisations performed. The basic philosophy of non-linear filtering and control throughout this work was based on the processes of linearising and updating the system in terms of the filter estimates at each sampling instant. This will impose a high computational burden. Simulations shown in Figure 7.7 and Figure 7.10 are the ship trajectories based on linearising and updating the system every two intervals and five intervals respectively, with a cost saving and no loss of accuracy.

Parameter estimation for the dynamic positioning problem is an essential technique by which the uncertainties within the system dynamics can be overcome. Grimble and Patton [49] did a substantial amount of work in this field and hence it has been summarised here for its relationship to the idea of non-linear control (Section 7.2).

C H A P T E R (8)

CHAPTER 8

OVERALL CONCLUSIONS

The major aims of the work in this case study was achieved successfully and reported in this thesis. From the basic design considerations and the related practical investigations, it has been shown that the Kalman filtering technique is suitable for the dynamic ship positioning problem under consideration. It uses the actual available information on the dynamical behaviour of the process generating the measurements as part of the filter structure. Although information about the model is included in the filter, model inaccuracies within the ship dynamics are a dominant limiting factor in the Kalman filter performance.

System dynamics were provided by GEC Electrical Projects from experiments on a model of the ship using a set of tank and wind tunnel tests for the three degrees of freedom. Some interaction between sway and yaw motions was considered and the whole system design for filter and control was carried out successfully for both motions simultaneously. Basic equations used to build the Kalman filter were based on the ship dynamics obtained from the above-mentioned experimental tests. The system measurements were the only source of information available for the filter from the outside world during its operation. A back-up taut-wire source of measurement is employed along with the acoustic system since water disturbances, such as fish passing and air bubbles, can cause a loss of the pulses required by the the set of the hydrophones to generate the desired measurements. Grimble and Patton [51] did some comparison work on the practicability of using Notch filters and PID controllers or the alternative Kalman filter and stochastic optimal control and showed

that a better system response could be obtained by using the latter scheme. In this work, a Kalman filtering scheme was implemented successfully using stochastic optimal control theory within dynamic positioning control for two vessels, "Wimpey Sealab" and "Star Hercules". The proposed scheme has been installed on the latter vessel and commissioned. The Kalman filter, while offering the most potential improvement in estimation accuracy, is inherently linear since it represents the linearised ship model. The required approximations can result in system and filter modelling errors. However, more realistic representations have been considered throughout the simulations of the system including non-linearities.

In the early stages of this work, linearised systems have been considered for Kalman filter implementation and a simple plant has been modelled but there is no reason to believe that the results obtained are not typical of what may be found using a more complex model. Several important factors have been studied and these impose a degree of limitation on the accuracy and ease of implementation of the Kalman filter algorithm for the dynamic positioning problem under consideration. These factors are:

(i) the accuracy of the filter structure as a true model of the actual plant,

(ii) the availability and uncertainty of the different parameters of the plant model,

(iii) the choice of process and measurement noise statistics and their corresponding covariance matrices affect the Kalman gain calculations and hence the elements of these matrices should be accurately chosen and fed into the filter.

(iv) on-board computer storage capacity to handle the complexity of the scheme structure and the related calculations and storage requirements.

Several investigations have been carried out to show the reliability and robustness of using the Kalman filter for estimation within the dynamic positioning control loop despite the above restrictions and limitations. These can be listed as follows:

(i) Introducing the reduced-order Kalman filter reduces the size of the filter, which has the advantage of minimising the modelling errors since the filter does not include the model of the directly measured thruster subsystem. An additional advantage with using this scheme is a reduction in the computer storage requirement especially when a high dimension filter is used for state and parameter estimations.

(ii) Full Kalman filter simulations show that the filter gain matrix becomes constant after approximately 20 seconds. One of the disadvantages of using the time-varying Kalman filter is the computational burden associated with the filter gain calculations, and hence partitioning the filter gain calculations into a time-varying region of up to 20 seconds and a constant region for the rest of the simulations shows a significant saving on the filtering and control process.

(iii) The mismatching problem was investigated by simulating the system with the Kalman filter using Beaufort number 5 dynamics, keeping the ship with a worst sea condition dynamics of Beaufort number 8. The system and filter responses showed some deviations in the filter estimates. Hence, to ensure good estimation accuracy, the filter structure should represent a higher Beaufort number than that expected of the real plant.

(iv) As mentioned above, noise statistics are an important factor in shaping the filter behaviour. Tests havebeen carried out by increasing

the measurement noise statistics of the system keeping the filter with only the usual information. The filter gave acceptable estimates to show its reliability up to a critical noise level (shown in Section 6.5) where the filter behaviour cannot be relied upon, corresponding to the case when the noise covariances were increased by 100 times.

Kalman filtering models for the dynamic positioning problem have been extended to include some of the system non-linearities. Such investigations have shown that a form of extended Kalman filter can be used to provide the necessary state estimates for closed loop non-linear control. The use of such an approach to control system design (Chapter 7) is shown to produce more realistic system responses. A practical algorithm for on-line estimation and control of a noisy non-linear system has been implemented with some computational load.

Further research can be concerned with the procedure of partitioning the non-linear system of Chapter 7. The linear constant part of the dynamics can be dealt with separately in the usual way using a linear Kalman filter with the advantages of reduced implementation cost.

REFERENCES

1. AL-TAKIE, A A: "Development of a dynamic ship positioning simulation", Research Report no.EEE/28/1979, Sheffield City Polytechnic.

2. AL-TAKIE, A A: "Documentation report on the selection of the optimal control performance criterion weighting matrices", Research Report, January 1980, Sheffield City Polytechnic.

3. AL-TAKIE, A A: "Kalman filtering techniques applied to the dynamic ship positioning problem", Research Report EEE/53/May 1980, Sheffield City Polytechnic.

4. AL-TAKIE, A A and GRIMBLE, M J: "Optimal control of non-linear stochastic systems with applications to dynamic ship positioning", International Conference on Systems Engineering, 14-16 September, 1982.

5. ANDERSON, B D O and MOORE, J B: "The Kalman-Bucy filter as a true time-varying Wiener filter", IEEE Transactions on Systems, Man, Cybernetics, April 1971, Vol SMC-1, No 2.

6. ASHER, R B and SIMS, C S: "Reduced-order filtering with state dependent noise", ISA 1978, pp 269-276.

7. ASTROM, K J and KALLSTROM, C G: "Identification of ship steering dynamics", Automatica, Vol 12, pp 9-22, 1976.

8. ATHANS, M: "On the design of PID controllers using optimal linear regulator theory", Automatica, Vol 7, pp 643-647, Pergamon Press, 1971, printed in Great Britain.

9. ATHANS, M: "The compensated Kalman filter", symposium on non-linear estimation, University of California, San Diego, September 15, 1971.

10. ATHANS, M: "The role and use of the stochastic linear-quadratic-Gaussian problem in control system design", IEEE Transactions on Automatic Control, Vol AC-16, No 6, December 1971.

11. BALCHEN, J G, JENSSEN, N A, MATHISEN, E and SELID, S: "Dynamic positioning of floating vessels based on Kalman filtering and optimal control", 0191-2216/80/0000-0852 $00.75, 1980, IEEE, 19th Proc Con Decis Control, Incl Sym Adap Proc, Vol 2.

12. BALCHEN, J G, JENSSEN, N A and SELID, S: "Dynamic positioning using Kalman filtering and optimal control theory", Automation in Offshore Oil Field Operation, eds Galtung, Rosandhaug and Williams, North-Holland Publishing Co, 1976.

13. BALL, A E and BLUMBERG, J M: "Development of a dynamic ship positioning system", GEC Journal of Science and Techn. Vol 42, No 1, 1975, 29-36.

14. BARNETT, S: "Introduction to mathematical control theory", Clarendon Press, Oxford, 1975.

15. BARTON, P H: "Dynamic positioning systems", GEC Electrical Projects Ltd, No 3493-108, Rugby, Warwicks, CV21 1BU.

16. BENDAT, J S: "Optimum filters for independent measurements of two related perturbed messages", IRE Transactions on Circuit Theory, March 1957.

17. BERGER, C S: "A damping indicator for multivariable systems", Dept Electrical Engineering, University of Monash.

18. BODE, H W and SHANNON, C E: "A simplified derivation of linear least square smoothing and prediction theory", Proc of IRE, April 1950.

19. BRINK, A W, VAN DEN BRUG, J B, TON, C, WAHAB, R and VAN WIJK, W R: "Automatic position and heading control of a drilling vessel", Third Ship Control Systems Symposium, 26-28 Sept 1972, Bath, UK.

20. CORRAL, D R and WILSON, D R: "Tracking accuracy of adaptive Notch filters for servo stabilisation", Division of Engineering,

20. cont. The Polytechnic of Central London, July 1978.

21. CURRY, RENWICK, E: "A separation theorem for non-linear measurements", IEEE Trans on Automatic Control, Oct 1969, Vol AC-14.

22. DAVIS, M H: "Linear estimation and stochastic control", 1977, Chapman and Hall, London.

23. ST. DENIS, M: "Some observations on the techniques for predicting the oscillations of freely-floating hulls in a seaway", Offshore Technology Conference, 6200 North Central Expressway, Dallas, Texas, 75206, Paper no OTC 2024.

24. EMARA-SHABAIK, H E and LEONDES, C T: "Non-linear filtering - the link between Kalman and extended Kalman filters", Int J Control, 1981, Vol 34, No 6, 1207-1214.

25. ENGLISH, J W and WISE, D A: "Hydrodynamic aspects of dynamic positioning", Vol 92, No 3, The North East Coast Inst of Engineers and Shipbuilders, December 1975.

26. FITZGERALD, R J: "Divergence of the Kalman filter", IEEE Trans on Automatic Control, Vol AC-16, No 6, December 1971.

27. FOTAKIS, I E: "Design of optimal control systems and industrial applications", Research Report EEE/77/June 1981, Sheffield City Polytechnic.

28. FOTAKIS, I E, GRIMBLE, M J and KOUVARITAKIS, B: "A comparison of characteristic locus and optimal designs for stochastic multivariable systems", Research Report EEE/48/February 1980, Sheffield City Polytechnic.

29. FRIEDLAND, B: "On the effect of incorrect gain in Kalman filter", IEEE Transactions on Automatic Control, October 1967, AC-12.

30. GELB, A: "Applied optimal estimation", MIT Press, 1974.

31. GOCLOWSKI, J and GELB, A: "Dynamics of an automatic ship steering system", IEEE Transactions on Automatic Control, Vol AC-11, July 1966.

32. GRIMBLE, M J: "S-domain solution for the fixed end-point optimal control problem", Proc IEE, Vol 124, No 9, September 1977.

33. GRIMBLE, M J: "Relationship between Kalman and Notch filters used in dynamic ship positioning systems", Electronics Letter, 22 June 1978, Vol 14, No 13.

34. GRIMBLE, M J: "The dynamic ship positioning control problem", Research Report EEE/22/1978, Sheffield City Polytechnic.

35. GRIMBLE, M J: "Solution of the linear-estimation problem in the s-domain", Proc IEE, Vol 125, No 6, June 1978.

36. GRIMBLE, M J: "Design of stochastic optimal feedback control systems", Proc IEE, Vol 125, No 11, November 1978.

37. GRIMBLE, M J: "A combined state and state estimate feedback solution to the stochastic optimal control problem", Research Report EEE/27/January 1979, Sheffield City Polytechnic.

38. GRIMBLE, M J: "Optimal control of linear systems with cross-product weighting", Proc IEE, Vol 126, No 1, Jan 1979, pp 96-103.

39. GRIMBLE, M J: "Design of optimal output regulators using multi-variable root loci", Research Report EEE/37/April 1979, Sheffield City Polytechnic.

40. GRIMBLE, M J: "Frequency domain solution to the optimum multivariable tracking problem", Trans MC, Vol 1, No 2, Apl-Jun 1979.

41. GRIMBLE, M J: "Solution of the stochastic optimal control problem in the s-domain for systems with time delay", Proc IEE, Vol 126, No 7, July 1979.

42. GRIMBLE, M J: "Design of optimal stochastic regulating systems including integral action", Proc IEE, Vol 126, No 9, September 1979.

43. GRIMBLE, M J: "Solution of the discrete-time stochastic optimal control problem in the z-domain", Int J Systems Sci, 1979, Vol 10, No 12, 1369-1390.

44. GRIMBLE, M J: "Frequency domain properties of Kalman filters", Research Report EEE/42/1979, Sheffield City Polytechnic.

45. GRIMBLE, M J: "Solution of Kalman filtering problem for stationary noise and finite data records", Int J Systems Sci, 1979, Vol 10, No 2, 177-196.

46. GRIMBLE, M J: "Frequency domain properties of Kalman filters", IEE Colloquium on Kalman filters and their applications, 17th Nov 1980, Savoy Place, London.

47. GRIMBLE, M J: "Introduction to linear and extended Kalman filters", SRC Vacation School, Stochastic Processes in Control Systems, University of Warwick, April 1981.

48. GRIMBLE, M J and AL-TAKIE, A A: "Optimal control of non-linear stochastic systems", Research Report EEE/60/September 1980, Sheffield City Polytechnic.

49. GRIMBLE, M J, PATTON, R J and WISE, D A: "The design of dynamic ship positioning control systems using extended Kalman filtering techniques", IEEE Oceans '79 Conference, San Diego, California.

50. GRIMBLE, M J, PATTON, R J and WISE, D A: "Use of Kalman filtering techniques in dynamic ship positioning systems", IEE Proceedings, Vol 127, Pt D, No 3, May 1980.

51. GRIMBLE, M J, PATTON, R J and WISE, D A: "The design of dynamic ship positioning control systems using stochastic optimal control

51. cont. theory", Optimal Control Applications & Methods, Vol 1, 167-202 (1980).

52. HADDAD, A H: "Minimum filtering with a class of non-linear systems", IEEE Transactions on Automatic Control, June 1968, AC-13.

53. HALAMANDARES, H and OZDES, D: "A Kalman filter augmented marine navigation systems", Satellite Positioning Corporation, 16033 Ventura Blvd, Encino, California, 91316, USA.

54. HALYO, N and CAGLAYAN, A K: "A separation theorem for the stochastic sampled-data LQG problem", Int J Control, 1976, Vol 23, No 2, 237-244.

55. HEFFES, H: "The effect of erroneous models on the Kalman filter response", IEEE Transactions on Automatic Control, July 1966, AC-11.

56. HUTCHINSON, C E: "An example of the equivalence of the Kalman and Wiener filters", IEEE Transactions on Automatic Control, April 1966, AC-11.

57. KAILATH, T: "A view of three decades of linear filtering theory", IEE Transactions on Information Theory, Vol IT-20, No 2, March 1974.

58. KALMAN, R E: "A new approach to linear filtering and prediction problems", Trans of ASME, March 1960, pp 35-45.

59. KALMAN, R E: "When is a linear control system optimal? ", Journal of Basic Engineering, March 1964.

60. KALMAN, R E and BUCY, R S: "New results in linear filtering and prediction theory", Trans of the ASME, March 1961, pp 95-108.

61. KLEINMAN, D L: "on an iterative technique for Riccati equation computations", IEEE Transactions on Automatic Control, February 1968, AC-13.

62. KLEINMAN, D L: "Optimal control of linear systems with time-delay and observation noise", IEEE Transactions on Automatic Control, October 1969, AC-14 .

63. KOSUT ROBERT, L: "Sub-optimal control of linear time-invariant systems subject to control structure constraints", IEEE Transactions on Automatic Control, Vol AC-15, No 5, October 1970.

64. KREBS, V: "Combined state and parameter estimation for a class of non-linear stochastic systems by modified non-linear filtering", Inst für Regelungstechnik, Technische Hochschule Darmstadt, Darmstadt, Germany (FRG).

65. KREYSZIG, E: "Advanced engineering mathematics", 3rd Edition, John Wiley & Sons, Inc, 1972, USA.

66. KWAKERNAAK, and SIVAN: "Linear optimal control systems", 1972, John Wiley & Sons Inc.

67. LEONDES, C T and PEARSON, J O: "Kalman filtering of systems with parameter uncertainties - a survey", Int J Control, Vol 17, No 4, 785-801, 1973.

68. LEVINE, W S and ATHANS, M: "On the determination of the optimal constant output feedback gains for linear multivariable systems", IEEE Transactions on Automatic Control, Vol AC-15, No 1, February 1970.

69. LJUNG, L: "Asymptotic behaviour of the extended Kalman filter as a parameter estimator for linear systems", IEEE Transactions Vol AC-24, No 1, February 1979.

70. MacFARLANE, A G J: "An eigenvector solution of the optimal linear regulator problem", J Electronics and Control, (14), pp 643-654, 1963.

71. MAHALANABIS, A K: "On minimising the divergence in discrete filters", IEEE Transactions on Automatic Control, April 1972, AC-17.

72. MARSHALL, S A and NICHOLSON, H: "Optimal control of linear multivariable systems with quadratic performance criteria", Proc IEE, Vol 117, No 8, August 1970.

73. MEARNS G M: "Dynamic positioning, its applications to offshore craft", The Inst of Marine Engineers, January 1978.

74. MEHRA, R K: "On the identification of variances and adaptive Kalman filtering", IEEE Transactions on Automatic Control, Vol AC-15, No 2, April 1970.

75. MELSA, J and JONES, S: "Computer programs for computational assistance in the study of linear control theory", 1973, McGraw-Hill, Inc, USA.

76. MENDEL, J M: "Computational requirements for a discrete Kalman filter", IEEE Transactions on Automatic Control, Vol AC-16, No 6, December 1971.

77. MEYER, G G L and PAYNE, H J: "An iterative method of solution of the algebraic Riccati equation", IEEE Transactions on Automatic Control, August 1972, AC-17.

78. MISSAGHIE, M M and FAIRMAN, F W: "Least squares observer design for continuous stochastic systems", Int J Systems Sci, 1978, Vol 9, No 2, 137-146.

79. NELSON, L W and STEAR, E: "The simultaneous on-line estimation of parameters and states in linear systems", IEEE Transactions on Automatic Control, February 1976, AC-21.

80. NEWMANN, M: "A continuous-time reduced-order filter for estimating the state vector of a linear stochastic systems", Int J Control, 1970, Vol 11, No 2, 229-239.

81. NICHOLSON, H: "Concepts of general system theory in the linear optimal control problem", Research Report No 5, Dept of Control Engineering, Sheffield University, November 1970.

82. OGATA KATSUHIKO: "Modern control engineering", 1970, Prentice-Hall Inc, Englewood Cliffs, NJ.

83. PANUSKA, V: "A new form of the extended Kalman filter for parameter estimation in linear systems with correlated noise", IEEE Transactions on Automatic Control, Vol AC-25, No 2, April 1980.

84. PAYNE, H J and SILVERMAN, L M: "On the discrete time algebraic Riccati equation", IEEE Transactions on Automatic Control, Vol AC-18, No 3, June 1973.

85. PORTER, B and WOODHEAD, M A: "Performance of optimal control systems when some of the state variables are not measurable", Int J Control, 1968, Vol 8, No 2, 191-195.

86. PRICE, C F: "An analysis of the divergence problem in the Kalman filter", IEEE Transactions on Automatic Control, December 1968, pp 699-702, **AC-13**.

87. PRICE, W G and BISHOP, R E D: "Probabilistic theory of ship dynamics", Chapman and Hall Ltd, 1974.

88. PRUSSING, J E: "A simplified method for solving the matrix Riccati equation", Int J Control, 1972, Vol 15, No 5, 995-1000.

89. QUIGLEY, A L C: "An approach to the control of divergence in Kalman filter algorithms", Int J Control, 1973, Vol 17, No 4, 741-746.

90. RUZICKA, J: "Optimal bounded regulator problem for continuous times stochastic systems with noisy observations", University of California, Los Angeles.

91. SAFONOV, M G and ATHANS, M: "Robustness and computational aspects of non-linear stochastic estimators and regulators", 0018-9286/78/0800-0717 $00.75, 1978, IEEE, **AC-23**.

92. SAITO, O, TAKEDA, H and FUKUSHIMA, K: "The effect of an erroneous model of coloured noise on the optimal filtering algorithm", IEEE Transactions on Automatic Control", October 1971, **AC-16**.

93. SAMANT, V S and SORENSON H W: "On reducing computational burden in the Kalman filter", Automatica, Vol 10, 61-68, Pergamon Press, 1974.

94. SARGENT, J S and ELDRED, J J: "Adaptive control of thruster modulation for a dynamically positioned drillship", Offshore Technology Conference, 6200North Central Expressway, Dallas, Texas, 75206, paper no OTC-2036.

95. SCHMID, G T: "Closed-loop control of stochastic non-linear systems", Automatica, Vol 7, pp 557-566, 1971

96. SIMON, K W and STUBBERUD, A R: "Reduced-order Kalman filter", Int J Control, 1969, Vol 10, No 5, 501-509.

97. SINGER, R A and SEA, R G: "Increasing the computational efficiency of discrete Kalman filters", IEEE Transactions on Automatic Control, June 1971, **AC-16**.

98. SMITH, M W A and ROBERTS, A P: "A study of the Kalman filter as a state estimator of deterministic and stochastic systems", Int J Systems Sci, 1979, Vol 10, No 8, 895-911.

99. SORHEIM, H R and GALTUNG, F L: "Wave filter performance evaluation", Offshore Technology Conference, 9th Annual OTC in Houston Texas, May 1977.

100. SRIYANANDA, H: "A simple method for the control of divergence in Kalman-filter algorithms", Int J Control, 1972, Vol 16, No 6, 1101-1106.

101. STEAR, E B and STUBBERUD, A R: "Optimal filtering for Gauss-Markov noise", Int J Control, 1968, Vol 8, No 2, 123-130.

102. VIT, K: "Iterative solution of the Riccati equation", IEEE Transactions on Automatic Control", April 1972,AC-17.

103. WILSON, D R and CORRALL D R: "The design of digital Notch networks for use in servomechanisms", IEEE Transactions on Industrial Electronics and Control Instrumentation, Vol IECI-20, 138-144, August 1973.

104. WISE, D A and ENGLISH, J W: "Tank and wind tunnel tests for a drill-ship with dynamic position control", Offshore Technology Conference, Dallas Texas 75206.

A P P E N D I C E S

APPENDIX 1

NOTES ON PER-UNIT SYSTEM OF TIME SCALING

All the equations of motion for both"Wimpey Sealab"and"Star Hercules" vessels have been represented in per-unit. Both time and amplitude scaling have been applied.

Consider the following general differential equation:

$$\frac{d}{dt}\underline{x}(t) = A\,\underline{x}(t) + B\,\underline{u}(t) \qquad \ldots\ldots\ldots\ldots\ldots (1)$$

which has been represented in a real time. Now suppose that time scale change from real time (t) to per-unit time ($t^{\backprime}$), where

$$t^{\backprime} = \frac{t}{t_b} \quad \text{and } t_b \text{ is the base time}$$

Then the plant differential equation will become:

$$\frac{d}{dt^{\backprime}}\underline{x}(t^{\backprime}t_b) = t_b(A\underline{x}(t^{\backprime}t_b) + B\underline{u}(t^{\backprime}t_b)) \qquad \ldots\ldots\ldots\ldots\ldots (2)$$

$$\dot{\underline{x}}_o(t^{\backprime}) = t_b(A\underline{x}_o(t^{\backprime}) + B\underline{u}(t^{\backprime}t_b)) \qquad \ldots\ldots\ldots\ldots\ldots (3)$$

where $\underline{x}_o(t^{\backprime})$ is the per-unit value of the state vector.

In order to determine the values of the control Q and R matrices, and hence the state feedback gain matrix, the maximum permissible deviations in the per-unit thruster control signals are required.

The general base units for the per-unit system differes for different kinds of vessels, which depend upon the size and the geometry of the vessel, and can be summarised for both"Wimpey Sealab"and"Star Hercules":

(i) "Wimpey Sealab" Vessel

Mass	(m)	= 5670	tonne
Length	(L_{pp})	= 94.49	metre
Gravitational Acc.	(g)	= 9.81	m/sec^2
Time	$\sqrt{L_{pp}/g}$	= 3.104	seconds
Velocity	$\sqrt{L_{pp}g}$	= 30.44	m/sec
Force	(mg)	= 55,620	KN
Moment	(mgL)	= 5,256,000	KN-m
Angular Velocity	$\sqrt{g/L}$	= 0.3222	rad/sec

From which:

The base time = t_b = 3.104 sec

The amplitude scaling factor = 95 m

Assuming that all the thrusters acting in one direction, the maximum force is (40) tones or (400) KN, then

$$\text{per-unit sway force} = \frac{400}{55.6 \times 10^3} = 0.007 \simeq 0.01$$

and the maximum torque is 90 m x 20 tonnes which is (1800) m tonne or (18000 KN metres, then

$$\text{per-unit torque} = \frac{18000}{5{,}256 \times 10^6} = 0.003 \simeq 0.004$$

The assumption has made that, the thruster time constant is to be (2) seconds or (2/3.104 = 0.644 pu) and hence,

$$b_1 = b_2 = 1/0.644 = 1.55$$

(ii) "Star Hercules"Vessel

Mass	m	= 4377	tonne
Length	L_{pp}	= 73	metres
Time	$\sqrt{L_{pp}/g}$	= 2.728	seconds
Gravitational Acc.	g	= 9.81	m/sec^2
Force	mg	= 42.940	KN
Moment	mgL_{pp}	= 3,134,500	KN.m

From which:

The base time = 2.728

and for (2) seconds thruster's time constant, which is (2/2.728 = 0.733 pu), $b_1 = b_2 = 1/0.733 = 1.364$.

APPENDIX 2

HIGH FREQUENCY MODEL PARAMETERS

By examining the high frequency part of the dynamics, the general structure of the system A-matrix for sway or yaw is:

$$\begin{bmatrix} 0 & T_b & 0 & 0 \\ 0 & 0 & T_b & 0 \\ 0 & 0 & 0 & T_b \\ -\alpha_4 & -\alpha_3 & -\alpha_2 & -\alpha_1 \end{bmatrix}$$

where T_b = 3.104 secs for "Wimpey Sealab" while the parameter α_1, α_2, α_3 and α_4 varies in proportion to the weather conditions as indicated in the following Table 1 for "Wimpey Sealab" vessel for Beaufort number 5 (calm sea) to Beaufort number 9 (the worst weather conditions), and the corresponding Beauforts number 5 and number 8 of Table 2 for "Star Hercules" vessel.

Beaufort No	α_1	α_2	α_3	α_4
5	4.594	4.384	2.988	1.470
6	3.663	2.698	1.452	0.556
7	3.166	2.119	0.974	0.341
8	2.794	1.789	0.754	0.251
9	2.545	1.353	0.486	0.131

Table No (1)

Beaufort No	α_1	α_2	α_3	α_4
5	4.037	3.853	2.626	1.292
8	2.455	1.572	0.662	0.22

Table No (2)

APPENDIX 3

CALCULATION OF THE KALMAN GAIN MATRIX

The position measurements are not defined in continuous form but are sampled at regular intervals. The system simulation and the Kalman filter have both been modelled using their discrete forms. The resulting discrete equations are as follows:

$$\underline{x}(k+1) = \Phi(k+1,k)\underline{x}(k) + \Delta\underline{u}(k) + \Gamma\underline{\omega}(k) \quad \ldots\ldots\ldots (1)$$

$$\underline{z}(k) = C\underline{x}(k) + \underline{v}(k) \quad \ldots\ldots\ldots (2)$$

with

$$E\{\underline{\omega}(k)\} = 0 \qquad E\{\underline{\omega}(k)\underline{\omega}^T(j)\} = Q\delta_{kj} \quad \ldots\ldots\ldots (3)$$

$$E\{\underline{v}(k)\} = 0 \qquad E\{\underline{v}(k)\underline{v}^T(j)\} = R\delta_{kj} \quad \ldots\ldots\ldots (4)$$

and where δ_{kj} is the Dirac function. The matrices Δ and Γ are related to their continuous-time counterparts by

$$\Delta = \int_0^{\tau_1} \Phi(\tau)B \, d\tau \quad \ldots\ldots\ldots (5)$$

$$\Gamma = \int_0^{\tau_1} \Phi(\tau)D \, d\tau \quad \ldots\ldots\ldots (6)$$

and

$$\Phi(k+1, k) \triangleq \Phi(\tau_1) \quad \ldots\ldots\ldots (7)$$

where τ_1 is the sampling interval.

The state estimate is given by calculating the predicted state

$$\hat{\underline{x}}(k+1|k) = \Phi(k+1|k)\hat{\underline{x}}(k|k) + \Delta\underline{u}(k) \quad \ldots\ldots\ldots (8)$$

and then calculating the estimated state at the instant $(k+1)$, using

$$\hat{\underline{x}}(k+1|k+1) = \hat{\underline{x}}(k+1|k) + K(k+1)(\underline{y}(k+1) - C\hat{\underline{x}}(k+1|k)). \quad (9)$$

The Kalman gain matrix $K(k + 1)$ can be obtained, first by calculating the predicted error covariance matrix

$$P(k + 1|k) = \Phi(k + 1|k)P(k|k)\Phi^T(k + 1|k) + \Gamma Q\Gamma^T \quad \ldots\ldots\ldots (10)$$

for some initial error covariance $P(k|k)$, and then calculating

$$K(k + 1) = P(k + 1|k)C^T\left[CP(k + 1|k)C^T + R\right]^{-1} \quad \ldots\ldots\ldots (11)$$

Finally, the error covariance matrix is obtained using

$$\begin{aligned} P(k + 1|k + 1) = &(I - K(k + 1)C)P(k + 1|k)(I - K(k + 1)C)^T \\ &+ K(k + 1)RK^T(k + 1) \end{aligned} \quad \ldots\ldots\ldots (12)$$

The above equations can be used iteratively to obtain the state estimate at any future sampling time, given the initial state and covariance.

APPENDIX 4

EXTENDED KALMAN FILTER/PROPAGATING THE CONDITIONAL MEAN OF THE STATE ESTIMATE AND ITS ASSOCIATED COVARIANCE

In order to extend the problem of optimal estimation and control for linear systems to the general case of a system with non-linearity, consider the following non-linear stochastic differential equations of the system dynamics:

$$\dot{\underline{x}}(t) = \underline{f}(\underline{x}(t), t) + \underline{\omega}(t) \qquad \ldots\ldots\ldots\ldots (1)$$

in which $\underline{f}$ is a function of the state $\underline{x}(t)$.

The problem will be the estimation of the state $\underline{x}(t)$ using the non-linear measurements, which is described in its discrete form as:

$$\underline{z}_k = \underline{h}_k(\underline{x}(t_k)) + \underline{v}_k \qquad k = 1, 2,... \qquad \ldots\ldots\ldots\ldots (2)$$

where $\underline{h}_k$ is a function of the state $\underline{x}(t_k)$ and depends on the index k at each sampling period.

Both $\underline{\omega}_k$ and $\underline{v}_k$ are white gaussian noise of zero mean, with $E(v_k) = E(\omega_k) = 0$ where $E(.)$ is the expected value of $\cdot$ and $E(v_k v_j^T) = R_k \delta_{kj}$, $E(\omega_k \omega_j^T) = Q_k \delta_{kj}$ and $E(\omega_k v_j) = 0$ for all k, j, since all the noise sequences are independent, where the Kronecker delta functions

$$\delta_{kj} = 0 \qquad k \neq j$$
$$= 1 \qquad k = j$$

Given the non-linear system equation of motion and the measurement equation, and the problem is to calculate the minimum variance estimate of $\underline{x}(t)$. The minimum variance estimate of $\underline{x}(t)$ is the conditional mean of the state $\underline{x}(t)$.

Suppose that the measurements data are given at time t_{k-1} and the conditional mean estimate of the state vector $\hat{\underline{x}}(t_{k-1})$ is known. Then by integrating both sides of equation (1) from time t_{k-1} to t_k, the propagated state at instant t_k will be:

$$\underline{x}(t) = \underline{x}(t_{k-1}) + \int_{t_{k-1}}^{t} \underline{f}(\underline{x}(\tau), \tau)d\tau + \int_{t_{k-1}}^{t} \underline{\omega}(\tau)d\tau \qquad .....(3)$$

taking the expectation, differentiation of both sides of equation (3), taking into consideration the noise characteristics mentioned above, produces:

$$\frac{d}{dt} E[\underline{x}(t)] = E[\underline{f}(\underline{x}(t), t)] \quad \text{where } t_{k-1} \leq t < t_k \qquad .....(4)$$

In equation (2) above, all the measurements taken up to time t_{k-1}.

$$E[\underline{x}(t_{k-1})] = \hat{\underline{x}}(t_{k-1}) \text{ is the initial condition}$$

Refer to equation (4). Over the time interval $t_{k-1} \leq t < t_k$, the solution of equation (4) is the conditional mean of $\underline{x}(t)$ which is:

$$\dot{\hat{\underline{x}}}(t) = E[\underline{f}(\underline{x}(t), t)] \quad t_{k-1} \leq t < t_k \qquad .....(5)$$

The initial condition is the conditional mean of the state at t_{k-1} which is assumed known.

The estimation error covariance matrix is defined as:

$$P(t) \triangleq E[(\hat{\underline{x}}(t) - \underline{x}(t))(\hat{\underline{x}}(t) - \underline{x}(t))^T] \qquad .....(6)$$

The differential equation for the estimation error covariance will be:

$$\dot{P}(t) = E[\dot{\underline{x}}(t)\ \underline{x}^T(t)] + E[\underline{x}(t)\ \dot{\underline{x}}^T(t)] - \dot{\hat{\underline{x}}}(t)\ \hat{\underline{x}}^T(t) - \hat{\underline{x}}(t)\ \dot{\hat{\underline{x}}}^T(t) \cdots (7)$$

substitute for $\dot{\underline{x}}(t)$ from equation (1) and for $\dot{\hat{\underline{x}}}$ from equation (5) into

equation (7):

$$\dot{P}(t) = E\left[(\underline{f} + \underline{\omega})\underline{x}^T\right] + E\left[\underline{x}(\underline{f} + \underline{\omega})^T\right] - E\left[\underline{f}\right]\hat{\underline{x}}^T - \hat{\underline{x}}\,E\left[\underline{f}^T\right]$$

$$= E\left[\underline{f}\,\underline{x}^T\right] + E\left[\underline{x}\,\underline{f}^T\right] - \hat{\underline{x}}\,E\left[\underline{f}^T\right] - E\left[\underline{f}\right]\hat{\underline{x}}^T + 2\int_{t_{k-1}}^{t} Q(t)\,\delta(t-\tau)\,d\tau$$

$$\dot{P}(t) = E\left[\underline{f}\,\underline{x}^T\right] + E\left[\underline{x}\,\underline{f}^T\right] - \hat{\underline{x}}\,E\left[\underline{f}^T\right] - E\left[\underline{f}\right]\underline{x}^T + Q(t) \qquad \ldots\ldots (8)$$

Refer to equation (5), denote $E\left[\underline{f}(\underline{x}, t)\right]$ as $\hat{\underline{f}}\,(\underline{x}(t), t)$.

Now expand $\underline{f}(\underline{x}, t)$ in a Tylar series about the current estimate of the state vector, then take the expectation of both sides to compute $\underline{f}(\underline{x}(t), t)$, as follows:

$$\underline{f}(\underline{x}, t) = \underline{f}(\hat{\underline{x}}, t) + \left.\frac{\partial \underline{f}}{\partial \underline{x}}\right|_{\underline{x} = \hat{\underline{x}}} (\underline{x} - \hat{\underline{x}}) + \ldots \qquad \ldots\ldots\ldots (9)$$

$$\hat{\underline{f}}(\underline{x}, t) = \underline{f}(\hat{\underline{x}}, t) + 0 + \ldots \qquad \ldots\ldots\ldots (10)$$

substitute the first-order approximation of $\hat{\underline{f}}(\underline{x}, t)$ from equation (10) into equation (5)

$$\dot{\hat{\underline{x}}}(t) = \underline{f}(\hat{\underline{x}}(t)) \qquad t_{k-1} \leq t < t_k \qquad \ldots\ldots\ldots (11)$$

To find an approximate differential equation for the estimation error covariance matrix, define matrix $F(\hat{\underline{x}}(t), t)$ whose ijth element is:

$$\underline{f}_{ij}(\hat{\underline{x}}(t), t) \triangleq \left.\frac{\partial \underline{f}_i(\underline{x}(t), t)}{\partial x_j(t)}\right|_{\underline{x}(t) = \hat{\underline{x}}(t)}$$

$$\dot{P}(t) = E\left[\underline{f}\,\underline{x}^T\right] + E\left[\underline{x}\,\underline{f}^T\right] - \hat{\underline{x}}\,E\left[\underline{f}^T\right] - E\left[\underline{f}\right]\hat{\underline{x}}^T + Q(t) \qquad \ldots\ldots\ldots (12)$$

using equation (9):

$$\dot{P}(t) = E\left[\underline{f}(\hat{\underline{x}}, t)\underline{x}^T + \left.\frac{\partial \underline{f}}{\partial \underline{x}}\right|_{\underline{x} = \hat{\underline{x}}} (\underline{x} - \hat{\underline{x}})\underline{x}^T\right] + E\left[\underline{x}\,\underline{f}^T\right] -$$

$$- \hat{\underline{x}}\, E\left[\underline{f}^T(\hat{\underline{x}},\ t) + \left(\frac{\partial \underline{f}}{\partial \underline{x}}\right|_{\underline{x} = \hat{\underline{x}}} (\underline{x} - \hat{\underline{x}}))^T\right] - E[\underline{f}]\ \hat{\underline{x}}^T + Q(t)$$

$$= \underline{f}(\hat{\underline{x}},\ t)\hat{\underline{x}}^T + \left.\frac{\partial \underline{f}}{\partial \underline{x}}\right|_{\underline{x} = \hat{\underline{x}}} E\left[(\underline{x} - \hat{\underline{x}})\underline{x}^T\right] + E\left[\underline{x}\ \underline{f}^T\right]$$

$$- \hat{\underline{x}}\ \underline{f}^T(\hat{\underline{x}},\ t) - E\left[\hat{\underline{x}}(\underline{x} - \hat{\underline{x}})^T\right] \left.\frac{\partial \underline{f}^T}{\partial \underline{x}}\right|_{\underline{x} = \hat{\underline{x}}} - E[\underline{f}]\hat{\underline{x}}^T + Q(t)$$

$$= \left.\frac{\partial \underline{f}}{\partial \underline{x}}\right|_{\underline{x} = \hat{\underline{x}}} E\left[(\underline{x} - \hat{\underline{x}})\,(\underline{x}^T - \hat{\underline{x}}^T)\right]$$

$$+ E\left[(\underline{x} - \hat{\underline{x}})\,(\underline{x}^T - \hat{\underline{x}}^T)\right] \left.\frac{\partial \underline{f}^T}{\partial \underline{x}}\right|_{\underline{x} = \hat{\underline{x}}} + Q(t)$$

$$= \left.\frac{\partial \underline{f}}{\partial \underline{x}}\right|_{\underline{x} = \hat{\underline{x}}} P(t) + P(t) \left.\frac{\partial \underline{f}^T}{\partial \underline{x}}\right|_{\underline{x} = \hat{\underline{x}}} + Q(t)$$

$$\dot{P}(t) = F(\hat{\underline{x}}(t),\ t)\ P(t) + P(t)\ F^T(\hat{\underline{x}}(t),\ t) + Q(t)$$

$$t_{k-1} \leq t < t_k \qquad \text{.....(13)}$$

Equations (11) and (13) are an approximate expression for propagating the conditional mean of the state and the estimation error covariance for $t_{k-1} \leq t < t_k$. Those equations have got the structure of Kalman filter and referred to as extended Kalman filter.